8-2013

THE INTERACTION OF MECHANICAL LOADING AND METABOLIC STRESS ON HUMAN CORTICAL BONE: TESTING ANTHROPOLOGICAL ASSUMPTIONS USING CROSS-SECTIONAL GEOMETRY AND HISTOMORPHOLOGY

Courtney Dianne Eleazer
celeazer@fiu.edu

To the Graduate Council:

I am submitting herewith a dissertation written by Courtney Dianne Eleazer entitled "THE INTERACTION OF MECHANICAL LOADING AND METABOLIC STRESS ON HUMAN CORTICAL BONE: TESTING ANTHROPOLOGICAL ASSUMPTIONS USING CROSS-SECTIONAL GEOMETRY AND HISTOMORPHOLOGY." I have examined the final electronic copy of this dissertation for form and content and recommend that it be accepted in partial fulfillment of the requirements for the degree of Doctor of Philosophy, with a major in Anthropology.

Benjamin M. Auerbach, Major Professor

We have read this dissertation and recommend its acceptance:

Graciela Cabana, Andrew Kramer, Katie Kavanagh

Accepted for the Council:
Dixie L. Thompson

Vice Provost and Dean of the Graduate School

(Original signatures are on file with official student records.)

THE INTERACTION OF MECHANICAL LOADING AND METABOLIC STRESS ON HUMAN CORTICAL BONE: TESTING ANTHROPOLOGICAL ASSUMPTIONS USING CROSS-SECTIONAL GEOMETRY AND HISTOMORPHOLOGY

A Dissertation Presented for the
Doctor of Philosophy
Degree
The University of Tennessee, Knoxville

Courtney Dianne Eleazer
August 2013

ACKNOWLEDGEMENTS

As is true of all doctoral candidates, I could not have accomplished this goal without the assistance and support of others. Those who have contributed to this research project, whether in an academic context or in the form of emotional support, deserve enormous credit for their efforts.

First, I would like to thank Ben Auerbach for his role in helping to shape this work. Ben accepted me as his first graduate student at the University of Tennessee knowing that my dissertation project would be a challenging endeavor (for both of us), and through these last six years he has met every bump in the road with exceptional optimism and encouragement. I am incredibly lucky to have had such a supportive and involved academic advisor and committee chair. I would also like to thank the remaining members of my committee: Graciela Cabana, Andy Kramer, and Katie Kavanagh, for providing insightful comments and advice that improved this research. Graciela has provided much guidance on the project's design, specifically the formulation of the research hypotheses and the broader implications to the anthropological discipline. She also graciously allowed me to cut samples and store equipment in her molecular anthropology lab. In addition, Andy and Katie's broad knowledge of mechanics and nutrition have helped structure my approach to interpreting these effects in archaeological samples. Together, the perspectives of my committee members have helped develop the project in ways that I would have not considered, and I am much appreciative of their guidance.

I would like to especially thank those researchers and colleagues not on my committee who have provided me with access to collections and resources as well as advice, without which

this research would not have been possible. I am forever indebted to Tosha Dupras. In addition to providing me with bone samples from Egypt (Kellis 2 cemetery, Dakhleh Oasis) for my pilot project and granting me permission to continue research at that site, she was integral to locating another cemetery sample when the Egyptian revolution prevented access to the Kellis skeletal remains and thwarted progress on this project. When it appeared that no other subadult skeletal collection was available for histological analysis, Tosha made it her mission to assist with finding a collection for me to conduct my research and placed me in contact with the Faculty of Medicine at Vilnius University. Without her assistance, it is likely that I would have had to abandon the project entirely.

I also wish to express my sincere gratitude to Rimantas Jankauskas, the curator of skeletal collections at the Vilnius University, for granting me access to the Alytus skeletal collection. Rimantas was always willing to go above and beyond in providing assistance and information. Thank you also to Agnius Urbanavicius and Justina Kozakaite for pulling boxes during data collection in Vilnius and allowing me to disturb their carefully curated collection. Agnius also took time out of his summer vacation to show me around his hometown of Alytus and pass along his knowledge of Alytus history, and for this I am incredibly grateful. Several doctoral students at Vilnius University aided with procuring bone samples as well. Lana Williams shared her extensive expertise in photographing pathological lesions and alleviated some of the burden of data collection by offering to photograph some pathologies herself.

I extend my deepest appreciation to Walter Klippel for allowing me to utilize histological equipment and supplies in the Mineralized Tissue Histology Laboratory and Zooarchaeology Laboratory at the University of Tennessee. Thank you also to the Department of Anthropology for funding a portion of this project through the Kneberg-Lewis Award. Additionally, I wish to

thank those researchers (in no particular order) whose ideas have helped shape my own and with whom I have had many insightful conversations over the years about my research: Libby Cowgill, Evan Garofalo, Valerie DeLeon, Robert Paine, Margaret Streeter, Susan Pfeiffer, Sam Stout, Danny Wescott, Dan Temple, Osborn Pearson, David Burr, and Chris Ruff.

I am immensely indebted to my family and friends who have supported me through this entire process. There are no words to express how much my parents have contributed to my academic career and how appreciative I am of their love and support. They have always supported me in my decisions and endeavors throughout my life. My brother, Ben, is about to embark on this same journey and I intend to provide him with the same encouragement (and bitter sarcasm/teasing) as he has bestowed on me. My best friend and platonic life partner, Linz, has been by my side throughout my college and graduate school years. Above all things, she has taught me how to laugh and not take myself too seriously. Thanks also to my in-laws—Rick, Jan, Joe, Katy, and Daniel—for accepting me into their family and being so understanding and supportive of my career goals.

To my fellow graduate students and ladies of the OVAL (Becky Kelso, Nicole Reeves, Amber Wheat, Brannon Hulsey, Frankie Pack, Hillary Parsons, Beatrix Dudzik), were it not for you I would have gone completely insane. Thank you for making me smile no matter the circumstances and being patient while I obsessed about osteons and cross-sections. You all have given me an incredible amount of academic and personal advice that I will continue to employ for years to come. All of you are beautiful, amazing women who have influenced and enriched my life more than you probably realize.

And finally, I especially thank my husband, Andrew Weidman, for having unwavering faith in me. Andrew, you are my rock. Thank you for taking care of me (and the house) and always being there for me. I couldn’t have accomplished this goal without your help.

ABSTRACT

This research investigates how the interaction of mechanics (i.e., physical activity) and metabolism (i.e., health status) shapes human cortical bone morphology during skeletal development. Understanding this interaction is important for research investigating human behavior from adult and subadult archaeological skeletal samples, as previous studies have demonstrated that interaction effects may confound the interpretation of either mechanics or metabolism independently from skeletal remains.

This study approaches this issue holistically through the analysis of human cortical bone morphology at dual scales (microscopic and macroscopic scales) and across multiple skeletal elements (femora, humeri, and ribs) exposed to different levels of mechanical loading. Because bone responds to environmental influences most strongly during growth, a *subadult* cemetery sample of 57 individuals from the medieval archaeological site of Alytus, Lithuania (A.D. 14th-18th centuries) was employed. Bone properties were compared among individuals who had experienced varying amounts of metabolic stress, as inferred from skeletal stress lesions. Analyses tested the hypothesis that to maintain proper bone strength, metabolic stress effects (i.e., bone loss) are increasingly attenuated as mechanical loading demands increase across the three skeletal elements.

Results suggest that mechanical loading compensates for metabolic bone loss at both macroscopic and microscopic scales. Macroscopically, loading attenuates metabolic bone loss by redistributing cortical bone further from the cross-sectional centroid, thus increasing bone strength properties and maintaining loading relationships across the skeleton. Additionally, although metabolic stress is associated with microscopic bone loss, this loss is distributed within

the skeleton in a way that may mitigate reductions in strength at the tissue-level (i.e., preferentially in elements with more macroscopic bone mass). While these results point to enhanced effects of loading relative to metabolic stress, both factors have a detectable influence on cortical morphology.

The interaction between mechanical and metabolic factors, therefore, must be considered when interpreting physical activity and health status from human skeletal remains. As the majority of adult cortical morphology is formed during skeletal development, when these factors are strongest, accounting for interaction effects is important for both subadult and adult studies. Thus, the implications of this study will assist in improving analyses of human biocultural adaptation in the past.

TABLE OF CONTENTS

LIST OF TABLES

LIST OF FIGURES

CHAPTER 1: INTRODUCTION

Biological anthropologists often examine cortical bone to deduce the influence of environmental factors, such as mechanics (i.e., physical activity) and metabolism (i.e., health status), on the skeletal morphologies of human populations. Such analyses are foundations for the behavioral reconstruction of past populations, models of diachronic changes in biocultural practices, and the understanding of biological and biocultural adaptation in humans (Agarwal, 2008; Ruff, 2008a; Pinhasi and Stock, 2011). Furthermore, many aspects of skeletal morphological variation within and among human populations are the product of individual ontogeny; adult skeletal properties and dimensions are largely shaped by factors encountered during growth and development (Cameron and Demerath, 2002; Ruff, 2003a; Pearson and Lieberman, 2004; Lewis, 2007).

A thorough understanding of the effects of mechanics and metabolism on human bone development, then, is fundamental to any osteological research on human skeletal remains. In adults, and especially in immature individuals (< 18 years of age), cortical bone reacts to the influence of mechanical and metabolic factors at both macroscopic and microscopic scales by altering its mass (i.e., quantity) and shape (i.e., distribution) (Turner, 2002; Bass et al., 2005). These alterations, in turn, influence bone strength by changing how forces encountered during physical activity (i.e., mechanical loading) are distributed within the bone (Martin et al., 1998; Currey, 2003).

Of the multiple components that comprise mechanical and metabolic factors, it is well documented that interaction effects between mechanical loading and metabolic stress (i.e., insufficient metabolism, poor health status) may significantly influence bone morphology (Ruff,

2006; Specker and Vukovich, 2007; Vicente-Rodriguez et al., 2008). However, until quite recently very few studies have attempted to examine this interaction in humans (Pearson and Lieberman, 2004; Ruff et al., 2006). Most researchers have examined these two environmental factors in isolation (Rauch and Schönau, 2001; Cohen and Crane-Kramer, 2007; Pinhasi and Stock, 2011). Even if it is not the explicit intention of these studies, such separation in the analyses of mechanical loading and metabolic stress effectively models these factors as independent actors in shaping bone morphology.

Interaction effects between the two factors may actually confound the accurate interpretation of each factor's influence (Kimmel, 1993; Frost and Schönau, 2000; Jee, 2000). Because the nature of this interaction is unknown, researchers have difficulty with interpretations of observed cross-sectional geometry or histomorphological bone properties that do not match *a priori* expectations for a human skeletal sample (e.g., Ruff and Larsen, 2001; Mays et al., 2009). Take, for example, a case where archaeological evidence suggests that a population is expected to exhibit greater bone strength due to increased activity over time. A researcher who, instead, documents a change in cross-sectional properties that indicates decreasing bone mass and strength would either interpret this pattern as reflecting an unexpected decline in activity or a decline in health status that has tempered an increase in activity. Interpretation will depend on whether the researcher believes the *a priori* assumptions are valid, creating a tautology. Additional research would be required to investigate whether changes also occurred in factors affecting metabolic stress, and if the decreases that occurred in cortical microscopic and macroscopic structure due to metabolic shifts interacted with the effects of mechanical loading. Thus, understanding the nature of the interaction of mechanical loading and metabolic stress has important implications for interpreting behavioral activity from skeletal samples.

This study evaluates mechanical and metabolic influences on cortical bone development through the analysis of cross-sectional properties and histomorphometry in an archaeological sample of immature humans. The study has been designed to examine the potential interaction of these influences through four objectives:

1) **Use of a developmental approach**. A developmental approach is taken through the use of an immature skeletal sample, as the effects of mechanical loading and metabolic stress are argued to be greatest during growth (Wang and Seeman, 2008). An archaeological sample is chosen to address the significance of a potential interaction on behavioral interpretations from cemetery samples (see Chapter 4 for a full discussion).

2) **Analysis of bone properties at multiple scales**. The study sets out to quantify bone mass at both macroscopic and microscopic scales in the same sample using cross-sectional properties and histomorphometry, respectively. This technique provides a more complete picture of overall effects of environmental influences on cortical bone structure.

3) **Comparison of bone properties across multiple skeletal elements**. Measurements of both cross-sectional properties and histomorphology are examined in three skeletal elements (i.e., ribs, humeri, femora) that are known to experience different levels of mechanical loading. Hypotheses regarding effects of physical activity on cortical structure are tested based on these loading differences.

4) **Comparison of bone properties between individuals of differing metabolic status**. Differences in bone properties are compared between individuals possessing one or more skeletal stress lesions and individuals without stress lesions. Comparisons between these groups test hypotheses concerning metabolic stress effects on cortical bone properties. Due to sampling bias in cemetery samples, interpretation of morphological differences between these two stress groups requires careful consideration. Skeletal remains with stress lesions represent chronic metabolic stress (individuals who recovered from one or several stress events and succumbed to death following a final stress event), whereas skeletal remains without stress lesions represent *either* acute stress (morbidity prior to skeletal response to a stress event) or death by non-metabolic causes (e.g., accidental death). It is not possible to distinguish between the two latter scenarios in archaeological samples (see Chapter 4 for full discussion).

The analysis of cortical structure at both scales provides benefits over the use of a single scale, as both macroscopic and microscopic bone mass contribute to bone strength (Seeman and Delmas, 2006), and the relative influence of mechanics and metabolism may vary depending on the scale of analysis (Davison et al., 2006). The estimation of cross-sectional geometric properties assumes that microscopic structure is homogenous within the section, yet recent evidence suggests that alterations in microarchitecture can have a disproportionately large impact on overall bone strength (Seeman, 2003; Dong and Guo, 2004; Burghardt et al., 2010). Though cortical bone may be capable of adapting to metabolic stress by maintaining bone strength despite changes in bone mass on the macroscopic level, bone loss at the microscopic level

resulting from metabolic causes may or may not be similarly mitigated (see Chapters 2 and 3 for a full explanation). This study is the first systematic attempt to investigate such an interaction at both scales in a subadult human sample.

As emphasized above, this research utilizes a developmental approach to ascertain potential mechanical and metabolic interactions. After skeletal maturity, bone is less responsive to environmental effects; a majority of adult cortical bone morphology (especially bone mass) reflects factors that affect cortical structure during development, rather than the influence of factors encountered during adulthood (Forwood and Burr, 1993; Kontulainen et al., 2001; Lieberman et al., 2001, 2003; Turner et al., 2003; Lewis, 2007; Rizzoli et al., 2010). This developmental perspective, then, is more sensitive to variations in skeletal properties that result from activity and metabolic differences among individuals and will assist in achieving a more comprehensive understanding of human behavioral variation.

This research tests specific hypotheses relating to the association of metrics indicative of skeletal mechanics and metabolism, both within and among individuals. The differential effects of mechanical loading and metabolic stress on the skeleton present an opportunity for the possible disentanglement of their effects, as well as developing an understanding of their mutual interactions. Mechanical loading increases bone mass and distribution *locally* (within the bone being loaded), while metabolic stress decreases bone mass *systemically* (across the skeleton) (Raisz, 1999; Ruff, 1999, 2006). Therefore, the relative influence of these factors should vary across individuals (with different health statuses and activity levels) and within individuals (across skeletal elements under dissimilar mechanical demands). Thus, the comparisons made among and within individuals in this study test whether differences in cortical bone structure follow expectations given these differential effects.

Research Questions and Hypotheses

Three central questions are posed in this dissertation: 1) How does the interaction between mechanical loading and metabolic stress influence macroscopic and microscopic cortical bone structure? 2) Does this interaction affect bone strength within and across individuals? 3) Does the interaction potentially restrict interpretations of physical activity and health status from skeletal samples? The subsequent hypotheses and background chapters are centered on these research questions, with the background chapters providing the justifications for the hypotheses.

The first set of hypotheses assessed in this study addresses the relationship between chronic metabolic stress (as inferred from skeletal stress lesions; defined in Chapter 3) and systemic bone loss. It is important to establish this relationship prior to addressing the main research question, as it is an essential research component that skeletal morphology reflects differences in the amounts of metabolic stress encountered by individuals. It is generally assumed that systemic bone loss occurs with chronic metabolic stress (Brickley and Ives, 2008), though local mechanical and hormonal factors are likely to mitigate this effect (Raisz, 1999, 2005). However, the distribution of bone loss with metabolic stress has not been thoroughly investigated in humans. With these issues in mind, two related hypotheses are examined:

1a. Individuals with skeletal stress lesions exhibit systemic macroscopic bone loss—indicated by reduced cortical area in all three skeletal elements—relative to individuals without lesions.

1b. Individuals with skeletal stress lesions have systemic microscopic bone loss—indicated by increased resorption, increased remodeling, and/or disrupted bone replacement during remodeling in all three skeletal elements—relative to individuals without lesions.

The second set of hypotheses addresses the interaction between mechanical loading and metabolic stress. As mechanical loading demands increase across the three different skeletal elements assessed in this study (ribs, then humeri, then femora), it is hypothesized that systemic reductions in bone mass due to metabolic stress are increasingly attenuated among these three elements in order to maintain proper bone strength. Therefore, this study anticipates that skeletal elements that experience the greatest mechanical loads (i.e., femora) demonstrate minimal reductions in bone mass and strength due to metabolic stress, while those under the smallest mechanical loads (i.e., ribs) show significant reductions. Humeri have intermediate levels of mechanical loading relative to femora and ribs, and so are expected to exhibit intermediate reductions in mass and strength.

2a. In individuals with skeletal lesions, periosteal bone deposition compensates for macroscopic bone loss that occurs endosteally, causing augmentations to cross-sectional properties that maintain bone strength. Mechanical compensation for macroscopic bone loss increases as loading increases (i.e., femora demonstrate the greatest compensation, ribs show little to no compensation, and humeri are intermediate). This pattern will not be present in individuals without lesions.

2b. Microscopic bone loss due to chronic metabolic stress will decrease relative to the increasing mechanical demands placed on an element (i.e., rib elements possess the most loss, femora the least loss, and humeri are intermediate).

2c. Microscopic bone loss indicative of chronic metabolic stress is located only in macroscopic regions of long bone cross-sections where reductions to bone strength would be minimized (i.e., along axes of minimum bending rigidity, I_{min}). This pattern should be more apparent in the femora relative to the humeri.

Support for the second set of hypotheses would suggest that researchers should infer physical activity from elements under the strongest mechanical demands and metabolic stress from those under the least mechanical influence. That is, local mechanical loading demands will attenuate the effects of cortical bone reductions that are the result of metabolic stress. On the other hand, rejection of the second set of hypotheses and support for the first set of hypotheses would indicate that metabolic stress has a significant effect on bone mass and strength regardless of the amount of mechanical loading. Additionally, if neither set of hypotheses is supported, the study's results would argue that loading activity has a strong influence on cortical bone structure regardless of the presence of metabolic stress. Therefore, if either of the latter two scenarios is upheld, the way in which human behavior is inferred from skeletal remains may require reevaluation to account for strong interaction effects between mechanical loading and metabolic stress.

CHAPTER 2: BONE FUNCTIONAL ADAPTATION AND MECHANICAL LOADING

Those who seek to study skeletal response to load find a literature replete with confusing and often contradictory experimental evidence.

- *Bertram and Swartz (1991)*

Bone is influenced over the course of an individual's lifetime by the mechanical forces to which it is exposed. This fundamental principle has been supported by extensive experimental and theoretical research and forms the basis for understanding behavioral variation in the archaeological record. This chapter reviews theoretical models of the functional adaptation of bone to activity and loading, and explores the extensive research about mechanical influences on human cortical bone. While both cortical bone and trabecular bone morphology are regulated by mechanical inputs, these background chapters focus on mechanical responses in cortical bone, as this study uses skeletal remains from an archaeological context, in which trabecular architecture is infrequently well preserved.

The subsequent review considers macroscopic and microscopic implications for the results of previous studies separately. Specifically, the discussion of previous research focuses on the variation in loading patterns across the human skeletal elements employed in this study, mechanical effects on immature bone during growth, and application of bone adaptation principles to anthropological samples. All material in this chapter refers to biological processes and outcomes that would occur in healthy, non-metabolically stressed individuals. Particular effects of metabolic stress on cortical bone are presented in Chapter 3.

Mechanical Loading: An Introduction

Numerous experimental and observational studies have demonstrated that bone responds to changes in mechanical loading. During physical activity, mechanical forces (loads) are applied to bone externally by the environment (e.g., gravity, activity, etc.) and internally by the action of muscles (Frost, 1990; Turner, 1998). The stresses (forces per unit area) applied to bone by these loads, produce deformations, or strains (changes in length per unit length), within the bone. The location of bone deformation depends on the type of stress (i.e., axial compression, tension, bending, twisting, and/or shear) (Currey, 1984; Martin et al., 1998; Carter and Beaupré, 2001). The stress of increased activity level enhances the strain incurred by bone, necessitating a compensatory change in bone volume and/or shape to maintain enough strength to prevent fracture. Likewise, decreased activity lowers strain levels, and in turn decreases the amount of bone necessary to meet strength demands; bone is removed to minimize the costs associated with the maintenance of extraneous tissue (Currey, 2002).

To maintain an "equilibrium" or "customary" strain level within the bone, bone structure must adapt to changes in strains at both the macroscopic and microscopic level (Lanyon, 1982; Carter, 1984; Frost, 1987; Turner, 1998). A "customary" strain level is maintained under a changing mechanical environment when macroscopic mass (size), macroscopic shape (distribution), and/or microstructure (e.g., osteon density or porosity) are modified, adjusting the distribution of strains within the bone (Martin and Burr, 1989; Currey, 2002). All three approaches involve modification to bone structure, but not the material properties of bone tissue itself. Changes in the collagen and mineral content of bone tissue occur throughout life, which *does* affect material properties and therefore mechanical properties of cortical bone (Evans, 1973; Pidaparti and Burr, 1992; Burr, 2002), but these are typically associated with senescence

(i.e., biological aging) and disease processes. Bone material properties vary little within and among healthy, active individuals within the same species (Cowin, 2001; Erickson et al., 2002; Currey, 2003; cf. Schwartz-Dabney and Dechow, 2003; Wang et al., 2010). The adaptive process of bone structural modification involves a self-regulating feedback mechanism, resulting in bone tissue being remodeled (i.e., removed and deposited; see "Processes of Bone Functional Adaptation" below on page 17) continuously over an individual's lifetime to preserve biomechanical competence and adapt to changes in loading behavior. This hypothesized feedback mechanism is the basic foundation for specific models of bone functional adaptation, as outlined below.

The term "bone functional adaptation" encompasses the full spectrum of specific theoretical models for *how* bone adapts to mechanical forces. It has been recently proposed as an appropriate term to describe the process of bone response to mechanical loading, and is a general application of concepts previously associated with "Wolff's Law" (Pearson and Lieberman, 2004; Ruff et al., 2006). Until the last decade, the term "Wolff's Law" was often used to refer to the general concept that bone morphology reflects its current and past loading history by adapting to its biomechanical environment. However, many have critiqued the use of this term, because its original meaning has since been discredited (Bertram and Swartz, 1991; Martin et al., 1998; Cowin, 2001; Pearson and Lieberman, 2004; Ruff et al., 2006). Wolff (1892) originally sought to delineate the mathematical principles by which the trabecular bone structure of long bone epiphyses adapts to alterations in the mechanical environment. Because "Wolff's Law," *sensu stricto*, does not adequately explain the principle of bone adaptation to mechanical forces in general, some authors propose avoidance of the term entirely (Martin et al., 1998; Cowin, 2001; Pearson & Lieberman, 2004), a trend that is reflected herein.

Models of Bone Functional Adaptation

Frost's Mechanostat Model

One of the first and most well-known models of bone adaptation was Frost's mechanostat model (Figure 1), which introduced the hypothesis that bone remodeling is regulated by a homeostatic, negative feedback loop that Frost likened to a thermostat (Frost, 1964, 1987, 1990a, 1990b, 2003). Under this model, mechanical strains induce alterations to bone strength only when they surpass a particular strain threshold. When strains are maintained within the customary strain window, no bone response occurs. However, strains that surpass the upper limit of this customary strain window stimulate bone deposition, which in turn decreases the strain incurred by the bone and thus returns it to mechanical equilibrium as a result of the shifted bone morphology. Conversely, a reduction in strain level below the lower limit of the customary window promotes bone resorption and a return to customary strain levels. The mechanostat model is one of the only equilibrium models to incorporate hypotheses for both macroscopic and microscopic responses to mechanical stimuli and is, therefore, useful for constructing hypotheses tested in this research study. Epigenetic regulatory models (Turner, 1992), while useful for models of woven bone formation and maintenance, are less appropriate for understanding the regulation of cortical bone and so are not considered further here.

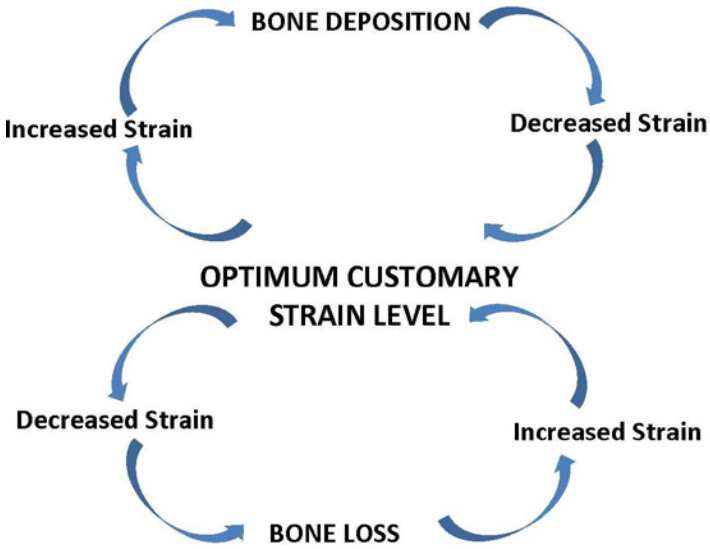

Figure 1. Diagram of Frost's mechanostat model of bone mechanical adaptation (adapted from Lanyon, 1982).

Turner's Mechanotransduction Model

Building on Frost's mechanostat model, Turner (1998) introduced refinements that assisted in understanding local responses in bone to loading at the cellular level. In his model, mechanical responses are facilitated by mechanotransduction, wherein osteocytes sense mechanical loads and transmit biological signals to activate or inhibit osteoblasts and/or osteoclasts (Jones et al., 1995; Henderson and Carter, 2002; Klein-Nulend et al., 2013). This process regulates structural changes at the tissue level, which may or may not accumulate to form macroscopic structural shifts (Rauch and Schönau, 2001).

In the mechanotransduction model, Turner provided three specific rules governing bone regulation. These rules have been crucial in the development of subsequent research into bone mechanical properties, and inform part of the basis for this study. The first rule states that bone

responds to dynamic rather than static loads. In addition to the magnitude of loading (i.e., static load), loading frequency and strain rate are significant determinants of bone remodeling response (Lanyon and Rubin, 1984; Rubin and Lanyon, 1984; Turner et al., 1994; Forwood and Turner, 1995; Turner et al., 1995). Experimental studies on rats have shown that increases in bone mass and strength require loading frequencies at or above a threshold of 0.5 Hz (Turner et al., 1994).

Second, only short durations of loading are required to stimulate an osteological response; extending the period of loading has diminishing returns in terms of bone formation. As loading duration increases, bone response diminishes, and bone cells become desensitized to mechanical forces (Rubin and Lanyon, 1984; Turner et al., 1994). Mechanosensitivity is reduced by 95% after only 20 loading cycles (Robling et al., 2001; 2006). After cessation of loading, bone cells will become "resensitized" to further mechanical stimulation; however, the time required for resensitization depends on the nature of the loading stimulus—its magnitude, frequency, and duration. Therefore, the loading conditions most conducive to osteogenic response are short bouts at frequencies above the customary strain level and punctuated by short periods of recovery (Srinivasan et al., 2002).

Last, osteocytes become less responsive to mechanical loads associated with a routine loading regime. Thus, structural changes are brought about not through continued cycles of normal loading but under abnormal strains. In some respects, an osteocyte can be said to acquire a memory of its past loading environment, which in turn allows the cell to recognize and adjust to new mechanical environments. Cellular accommodation, by way of cytoskeletal restructuring and/or genetic expression, appears to occur in response to a habitual loading stimulus (Robling et al., 2000; Burr et al., 2002). Changes in the strain environment will induce alterations to

cytoskeletal organization and intercellular protein expression and, thus, alter the mechanosensitivity of the cell (Rubin et al., 2002).

Carter and Beaupré's Mechanobiology Model

Using Frost's and Turner's feedback loop models as a foundation, Carter and Beaupré (2001) proposed a more complex bone adaptation hypothesis that, unlike previous models, incorporated the influence of developmental factors (Figure 2). According to their mechanobiology model, bone growth can be deconstructed into two components: a biological component and a mechanobiological component. The biological component encompasses intrinsic growth processes regulated by genes, hormones, and factors such as metabolic status. The mechanobiological component, however, represents the bone growth (i.e., modeling; see "Processes of Bone Functional Adaptation" below on page 17) that occurs to maintain an optimum strain level within the bone in response to encountered mechanical loads. These two components combine to affect bone morphology across ontogeny; with increasing age, the biological component becomes less influential and the mechanobiological component increases in importance (Carter and Beaupré, 2001). Simulation and empirical studies verify that the mechanobiology model predicts long bone geometric properties and bone acquisition during growth quite accurately (van der Meulen et al., 1993, 1995, 1996, 1997; Carter et al., 1996).

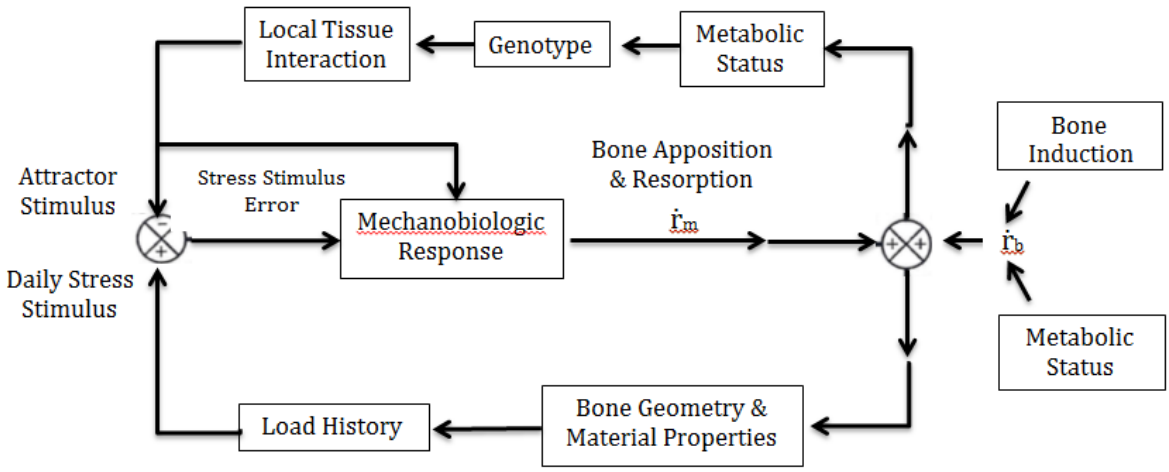

Figure 2. Diagram of the mechanobiology model of bone mechanical adaptation (adapted from Carter and Beaupré, 2001).

The greatest contribution the mechanobiology model has made to understanding bone functional adaptation is its appreciation of intrinsic factors that may affect the threshold (or "attractor stimulus") for osteological response. This aspect of the model makes it especially relevant to the current study's focus on the interaction between extrinsic mechanical influences and intrinsic metabolic factors. The attractor stimulus is a strain level locus surrounded by a "lazy zone," or region where changes in strain result in little to no net bone gain or loss. Only substantial changes in mechanical loading will result in strains beyond the lazy zone, causing bone deposition or resorption. The model allows for biological disturbances (e.g., metabolic status), factors not incorporated into either the mechanostat or mechanotransduction models, to influence bone deposition and resorption directly through the input parameter $\dot{r}_b$ (Figure 2). This input parameter is filtered through either the upper or lower feedback loop to affect the output parameter ($\dot{r}_m$)—mechanobiological loss or gain of bone through resorption or through apposition, respectively. Non-mechanical systemic factors (e.g., metabolic status, genetics, local

tissue interactions) may also affect net bone mass by indirectly altering the mechanical strain level locus itself (i.e., the upper feedback loop in Figure 2). The lower feedback loop contains variables that influence the daily stress stimulus experienced by the bone, such as bone geometric properties and loading history.

Processes of Bone Functional Adaptation

Bone responds to mechanical loading through two processes: modeling and remodeling. Cortical bone modeling involves *either* deposition or resorption at the periosteal or endosteal surfaces that occur *independently* of one another by the actions of osteoclasts and osteoblasts, respectively. Remodeling, in contrast, involves the coordination of both osteoblasts and osteoclasts to resorb and deposit bone *simultaneously*, removing older bone and replacing it with new bone matrix (Frost, 1990b). In short, modeling tends to alter the gross morphology—shape and size—of bone, while remodeling tends to maintain existing bone geometry as well as alters tissue-level structure.

Biomechanical loading during growth induces modeling to maintain bone strength as the bone grows in size (Enlow, 1963; Frost, 1988; 1990a), sculpting the bone according to its genetic plan through mechanical stimulation (Wong and Carter, 1990; Henderson and Carter, 2002). Modeling is most active during infancy and slowly subsides after skeletal maturity, at which time remodeling activity becomes more predominant (Frost 1964a, 1990a). Specifically, with respect to long bone diaphyses, modeling functions mostly to increase bone strength throughout ontogeny by depositing bone periosteally while removing it endosteally as the bone grows proximodistally (Rubin and Lanyon, 1984a, 1984b; Biewener et al., 1986; Bass et al., 1998; Ruff et al., 1994; Lieberman and Pearson, 2001). The opposite is true of the metaphyseal portions of

the growing long bone, where expansion of the periosteal collar involves removal of the periosteum and deposition at the endosteum to preserve its morphological function (Enlow, 1963). A similar process occurs in ribs to accommodate expansion of the thorax during growth; however rib cortices tend to drift cutaneously as bone is resorbed periosteally from the pleural side and endosteally from the cutaneous side, while bone is simultaneously deposited periosteally on the cutaneous side and endosteally on the pleural side (Epker and Frost, 1966; Landeros and Frost, 1964; Streeter, 2005).

Remodeling occurs throughout the lifecycle, turning over small packets of bone at a time and eventually culminating in the replacement of the entire adult skeleton every seven to ten years. This is achieved through groups of cells called basic multicellular units (BMUs), which are composed of roughly 10 osteoclasts, hundreds of osteoblasts, and their associated blood vessels and nerves (Frost, 1963; Sims and Gooi, 2008). Bone remodeling is surface dependent; BMUs can be generated at any bone surface that is lined with osteogenic connective tissue (i.e., trabecular, periosteal, endosteal, intracortical, and Haversian canals) (Hattner et al., 1965).

Changes in cortical bone microstructure occur through intracortical remodeling, the process by which secondary osteons (i.e., Haversian systems) are created. Secondary osteons form when BMUs tunnel through cortical bone and replace old, damaged tissue. These structures are called *secondary* osteons because they develop after the affected tissue has ossified and require the resorption of preexisting bone tissue prior to formation. Primary osteons, on the other hand, develop without resorption as the spaces within woven bone are filled by concentric lamellae (Hall, 1965).

A brief overview of the intracortical remodeling process is presented here in support of the rationale behind the research hypotheses on microscopic adaptations to mechanics and

metabolism. Each BMU undergoes three lifecycle stages: activation, resorption, and formation (Frost 1964b, 1969). The first step in remodeling occurs with activation of osteoclast formation through the fusion of monocytes, a process that takes about three days to complete (Martin et al., 1998). These newly formed osteoclasts begin to resorb bone at a rate of about 40 μm per day, tunneling through the bone cortex (Frost, 1964b). This osteoclast activity forms a resorptive space in cross section, an empty space within the cortical layer delineated by a rugged outline. Eventually, the osteoclasts experience apoptosis, which signals the initiation of osteoblast formation from precursor cells especially found in the medullary cavity. In a BMU tunnel, the reversal from osteoclastic to osteoblastic activity creates an empty space between the resorptive and formative regions along the tunnel's length. This space represents the lag time between resorption and formation, caused by the differential activity rates of both cell types; an osteoblast can secrete one micrometer of bone per day, while an osteoclast resorbs tens of micrometers of bone per day. This reversal line coincides with the future cement line of the secondary osteon, a hypermineralized line delineating the border between the bone cortex and the newly created Haversian system (Frost, 1969).

After proliferating and lining the resorptive cavity, osteoblasts deposit concentric layers of osteoid (unmineralized bone matrix) onto this reversal line, slowly reducing the size of the remodeling space. After each layer (or osteonal lamella) is deposited, it will begin to mineralize with the older lamellae on the periphery mineralizing first. Mineralization occurs through the deposition of mineral crystals within and between collagen fibers of the organic bone matrix (Frost, 1963). About 75% of osteon mineralization occurs in the first few days after formation; the remaining portion occurs slowly over the next year or so (Ortner, 2003; Fuchs et al., 2008). Once the BMU is isolated within the bone's cortex, a constant vascular supply is needed to

provide nutrients to the working cells, including the osteoblasts that are enclosed in the developing matrix; these embedded osteoblasts become osteocytes. Thus, at the center of each osteon is a Haversian canal that contains blood vessels for nutrient supply within the bone tissue (Martin and Burr, 1989; Martin et al., 1998).

There are two purposes for intracortical remodeling, which in turn affect the interpretation of mechanics and metabolism from cortical bone. “Targeted” remodeling is a mechanical adaptation to loading that replaces old, damaged bone tissue (Burr, 2002; Parfitt; 2002; Martin; 2007). This form of remodeling is the subject of both Frost’s and Turner’s models. In contrast, “stochastic” (also termed “non-targeted”) remodeling is hypothesized to be a normal part of mineral homeostasis, which theoretically occurs in random locations with respect to loading to maintain levels of essential nutrients in the bloodstream (Martin and Burr, 1982; Burr, 2002; Martin, 2004).

As bone tissue ages, microscopic damage in the form of microstress fractures occurs through mechanical usage, and without intervention, would eventually accumulate to form larger fractures. The purposes of targeted remodeling are not entirely understood. However it has been proposed that secondary osteons maintain bone strength through various methods: their formation replaces fatigue-damaged tissue (Carter, 1984; Frost, 1987); their shape—especially the cement line—prevents microcrack propagation (Frost, 1960; Schaffler et al., 1995); or, perhaps, their presence and concentration prevents microdamage by anticipating potentially weakened areas (Parfitt, 2002). In any of these scenarios no *ultimate* changes to mass occur because equal amounts of bone tissue are removed and replaced; although remodeling *temporarily* reduces microscopic bone mass, as resorption of damaged tissue increases porosity and newly-formed, unmineralized bone is less dense than completely mineralized bone tissue

(Carter and Hayes, 1977; Boivin et al., 2000). Targeted remodeling produces higher osteon counts in areas of the cross-section that experience the greatest loading stresses (e.g., I_{max}, periosteal surface) (Lieberman et al., 2003; Drapeau and Streeter, 2006). Remodeling also increases in cases of disuse, when the strain stimulus drops below a particular threshold (Martin, 2000), though significant periods of unloading are required to initiate such a response (Frost, 1997; Skerry, 2008).

The processes of stochastic remodeling are less well understood. As discussed in Chapter 3, bone acts as a reservoir for minerals, especially calcium, and so remodeling is the mechanism by which these elements are released for use elsewhere in the body. Even though the specific factors that initiate this homeostatic process are complex, and the reasons for some bone regions being resorbed rather than others is not resolved, the existence of this apparently stochastic replacement of bone alone speaks to the complexity of environmental inputs and pathways associated with BMU initiation. The sensitivity of BMUs to both mechanically driven and homeostatic cellular processes suggests that bone is able to prioritize different needs in order to maintain mechanical competency (Parfitt, 2002). Both types of remodeling—targeted and stochastic—occur simultaneously within cortical bone, and would theoretically vary in their relative frequencies depending on the region and its strain stimulus. The relationship between these kinds of remodeling is further discussed in Chapter 3.

Loading Variation Within the Skeleton

As discussed above, mechanical loading has a localized influence on bone through mechanotransduced osteocytic regulation of osteoblasts and osteoclasts, which are activated for targeted remodeling. Loading effects, therefore, are generated within the particular mechanically

active skeletal element, and vary both across and within skeletal elements with distinct habitual loading patterns (Lieberman et al., 2001, 2003; Rauch and Schönau, 2001; Peck and Stout, 2007). Thus, morphological adaptations to mechanical loading are greatest in bones that experience the highest loads and decrease with lower dynamic loading activity (Turner et al., 2002). From this context, the following sections describe the relative influence of mechanics on cortical bone in the three skeletal elements of interest to this study: ribs, femora, and humeri.

Ribs

The rib cage experiences lower strains relative to long bone elements, mainly through muscular action during respiration (Stein and Granik, 1974). Rib elements are not directly involved in locomotor behavior or manipulative tasks, though they would hypothetically be under higher loads during increased physical activity and the subsequent rise in respiration rate. However, Tommerup et al. (1993) found no effect on rib morphology with increased breathing rate during exercise in sows, demonstrating that loading has a primarily limited, localized effect on bone rather than a systemic one. For this reason, ribs are often examined for health status in skeletal samples. This is because they are thought to be more representative of hormonal influences and metabolic stress (Sedlin, 1964; Ott et al., 1999; Vajda et al., 1999), without the confounding influence of mechanical loading, to which they are less responsive than long bones (Raab et al., 1991; Tommerup et al., 1993).

This does not imply that ribs fail to adapt functionally to the mechanical loads placed on them. Several experimental studies utilizing three-point bending and tensile loading have tested the mechanical material properties and cortical geometry of ribs and noted adaptations to strain level variations within the rib cage (Granik and Stein, 1973; Schultz et al., 1974; Stein and

Granik, 1976; Yoganandan and Pintar, 1998; Stitzel et al., 2003; Cormier et al., 2005; Kemper et al., 2005; 2007). This variation is not driven by differences in bone material properties, which vary little within and among ribs; rather, cross-sectional geometric properties vary significantly by location in the rib cage (Kemper et al., 2005).

Additionally, compared to long bones, rib elements contain high amounts of medullary tissue, undergo significant modeling and remodeling as the thorax expands during growth, and therefore have a younger effective tissue age (Robling and Stout, 1999; Cho and Stout, 2001; Streeter, 2005). Because bone turnover is higher in ribs, they are expected to capture comparatively recent events in an individual's mechanical and metabolic history (Pfeiffer et al., 2006).

Femora

The human lower limb is under the strongest magnitude of loading because it is weight-bearing (supports body mass) and sustains bending and torsional loads during bipedal locomotion (Ruff, 2003a, 2003b). Evidence for the hominin lower limb being a highly functionally adapted structure comes from numerous analyses of diaphyseal robusticity (defined as bone strength relative to mechanically-relevant body size; Ruff et al., 1993). The lower limb has higher strength properties than the upper limb across many modern, adult human and fossil hominin samples (Ruff et al., 1984; Ruff and Larsen, 2001; Wescott, 2001; Shackelford, 2007; Ruff, 2008b, 2009). Femoral strength properties are strongly associated with variation in mobility patterns (Ruff, 1987, 1999; Ruff et al., 1993; Trinkaus and Ruff, 1999; Ruff and Larsen, 2001; Wescott, 2006; Stock, 2006). Mechanically, within individuals, there is a correlation between femoral shape and bending loads about the hip (Ruff, 1987, 1995). Histomorphometric

studies have also found higher rates of remodeling in femora relative to other bones (Kerley, 1965; Evans and Bang, 1967; Robling and Stout, 2000; Tersigni, 2005). Additional consideration of both geometric properties and histological properties of the femur is presented later in this chapter.

Humeri

Loading in the adult human upper limb is intermediate relative to the rib cage and lower limb, because it is generally not habitually used in locomotion but is loaded during manipulative tasks (Sumner and Andriacchi, 1996; Ruff, 2003a, 2003b). Without locomotor constraints, the human humerus exhibits directional asymmetry in diaphyseal size and robusticity, which likely corresponds with lateralized behaviors across a wide range of human populations (Auerbach and Ruff, 2006). Although the humerus has lower values for properties associated with bone strength, as mentioned above, observations of marked humeral asymmetry in tennis and racquetball players (Jones et al., 2001; Kontulainen et al., 2002; Bass et al., 2002) further demonstrates that the upper limb may be subject to high mechanical loads, and that the upper limb has less mechanical constraint than the lower limb.

The unique functional role of the humerus in humans is also demonstrated during the transition from crawling to walking in toddlers. Prior to bipedal walking, infant lower and upper limb strength proportions more closely mimic those of quadrupedal animals; however, after walking commences, humeral strength proportions slowly decline, while femoral strength rises (Ruff, 2003a, 2003b; Cowgill, 2010). In fact, due to lowered mechanical stress and intracortical remodeling rates in humeri relative to femora, use of upper limb elements in adult

histomorphological age estimation has been encouraged, as humeri appear to provide better age estimates than highly mechanically-stressed elements (Tersigni, 2005; Robling and Stout, 2008).

Mechanical Influences on Immature Bone

Regardless of which skeletal element is examined, research has shown that the bone of immature individuals is more responsive to environmental factors and perturbations, including mechanical loading, than adult bone (Bertram and Schwartz, 1991; Forwood and Burr, 1993; Lieberman et al., 2001, 2003; Turner et al., 2003). After skeletal maturity, it becomes increasingly difficult to increase bone strength (Kontulainen et al., 1999, 2001), because adult osteogenic response is lowered relative to immature individuals (Kotev-Emeth et al., 2000; Lieberman et al., 2003; Guadalupe-Grau et al., 2009). This is especially true in older adults in which alterations in hormone levels (e.g., estrogen and testosterone), as well as the senescence of osteoblasts and osteoprogenitor cells, disrupt the balance between bone resorption and formation, tipping the scales in favor of bone loss (Teitelbaum et al., 1996; Nishida et al., 1999). Thus, the maximization of peak bone mass early in development mitigates excessive bone loss caused by aging (i.e. osteoporosis) and other metabolic disturbances.

Numerous studies have demonstrated that adequate exercise is required for optimal skeletal development throughout childhood and adolescence (Bonjour et al., 1994; Goulding et al., 2000, 2001; Hernandez et al., 2003; Ward et al., 2007) and contributes significantly to maintenance of bone mass, and thus prevention of osteoporosis, into adulthood (Kannus et al., 1995; Puntila et al., 1997; Cooper et al., 2006; Rizzoli et al., 2010). In fact, studies suggest that the majority of bone mineral content of the adult skeleton is formed during childhood and early adolescence, the amount of which is modulated by activity levels (Bailey et al., 1999; Harel et

al., 2007). Consequently, inactivity (along with malnutrition; see Chapter 3) in children and adolescents is one of the most significant causes of adult osteoporosis and has become an increasingly alarming health concern within the past few decades. Because bone is considerably sensitive to intrinsic and extrinsic inputs during growth, much of adult cortical bone morphology reflects skeletal loading history and physical activities *prior* to and coinciding with early skeletal maturity (Haapasalo et al., 1998; Bass et al., 2002; Pearson and Lieberman, 2004; Shaw and Stock, 2009a, 2009b). Therefore, studies using archaeological subadult samples can provide optimal resolution of environmental influences on bone.

Physical Activity Among Immature Humans

Researchers have recognized for some time that immature bone is highly sensitive to mechanical inputs, and this directly impacts the interpretation of physical activity and behavior from skeletal samples. Only recently, though, has immature bone been the subject of biomechanical studies in anthropology (Pearson and Lieberman, 2004; Ruff et al., 2006). Historically, adult cortical bone has been examined to interpret loading behavior in human populations (e.g., Ruff, 2008a). Based on the knowledge of bone responses to loading during growth, there would arguably be tremendous benefit in turning attention toward the ontogeny of cortical morphology and its relationship with activity during growth.

Research that has begun to explore biomechanical effects on bone during ontogeny has shown strong relationships between immature bone morphology and loading behavior (Ruff, 2003a, 2003b; Cowgill and Hager, 2007; Ruff, 2007; Cowgill, 2010; Cowgill et al., 2010; Garofalo, 2012). Collectively, these studies provide new perspectives on variation in population activity, as well as new topics that the study of adult skeletons cannot address; for example,

research on subadult remains sheds light on the initiation of cultural participation in subsistence-related behaviors by children, as well as morphological development during the onset of bipedal walking (Cowgill, 2008; Cowgill, 2010; Garofalo, 2012).

The focus on adult bone in anthropology is due, in part, to a misconception of physical activity during growth: that subadults do not engage in typical adult behaviors. Ethnographic research, though, reveals that older children and adolescents frequently engage in activities similar to those of the adults in their population (Moberg, 1985; Bradley, 1993). In contrast to postindustrial urban societies, children as young as six years old contribute significantly to the work force in past and non-industrial societies (and industrial societies prior to laws restricting child labor), especially providing aid in subsistence-related tasks (Bradley, 1993; Bird and Bird, 2000; Kamp, 2001; Bird-David, 2005). Prior to the age of six, the activities typically require minimal strength and skill and, if labor-related, are more energetically costly in terms of yield than tasks performed by adults. It has been argued that insufficient brain development, coordination, and experience cause individuals under the age of six to be unable to contribute significantly to a cultural economy (Kaplan, 2000; Hewlitt and Lamb, 2005).

Between the ages of six and ten, labor activities become increasingly similar to the adult pattern, and after age ten they mimic the gender-specific tasks of same-sex adults (Bradley, 1984, 1993; Hill and Hurtado, 1996; Bock, 2005). Although subadults are less productive laborers in general, this deficiency is likely due to smaller body size and strength rather than a lack of knowledge and experience or inadequate intelligence (Bird and Bliege Bird, 2002, 2005; Blurton Jones and Marlow, 2002; Bock, 2005). Smaller body size and strength appears to affect such factors as walking speed and upper arm fatigue, especially increasing the energetic costs

associated with foraging and hunting (Blurton Jones and Marlow, 2002; Bock, 2005; Gurven et al., 2006).

Subadult activities can make a significant contribution to the subsistence economy of both hunter-gatherer and agricultural communities. Although subadults are oftentimes left with the tasks deemed tedious and unchallenging by adults (Bradley, 1993), their foraging behavior and agricultural labor leave traces in the archaeological record, though it is difficult to distinguish their activities from those of adults (Sofaer Derevenski, 1997; Bird and Bird, 2000; Kamp, 2001). Given this lack of discernable activity patterns in archaeological contexts, ethnographic studies have been essential in ascertaining the influence of immature subsistence activities on cultural economy. In foraging societies, subadults hunt small, easily captured game (e.g., lizards, birds) and collect food items low to the ground (e.g., eggs, shellfish, nuts, tubers) (de Boer et al., 2000; Bird and Bliege Bird, 2000, 2002, 2005; Tucker and Young, 2005). These resources tend to provide a significant portion of their daily caloric intake and, in some cases, fulfill their nutritional needs entirely (Bird and Bliege Bird, 2005; Hawkes et al., 1995). While foraging, individuals over the age of six are more likely to travel large distances away from the home base in search of food resources (Hawkes et al., 1995), increasing the loads placed on their lower limbs during locomotion relative to their upper limbs. Approaching adolescence, foraging production in subadults increases beyond sustaining individual caloric needs and attains an important role in supplying the community resource base (Tucker and Young, 2005).

In agricultural societies, children and adolescents are considered an essential asset to economic success and form a more vital component of the work force than in foraging communities (Bradley, 1993; Moberg, 1985; Porter, 1996). The activities of subadults are more varied and include household chores, such as cleaning, cooking, fetching and carrying water, and

caring for smaller children. They also are expected to care for domesticated animals, engage in animal husbandry, and participate in the maintenance of crops (White, 1975; Pomeroy, 1987; Porter, 1996). In agricultural groups, high demands for labor place strong incentives on families to have many offspring to assist with daily tasks (Cain, 1977; Moberg, 1985; Ratha and Mahakud, 1988; Porter, 1996), and a strong correlation exists between the utilization of child labor and economic production (Nag et al., 1978). Compared to foraging societies, subadults in agricultural communities also generally perform more gender-specific duties that mirror those of adult males and females (Bradley, 1993; Porter, 1996; Sofaer Derevenski, 1997). For both females and males, the hours spent engaged in subsistence activities generally increase during adolescence, until the adult workload is achieved (White, 1975; Nag et al, 1978). For example, in Bangladesh, young children work on average five hours a day until they reach 13-15 years of age, at which time their workload is raised to the typical adult work commitment of 9 hours (Caine, 1977).

These studies underscore the need for further research on skeletal responses to mechanical stresses in subadults and a more complete understanding of cortical bone development. Behavioral analyses of skeletal samples would benefit from the inclusion of immature individuals wherever possible, as environmental factors will have the strongest influence on this portion of the population and produce lasting effects into adulthood. Understanding the impact of environmental effects on adult bone morphology in archaeological samples, therefore, necessitates examination of subadult skeletal remains, and is therefore the focus of this study. In light of the background provided, the remainder of this chapter reviews the specific methods applied to studying the macroscopic and microscopic properties of human bone, and the relevant findings of research that has used these approaches. Consideration is given

to applications of these methods to archaeological samples, particularly to immature skeletal remains.

Bone Mass, Balance, and Strength

Optimization theory is an essential concept in bone morphology studies (Currey, 1984, 2002, 2003; Lieberman et al., 2003). This theory proposes a trade-off between bone strength and bone mass. To be optimally adapted, bones must be able to resist external forces without fracturing but must also be light enough to be moved efficiently through muscular action. While adding bone mass will certainly reduce the risk of fracture by distributing forces over a wider area, increasing bone mass will eventually compromise the function of the element due to the high metabolic costs associated with its movement. Therefore, if the skeleton optimally balances these two competing functions, bone strength will be maximized while minimizing increases to bone mass. Optimization is especially important in the long bones of vertebrate limbs, where elements are specially adapted to locomotor behaviors (Currey, 1984, 2002, 2003).

Thus, retention of bone strength is closely related to the maintenance of bone mass within certain limits. In order to maintain bone strength, macroscopic and microscopic bone mass must often be conserved to resist typically encountered loads within the customary strain window (i.e., the lazy zone). Bone mass is maintained when resorption and formation are balanced (Seeman and Delmas, 2006). Negative bone balance occurs when resorption exceeds formation, causing reduced bone mass; positive bone balance results when the opposite conditions occur and bone mass increases (Frost, 1990a, 1990b; Parfitt, 2002; Grynpas, 2002). In healthy subadults and young adults, bone remodeling is a balanced process—old, damaged bone is replaced by an equal amount of new bone matrix. However, with increasing age, resorption begins to exceed

formation (Hattner et al., 1965; Martin and Seeman, 2008). Likewise, low levels of loading or cessation of loading altogether (e.g., spaceflight or extended bed rest) can cause quiescence in remodeling or asymmetric bone turnover (that is, more resorption) to restore customary strain levels (Baldwin et al., 1996). In this "disuse-mode" remodeling, more bone is resorbed than created, resulting in permanent bone loss in trabecular and cortical envelopes (Jee and Li, 1990; Li et al., 1990; Li and Jee, 1991). Similarly, metabolic bone diseases and other illnesses that interrupt bone balance also have drastic effects on bone strength by promoting negative bone balance (see Chapter 3). This relationship between bone mass and bone strength drives the hypotheses set forth in this project.

In light of optimization theory, bone may exhibit multiple solutions to changes in loading that add complexity to a simple model of bone mass conservation. With increases in loading stimulus, cortical bone strength can be maintained in three ways: 1) adding macroscopic bone mass (e.g., to the periosteal or endosteal surfaces), 2) redistributing macroscopic bone further away from the mechanical centroid (the neutral bending or torsional axis, often modeled as the center of a long bone cross-section), or 3) increasing osteonal remodeling to reduce the incidence of microcracks (Martin et al., 1998; Currey, 2003). The following section, *Macromorphology*, reviews these specific mechanical alterations in macroscopic cortical bone structure and their impact on interpretations of cortical morphology. Next, the *Micromorphology* section discusses mechanical adaptations in cortical bone microstructure. Each section begins with a description of morphological adaptations to loading followed by a summary of previous studies in living humans, as well as anthropological applications of these studies to human skeletal samples. These studies form the foundation upon which the current analysis is based.

Macromorphology

Basic Structure

Given the response of cortical bone to mechanical loading, a strong relationship ought to exist between loading patterns and cortical bone morphology. This assumed relationship forms the basis of all studies examining size and shape changes in human long bone cross-sectional geometry with differences in loading both within and among individuals. By modeling long bone diaphyses as hollow, static beams, the resistance of a bone to different types of mechanical loads can be calculated using engineering Euler-Bernoulli beam theory (Huiskes, 1982; Ruff and Hayes, 1983). The area of bone within a cross-section (i.e., total area [TA] and cortical area [CA]) is proportional to its strength under axial compression and tension forces. Macroscopic modeling and remodeling to specific bone surfaces regulate the amount of bone within the cross-section. Cortical area is increased by adding bone to the periosteal surface, where the maximum strain occurs (as it is farthest from the neutral plane where strains equal zero), and /or reducing the rate of bone resorption at the endosteal surface (Lazenby, 1990b; Ruff et al., 1994).

However, long bones rarely undergo pure axial loads and most often experience some combination of compression and tension, which results in bending (Biewener, 1983; Rubin and Lanyon, 1982; Bertram and Biewener, 1988). The distribution of bone about the neutral axis, where strain levels are zero, is proportional to a bone's resistance to bending and torsional loads. Second moments of area (I_x, I_y, I_{max}, I_{min}) quantify bending rigidity about a particular bending axis. I_x and I_y estimate bending rigidity in the anteroposterior and mediolateral planes, respectively. The I_x axis is parallel to the mediolateral plane and estimates bending rigidity when the bone is bent in the anteroposterior plane. Likewise, the I_y axis estimates rigidity when the

bone is bent mediolaterally, and this axis falls in the anteroposterior plane. I_{max} and I_{min} represent the maximum and minimum bending rigidities within the diaphysis, and therefore, the location of these second moments of area will vary based on the shape of the cross-section. The location of maximum bending rigidity in relation to anatomical axes (I_x and I_y) is expressed as the angle between two axes (theta, θ). By summing two respective second moments of area (e.g., I_{max} and I_{min} or I_x and I_y), the bone's torsional strength (polar moment of area, J) is calculated (Ruff and Hayes, 1983). The polar moment of area is a good indicator of overall rigidity, as it is proportional to twice the average bending rigidity. To account for the fact that the maximum strains in bending and torsion occur on the periosteal surface, second moments of area are often divided by the distance between the centroid and the outermost surface. The resulting section moduli (i.e., Z_x, Z_y, Z_{max}, Z_{min}) represent bending strengths rather than rigidity in bending. The polar section modulus (Z_p) is the section modulus equivalent of the polar moment of J and is a good index of overall torsional strength (Ruff, 1995, 2002).

Some caveats should be noted about the use of beam theory as summarized. Given the vagaries of absolute material properties among bones, it is important to note that none of the cross-sectional properties calculated (I, J, or Z) are the *absolute* values for bone rigidity and strength, but they are considered to be *proportional* to these values. Though, when similar methods are applied across individuals, strength properties will be proportional to the actual values and comparisons will reflect morphological differences between individuals. In addition, experimental evaluation of strain gauge data shows that the neutral axis is not always located on the cross-sectional centroid, but rather shifts depending on the mechanical loading environment of the bone. This suggests that second moments of area and section moduli do not reflect true *in vivo* bone strength but are simply an imperfect approximation of strength (Lieberman et al.,

2004). Nevertheless, cross-sectional properties calculated on the centroid are well correlated with those calculated on the experimental neutral axis (Lieberman, 1997). Additionally, shifts in neutral axis location in dynamic loading cannot be accounted for in static models, and in cases where mechanical loading conditions are unknown, geometric properties are the best method for estimating bone strength (Ruff et al., 2006; Ruff, 2008b).

The properties outlined above vary not only with the amount of bone present, but with its distribution as well. A reduction in cortical area does not result in a reduction in strength and rigidity if the bone is distributed farther from the centroid of the cross-section, resulting in larger second moments of area and section moduli and distribution of loads over a wider area (Lazenby, 1990; Frost and Schönau, 2000). Periosteal deposition coupled with more modest endosteal resorption during growth allows for the development of wider, stronger diaphyses and is required to maintain adequate cross-sectional strength for increasing body mass and bone length (Figure 3; Ruff, 2003a, 2003b).

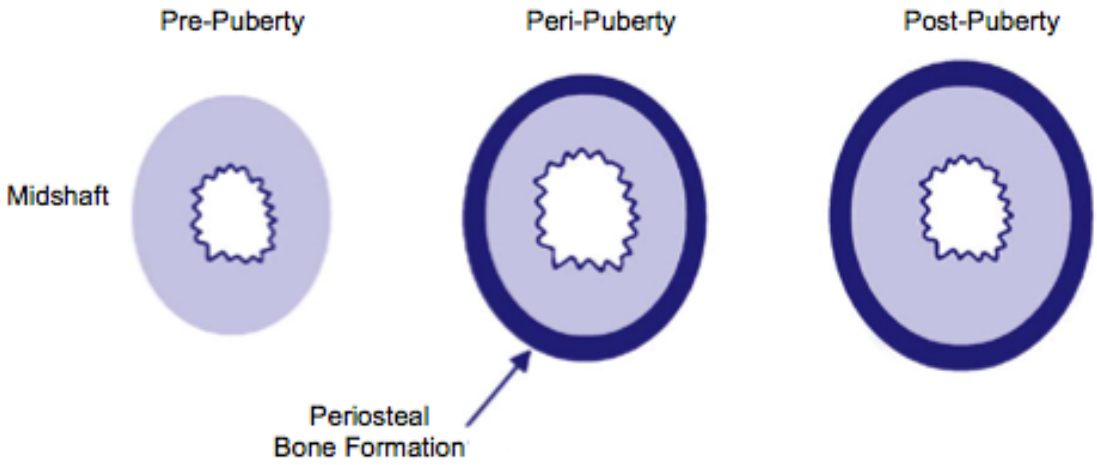

Figure 3. Diagram of periosteal deposition and endosteal resorption during growth. Note that with the onset of puberty, modeling increases periosteal bone first, followed (with sufficient dynamic loading) by some endosteal apposition by the end of puberty.

Endosteal resorption serves to remove bone from the area of the cross-section under the least strain, while periosteal deposition increases bone mass in the area of highest strain (Ruff et al., 1994). Periosteal deposition is an efficient means of adding bone mass in response to increased loads while minimizing bone weight, because a small volume of bone can be added periosteally and provide a considerable improvement in mechanical strength compared to endosteal deposition (Jones et al., 1977; Lazenby, 1990b; Bertram and Swartz, 1991; Ruff et al., 1994; Bass et al., 1998). Increased loads incurred by a bone, whether due to growth-induced alterations in body composition or increased physical activity, lead to intensified modeling rates. Under these conditions, resorption on the endosteal surface and deposition on the periosteal surface will increase relative to elements under less strain, though modest increases in endosteal bone may occur through mid-adolescence (Bass et al., 2002; Ruff et al., 2006). On the other hand, reduced loading strain stimulates bone resorption at the endosteal surface and the cessation of periosteal deposition (Lanyon and Rubin, 1984; Biewener and Bertram, 1994).

Therefore, the lack of correlation between bone mass and bone strength in long bone diaphyses is important to recognize when considering the effects of metabolic bone loss on macroscopic bone mass, which occurs preferentially at the endosteal surface (see Chapter 3). As loading demands increase among different skeletal elements, *low* macroscopic bone mass does not necessarily equate to *inadequate* bone mass for resisting loads. Therefore, analyses of the distribution of bone are more salient to the questions asked in this study than simple measurements of overall bone mass (i.e., total area and cortical area), or bone mineral content and density. However, research on bone mineral content and density has been important to establishing the effects of activity on bone in living subjects.

Clinical Studies

Bone Mineral Density. Clinical research on the effects of exercise in living humans has proven quite useful in understanding mechanical alterations in cortical bone mass. As reviewed below, numerous studies have documented increased bone mineral content (BMC) and bone mineral density (the amount of mineral per square centimeter of bone tissue) across multiple skeletal locations with increased physical activity in adults and subadults. These analyses typically examine locations in appendicular elements (e.g., femoral neck, distal radius) and/or axial elements (e.g., lumbar spine) that are not investigated in anthropological contexts. Although femoral and humeral diaphyseal midshafts are occasionally analyzed, rib elements are not a common location of interest in clinical settings. However, the general skeletal findings of these studies, especially those involving subadults, inform hypotheses set forth in Chapter 1 for long bone elements. The findings of this body of research are described here to establish patterns of mechanical adaptation in subadults, as well as advocate for more focused structural analyses of cortical bone in immature samples. In addition, the limitations in the application of the methods for examining both bone mineral content and density are reviewed in light of the goals of this study.

Bone mineral density (BMD) varies significantly with variation in quantity and quality of dynamic activity. High, frequent dynamic skeletal loading (i.e., “high impact” activities) in adults—such as encountered in volleyball, soccer, hockey, running, and weightlifting—is associated with significant BMD increases in loaded elements relative to non-athletic controls, regardless of the skeletal location (Heinrich et al., 1990; Karlsson et al., 1993; Taaffe et al., 1995; Alfredson et al., 1996, 1997, 1998; Pettersson et al., 1999). Conversely, low-impact and non-weight bearing exercise (e.g., swimming) has less effect on bone strength between athletes

and controls (Block et al., 1989; Heinonen et al., 1993). Increased activity level in adult non-athletes also results in increased BMD, although the response is modest in comparison to the differences between athletes and non-athletic controls (Menkes et al., 1993; Heinonen et al., 1996; Kerr et al., 1996; Nickols-Richardson et al., 2007). Cessation of exercise, as occurs with decreased athletic training and immobilization during bed rest, has been linked to considerably reduced bone mineral densities (Tilton et al., 1980; LeBlanc et al., 1990; Schneider et al, 1995; Valdimarsson et al., 2005).

While adult exercise studies have detected differences in bone mass in association with activity level, lowered adult osteogenic response suggests that not all of these differences can be explained by loading effects encountered after skeletal maturity. Exercise studies on children and adolescents have revealed comparable results to adult exercise studies, though osteogenic response is heightened and the effects of activity far exceed those of adult studies. McCulloch et al. (1992) compared BMC in the calcaneus and distal radius across adolescent competitive swimmers, soccer players, and controls. Results indicated that swimmers of both sexes had the lowest calcaneal BMC and soccer players had the highest, whereas no differences were present in the radius between activity groups. The authors concluded that extended periods of time spent in a weightless, buoyant environment would preferentially affect weight-bearing bones, supporting previous analyses of astronauts experiencing prolonged space flight (Smith and Gillian, 1987; LeBlanc et al., 2000).

Since McCulloch et al.'s publication, several additional studies have documented BMD differences ranging from 5% to 40% in immature individuals participating in high-impact sports (e.g., ballet, soccer, and gymnastics) compared to those engaged in low-impact activities (e.g., walking), low- or non-weight bearing exercise (e.g., cycling, swimming), and no athletic activity

(Young et al., 1994; Kannus et al., 1995; Dyson et al., 1997; Bass et al., 1998). In addition to exercise types, immature BMD also varies with overall activity level. For example, Meyer et al. (2011) detected an increase in total body, femoral neck, and total hip BMD in primary school children introduced to a 9-month physical activity intervention program. A three-year follow up on the oldest children showed that high BMD values were maintained into adolescence relative to controls, suggesting that physical activity encountered early in life may have long-term effects on bone density (Meyer et al., 2013).

Although BMD accounts for up to 40% of variation in bone strength and is a good predictor of fracture risk (Wachter et al., 2002), it is not a mechanical property and does not encapsulate the majority of variation in bone strength caused by differences in bone structure (Ruff et al., 2006). Recent studies have demonstrated that adjustments in mechanical properties sometimes occur without modifications to bone mineral density (Ashizawa et al., 1999; Haapasalo et al., 2000). For example, comparing dominant and non-dominant arms in adult tennis players, Ashizawa et al. (1999) found that the radii of dominant forearms exhibited significantly higher total areas and cortical areas, though BMD was actually lower in the dominant forearm.

Moreover, as noted, methods used for examining BMD do not account for the properties of interest in this study, namely cortical cross-sectional geometry and histological evidence of bone turnover or maintenance. The most widely used technology for calculating BMD, single-energy X-ray absorptiometry (SXA) and dual-energy X-ray absorptiometry (DXA), cannot adequately distinguish between trabecular and cortical bone, though recent techniques have improved this distinction (Zabeze et al., 2013). BMD itself is not a measure of true density, because it cannot distinguish between areas containing ossified tissues and those that do not

(Prentice et al., 1994), though it is a standard measurement by which differences in bone size can be compared across groups under the same methodological conditions and is strongly correlated with risk of fracture in adults (Stone et al., 2003) and subadults (Clark et al., 2002, 2008; Bianchi, 2007). However, only true bone density can assist with understanding more nuanced changes in bone strength with environmental and behavioral factors. New, alternative methods such as quantitative computed tomography (QCT) and peripheral quantitative computed tomography (pQCT) provide the ability to measure geometric properties as well as volumetric BMD rather than areal BMD. These alternative methods involve high doses of radiation and are more expensive, and therefore, less widely available (cf. Shaw and Stock, 2009a, 2009b).

Another complication is that the calculation of BMD (BMC ÷ bone area or bone width) assumes that BMC and bone area are linearly proportional—an increase in BMC is associated with the same percentage increase in bone area—though this relationship has not been verified. Therefore, assumptions of linearity can lead to spurious correlations among BMD and other variables (e.g., caloric intake, energy expenditure) simply due to their relationship with overall body size, and standardizations by body size measures (e.g., body mass index, BMI) are not likely to account completely for bone and body size differences (Prentice et al., 1994). For the reasons outlined above, researchers have called for more honed examinations of cortical bone morphology to determine the structural factors (including cross-sectional geometry, osteonal remodeling, and microscopic porosity) that determine overall bone strength (Seeman, 2003b; Daly, 2007). The present study, then, joins a broad literature in attempting to address this appeal.

Macroscopic Bone Structure. Clinical studies have been fundamental in establishing surface-specific modifications to the cortical structure of long bone diaphyses, and how they

differ in immature individuals compared to adults. These studies, moreover, establish macroscopic changes in bone in response to loading that BMD studies, as reviewed above, are unable to accurately reveal due to confounding factors. While some studies have shown increases in cross-sectional strength properties in concert with increases in BMD, most have focused instead on establishing the manner in which cortical bone is modified in relation to the age at which individuals engage in activities, the intensity of those activities, and how their effect on bone changes over time.

As explored in the previous subsection, studies of BMD have established a basic understanding about the relationship of activity levels and bone response. Yet, as established, augmented levels of BMD do not necessitate changes in macroscopic shape, or vice versa, and the relationship between the two is not often clear. Bass et al. (1998), for example, detected greater BMD in the lumbar spine and femoral midshaft of pre-pubertal female gymnasts relative to controls, which the authors inferred as being caused by changes at the endosteal rather than the periosteal surface, though this hypothesis could not be confirmed with BMD data alone. Other studies have found potential relationships between increased cortical area and greater BMD. Dyson et al. (1997) established that cross-sectional area in the distal radii of 7 to 11 year-old female gymnasts were 11% greater compared with controls, and argued that higher trabecular and cortical BMD in gymnasts indicated exercise-induced mass increases through either thicker trabeculae, endosteal deposition, and/or inhibited endosteal resorption. In contrast, cortical BMD at the radial midshaft in pre-pubertal male and female gymnasts was not different from controls in a different study, despite significantly greater total and cortical areas in the gymnasts (Ward et al., 2005). This emphasizes the potential incongruity of cortical bone macroscopic structural variation and bone mineral density.

Given this ambiguity, emphasis has been placed on the examination of cross-sectional geometry instead of BMD to understand the effects of activity on bone, especially ontogenetically. Heinonen et al. (2002), for instance, discovered increased cortical area in the radial diaphyses of adult female weightlifters relative to controls, a difference associated in other studies with increased BMD. Similarly, Daly and Bass (2006) found a significant correlation between time engaged in weight-bearing physical activity and femoral cross-sectional areas and polar moment of area. Studies like these in adult populations are helpful for understanding lifetime activity effects on bone structure; however, because bone is more responsive to activity in subadults, the relationship between loading and macroscopic structure are more strongly illustrated by growth studies.

A major finding of growth studies, which has already been noted in the discussion of cross-sectional properties, is that activity has a disproportionate effect on younger individuals, and these effects are retained into adulthood. In a longitudinal study of non-athletic boys and girls, highly active children maintained 5-10% greater femoral and radial bone mass in adolescence than children who had experienced lower activity levels before puberty (Slemenda et al., 1991, 1994). Tennis training during growth has been associated with increased adult total and medullary bone areas in the proximal humerus and radial midshaft (Haapasalo et al., 2000; Kontulainen et al., 2002). Similarly, Forwood et al. (2006) presented strong evidence for the beneficial effects of daily exercise during growth when they found that physical activity was a significant predictor of peak cross-sectional area and section modulus in the femoral neck into adulthood.

Researchers have also shown that cortical bone strength varies over the course of ontogeny with rates of growth and, thus, age and body size. In their 1996 paper, van der Meulen

et al.'s study on immature cross-sectional strength properties indicated a strong relationship between femoral midshaft diaphyseal strength properties and body mass throughout ontogeny, leading the authors to conclude that mechanical loading was the main determinant of long bone cross-sectional (i.e., appositional) growth. During development, long bone strength must continually meet mechanical demands as they fluctuate with changes in body mass, bone length (i.e., linear growth), and muscular strength, with bone strength typically lagging behind adjustments in these three factors (Rauch and Schönau, 2001; Ruff, 2003b; Cowgill et al., 2010). This relationship is clearly visible during the pubertal growth spurt, when rates of growth in bone length far exceed those in mass and strength, raising the risk of fracture to the highest levels that occur in subadults (Bailey et al., 1996; Bonjour and Rizzoli, 1996; Bass et al., 1999).

Furthermore, the osteogenic response of diaphyseal surfaces, and thus structural geometric changes, will also vary during ontogeny. The ratio of periosteal and endosteal border expansion is similar between the sexes up until puberty; as explained previously, bone is added periosteally and resorbed endosteally. During puberty, rising estrogen levels in females inhibits periosteal deposition while simultaneously stimulating endosteal deposition (Ruff et al., 1994; Seeman, 2001). This phenomenon has been confirmed in young female tennis players who demonstrate more activity-related periosteal deposition and resistance in bending prior to puberty, but endocortical deposition and minimal improvements to bending strength during and after puberty (Haapasalo et al., 1996; Bass et al., 2002). Except for this small window of time during puberty, bone deposition typically occurs at the periosteal surface in subadults and young adults, because a small volume of bone can be added periosteally and provide the same improvement in mechanical strength that would occur with considerable endosteal deposition (Jones et al., 1977; Lazenby, 1990b; Bertram and Swartz, 1991; Ruff et al., 1994; Bass et al.,

1998). This mechanically inefficient deposition in pubertal females, then, may serve as calcium reservoir for pregnancy and lactation (Schönau et al., 2001). Thus, hormonal effects, in addition to activity variation and the age of onset for loading (not to mention stress and diet; see Chapter 3), are important in shaping ontogenetic changes in diaphyseal cross-sectional properties.

After skeletal maturity and with advancing age, bone remodeling becomes "uncoupled": periosteal deposition is limited to a few millimeters and endosteal resorption continues to cause net cortical bone loss (Balena et al., 1992; Robling et al., 2002). This uncoupling in adults is known to occur in both appendicular elements (Ruff and Hayes, 1982) and ribs (Sedlin et al., 1963; Takahashi and Frost, 1966). In older adults, mechanical loading cannot reverse bone loss but may maintain it, mainly through inhibition of endosteal resorption rather than periosteal deposition (Szulc et al., 2006). Net bone loss is higher in women due to an increased propensity for periosteal apposition in males (Russo et al., 2003). Bone strength in healthy adults, however, does not decrease as much as one might think based on evidence of reduction in cortical area alone; minimal periosteal deposition may compensate for age-related endosteal resorption, resulting in increased second and polar moments of area and potentially compensating for net losses in cortical area (Lazenby, 1990b; Seeman, 2003b), although the capacity for compensation is dependent on the rate and extent of bone loss (Szulc et al., 2006).

Application to Anthropology

Adult Research. The examination of cross-sectional geometry in skeletal remains has been an indispensable tool for reconstructing behavior among past human populations. Studies typically examine cross-sectional properties of long bone diaphyses to develop inferences about terrestrial mobility, body mass, habitual loading behaviors, and subsistence strategy in both

archaeological (Ruff et al., 1984, 1999; Bridges et al., 2000; Stock and Pfeiffer, 2001, 2004; Weiss, 2003; Stock, 2006; Wescott, 2006) and paleoanthropological contexts (Ruff et al., 1993; Ruff et al., 1999; Trinkaus et al., 1999; Pearson, 2000; Sladek et al, 2006; Shackelford, 2007; Ruff, 2008b; Ruff, 2009). Special attention has been given to the shift in activity from foraging to agricultural subsistence strategies (Ruff and Hayes, 1983a, 1983b; Ruff, 1988; Bridges, 1989, 1991; Ruff and Larsen, 1990; Larsen and Ruff, 1991; Ruff, 1994, 1987, 1999; Bridges et al., 2000). The current study has potential implications for this area of research, because interpretations of subsistence-related activities from skeletal remains are complicated by the inability to address the interaction between mechanics and metabolism.

Several studies have documented a decrease in diaphyseal strength properties after the transition to agriculture (Ruff et al., 1984; Larsen et al., 1990, 1995; Ruff and Larsen, 1990; Larsen and Ruff, 1991). Ruff et al., (1984) found a reduction in almost all femoral cross-sectional properties in agricultural groups of the Georgia Coast, which lead these authors to conclude that reduced loading on the lower limb (likely caused by increased sedentary behavior) was causing alterations in the size and shape of cortical bone.

However, not all evidence confirms a reduction in activity level with agricultural subsistence. Bridges (1989, 1991) inferred a rise in activity level and work load with the intensification of maize agriculture in Northwestern Alabama. Mississippian groups in this region exhibited stronger femora relative to their Archaic hunter-gatherer predecessors and reduced bilateral asymmetry in their humeri. Bridges interpreted these results as being caused by a shift from mostly unimodal to bimodal tasks in the upper limb, mainly through the extended use of the bow and arrow over the atlatl in males and corn processing in female. Unlike early studies by Ruff and colleagues, these comparisons were made without size-standardization, and

discrepancies in the findings of Bridges' studies and those of Ruff and colleagues were potentially driven by body size differences. In a more recent comparison of size-standardized diaphyseal properties, Bridges and colleagues (2000) found slightly different and more complex patterns in west-central Illinois that are unlike those of either the Georgia Coast or Northwestern Alabama. In this region, only females demonstrated both femoral and humeral strength increases over time with the introduction of maize between the Middle and Late Woodland, and male right humeral strength declined. The most significant changes occurred in the Mississippian period, when maize became a predominant component of the diet (Bridges et al., 2000).

Multiple variables likely contribute to these and other inconsistencies between observed long bone diaphyseal strength and expected activity patterns in archaeological skeletal samples, as cortical bone morphology is a complex phenomenon resulting from multiple causal factors. When interpreting habitual loading activity from diaphyseal cross-sections, the investigator is in fact documenting an aggregation of continuous modifications to cortical structure that occur over the course of an individual's lifetime. Complicated patterns across skeletal elements and among individuals may arise if they are engaged in highly variable activities throughout their life, especially if there are differences in activity during childhood, adolescence, and young adulthood (Pearson and Lieberman, 2004). Additionally, an inadequate knowledge of a human population's behavioral activities makes it difficult to construe meaning and ultimate causation from structural shifts in morphology without providing *ad hoc* explanations to support *a priori* hypotheses.

Moreover, other mechanically driven factors may be causing variation in long bone diaphyses that are not necessarily readily apparent. For example, when considering multiple skeletal samples in different regions within North America, Ruff (1999, 2008) found that terrain could be driving the differences present in lower limb cortical area and torsional strength

between agricultural and pre-agricultural groups. In fact, variation in lower limb proportions may additionally affect the cross-sectional strength properties among groups (Higgins and Ruff, 2011), which in turn relates to terrain—shorter lower limbs, especially tibiae, provide mechanical advantages in more hilly geography. Stronger femora in populations occupying more mountainous regions could account for the patterns previously attributed to subsistence. Moreover, non-mechanical factors are known to influence cross-sectional geometric properties (e.g., nutrition, metabolic status, and genetics), and these may have significant effects on mechanical interpretations from human skeletal samples (see Chapter 3). And finally, with increasing bone loss associated with aging, adult morphological patterns may not reflect recent mechanical effects as accurately as immature bone.

Ontogenetic Research. Even though far fewer assessments have been made of mechanical adaptations in immature populations, a growing body of research into developmental processes underlying adult long bone strength has provided a foundation from which to expand investigations. The majority of these studies involve the acquisition of adult femoral to humeral strength proportions, yet recent work on shape changes in long bone elements points to unique loading patterns in subadult populations relative to adults.

Sumner and Andriacchi (1996), in one of the first studies, compared humeral and femoral strength proportions across ontogeny in a skeletal sample from Grasshopper Pueblo. They found that early in ontogeny the two limb bones possessed similar strength proportions relative to bone length but that higher rates of increase in diaphyseal robusticity in the femur prior to the age of ten were responsible for creating the divergent adult strength ratios between these two elements. Ruff (2003a, 2003b) refined their study and detected ontogenetic shifts in relative limb bone

strength that establish the association between development of diaphyseal cross-sectional properties and mechanical loading both with and without the influence of body mass. Ruff (2003a) found stronger correlations between immature human growth velocity in femoral strength and that of body weight times bone length compared to growth velocity in stature and muscle size. In the humerus, however, growth velocity in strength has a lower correlation with body weight multiplied by humeral length than the femur but a clear association with forearm muscle area in males.

In immature baboons and humans, Ruff (2003b) observed the appearance of human-like femoral to humeral strength proportions only after the transition to bipedal walking (around roughly one year of age), with femoral strength increasing gradually during growth and humeral strength declining after cessation of crawling. Peaks in strength properties in both the humerus and femur during infancy are associated with the initiation of walking and mark the divergence between femoral and humeral growth trajectories (Ruff, 2003a). Prior to the acquisition of bipedal locomotion, human infant morphology was similar to baboons and other quadrupedal animals. While adult femoral to humeral strength proportions did not develop until late adolescence, adult length proportions were present at birth. Likewise, femoral to humeral length proportions increased slightly during growth, however, initiation of walking appeared to have no effect on bone length growth trajectories (Ruff, 2003b).

Cowgill (2008; 2010) conducted the first thorough analysis of subadult strength properties in more than one human sample. Her analyses in both Holocene and Late Pleistocene populations confirmed the diaphyseal strength proportion patterns outlined by Ruff (2003a, 2003b) associated with the transition to bipedal walking, as well as the disparities in growth velocity between long bone strength, body mass, and bone length that cause cross-sectional

geometric properties to lag behind changes in body size (Ruff et al., 1994). In addition, results suggested that population differences in limb strength properties appear by the skeletal age of six, supporting ethnographic research of young children engaging in adult-like behavior and activities by this developmental stage across many human groups. Humeral asymmetry developed slowly in these populations, with adult values being obtained after 12 years of age, a pattern indicative of increased unilateral limb use with age in populations with high adult asymmetries.

The findings most relevant to the current study were the slow emergence of adult femoral and tibial shape during growth (Cowgill, 2008). The femur, for example, is medio-laterally reinforced (i.e., I_{max} tends to fall near I_x) until adolescence, when a femoral pilaster forms and bone mass is shifted in the anterioposterior direction. Cowgill (2008) attributed disparities in lower limb diaphyseal shape between younger and older subadults to the relatively late attainment of the bicondylar angle (around 6 years of age), prior to which bending moments about the hip are mostly mediolaterally oriented. This hypothesis was validated in a kinematic study of immature gait that showed significantly higher mediolateral ground reaction forces in toddlers relative to adults, which were due to a wider stance and waddling gait (Cowgill et al., 2010). These results impact the current study, which assesses geometric and microstructural properties along femoral and humeral axes of bending rigidity.

Micromorphology

The proper mechanical function of a bone depends not only on its arrangement (e.g., size and shape) but also on the properties of the bone tissue material itself. Some of this is reviewed above in the discussion on bone mineral density (BMD) responses to activity. Although

macroscopic cortical bone structure is arguably the principal determinant of bone strength, adjustments in microarchitecture can significantly influence resistance to mechanical forces as well (Parfitt, 1984; Currey, 1988; Schaffler and Burr, 1988; Martin and Ishida, 1989; McCalden et al., 1993; Martin et al., 1998; Yeni and Norman, 2000; Seeman, 2003). Microstructural variation appears to affect the distribution of strains within bone on the local level, which accumulate to create effects at the organ level that cannot be explained by total bone mineral content and density alone (Currey, 2003; Hoc et al., 2006). Along with evidence of mechanical alterations to macroscopic properties, this histological response demonstrates that bone adapts to mechanical inputs at multiple biological levels. In other words, bone's hierarchical organization ultimately dictates its mechanical properties (Katz, 1980; Cowin, 2001). Therefore, variation in bone tissue organization is correlated with mechanical loading regime both among skeletal elements and within specific regions of elements (Lanyon and Baggott, 1976; Carter et al., 1980; Carter, 1984, 1987; Burr, 1992; van der Meulen et al., 1996; Reilly et al., 1997; Skedros et al., 1994a, 1994b, 1996, 1997, 2000, 2001a, 2001b).

Historically, investigations of mechanical effects on microscopic structure have been limited when compared to macroscopic bone density and cross-sectional properties as investigated across multiple disciplines. Generally speaking, histological methods are more common in anthropological analyses of skeletal samples than in clinical settings; primary focus in the clinical literature has remained on large changes in cortical size and shape and their mechanical consequences (e.g., DXA), with the expectation that further research will clarify the relationship between organ and tissue level structure (Cooper et al., 2006, 2007; Davison et al., 2006). Until recently, with the advent of high-resolution imaging (i.e., microCT), it has not been possible to assess tissue-level properties without resorting to destructive methods (Cooper et al.,

2007). Clinical studies were initially restricted to experimental research on non-human animals or minimally invasive biopsies (e.g., iliac crest biopsy) from living human subjects. Therefore, regions predominantly comprised of cortical bone (e.g., long bone diaphyses, ribs), which are typically analyzed in skeletal samples, are not frequently used in living humans to assess microstructure, though experimental studies on animals have shed some light on this area of research (Lanyon et al., 1979; Lieberman and Crompton, 1998; Skedros et al., 2001).

Histological methods for investigating bone tissue organization (e.g., light microscopy, microradiography, back-scattered electron microscopy, and nanoindentation testing), despite largely being destructive, provide advantages over microCT in being able to clearly isolate histological structures other than porosity (i.e., osteon size, osteon cortical area) and assist with calculations of intracortical remodeling rate (Cooper et al., 2007). An important limitation to the use of histological techniques is that these methods are often more time-consuming relative to high-resolution imaging, and, more significantly, are greatly restricted due to their destructive nature. Their utility for understanding whole bone strength, however, cannot be understated. The calculations associated with cross-sectional geometric properties, for example, assume homogenous microstructure (i.e., isotropy) throughout the cortical area (Ruff, 1999), though long bone tissue is known to be anisotropic (Turner et al., 1999). Diaphyses that appear to have strong cortical structure using macroscopic analyses may be mechanically weaker if the cortical bone is comprised of inferiorly organized or structurally compromised bone tissue (Keller et al., 1990; Martin and Boardman, 1993). While this fact certainly does not negate the importance of geometric properties for understanding bone strength, further research into covariation of bone structure at both scales is necessary to fully understand how their relationship shapes bone strength.

Osteonal Remodeling Rates and Loading Behavior

Within the past few decades, a rise in bone microstructure research has generated a new appreciation for its influence on cortical bone properties. As stated previously, although intracortical remodeling is not a completely understood phenomenon, it is clearly connected with replacing fatigue-damaged bone (Mori and Burr, 1993; Burr, 2002; Parfitt, 2002; Martin; 2007) and possibly preventing the propagation of additional microcracks (Martin and Burr, 1982; Schaffler et al., 1995). This skeletal response seems to be mediated by mechanotransduction, the load-induced cellular responses associated with formation and resorption. Though the exact mechanisms of mechanotransduction are still elusive, osteocytes appear to "sense" mechanical signals through their fluid-filled canalicular networks, leading to secondary cytogenic signals sent to osteoblasts and osteoclasts via cytokines (Frost, 1973; Burger and Klein Nulend, 1999; Cowin et al., 1991; Martin, 2000). Microdamage has been associated with reduced fluid flow and osteocytic cell death, which in turn are linked to the initiation of osteoclastic activation and remodeling (Noble et al., 1997; Verborgt et al., 2000).

Contrarily, some authors have proposed that osteonal remodeling weakens cortical bone. Skeletal elements with high rates of remodeling were shown to be weaker in tension, compression, bending, and shear than primary bone, due to the temporary increase in porosity and generally less mineralized bone being deposited in newly-created Haversian systems (Reilly and Burstein, 1974, 1975; Carter et al., 1976; Carter and Hayes, 1977). However, *fully mineralized* osteonal bone is actually stronger in compression than non-remodeled bone (Hert et al., 1965), is stronger than older, damaged primary bone (Schaffler et al., 1989, 1990), and contains collagen fibers reoriented along axes of tension where bone is the weakest (Martin and Burr, 1982; Riggs et al., 1993). Furthermore, based on mounting evidence of a strong association

between higher stain stimuli and increased remodeling rates, researchers now agree that targeted remodeling is a necessary bony response that improves mechanical properties.

Higher rates of osteonal remodeling occur in conditions of increased loading and in skeletal elements and bone regions under higher mechanical strains (Bouvier and Hylander, 1981; Rubin and Lanyon, 1984, 1985; Schaffler and Burr, 1988; Burr et al., 1985; Mori and Burr, 1993; Goodship and Cunningham, 2001; Lieberman and Pearson, 2001; Lieberman et al., 2003). In an *in vivo* avian model, Rubin and Lanyon (1984, 1985) found that cessation of loading resulted in substantial bone loss through increased resorption both endosteally and intracortically; however only minor exposure to strain stimulus above the "lazy zone" was required to cause increased remodeling and restore bone balance.

Lieberman and Crompton (1998) proposed that remodeling responses to strain would optimize strength over mass; specifically, intracortical remodeling would increase along the proximo-distal limb axis in cursorial mammals (i.e., sheep). Distal limb elements are more energetically costly to move and therefore more slender than proximal segments; the distal elements demonstrate higher strain levels due to this slenderness and consequently increased remodeling. These results further support the optimization model for bone at both the macroscopic and microscopic levels; however, humans are non-cursorial animals, and so may not demonstrate this same pattern in the lower limb. The human tibia does not appear to have reduced bending and torsional strength or higher rates of osteonal remodeling relative to the femur (Drapeau and Streeter, 2006).

Nevertheless, experimental studies indicate that remodeling occurs preferentially along axes under the greatest loads to bolster these areas from potential microdamage and mechanical failure. Lanyon et al. (1979) compared *in vivo* strain gauge data with mechanical testing of

immature and mature sheep radii and recorded higher rates of osteonal remodeling in the more highly strained and compressed caudal cortex of the midshaft diaphysis relative to the cranial cortex. Skedros et al. (2001) has also reported variation in both geometric and material properties within diaphyseal cross-sections of immature mule deer calcanei (a compression-tension bone) that supports expectations according to the mechanostat model. Relative to the compression cortex (i.e., cranial), the tension cortex (i.e., caudal) contained evidence of increased remodeling: high porosity, greater percentages of osteonal bone per area, larger numbers of incompletely formed osteons, and larger osteons, all of which would be expected given that bone is weaker in tension than compression. Higher rates of remodeling in this cortex suggest mechanical adaptation to higher strains. Additionally, compared with the medial and lateral cortices (closer to the neutral axis—where strains are lowest circumferentially), the compression and tension cortices exhibited greater numbers of osteons and newly formed osteons, increased percentage of osteonal bone per area, and increased porosity.

Comparisons of microstructure within human long bone cortices have been limited to a few studies in adult femoral diaphyseal midshafts and have focused on porosity distributions due to their association with age-related osteoporosis; only a handful have compared porosity along axes of bending rigidity. However, these studies, along with that of Skedros et al. (2001), help inform hypotheses regarding the distribution of targeted remodeling versus stochastic remodeling within long bone cortices in relation to mechanical and metabolic demands. Multiple studies confirmed nonuniform porosity distributions with increased porosity present in the more highly strained periosteal region relative to the endosteal region (Jowsey, 1960; Martin et al., 1980; Martin and Burr, 1984; Bousson et al., 2001).

In one of the only assessments of circumferential differences in porosity distribution within femoral cortices, Thomas et al. (2005) documented the highest levels of porosity in the posterior cortical section followed by the anterolateral section and the lowest levels of porosity in the medial and lateral portions. These results are similar to those of Skedros et al. (2001), except that the posterior cortex in humans is under mostly compression in bending, not tension. Differences between the sections became more pronounced with advancing age, as porosity levels increased, presumably due to unbalanced remodeling. However, increased porosity can result from increased balanced remodeling, disrupted osteon filling, and/or increased resorption spaces; therefore, the relationship between porosity and remodeling rates is tenuous. Individuals in the sample were not osteoporotic, and the question remains whether this same pattern would persist under conditions of metabolic disturbance and potential microscopic bone loss (see Chapter 3).

There is some evidence of regional variation in osteonal remodeling in the human femoral diaphysis; however no work has evaluated these variables thoroughly in relation to mechanical axes. In a study on the effects of sampling location within the femoral cortex on histological age estimates, regions of interest within the anterior cortex tended to possess the lowest rates of percent osteonal bone and were the most variable in amounts of osteonal bone compared to other subsections (Pfeiffer et al., 1995). In general, anatomical axes (e.g., anterior, posterior, medial, and lateral) possessed more variability in percent osteonal bone than mechanical axes (I_{max} and I_{min}), but the authors did not assess differences between I_{max} and I_{min}. When all eight regions of interest from each cortex section are considered together rather than separately, percentages of remodeled bone mimic the results of Thomas et al. (2005) and suggest higher rates of remodeling in highly strained portions (see Table 1 in Pfeiffer et al., 1995).

Additionally, unlike evidence for porosity distribution, more osteonal bone was present in endosteal sections compared to periosteal sections (Pfeiffer et al., 1995).

Previous research on microstructural variation within the human femur provides a basis from which to test hypotheses concerning the distribution of targeted remodeling within immature long bone diaphyses. In this study, this distribution will be contrasted with that expected for metabolic bone loss in relation to mechanical axes (Hypothesis 2c in Chapter 1). "Stochastic" osteonal remodeling also occurs to maintain mineral homeostasis, and the structural results of this process take place simultaneously with targeted remodeling (see Chapter 3 for a full discussion).

Remodeling Rates and Age

Intracortical remodeling is a predictable biological process subject to quantitative analysis, chiefly because it involves coordinated removal and replacement of units of bone tissue. Rates of remodeling can be modeled mathematically and hypotheses tested based on expectations, providing a means of identifying inaccuracies in our assumptions and assist with improving future research (Frost, 1964, 1969). This procedure forms the basis for estimating age-at-death in skeletal remains through calculation of osteon population density or percentage of the cortical bone containing secondary osteons (Kerley, 1965; Ahlqvist and Damsten, 1969; Thompson, 1979; Stout and Paine, 1992). Because structural modifications to adult cortical bone occur mainly through remodeling rather than modeling, as an individual ages the number of osteons and percentage of remodeled bone (e.g., percent osteonal bone, osteon population density) increases. Eventually, as bone tissue age rises and remodeling continues osteons may begin to overlap one another and partially or entirely obliterate older osteons. This process

creates fragmented osteons, which have been shown to positively correlate with age in adults (Stout and Paine, 1992; Chan et al., 2007). Though osteonal overlap may erase evidence of previous remodeling events, correction factors can be applied to assist with age estimations in skeletal remains and to improve estimates of bone turnover rates (Frost, 1987).

Very little is known about osteonal remodeling rates during growth in relation to adults other than they are higher (Jowsey, 1968; Currey, 1984). One confounding factor in comparing remodeling rates in subadults is that, due to rapid modeling and cortical drift, at any given point during ontogeny cortical bone is comprised of multiple bone layers of varying tissue age. The average tissue age of a bone can be considerably younger than the individual's age-at-death, depending on rates of modeling and macroscopic remodeling. Although young adults retain some cortical tissue that was deposited during development, adult variation in mean tissue age is lower due to diminished modeling rates (Goldman et al., 2009; Maggiano, 2012). During growth, modeling causes bone shape to "drift" in the direction dictated by the mechanical environment, directing the distribution of tissue layers within the cortex (Enlow, 1963; Wu et al., 1970; Maggiano, 2012).

Further complicating matters, modeling processes in subadults preferentially remove the oldest bone tissue that is most likely to contain osteons. During expansion of periosteal and endosteal borders, the oldest bone is removed endosteally; therefore, modeling will result in the removal of the most highly remodeled portion of the cortex and the addition of primary bone (i.e., circumferential lamellae) periosteally. This primary bone will subsequently become remodeled as it becomes incorporated into the midcortical region and then, in turn, the endosteal region where it is eventually subject to resorption. In human subadults, the relationship between cortical modeling and remodeling has not been thoroughly explored, and any effect that cross-

sectional shape changes across ontogeny would have on remodeling rates is unknown. Nevertheless, taking this potential variation into account, one can ask how such circumstances could enhance or mitigate the ability of bone to structurally adapt to mechanical and metabolic demands.

Application to Anthropology

Adult Research. Examination of cortical bone microstructure in anthropological contexts primarily involves documenting metabolic disturbances (see Chapter 3) and estimating age-at-death, though the distribution and size of osteons have previously been used to infer behavioral factors from human skeletal samples. Abbott et al. (1996) proposed that high macroscopic skeletal robusticity in the lower limb of Pleistocene populations relative to late Holocene populations could be explained by their lower osteonal turnover, which would increase strains and thus induce periosteal apposition; however, recalculation of the data has shown that Pleistocene and Holocene groups have very similar remodeling rates in the lower limb (Streeter et al., 2010).

Comparing Pecos Pueblo Native Americans to 20th-century Europeans and Americans, Burr et al. (1990) found smaller Haversian canals in Pecos females and higher osteon population densities in Pecos males than modern populations. The authors interpreted these results as evidence that higher activity in Native American groups led to greater bone mass maintenance, supporting similar results on geometric properties of the femur in the Pecos group (Ruff, 1991; Ruff and Hayes 1983a, 1983b). Using samples of Late Stone Age foragers from South Africa and historic 18th and 19th century Europeans and British Canadians, Pfeiffer et al. (2006) expected to find greater variation in femoral osteon size relative to ribs (due to its more variable

loading regime) and more variable Haversian canal areas in ribs (argued to be higher in remodeling activity due to greater turnover). However, rib osteon size was smaller than femoral osteon size, and variation in osteon size was similar in the two skeletal elements within samples. These results lead Pfeiffer and colleagues (2006) to conclude that osteon size was a poor indicator of physical activity in past human populations, though they did call for more focused experimental and theoretical approaches to understanding variation in cortical remodeling and the factors that control its variability. Since this publication, few investigations of remodeling have been conducted to infer behavior from anthropological skeletal samples.

What these research studies did not take into account was the potential variation in microstructure caused by differences in metabolic status and nutrition. It is possible that some mechanical comparisons could be confounded by variation in metabolic activity among or within groups, as well as different age distributions among samples. A more complete understanding of what effect inferior metabolic status has on osteonal remodeling is needed to validate the utility of histological analyses on archaeological bone.

Ontogenetic Research. Histomorphometric analyses of immature human remains are extremely rare, especially in anthropological disciplines. The vast majority of these anthropological studies have explored subadult rib histological features to describe the normal growth processes that determine adult rib morphology. This dissertation represents the first anthropological examination of immature human bone histology to include a biomechanical component.

Pfeiffer (2006) examined rib sections from Spitafields subadult remains of known age and sex, noting the shift in bone types (e.g., woven, primary, secondary) with age as well as

measuring Haversian canal and osteon areas. She found that the number of secondary osteons relative to cortical area increased with age, and secondary osteons in the ribs appeared around the same age (as early as 1 year) as in the femur. In addition, subadult osteon dimensions were indistinguishable from their adult Spitafields counterparts. These findings were important for future studies, especially because they overturned ideas previously thought by researchers, namely that subadult bone did not remodel frequently enough, or similarly to adults, to warrant histological examination (Martin, 1983). Furthermore, from Pfeiffer's study it is clear that rapid modeling in subadult rib elements does not lead to a loss of evidence of intracortical remodeling that precludes quantitative assessment, opening up new potential avenues of inquiry into osteonal remodeling during growth.

Streeter (2005) supplied the first systematic evaluation of developing rib cortical bone. She assessed autopsied rib sections from metabolically normal subadults and found significant relationships between macroscopic and microscopic measures and age. Total area, medullary area, cortical area, and osteon population density were each highly positively correlated with age, while percent cortical area was negatively correlated with age. She also found that the percentage of drifting osteons decreased with age, while the average size of secondary osteons did not change during ontogeny. These results demonstrate that rib modeling and remodeling during development is similar to that of long bones. Additionally, the high percentage of drifting osteons in subadult ribs supports the hypothesis that resorption of larger bone packets by BMUs is associated with higher metabolic requirements of young individuals. The implications of these findings are considered further in the next chapter.

CHAPTER 3: METABOLIC INFLUENCES ON BONE

How many infants, daily how many children, how many flowering youths, how many robust young men are borne with weeping and great grief to the tomb.
- John Longland, Bishop of Lincoln, Canterbury (1520s)

The homeostasis of organismal metabolism is of central importance to maintaining good overall health. Perturbations in homeostatic maintenance are indicative of deviations in the mechanisms that regulate metabolism, whether they are induced by hormonal, enzymatic, dietary, or other causes. These shifts are a natural component in the reaction of an organism to both intrinsic and extrinsic demands, especially in relation to changing environments or abnormal physiology (i.e., disease processes) (Brand, 1997). It is when these deviations result in a steady state unfavorable to these demands, or when a steady regulatory state cannot be achieved, that conditions detrimental to the organism occur and result in pathological consequences. Some of these may take the form of changes in rates of growth, while others result in abnormal shifts in hormonal or other chemical levels, which, in turn, may have long-term consequences on health and longevity (Brand, 1997). As bone serves a dual function—resistance to and conduction of mechanical loads and a reservoir for both minerals and some cell types—it is a fundamental part of an organism's metabolism and metabolic regulation.

Biological anthropologists utilize skeletal evidence of metabolic disturbance to provide vital insight into dietary practices and health status among past human populations. These analyses have traditionally relied on the assessment of skeletal stress lesions to make inferences about the prevalence of particular diseases in skeletal samples, yet quantification of bone mass is also used as a general indicator of metabolic status in individuals. This chapter reviews the literature on health interpretation from bone pathology in the skeletons of past peoples and living

humans with specific emphasis placed on metabolic disorders and their influence on cortical bone mass and structure. Results of previous research are considered in this chapter separately by scale—macroscopic and microscopic analyses. The chapter also focuses on metabolic effects among immature populations, with emphasis on how responses to metabolic disturbances are more pronounced in subadults than in adults. The contents build upon basic concepts outlined previously in Chapter 2 concerning the relationships among bone mass, structure, and strength under non-pathological conditions, calling attention to the mechanisms by which metabolic disorders modify these relationships.

Metabolic Stress: An Introduction

Metabolic stress involves a complex array of physiological responses to biological, cultural, and environmental factors that govern the processes underlying metabolic regulation. Biological factors, such as disease and nutritional deprivation (whether due to deficient diet or malabsorption of nutrients), are mediated by cultural factors (e.g., subsistence strategy, socioeconomic status, access to resources, cultural norms on health care, population size, sanitation) and environmental factors (e.g., climate, exposure to pathogens and infectious disease) in a complex web of interactions that impact on the overall health status of a community (Figure 4; Goodman et al., 1984, 1988; Goodman and Armelagos, 1989; Goodman, 1991). Models of health stress are improved by the acknowledgement of these interactions between cultural and biological stressors.

According to the biocultural perspective of Goodman et al. (1984, 1988), environmental stressors and cultural stressors are filtered through a cultural buffering system that may or may not buffer an individual from stress. If the cultural buffering system is unable to buffer against

the stress, the stressor will then be filtered through the physiological status of the individual. Depending on the severity of the stress, an otherwise healthy person may be able to fight off the affliction without any physiological distress (i.e., the stressor does not shift an individual outside a metabolic steady state). However, if the individual is already immune-compromised, for example, or the stress is too intense (or perhaps even of a long duration that exceeds a particular threshold), the homeostatic steady state will be compromised and an osteological response may occur.

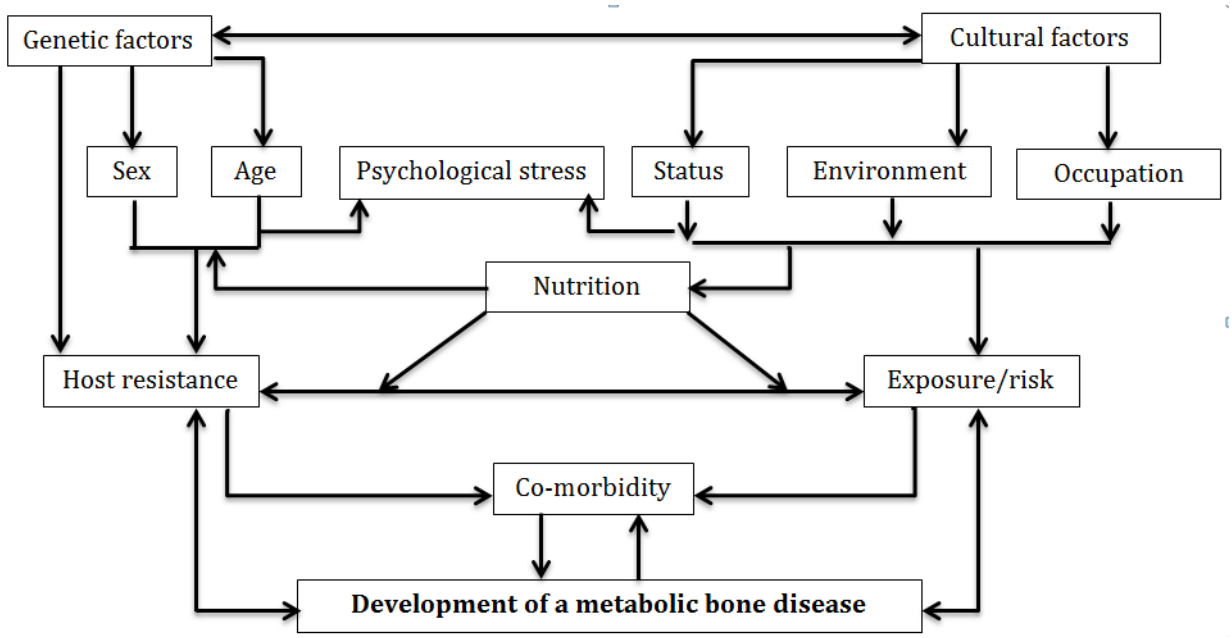

Figure 4. Diagram of the complex relationships among factors influencing metabolic status (adapted from Brickley and Ives, 2008).

Models like those developed by Goodman and colleagues have highlighted intricate relationships among stressors, such as the synergistic effect between nutrition and infectious disease. Inadequate nutrition inhibits the ability to fight off infections and, conversely, infections

may reduce the ability of the digestive system to absorb nutrients (Huss-Ashmore et al., 1982; Bennike et al., 2005). Therefore, nutritional insufficiency would be due to either poor dietary intake or an inability to properly absorb dietary nutrients due to pathogenic infection, two circumstances that are governed by cultural factors (Holland and O'Brien, 1997; Blom et al., 2005; Walker et al., 2009). This synergistic effect is discussed further with respect to immature individuals below.

The Osteological Paradox and Paleopathology

Before discussing the combinatory effects of stressors on subadult skeletons, consideration should be given to the contradictory nature of paleopathological study and metabolic disturbance effects on skeletal remains, an inconsistency termed “the osteological paradox” (Wood et al., 1992). Wood and colleagues cautioned researchers against reconstructing health from cemetery samples and questioned the common assumptions made in paleopathological analysis. The authors pointed out a paradox in the composition of skeletal assemblages: they only contain information regarding the health status of non-survivors and cannot reliably represent the full range of morbidity and mortality experienced by the living population. Selective mortality biases the archaeological record toward the frailest individuals, creating a distorted view of the prevalence of disease in past populations (Saunders and Hoppa, 1993). Additionally, an intrinsic property of archaeological cemetery samples is their hidden heterogeneity in risk of illness and death (Ortner, 1991; Wood et al., 1992). Individual frailty and mortality risks vary. The inability to account for this variation limits meaningful interpretations of population health, as populations are composed of numerous groups with inherently different frailty and mortality rates that will not all be captured in skeletal assemblages.

Inferences about health are also constrained by our ability to identify and effectively interpret the etiology of skeletal pathologies. Non-specific indicators of metabolic stress (e.g., dental enamel hypoplasia, cribra orbitalia, porotic hyperostosis) have traditionally been used as a general indication of poor health in archaeological samples and are not without their own caveats (Larsen, 1997; Lewis and Roberts, 1997). With the exception of dental enamel hypoplasias (cf. Ritzman et al., 2008), the temporal proximity of these indicators to the metabolically insulting event is ambiguous. More practically important, depending on the degree of preservation, much information useful to paleopathological assessments can be lost in archaeological bone; lesions and the elements exhibiting them might be obliterated due to taphonomic alteration. In addition, the majority of skeletal stress lesions are of unknown etiology; there are multiple physiological pathways that lead to their presence and severity within the skeleton (Wapler et al., 2004; Walker et al., 2009). Therefore, they cannot be used to make particular medical diagnoses, although in some cases their unique distributions and patterns alongside historical and contextual information may allow proper attribution to a particular disease process (Huss-Ashmore et al., 1982; Ortner, 2003; Lewis, 2007).

Furthermore, whether individuals with skeletal stress lesions are “healthy” or “unhealthy” has been rigorously debated. Both Wood et al. (1992) and Ortner (1999) argued that, contrary to previous interpretations, a stress response indicates adaptive ability; individuals who live long enough to develop a skeletal response represent those who were healthy enough to adjust to the insulting factor (e.g., form an immune response to infectious disease). It is widely recognized that in order for some skeletal lesions to develop (such as enamel defects), an individual must first recover from a stressful event, meaning that skeletal remains exhibiting stress lesions may actually represent the healthier individuals within a population. Even if an individual does not

recover from the insulting event, in the case of all skeletal lesions, she or he would have needed to survive long enough to present a skeletal indicator. Those without stress lesions, then, are likely to have succumbed to a stressful event quickly, before initiation of a skeletal response or have died from other causes (e.g., accidental or violent death). However, Goodman and Martin (2002) maintained that a skeletal response indicates increased morbidity or frailty within a population (the presumed scale of interest) and not necessarily individuals, further highlighting a need for clarity in interpretive approaches and assumptions to documenting health from skeletal remains.

An additional consideration for paleopathological analyses is the unpredictability of disease processes themselves. Many diseases do not affect the skeleton. We know from modern clinical settings that the degree of disease expression is inconsistent among individuals, and some diseases only variably leave traces on the skeleton in the form of observable lesions or gross osteological pathologies. For example, infection with *Mycobacterium tuberculosis* has a long incubation period, but may kill an individual within weeks of the onset of symptoms (Lincoln and Sewell, 1963), especially if the disease manifests as extrapulmonary (e.g., resulting in meningitis) (Feja and Saiman, 2005). The incubation period, rate of infection, and mortality of the disease varies. Moreover, in the small percentage of tuberculosis infections that spread to the parietal pleura or outside the pleural cavity and become chronic, it takes *years* for the infection to manifest in the skeleton enough to produce an abscess and ultimately the skeletal lesions that paleopathological analysis associates with the infection (Dabernat and Crubézy, 2010). It is possible for an individual to succumb to the infection (or another infection due to compromised immunity) long before a skeletal abscess forms.

Thus, metabolic stress does not induce a local or systemic skeletal response until a threshold of severity is reached (Goodman et al., 1988), and this typically occurs after other organ systems have been exhausted (Lewis, 2007; Brickley and Ives, 2008). This threshold is inconstant and depends on multiple biological factors discussed above, including the individual's prior health status, sex, age, ethnicity, and nutrition, as well as cultural factors. Therefore, drawing a dividing line between groups with skeletal lesions and those without lesions, as biological anthropologists must often do, will not encapsulate the full range of morbidity and mortality experienced by a population.

Nevertheless, these limitations do not invalidate the exploration of health in past human populations as long as realistic interpretations are made within the bounds and limits governed by the nature of the data (Goodman, 1993; Cohen et al., 1994; Konigsberg and Frankenburg, 1994; Wright and Yoder, 2003). The osteological paradox described by Wood et al. (1992), though framed as a severe critique of paleopathological and paleodemographic examinations, has actually assisted the anthropological discipline in improving the scientific rigor of interpretations made about skeletal pathologies. Emphasizing multiple indicators of stress rather than attempting to make specific diagnoses of individual skeletal pathological conditions has contributed to improved inferences of population health and adaptability (Goodman and Armelagos, 1989; Goodman, 1993; Armelagos, 2003). Focus on population level morbidity and mortality in lieu of specific and extreme pathological cases has advanced our understanding of health stressors in past populations (Goodman and Martin, 2002).

Moreover, adjustments in the perceptions of "stressed" and "non-stressed" groups, an approach taken in this research project (wherein metabolic stress is instead categorized as "chronic" versus "acute/non-metabolic" based on skeletal stress lesion presence and absence,

respectively), enhances and clarifies comparisons within a population, especially with regard to expectations of skeletal response to metabolic stress (Goodman et al., 1993; see the *Methods* section in Chapter 4 for a full discussion).

Metabolic Influences on Immature Populations

Due to the increased metabolic demands required for healthy growth and mediated by undeveloped immune systems, the skeletal effects of metabolic stress are much more pronounced in subadults compared to adults. These conditions make the immature individuals within a population, especially infants and young children, most susceptible to environmental pathogens and infectious agents and, thus, nutritional insufficiency (Lewis, 2007). Skeletal responses to these stressors include a reduction in stature due to retarded bone growth (Hummert and Van Gerven, 1983; Jantz and Owsley, 1984; Mensforth, 1985; Eveleth and Tanner, 1990; Humphrey, 2000), development of stress lesions (Huss-Ashmore et al., 1982; Goodman and Armelagos, 1988, 1989) and bone loss (Armelagos et al. 1972; Hummert, 1983; Van Gerven et al., 1985). For these reasons, subadults are considered sensitive indicators of biocultural change in archaeological populations (Blakely and Armelagos, 1985; Goodman et al., 1998; Lewis, 2007).

The synergistic relationship between nutrition and infectious disease is a main contributor to metabolic stress in subadults, especially in various past societies. This is particularly evident in the weaning of infants. A number of factors influence this synergistic effect, in particular: early weaning practices, the introduction of environmental pathogens (especially with the introduction of food), and the tendency for ancient weaning foods to contain inadequate nutrients (Katzenberg et al., 1996; Herring et al., 1998). Weaning an infant too early (prior to complete immune system development) potentially exposes the infant prematurely to harmful bacterial and

parasitic infections (e.g., microbes, helminth) present in food. These infections lead to chronic diarrhea followed by the inhibition of nutrient absorption and an increased risk of anemia (Foote and Marriott, 2003; Blom et al., 2005). After six months of age, infants require some solid foods in their diet, leading to the situation known as the "weanling's dilemma" (King and Ulijaszek, 2000). Delaying the onset of weaning will deprive the infant of a proper diet, yet introducing weaning foods will increase risk of infection. Likewise, historically common Eurasian and African traditional weaning foods (e.g., unpasteurized cow and goat milk), in addition to containing infectious pathogens, place significant restrictions on growth because they lack essential nutrients and antibodies present in human breastmilk (Sazawal et al., 1995). In agricultural societies, the addition of cereals to animal milk to form a soft, weaning gruel creates additional depletions in nutrients due to cereal phytates blocking calcium absorption in the gut (Dunnigan and Henderson, 1997; Binns, 1998).

Although metabolic stressors have the most significant impact on health during infancy and early childhood, early stress-inducing events increase susceptibility to additional stressors well into late childhood and adolescence (Goodman and Armelagos, 1989; Lewis, 2007). Perturbations to metabolic homeostasis continue throughout ontogeny, and are caused by multiple factors, including nutrition, disease, and psychosocial stress (Stratakis et al., 1995). These are known to induce growth retardation, although catch-up growth is likely to erase these effects in early and late adolescence (Prader et al., 1963; Bogin, 1999). But, as evidenced by cemetery demographics, subadults often do not survive long enough to recover from stress events.

There is a general perception among historians and archaeologists that subadults were viewed and treated differently from adults in the past (as discussed regarding activity in Chapter

2), as well as in comparison with modern subadults, and this disparity included decreased access to nutritious foods and healthcare compared with modern-day practices (Pollock, 1983). The site sampled for the research conducted herein is located in Eastern Europe, and so understanding the past treatment of subadults in Europe provides an appropriate context. For instance, there were often few, if any, laws or social customs preventing physical child abuse (Glencross and Stuart-Macadam, 2000).

In his pioneering work on the history of medieval European childhood, Ariès (1962) proposed that modern conceptions of childhood arose during the Industrial age, whereas beforehand parents treated their children unsympathetically, expecting them to behave no differently than adults. This apparent coping mechanism for the high rates of child mortality is purported to have led to mistreatment and neglect. Though this hypothesis has been extensively debated and shown to be a spurious generalization (cf. Pollock, 1983; Sofaer Deverenski, 2000), continued research on childhood in archaeological contexts has shown that life was often difficult for immature individuals. By late childhood and adolescence cultural expectations for self-sufficiency and independence were common; such expectations could have been accompanied by high physiological stress, as young individuals coped with increased risks of poor health and occupational hazards (Bogin, 1999). The accumulated effects of these metabolic insults, arising from social practices and environmental conditions, may be evidenced by the examination of metabolic bone disorders in past populations.

Metabolic Bone Disorders and Bone Loss

Despite the caveats introduced by the osteological paradox, bone mass is frequently employed as an overall indicator of health in skeletal assemblages, based on correlations between

numerous metabolic diseases and systemic bone loss (Brickley and Agarwal, 2003). Metabolic bone disorder is defined here as any condition that disrupts bone modeling and/or remodeling processes. These disorders upset bone balance by interrupting mineral homeostasis pathways and, thus, tipping the scales in favor of bone resorption; however, they may additionally manifest as decreases in bone *quality* (i.e., mineralization or material properties) (Marie et al., 1982; Grynpas and Holmyard, 1988; Parfitt, 1998), which are quite difficult to evaluate in archaeological bone due to diagenesis (Stout, 1978; Grynpas, 2003). (Diagenesis is the combined effect of environmental factors on changes to the chemical and structural properties of bone in a burial context.) Metabolic bone loss, referred to as secondary osteopenia (in contrast to the primary osteopenia caused by advanced age), is correlated with increased bone fragility and risk of fracture (Turner, 2002; Brickley and Ives, 2008). When incurred during growth, metabolic bone disorders might affect long-term health and survival later in life (Cameron and Demerath, 2002) and may increase the risk of developing adult osteopenia and osteoporosis (Grech et al., 1985).

One of the main functions of the skeleton is to act as a calcium reservoir; any condition that lowers serum calcium or inhibits calcium absorption will stimulate bone resorption to release these stored nutrients into the bloodstream (Rizzoli and Bonjour, 1999; Parfitt, 2003; Shapiro and Heaney, 2003). The complex interactions between numerous essential nutrients and hormones create multiple pathways that influence calcium metabolism (Figure 5). Deficiencies in essential nutrients (e.g., protein, phosphorous, vitamin C, vitamin D, potassium, and magnesium) disrupt calcium metabolism. However, metabolic disorders are best understood as caused by disturbances in the normal balance of ratios between nutrients rather than simply deficiencies in them (Huss-Ashmore et al., 1982; Mailhot et al., 2007). For example, having

adequate or extremely high levels of calcium in the diet is less osteogenic than an optimal balance of calcium and phosphorus (Shapiro and Heaney, 2003). Additionally, several hormones (e.g., estrogen, parathyroid hormone, calcitonin, glucocorticoids) influence bone resorption and formation, and circumstances affecting their synthesis or concentrations within the body, including factors arising from diet, also influence mineral homeostasis (Raisz, 1999, 2005).

Multiple metabolic diseases are responsible for bone loss, although not all of them are easily identified in human skeletal samples. The complex etiology, cellular pathways, and skeletal consequences of these disorders are beyond the scope of this project; however, the most

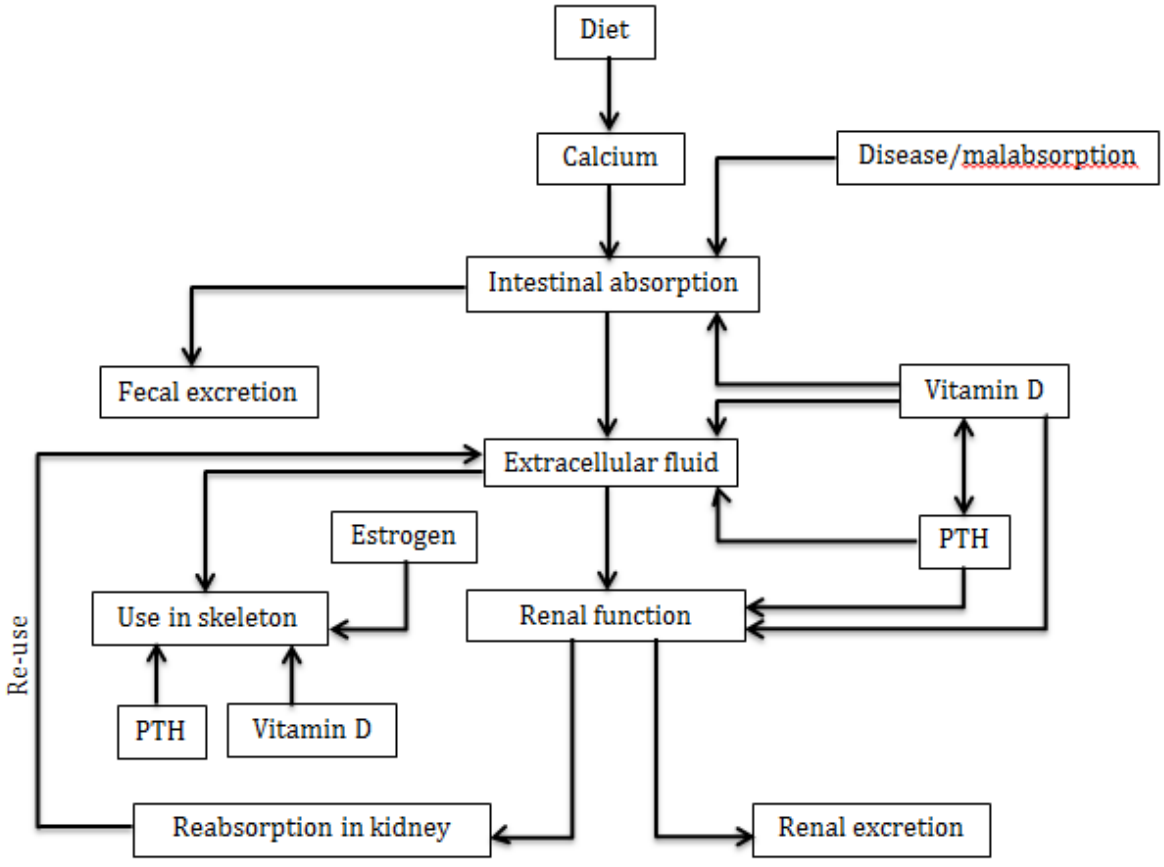

Figure 5. Diagram of the complex mechanisms regulating calcium metabolism (adapted from Brickley and Ives, 2008).

relevant ones that affect subadults are explained briefly below with an account of their effects on bone mass. This information is presented to demonstrate how prevalent bone loss can be in the archaeological record at the macroscopic and microscopic level, especially in subadults, and serves as an argument for comparing bone mass among stress groups within the study sample (see *Methods* in Chapter 4 for specific descriptions of metabolic stressors in the study sample).

Scurvy

Deficiency in vitamin C, referred to as scurvy, is a common affliction in subadults. Vitamin C is necessary for collagen formation and proper immune function, and individuals lacking this nutrient are prone to hemorrhage and commonly develop anemia (Clark et al., 1992; Ortner, 2003). Scurvy is common in early-weaned infants, as vitamin C is present in high levels in the breastmilk of healthy women and relatively low in cow's milk (Grewar, 1965; Severs et al., 1961; Fain, 2005) and cereals (Brickley and Ives, 2008). Individuals suffering from scurvy exhibit decreased osteoblastic activity and restricted osteoid deposition (Ortner et al., 2001; Fain, 2005; Brickley and Ives, 2006). Subadult scurvy is associated with radiologically detected osteopenia across the skeleton, but osteopenia manifests especially in elements containing mostly trabecular bone (e.g., vertebrae and pelvis) and rib elements (McCann, 1962). In severe cases, cortical thinning occurs in long bone diaphyses (Grewar, 1965). Histological studies have found generalized cortical osteopenia in adults (Bourne, 1942), but no studies have assessed histological features of scurvy in subadults.

Rickets and Vitamin D Deficiency

Vitamin D plays a significant role in mineral metabolism and immune response and, furthermore, is crucial for the proper mineralization of freshly deposited osteoid (Cowin, 2001).

Vitamin D regulates calcium homeostasis by promoting intestinal absorption of minerals and governing renal absorption and excretion to maintain adequate serum levels of calcium and phosphorous (Heaney, 1997). Synthesis of vitamin D is reliant on skin exposure to the sun as well as dietary intake (Pettifor, 2003); therefore, cultural practices (e.g., clothing, occupation), climate, and seasonality affect the prevalence and severity of vitamin D deficiency and were likely the chief factors in the etiology of this disease in past populations (Mays et al., 2006).

Vitamin D deficiency in children leads to rickets, a pathological condition characterized by decreased bone mineralization and increased bone loss (Hollick, 2006). Infantile rickets is more prevalent in malnourished mothers and within societies with inadequate weaning foods (Jelliffe, 1955; Pettifor, 2004). High amounts of cereals in the diet also cause calcium imbalance and vitamin D deficiency when phytates bind to calcium molecules, preventing their absorption (Dunnigan and Henderson, 1997). Rickets is associated with radiological appearance of generalized osteopenia; in the long bones high porosity, as well as trabecular and cortical bone loss, are noted (Pettifor and Daniels, 1997). In histological sections, rachitic cortical bone exhibits diminished bone formation, poorly organized bone, increased resorption spaces (especially converging ones), and mineralization defects (Mankin, 1974; Pitt, 1988).

Non-specific Metabolic Diseases

Other generalized metabolic disorders (e.g., pellagra, protein-calorie malnutrition, hyperparathyroidism, anemia) are linked to bone loss but do not present as diagnostic diseases in archaeological samples. All of these conditions result in secondary osteopenia at both the macroscopic and microscopic levels and are often exacerbated by the biological, cultural, and environmental factors outlined above (Ross, 1998; Christiansen, 2001; Mays et al., 2001; Paine

and Brenton, 2006). As stated previously, subadults are highly susceptible to these types of disorders, especially in communities that experience high rates of infectious disease and wherein sanitation conditions promote factors contributing to high prevalence of chronic diarrhea. Macroscopically, secondary osteopenia manifests as cortical thinning and reduced bone formation rates, while histologically it is defined by increased resorption spaces, incomplete osteon filling, and greater osteon size (Martin and Armelagos, 1979; Burr et al., 1997; Zink et al., 2005; Peck and Stout; 2007).

Metabolic Bone Loss and Bone Strength

As discussed in Chapter 2, bone mass and bone strength are strongly interrelated, although in long bone diaphyses the relationship between bone mass and strength is less straightforward. Otherwise, depending on the strain stimulus, amount of resorption, and location of deficits, bone loss (i.e., reductions in bone mass) potentially will result in reductions to bone strength (Lambert et al., 2005; Seeman and Delmas, 2006). Reduced bone mass leads to greater strains within the bone under a given magnitude of force and stimulates bone deposition to return strains to the customary level and avoid fracture (Frost, 1987, 1990a, 1990b). However, this negative feedback loop within the mechanostat model applies only in non-pathological cases; the ability to respond to bone loss with bone deposition is highly dependent on the individual's metabolic status, as well as age, sex, and ethnicity (Parfitt, 2003). In other words, bone loss leads to bone fragility in situations of failed adaptation. In addition to reduced bone mass, metabolic deficiencies in bone *quality* (i.e., microarchitecture, mineralization, and mechanical properties) also affect strength (Grynpas, 2003). Accretion of under-mineralized bone tissue, for instance, leads to weakened areas and increased strains (Parfitt, 1986; Martin and Ishida, 1989; Fratzl-

Zelman et al., 2011). However, as mineralization cannot be adequately assessed in archaeological populations (due to diagenesis, among other factors), the remainder of the chapter will focus on bone mass structural changes, specifically which surfaces experience loss and how strength is subsequently affected.

Morphologically, declines in cortical bone strength are attained in three ways: 1) reductions of macroscopic bone mass through endosteal resorption; 2) more generalized reductions of cross-sectional geometric strength properties through bone loss or changes in shape; and 3) disruptions to the osteonal remodeling processes (Martin et al., 1998; Currey, 2003). Each of these structural alterations has been connected with metabolic bone disorders. The following section, *Macromorphology,* focuses on macroscopic reductions in cortical bone mass and their effect on bone structure. The *Micromorphology* section discusses pathological modifications to microscopic structure with implications for whole bone strength.

Extensive clinical research has been the foundation upon which researchers have achieved an understanding the etiology of these cortical bone reductions. Age-related and disorder-driven osteoporosis has been especially valuable in underscoring the structural consequences and mechanisms underlying metabolic bone loss. Osteoporosis is referenced here even though it does not directly apply to metabolic disturbances in subadults, as osteoporosis is itself a metabolic bone disorder and the mechanisms underlying bone loss are similar to processes in subadults. In fact, most clinical studies have focused on osteoporosis, as it has become an increasing health concern in the past few decades, and less research has been performed on nutritional deficiencies and their effects on bone strength. Anthropological research exploring bone loss in human skeletal samples is also presented in light of these clinical

findings. These studies help shape the hypotheses set forth by the current analysis by establishing the morphological shifts in cortical bone caused by metabolic stress.

Macromorphology

Basic Structure

Metabolic bone loss at the macroscopic level typically occurs from excessive cortical resorption at the endosteal surface (i.e., near the neutral axis), where strains are lowest, resulting in an expanded medullary cavity and reduced cortical area. This process occurs in both ribs (Paine and Brenton, 2006; Agnew and Stout, 2012) and long bone diaphyses (Garn et al., 1964, 1969; Frost, 1966; Lazenby, 1990a, 1990b). Under compression and bending loads, long bones experience increased strain due to endosteal bone loss, generating bone deposition at the periosteal surface—where strains are the highest—to restore customary strain levels (Lazenby, 1990b). As discussed in Chapter 2, this adaptive compensation results in the redistribution of a smaller amount of cortical bone further from the centroid of the cross-section and, therefore, increased strength in bending and torsion. Such restructuring is advantageous in terms of tissue economy; given reduced cortical thickness, a small amount of bone added periosteally produces significant improvements in resistance to loading. However, in cases of metabolic stress, physiological resources may not be available to allow for periosteal deposition (Szulc et al., 2006; DeVista et al., 2007), though the conditions required to cause such disturbance in normal bone balance processes are variable and unclear.

Periosteal compensation disrupts the direct correlation between bone mass and bone strength, making the investigation of metabolic effects on strength more complex. Lack of

consideration for structural compensation has limited analyses of metabolic bone disease; reductions in cortical area do not necessarily indicate reduced strength. Yet, a recent appreciation of the complexity of bone functional adaptation in response to both mechanical and metabolic inputs has improved understanding of morphological shifts in cortical structure and informed analyses of bone in archaeological contexts.

Experimental Non-Human Animal Studies

Experimental studies utilizing non-human animals have been key to understanding metabolic effects on cortical bone, because studies using humans are limited in experimental control and involve the application of invasive techniques. Researchers control and account for factors such as dietary intake, exercise, hormone levels, and the type and severity of metabolic disturbance in experimental studies. Model animal subjects can also be sacrificed to investigate bone properties through destructive methods, such as mechanical testing and histomorphometry. As reviewed in Chapter 2 and above, non-invasive imaging methods are inadequate in revealing many of these properties. Early studies on malnourished pigs and cockerels were among the first to demonstrate expanding medullary areas in long bone cross-sections coincident with reduced periosteal apposition (Dickerson and McCance, 1961; Pratt and McCance, 1961; McCance et al., 1962); these studies showed that severe calorie restriction increases bone resorption and inhibits bone formation. However, these experiments were conducted with small sample sizes and did not calculate the cross-sectional geometric properties that account for bone mass distribution (e.g., second moments of area and section moduli). Therefore, while foundationally informative, their conclusions were somewhat limited in scope.

Recent, focused animal studies have revealed more about the location-specific and time-dependent skeletal effects of malnourishment-induced metabolic stress. Guinea pigs are good model organisms for human diseases, as human disorders (especially scurvy) may be induced in them that other model organisms will not develop. Induction of scurvy in developing guinea pigs caused decreased body weight, shorter femoral length, reductions in BMD at the distal and midshaft of the femur, and reduced trabecular number and thickness at the proximal tibia than occurred in control animals (Kipp et al., 1996). Most importantly, calculations of bending strength showed no significant differences between the experimental and control groups for the femur, indicating that, despite systemic effects of vitamin C deficiency on bone mass, femoral strength was not reduced. However, scorbic animals did exhibit lower vertebral body strength relative to controls (Kipp et al., 1996). Skeletal site-specific differences in responses to metabolic stress, then, occurred, with more adaptive compensation in appendicular long bones than in axial elements, wherein the amount of cortical bone is reduced relative to trabecular bone.

Rats and mice, which are frequent models for malnutrition and osteoporosis research, have offered crucial insight into mechanisms of bone loss and potential treatment options. Ammann et al. (2000, 2002) demonstrated depressed periosteal apposition and enhanced endosteal resorption in the midshaft tibiae of ovariectomized and protein-deficient adult rats. This supports early findings in pigs and cockerels, though these effects were not present until 16 weeks following a protein-deficient diet. After 8 weeks of a low-protein diet, the only detectable deficits were low BMD at sites containing high proportions of trabecular bone (i.e., proximal tibia, lumbar spine, proximal and distal femur) (Ammann et al., 2000). The authors proposed that metabolic stress might have an earlier effect on trabecular bone because of its relatively higher turnover rate, though continued malnutrition would eventually lead to cortical reductions. These

conclusions were further supported by reversal of protein-deficiency in these rats, whereby the tibial midshaft was delayed in its osteogenic response to the restoration of a normalized diet in comparison with skeletal elements comprised of more cancellous bone (Ammann et al., 2002).

Devlin et al. (2010) found similar reductions in body mass, bone length, and trabecular and cortical BMD at the midshaft and distal femur and the lumbar spine in calorie restricted, immature mice. After adjusting for differences in body mass, reductions in femoral cortical area and cross-sectional strength properties were not significantly different between experimental and control groups after 3 weeks of dietary restriction, but these were significantly lower in the experimental group after 9 weeks. However, after 12 weeks, alterations to material properties (inferred from three-point mechanical testing) suggested that malnourished mice were compensating for inferior macrostructure by altering local elastic modulus.

These results underscore the need for investigations of microarchitecture and quality in addition to macroscopic analyses. Furthermore, despite reduced total body fat, malnourished mice possessed higher femoral bone marrow adiposity than controls. Marrow adipocytes have an antagonizing effect on osteoblasts and osteoclasts and, thus, have been linked to reduced osteogenesis. This relationship may be responsible for expanded medullary areas and enhanced endosteal resorption in human adolescents and young adults (Iorgi et al., 2008; Bredella et al., 2009; Casazza et al., 2012). Additionally, although bone reductions were present in the vertebrae, the effect was less than what was observed in the femur (Devlin et al., 2010). The authors hypothesized that calorie restriction may cause greater deficits in cortical and trabecular bone in the appendicular skeleton relative to the axial skeleton during growth, perhaps as an adaptation to preserve hematopoietic stem cells.

These studies have important implications for the research presented in the following chapters. Like the formation of skeletal stress lesions, metabolic bone loss is variable in its degree of expression, timing of response, and distribution within the skeleton. The physiological stressor must be a certain duration and magnitude to affect cortical bone; therefore, the osteological signatures of these stressors are more likely to be present in individuals from cemetery samples who experience and recover from chronic stress and not in those who succumb to a stressor quickly. Whether predisposition to metabolic bone loss in appendicular elements holds true for immature humans remains to be seen; however, its existence would refute the mechanostat model. Higher rates of bone loss in the human femur relative to axial regions suggests heightened importance of metabolic over mechanical demands, in terms of ultimate effects on bone strength. Studies such as those discussed above and in the following subsection highlight the complex relationships among environmental factors and caution against wholesale acceptance of bone optimization theory.

Human Clinical Studies

The bone-specific and surface-specific effects of metabolic disorders demonstrated in experimental animal studies are generally supported by research of human responses to metabolic stressors. Most human clinical studies can be categorized into two groups: those that correlate BMD and/or strength properties with dietary intake deduced from questionnaires and those that monitor bone properties under specific levels of vitamin supplementation. These analyses have documented strong positive relationships between adequate dietary mineral levels (especially calcium) and BMD, as well as peak bone mass, across multiple skeletal locations in both adults (Chiu et al., 1997; Riggs et al., 1998; Heaney, 2000; Kumar et al., 2010) and

immature individuals (Matkovic et al., 1990; Specker and Binkley, 2003; Vatanparast et al., 2007; Prais et al., 2008). These relationships underscore the systemic response of bone to metabolic demands. Most research outcomes have influenced clinical methods for reducing or preventing osteoporosis; however the subjects are typically healthy individuals without significant nutritional deficiencies. Thus, research using human subjects experiencing chronic malnutrition is more relevant to this study. For this reason, discussion of human subjects research focuses on conclusions drawn from studies of individuals suffering from anorexia nervosa.

Anorexia nervosa (AN) is a psychopathological eating disorder that disproportionately affects female adolescents and young adults, and is associated with reductions in body weight, lean body mass, and percent body fat, as well as diminished trabecular and cortical BMD. Researchers have estimated that roughly 90% of adult and adolescent women with AN have osteopenia and about 40-50% have osteoporosis, suggesting that bone loss is almost a universal trait of this disorder (Legroux-Gerot et al., 2007). This bone loss is commonly permanent, despite full recovery from the disorder, which typically occurs after the cessation of growth (Kooh et al., 1996).

Although evidence points to uncoupled mineral metabolism in AN, the exact mechanisms of bone loss are poorly understood, mainly due to over-reliance on evaluating BMD through imaging methods (e.g., DXA) that are incapable of calculating true bone material losses (see Chapter 2 for a full discussion). As reviewed above, multiple hormonal and nutritional factors contribute to metabolic deprivation leading to bone loss; the chronic undernutrition in AN patients is linked to low levels of estrogen, insulin-like growth factor I (IGF-I), vitamin D, leptin, and testosterone (Fernandez-Garcia et al., 2009). Amenorrhea is common in females with AN, and the associated estrogen deficiency is likely responsible for significant bone mass reductions

in many cases (Klibanski et al., 1995; Munoz et al., 2002), though it is certainly not the only factor contributing to low bone mass (Bachrach et al., 1990; Valla et al., 2000; Roberto et al., 2008), and males with AN also suffer significant bone loss (Castro et al., 2002; Misra et al., 2008).

Studies of AN are relevant to the present study especially because of their capacity to compare effects of body mass (i.e., mechanical effects) with those that arise from undernutrition (i.e., metabolic effects). Galusca et al. (2008), for example, compared constitutionally thin (non-anorexic) women with low body mass to anorexics and controls. Results of their study indicate that low bone mass and strength in anorexics and other chronically undernourished individuals may be more closely associated with the relationship between nutrition and body mass rather than simply nutritional factors themselves. Despite constitutionally thin women having significantly higher fat mass and no indication of abnormal bone turnover (i.e., normal urinary bone markers), both constitutionally thin women and anorexics possessed decreased BMD at the femoral neck and lumbar spine and reduced bending strength at the radius and tibia (with effects greater at the tibia than the radius). However, significantly reduced cross-sectional geometry at the femoral neck and shaft in adolescent anorexics relative to controls persisted even after adjusting for lean mass, suggesting that metabolic *and* loading factors may both affect the lower limb (DeVista et al., 2007). There did not appear to be periosteal compensation for expanded endosteal borders in these individuals, providing support for the possible influence of metabolic disturbance on even strongly loaded skeletal elements (DeVista et al., 2007).

Moreover, analyses of reductions in BMD that occur with AN reveal differential responses to systemic metabolic stress throughout the skeleton, particularly during growth, though the variation in specific skeletal location effects remain unclear. Positive relationships

have been found between BMD deficits and weight loss (Baker et al., 2000; Wong et al., 2004) and with longer durations at lower weight (Hotta et al., 1998). The most drastic effects on BMD take place prior to peak bone mass—that is, during growth—and the affected skeletal locations appear to vary depending on the age of metabolic disturbance and the magnitude of mechanical influence. Seeman and colleagues (2001) discovered that adult AN onset resulted in modest reductions in bone mass mostly in the spine, whereas onset prior to puberty, and especially during early puberty, caused considerable deficits in both lumbar vertebrae *and* femora. They concluded that rapid appendicular growth during early ontogeny was responsible for the differences in axial and appendicular skeletal responses to undernutrition.

Similarly, in adult women who developed AN as adolescents, reduced adult cortical BMD was most pronounced in the radius relative to the hip and spine (Milos et al., 2005). Seeman et al. (1992) documented hormonal effects on the lumbar vertebrae but not femora in anorexic women taking oral contraceptives, but anorexic women who exercised possessed higher BMD at the femoral neck than sedentary controls and sedentary anorexics. From these results, the authors inferred that axial regions may be more sensitive to hormonal inputs, while appendicular areas may respond better to weight-bearing exercise. These studies suggest skeletal site-specific differences in relative responses to local mechanical and systemic metabolic inputs.

While AN reductions in BMD are well-documented, researchers have scrutinized them, as these studies are not able to directly measure *actual* bone loss in malnourished individuals. The critiques raise an important caveat in using the results summarized above uncritically to inform expectations for the present study. In a recent article, Bolotin (2011) gives a strong argument for questioning results from AN studies utilizing DXA and other such imaging techniques, as it is widely-known that that this imaging method will misestimate differences in

bone mass under conditions of altered extra-skeletal fat and intraosseus marrow conditions. Therefore, BMD studies on malnourished individuals are particularly prone to inaccuracy. Errors would be especially predominant in skeletal locations with high trabecular bone, such as the lumbar spine and femoral neck, the only sites which have shown consistent evidence of bone loss with AN across numerous studies.

A combination of cross-sectional geometric and histomorphometric analyses at the same skeletal sites would be beneficial in confirming or denying the existence and location of possible metabolic bone loss; such studies are rare in the clinical literature, and when histomorphometric analyses are incorporated, they frequently involve trabecular architecture, rather than cortical histology, in conjunction with trabecular or cortical BMD as supplementary evidence of bone loss (see *Micromorphology* below). Without such methodologies, it is difficult to deduce the exact effects of bone loss on cortical strength. For example, decreased trabecular microarchitecture at the distal radius in AN patients without a concomitant reduction in BMD at this site (Lawson et al., 2010; Bredella et al., 2008) is difficult to interpret, as DXA cannot distinguish between cortical and trabecular bone. Furthermore, few AN studies take into account loading differences between skeletal sites or variation in activity levels between individuals, which could have a significant influence on how metabolic bone deficits are distributed within the body.

Application to Anthropology

The advantage of clinical and experimental studies is that the etiologies of conditions, as well as the pathological conditions, are documented with respect to osteological effects. Yet, anthropological perspectives contribute unique insight into skeletal mass and health through the

appreciation of individual variation and capacity for human biocultural adaptation to stressful events. The nature of skeletal samples from past populations also permits exact evaluation of cortical bone macrostructure through methods (e.g., cross-sectional geometry) more conducive to understanding the effects of metabolic shifts on bone strength than is possible in clinical studies.

Adult Research. In biological anthropology studies, reduced cortical area in various skeletal elements has been used to infer health status in adult skeletal samples. For example, reduced macroscopic bone mass in ribs was found in association with pellagra in 20th-century black South Africans from the Raymond Dart skeletal collection (Paine and Brenton, 2006; Brenton and Paine, 2007). In this sample, reduced rib mass was correlated with pathological indicators of non-specific metabolic stress associated with malnutrition, including dental caries, cribra orbitalia, enamel hypoplasia, periostitis, and osteomyelitis (Paine and Brenton, 2006).

Likewise, long bone cortical loss has previously been used to indicate metabolic stress (Garn et al., 1964, 1969; Martin and Armelagos, 1979; Martin et al., 1985; Mays et al., 2009) and track dietary shifts in past populations (Garn, 1970; Pfeiffer and King, 1983; Cook, 1984; Bridges, 1989; Larsen, 1995). Periosteal compensation for increased medullary area in the metacarpals of malnourished, living Guatemalan boys demonstrated the influence of metabolic bone loss on long bone cortices (Garn et al., 1964, 1969). Many other studies have shown a global trend towards increased osteopenia in agricultural groups relative to foraging societies (Cohen, 1989; Martin et al., 1984; Ulijaszek, 1991; Larsen, 2003). This tendency for inferior skeletal health to accompany agricultural subsistence may be due to intensifying reliance on cereals, which are poor sources of vitamins C, A, and D, as well as having low levels of iron, calcium, and sodium (Brickley and Ives, 2008).

Complex and unexpected patterns in diaphyseal robusticity within and between human populations have also shed light on potential nutritional effects. Most of these insights emerge from comparisons between human populations with dietary differences, dissimilar subsistence strategies, or varying activity levels. For instance, foraging adults from groups that lived in the Western Great Basin had extremely low femoral CA relative to other foraging groups but high femoral TA and J, as well as greatly reduced humeral CA and J (Larsen et al., 1995). The presence of high strength in the femur in spite of reductions to bone mass indicates higher mechanical loading in the lower limb, and thus greater mobility or movement in a more rugged environment; however, the low CA in both the femur and humerus was argued to be indicative of some type of systemic metabolic influence (Larsen et al., 1995; Larsen, 1997).

Fewer studies have made comparisons of cross-sectional geometric properties among subgroups within populations to assess dietary differences (e.g., due to socioeconomic status or social hierarchy). Based on burial location in mounds versus villages at the Dallas Site in East Tennessee, Hatch et al. (1983) found smaller CA in the femoral midshafts of high status adults relative to low status adults. Though high status individuals frequently engage in less physical activity than low status individuals (Maggiano et al., 2008)—which in turn could have accounted for decreased cortical bone in mound burials (Hatch et al., 1983)—this trend could also be due to nutritional differences. Improved nutrition is not a universal characteristic of high status individuals (Danforth, 1999; Buzon, 2006). Evaluation of cross-sectional strength properties in addition to cortical area in this population and the comparison of both highly loaded and relatively less loaded skeletal elements could possibly have improved the ability to effectively ascertain the cause of reduced macroscopic bone mass among status groups. Studies of bilateral

directional asymmetry in the upper limbs, similarly, would also shine light on possible causes (e.g., Stock and Pfeiffer, 2004).

Like many clinical studies, anthropological examinations of metabolic status tend to draw exact associations between diet and macroscopic bone mass without attempting to account for the influence of mechanical loading. Comparisons are frequently made within the same element across populations with potentially different and unknown physical activity. As discussed previously, measures of cortical area may relay incomplete information on bone health due to mechanical adaptations (Ruff and Larsen, 1990; Ruff, 1992; Pfeiffer and Lazenby, 1994). Accounting for mechanical effects is especially important when the skeletal location of interest is under strong loading demands (i.e., long bones), and recent appreciation of this fact has led to increased reliance on regions that experience less mechanical loading (e.g., rib cage) for metabolic assessments (Robling and Stout, 2003; Agnew and Stout, 2012).

Crucial to the present study, although this approach is certainly the more suitable one for metabolic studies, overreliance of analyses on a particular skeletal region of interest and a single environmental factor of interest has restricted the ability to shed light on interaction effects between mechanics and metabolism within the body. Furthermore, due to this restriction in research the systemic manifestation of macroscopic bone loss due to metabolic stress has not been thoroughly demonstrated in an archaeological sample, though systemic effects are frequently presumed (see Hypothesis 1a in Chapter 1). Only if systemic bone loss were evident among all skeletal elements, regardless of the magnitude of mechanical loading, would the strong metabolic influences warrant examination of any single skeletal location for health status.

Ontogenetic Research. Subadult skeletal remains present additional methods to those available in adult skeletons for examining the effects of metabolic stress macroscopically. Long bone growth (both linear and appositional) is considered a sensitive indicator of metabolic status in modern and past populations (Hoppa, 1992; Saunders et al., 1993b; Mays, 1999; Stinson, 2000; Lewis, 2002; Pinhasi et al., 2005, 2006). Ribs, however, have not been systematically analyzed in subadults to infer health. In one of the first analyses of health effects on subadult cortical bone, Cook (1979) interpreted a decline in early childhood long bone cortical thickness as an indication of weaning stress.

This conclusion carried over into other analyses, which refined Cook's findings. For example, in an exceptionally malnourished population in Sudanese Nubia (Kulubnarti), premature osteoporosis was potentially induced through lifelong nutritional inadequacy due to over-reliance on agricultural crops (Martin et al., 1985; Hummert, 1983). Tibial bone length appeared to be maintained throughout growth among the Kulubnarti, but deficits in percent cortical area and second moments of area indicated greater endosteal resorption immediately after weaning and following age twelve (Hummert, 1983; Van Gerven et al., 1985). Rapid increases in second moments of area tended to follow periods of enhanced bone loss, so that subadults were mimicking adaptive responses documented in postmenopausal women at Pecos Pueblo, described by Ruff and Hayes (1983) (Van Gerven et al., 1985). However, once subadult samples were examined from a variety of sites representing different subsistence practices and health statuses, Cowgill (2008) demonstrated that this pattern was evidently a consequence of normal growth patterns and not a convincing indicator of metabolic stress. The patterns appear to occur due to cortical area lagging behind growth in bone length and body mass, especially in individuals who have low mass for their statures (Ruff et al., 1994; Ruff, 2003a; Cowgill, 2008).

A recent analysis of subadult cross-sectional geometry has returned results that conflict with those connecting dietary insufficiency and low bone mass in adults. Garofalo (2012) compared high and low status subadults from the Barton-upon-Humber cemetery and found no statistically significant differences in body size, bone length, growth trajectories, and articular dimensions, though these differences would be expected. However, high status individuals tended to have greater diaphyseal cross-sectional properties for size in the humerus, femur and tibia, although results do not reach significance until the age of 14 and only in the femur. This pattern does not support the hypothesis that high status children and adolescents were engaged in less manual labor than those of low socioeconomic status. Also contrary to expectations, high status subadults under the age of four possessed *lower* percent cortical areas and higher medullary areas compared to low status individuals of the same age, though this difference was not statistically significant due to small sample sizes. These results point to inadequate nutrition (e.g., improper feeding practices among higher classes) and more vigorous mechanical loading before mid-adolescence in higher status individuals.

Garofalo (2012) proposed that such unexpected patterns could be caused by selective mortality. High status infants and children may have had better access to medical care, and therefore, unhealthy individuals were more likely to survive long enough to develop reduced cortical area. Similarly, low status individuals with limited healthcare would have succumbed to acute illnesses quickly, entering the mortuary sample prior to skeletal response and appearing healthier based on cortical morphology. Though she eliminated subadults with systemic skeletal lesions from her sample, Garofalo did note that high status individuals were more prone to advanced and long-standing lesions (e.g., bone deformation). This research has been significant in documenting key points to be addressed in the present study; namely, the effects that selective

mortality and hidden heterogeneity have on bone mass and strength properties, in addition to traditional paleopathological evaluations, should be further investigated in subadult skeletal samples. In the present study, it is conceivable that individuals with non-specific stress lesions represent high status or "healthier" individuals; however the presence of such lesions is likely to correlate with propensity for metabolic bone loss given the extended duration of stress, regardless of whether the individuals are considered "healthy" or "unhealthy" (see Chapter 4, *Methods*).

Micromorphology

Basic Structure

Microscopically, metabolic bone loss reduces bone strength mainly through increased porosity (higher numbers of resorption spaces, larger resorption spaces, and/or incomplete osteon filling) (Martin and Armelagos, 1979; Marie et al., 1982; Burr and Martin, 1989; Burr et al., 1997; Wachter et al., 2001; Zink et al., 2005; Peck and Stout; 2007). This microscopic bone loss appears to allow for increased nutrient transport within the bone (Metz et al., 2003) but also simultaneously reduces tissue mass, leading to increased local strain (Stout and Simmons, 1979; Pettifor et al., 1984). Even if the individual is eventually able to recover from the metabolic disturbance and fill in these pores with bone matrix to form secondary osteons, bone strength will remain temporarily reduced for some period of time by a rise in unmineralized osteoid matrix (Carter and Hayes, 1977; Boivin et al., 2000; Grynpas, 2003). Such conditions result in reduced material stiffness, resulting in excessive flexibility and deformation under loading and a predisposition to fracture (Seeman and Delmas, 2006).

It has been proposed that occurrence of these deficits would be random (i.e., stochastic) with respect to strain levels within the bone (Martin and Burr, 1982; Burr, 2002; Parfitt, 2002; Martin, 2004). Increased stochastic remodeling would theoretically be distinguished from loading-induced porosity by its widespread location within the cross-section; that is, stochastic porosity would not be restricted to regions with the highest strains. However, it has also been argued that, were porosity to occur without regard to existing bone geometry, weak geometry could potentially be coupled with weak tissue properties and cause especially maladaptive consequences to a bone's failure resistance (Lazenby, 1986; Rosenbaum Chou et al., 2008). Little work has been done on the distribution of remodeling and porosity within cortical bone cross-sections, and it remains possible that BMUs respond to metabolic needs advantageously by removing bone from regions where reductions to bone strength are minimized (i.e., endosteal surfaces and along I_{min}). This certainly appears to be the case with respect to targeted remodeling, as discussed in Chapter 2. It is also unknown to what extent structural alterations to geometric properties are able to offset microscopic bone loss, though even small increases in cortical porosity are able to degrade bone strength regardless of geometry (see below). There is some indication that metabolic stress causes microscopic changes that eventually culminate in macroscopic deficits; therefore, histological studies may be more sensitive to detecting metabolic disturbances on cortical bone than macroscopic analyses.

Porosity and Bone Strength

Many studies have shown that mechanical properties of bone depend on microscopic bone mass, especially the amount of microscopic porosity (Currey, 1988; Schaffler and Burr, 1988; Martin, 1993; Wachter et al., 2002). In fact, even small increases in porosity of a few

percentage points have disproportionally large consequences on bone strength (Davison et al., 2006; Turner, 2002; Dong and Guo, 2004).

Few studies have investigated metabolic effects on rib intracortical porosity, and those that have commonly focused on osteoporosis and rib strength. Ribs are proposed to lose more bone mass with age than any other skeletal element (Epker and Frost, 1965); few studies have been conducted to confirm this assertion with respect to metabolic bone disorders. Early research documented a rise in rib endosteal resorption with advancing age but few changes in intracortical porosity (Epker et al., 1965). Yet, recently, Agnew and Stout (2012) refuted this hypothesis. They found that *absolute* percent cortical area (defined as percent cortical area minus percent total intracortical porosity) was a more accurate measure of bone loss in aging ribs than percent cortical area alone. This occurred due to exceptionally high levels of intracortical porosity in elderly rib sections that could not be accounted for by measures of total cortical area (which fails to include microporosity). Based on their results, the authors proposed that the role intracortical porosity plays in raising the incidence of rib fractures may be underestimated; therefore, conclusions about the resistance of bone to loading drawn from cortical area alone may be erroneous (Agnew and Stout, 2012).

Most studies of long bone diaphyseal cortical bone have focused on osteoporotic changes in the adult femur and offer essential information concerning the morphological consequences of metabolic bone disorders. For instance, age-related increases in cortical bone porosity at the femoral neck have been linked to elevated risk of fracture (Bell et al., 1999a, 1999b; Yeni and Norman, 2000). In the adult femoral midshaft, porosity increases with age in non-pathological cases (Currey, 1964; Jowsey, 1966; McCalden et al., 1993; Bertelsen et al., 1995; Feik et al., 1997; Stein et al., 1999; Bousson et al., 2000, 2001; Thomas et al., 2005), and these increases are

more enhanced in osteoporotic individuals. Additionally, results of mechanical testing show that Young's modulus and shear modulus are significantly negatively correlated with porosity in femoral cortical bone (Dong and Guo, 2004), as well as radial and tibial cortical bone (Burghardt et al., 2010). Other metabolic bone disorders, such as malnutrition, may also cause extensive intracortical bone loss in both rib and long bone elements (see below); however, whether these deficits are evenly distributed within the skeleton or vary depending on the biomechanical demands placed on skeletal elements has not been explored thoroughly or in a subadult sample (see Hypotheses 1b and 2b in Chapter 1).

The exact etiology and manifestation of metabolic increases in cortical porosity still remains uncertain. For instance, highly porous bone may not result from merely an increase in the number of pores but the size of pores. Stein et al. (1999) reported that elderly humans did not possess greater numbers of pores their femoral diaphyses relative to younger adults, but rather a greater proportion of large pores. Likewise, Bousson et al. (2001) found increased pore size and number with age in the femoral midshaft of individuals under the age of 60, whereas elderly subjects exhibited decreased pore number and increased pore size. This phenomenon was also detected at the femoral neck (Bell et al., 1999). It is unclear, however, whether this trend is caused by increased osteoclastic activity *within* BMUs (resulting in larger resorption spaces), higher numbers of active BMUs overlapping to form larger pores, lags in osteon filling stemming from inhibited osteoblastic activity, or some combination of all these processes (Srinivasan et al., 2000). There are multiple pathways that could cause similar morphological results, and these conditions may vary with factors such as the type and duration of metabolic stress or the skeletal location.

Additionally, metabolic bone loss appears to occur simultaneously with macroscopic alterations, yet also independently of them. Several studies have documented elevated levels of cortical porosity in addition to thinning cortices in the femoral neck of patients with fractures relative to age-matched controls (Barth et al., 1992; Bell et al., 1999). However, Squillante and Williams (1993) found no differences between fracture and non-fracture groups in total femoral neck cortical area, though cortical porosity was higher in individuals with fractures, indicating that tissue-level modifications may influence bone strength regardless of macroscopic mass (macroscopic distribution was not taken into account). These results support findings by Yeni and colleagues (1997, 1998), who demonstrated a negative relationship between cortical porosity and bone toughness in human femora and tibiae that occurred independently of bone mineral density. Furthermore, Yeni et al. found that an increase in cortical porosity of as little as 5% caused a 50% decline in toughness.

Microscopic bone loss has surface-specific effects on cortical bone, which vary with factors such as age and sex, but generally supports the theory that bone mediates metabolic needs in an attempt to maintain bone strength. Microscopic variation within cortical cross-sections has been documented both radially (between periosteal and endosteal envelopes) and circumferentially (between anatomical axes and cortical sections) (e.g., Thomas et al., 2005). Very little is known about the distribution of metabolic bone loss within cortical bone in children and adolescents, but effects in adult long bones point to strength conservation in bones and bone regions with high loading demands. Bousson et al. (2001) found that the distribution of intracortical porosity in the femoral midshaft was uniform in adult males but occurred predominantly on the endosteal surface in females, resulting in cortical thinning. In this case, bone was removed from the area of the cross-section under the least loading. However, the

authors did not evaluate cross-sectional geometry to determine if periosteal compensation occurred in these women. Therefore, it is not clear whether females maintained femoral strength (despite the appearance of macroscopic net bone less) relative to males who displayed normal, yet porous, cortices.

In a similar study on adult males, Martin et al. (1980) found comparable patterns but, moreover, showed potential biomechanical mediation of systemic age-related porosity in the femur, humerus, and metacarpal. Microscopic losses with age were greatest in the humerus and least in the metacarpal, while the femur exhibited intermediate deficits. Martin and colleagues postulated that this pattern may reflect the relative degree of biomechanical influence in these elements, assuming that even sedentary, elderly men would continue to use their hands. In addition, while increased geometric properties in all three elements appeared to compensate for microscopic losses, these properties declined in the most elderly individuals (Martin et al., 1980), which may indicate adaptive failure under extended metabolic disturbance. As geometric response to metabolic disturbance will vary depending on the physiological status of the individual, microscopic losses may be even more detrimental to bone strength under conditions of malnutrition if macroscopic compensation does not take place.

A notable study on porosity distributions along mechanical axes found increased porosity along I_{min} relative to I_{max} in a small sample of healthy adult femoral midshafts (Lazenby, 1986). In a human femur, bending about the axis of maximum bending rigidity will generally cause tension and compression forces in the two cortical sections bisected by I_{min}; and, thus, increased porosity along I_{min} represents a mechanical advantage relative to other scenarios, because it reduces bending rigidity about I_{max} (where the bone is most resistant to bending). This scenario would make I_{max} and I_{min} values within a cross-section more similar to one another. Conversely,

if porosity were to increase along I_{max}, I_{min} bending rigidity would be diminished significantly relative to I_{max} and cause great disparity between I_{max} and I_{min} values (Rosenbaum Chou et al., 2008). From these results, Lazenby concluded that net bone loss will occur in regions of long bone diaphyses where strength will not be compromised; in other words, adaptive bone balance involves coupling of weak microscopic properties (i.e., increased porosity) with strong geometric properties (i.e., along the axis of minimum bending rigidity). This hypothesis is tested with regard to metabolic bone disorders and the distribution of bone loss within long bone cross-sections (see Hypothesis 2c in Chapter 1).

Application to Anthropology

Adult Research. As reviewed above, researchers have thought that metabolic disturbances cause extensive, systemic shifts in microarchitecture that reduce bone strength. However, the research methodologies applied (i.e., DXA and mechanical testing) have precluded visualization of these alterations and their interaction with macrostructure. Anthropological analyses, in relying mostly on skeletal samples rather than living humans, have been able to provide critical insight into metabolic effects on osteonal remodeling by utilizing histomorphometric methods.

Histomorphological analyses are relatively rare in anthropology due to their destructive nature, despite the fact that they can provide critical knowledge on metabolic diseases and processes (Schultz, 2001). Osteonal remodeling rates are used to infer metabolic status differences among populations with varying subsistence strategies. For example, the low calcium and high phosphorous content of maize may explain the early findings of higher remodeling rates in rib cortical bone among maize agriculturalists compared to hunter-gatherers (Stout and

Teitelbaum, 1976; Stout, 1989; Stout and Lueck, 1995). Contrarily, *reduced* rib osteon population densities were found in cases of pellagra and non-specific malnourishment in South African skeletons, and this lowered remodeling correlates with skeletal indicators of metabolic stress (Paine and Brenton, 2006; Brenton and Paine, 2007). Though these results refute expectations for increased stochastic turnover with metabolic stress, high endocortical resorption in the South African sample could be responsible for the lowered osteon counts by eliminating remodeling events. Thus, when comparing intracortical remodeling rates, it is important to be aware of potential interactions between macroscopic and microscopic properties that may affect nutritional and behavioral interpretations.

In addition to osteon remodeling rates, comparisons across human populations in the rate of osteon filling and mineralization have provided evidence of stress and unique methods for documenting metabolic bone disorders. Unlike remodeling rates or porosity, histological features of disrupted remodeling (i.e., Type II osteons, zonal osteons, incompletely formed osteons) are more directly characteristic of metabolic stress and have been documented in maize-dependent populations, as well as agriculturalists with protein-calorie malnourishment (Richman et al., 1979; Martin and Armelagos, 1979, 1985; Erikson, 1980). Type II osteons form by intra-osteonal remodeling of a pre-existing osteon to release nutrient reserves in bone, and their presence is correlated with skeletal stress lesions (Richman et al., 1979; Eriksen, 1980). Zonal osteons represent slowed osteon formation; they contain a hypermineralized growth arrest line, which forms after a stressful event has passed and normal bone deposition resumes (Pankovich et al., 1974; Stout and Simmons, 1979; Parfitt, 1983). Higher proportions of incompletely formed osteons suggest arrested osteon development and lead to increased porosity and high rates of under-mineralized tissue (Mosekilde, 2008). For incompletely formed osteons to be attributed to

metabolic stress, they must occur at a higher rate than normal targeted remodeling. These histological properties are utilized in an attempt to help distinguish metabolic bone disorders from normal remodeling effects.

One of the first paleopathological analyses to use histological properties unique to metabolic stress was conducted on femora from adult Nubian agriculturalists (Martin and Armelagos, 1979, 1985). Combined with high rates of skeletal lesions, these individuals had low percent CA, large resorption spaces, and higher numbers of incompletely formed osteons. Females who died between the ages of 20 and 29 were more at-risk for skeletal deficits than males, and no periosteal compensation was documented that could have possibly offset this disrupted remodeling. Nutritional stress in this population combined with childbearing metabolic demands (i.e., pregnancy, lactation) could explain the sexual differences in this age cohort (Martin and Armelagos, 1979). In addition, males possessed higher frequencies of zonal osteons, perhaps because females did not have enough calcium resources to continue mineralization after growth arrest, which would also explain the higher number of forming osteons in females (Martin and Armelagos, 1985).

In comparisons of overworked and undernourished African Americans from the post-Reconstruction South (Cedar Grove) to prehistoric and healthy modern populations, Cedar Grove exhibited decreased femoral cortical thickness and cortical areas, as well as increased resorption spaces and a higher proportion of incompletely formed osteons (Martin et al., 1987). These differences were most obvious near the endosteal surface in both sexes and all age cohorts. Most interestingly, lower percent CA was correlated with higher numbers of resorption spaces and incompletely formed osteons, indicating that bone loss was occurring simultaneously at both macroscopic and microscopic scales at Cedar Grove (Martin et al., 1987). While this study

suggests that metabolic bone loss can occur at both scales in a heavy loaded long bone such as the femur despite extensive physical activity, it is difficult to attribute these morphological differences to either mechanics or metabolism without including elements under relatively larger metabolic influence as a baseline comparison (cf. Robling and Stout, 2003).

Very few studies have compared microscopic structure in rib and long bone elements from the same individuals. Quite recently, Skedros and colleagues (2013) assessed osteon dimensions in ribs and long bones from a wide range of human and non-human species to evaluate hypotheses regarding their different roles in metabolic and mechanical activities. As ribs are highly sensitive to metabolic factors, the authors hypothesized that rib Haversian canals and osteon walls would demonstrate positive allometry; larger Haversian canals relative to osteon size has previously been suggested as a mechanism for increasing surface area for calcium exchange. Likewise, long bones ought to possess negative allometry in these dimensions, because slight increases in porosity are detrimental to skeletal elements under high loading demands, and smaller Haversian canals relative to osteon size would limit pore size. However, the existence of both positive and negative allometric relationships among the various samples Skedros et al. tested led to rejection of these hypotheses. A major conclusion of the study was that, although rib osteons tend to be larger and more variable in size than long bone osteons in modern humans, Haversian canals are not significantly different between ribs and long bones. This points to consistent conservation of bone tissue mass regardless of the skeletal element and further supporting the notion that limits to porosity are essential to maintain mechanical advantage in bone. However, this study included only one metabolically stressed sample (rib elements from Kulubnarti Sudanese Nubians), and, quite interestingly, their rib osteons were negatively allometric.

Not having the corresponding long bone elements from the Kulubnarti sample, Skedros et al. (2013) stated that either increased physical activity or poor health could have contributed to this pattern, although it is hard to imagine that loading could be responsible given that increased activity does not induce rib remodeling (Tommerup et al., 1993). The authors interpreted the overall findings to mean that calcium exchange is sufficient across Haversian canal surfaces to maintain mineral homeostasis in the short-term (e.g., between meals), without need for rib cortical remodeling. Yet, long-term metabolic demands (e.g., pregnancy, lactation, and metabolic deficiency) may be necessary to induce cortical bone turnover. By incorporating metabolically stressed subadults, this dissertation builds on these findings and tests the relationship between Haversian canal size and osteon size across ribs and long bones within the same skeletal sample (see Hypothesis 2b in Chapter 1).

Ontogenetic Research. Histological studies on subadult cortical bone in archaeological samples are exceptionally scarce. As previously discussed, this research has described cortical microstructural development and how healthy adult cortical morphology is attained (especially in rib elements). Such research provides a baseline with which to compare and identify subadult metabolic bone disorders and microscopic bone loss. This dissertation is the first systematic anthropological examination of metabolic stress effects on human cortical bone microstructure during growth. Streeter (2005) identified greater percentages of drifting osteons in subadult ribs relative to adult ribs, indicating greater metabolic demands during growth. Based on her findings, there may be greater percentages of large osteons (perhaps also more incomplete osteons) in subadults experiencing chronic metabolic stress relative to subadults experiencing brief or no metabolic stress (see Hypotheses 1b and 2b in Chapter 1).

In one of the few anthropological explorations of subadult long bone histology, Doppler et al. (2006) qualitatively assessed femoral cortical cross-sections from the anterior diaphyses of 63 subadults from an early medieval Bavarian cemetery. Some individuals had large resorption spaces and low rates of remodeling for age, which the authors interpreted as indicative of pathological disruption. They inferred that metabolic bone loss could potentially exist in individuals despite the absence of gross morphological lesions. However, the exclusion of individuals from their sample with skeletal stress lesions and, more importantly, the lack of quantitative assessment and statistical comparison both within the site and with reference populations make these results potentially spurious. Nevertheless, this study did find (qualitatively) advanced remodeling rates during the mid-childhood growth spurt and increased numbers of forming osteons in adolescence (Doppler et al., 2006), which may demonstrate physiological responses at the tissue level that accompany alterations in body mass and height. Overall, this study illustrates that quantification of histological variation in subadult cortical bone potentially provides a wealth of information to be gleaned from comparisons between paleopathological groups.

CHAPTER 4: MATERIALS AND METHODS

This chapter discusses the human skeletal sample analyzed in this study and analytical methods used to address the research questions and hypotheses presented in Chapter 1. Details about the archaeological sample and its context, along with sampling strategies and techniques, are provided in the *Materials* section below. In the *Methods* section, specific aging methods, assessment of metabolic stress, measurements taken from the skeletal remains for analyses, and statistical techniques are described.

MATERIALS

For this study, a single cemetery sample was investigated, rather than several samples. This strategy was used to reduce potential variation in activity levels and stress factors that could exist among individuals or groups buried in different cemeteries, and which would, in turn, complicate analyses into interaction effects between mechanical and metabolic factors. Of course, it is not established that activity levels among individuals buried in the sampled cemetery were uniform, but use of a single cemetery minimizes considerable activity and dietary differences that might have existed among geographically or temporally dispersed samples. The skeletal sample appropriately meets requirements that will allow assessment of the research objectives: the site from which the sample is taken has a significant number of well-preserved subadult burials representing a wide age range; skeletons are from associated, primary burials; a rib, humerus, and femur bone can be sampled from each individual; bone microstructure is exceptionally intact (diagenesis is limited for an archaeological sample); and historical

documentation of the population buried at the cemetery confirms the presence of significant health stressors (including malnutrition) at the site.

The Alytus Archaeological Site

History

The sample chosen for this study's analyses was obtained from an archaeological cemetery site in the medieval town of Alytus, Lithuania (Figure 6). This urban center was occupied during the late 14th to early 18th centuries A.D., the period in which modern-day Lithuania was the Grand Duchy of Lithuania (GDL). The site is the largest archaeological cemetery that has been excavated in Lithuania, and is located roughly 500 meters northwest of the Alytus hill-fort on the western bank of the Nemunuas River (Figure 6). Excavation of the cemetery was performed between 1984 and 1986, uncovering 1152 intact and 300 disturbed graves (Svetikas, 2003) (Figure 7). Although written sources about Alytus are scarce, and there is no historical documentation of social stratification in Alytus specifically, like most late medieval duchies, GDL society was based on feudalism (Dubonis, 1996). A full range of social classes, from noblemen to peasants, would have populated Alytus. Compared to most medieval villages in the GDL, Alytus is considered a small urban center, experiencing modest economic development and a large population size (with a peak population size estimated to be 2,500) (Miškinis, 1989).

The first record of Alytus as an official town center was associated with the construction of the hill-fort fortification circa A.D. 1365 with a village forming soon thereafter in A.D. 1370 (Navickas, 1988). Multiple invasions during the Teutonic Wars devastated the Alytus population; however, the adoption of Roman Christianity within the GDL in A.D. 1387

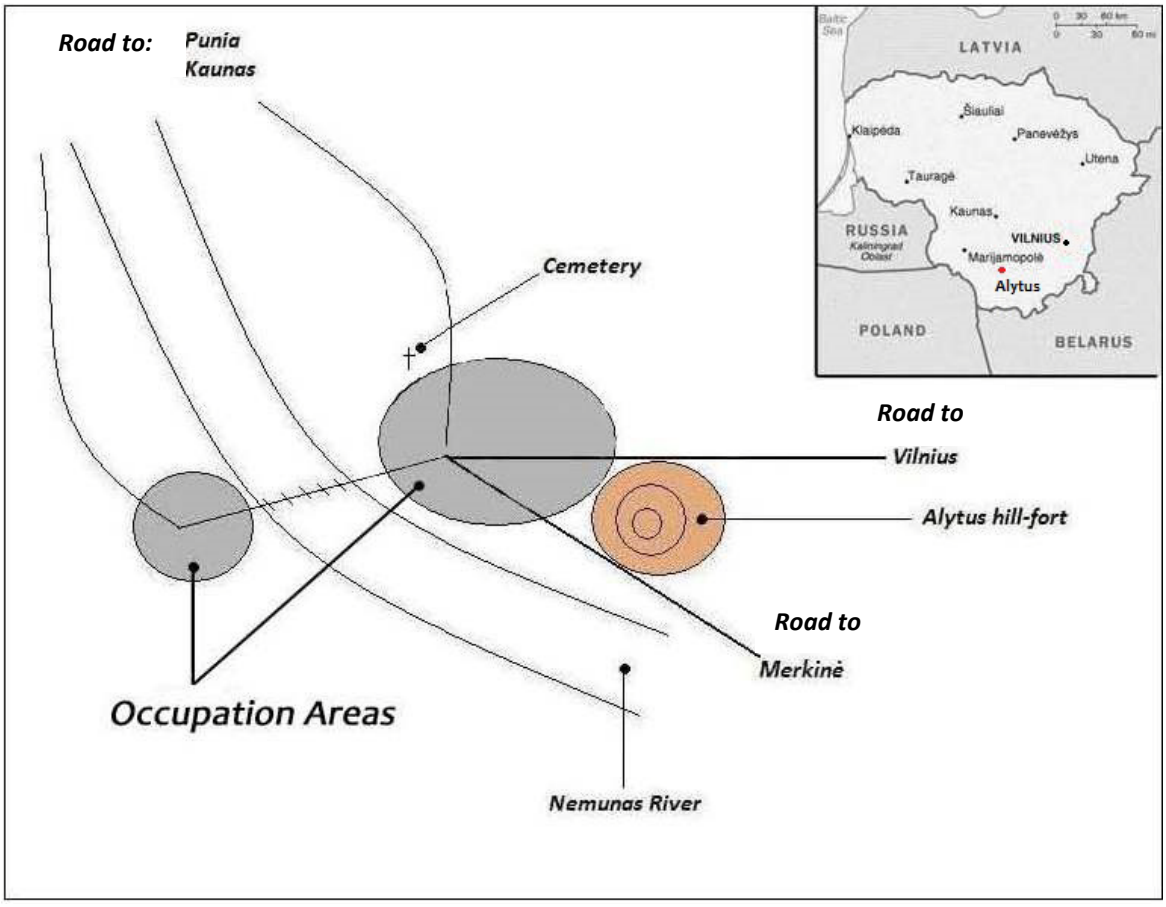

Figure 6. Schematic representation of the Alytus cemetery and location of the Alytus town in modern Lithuania (adapted from Kozakaitė, 2011).

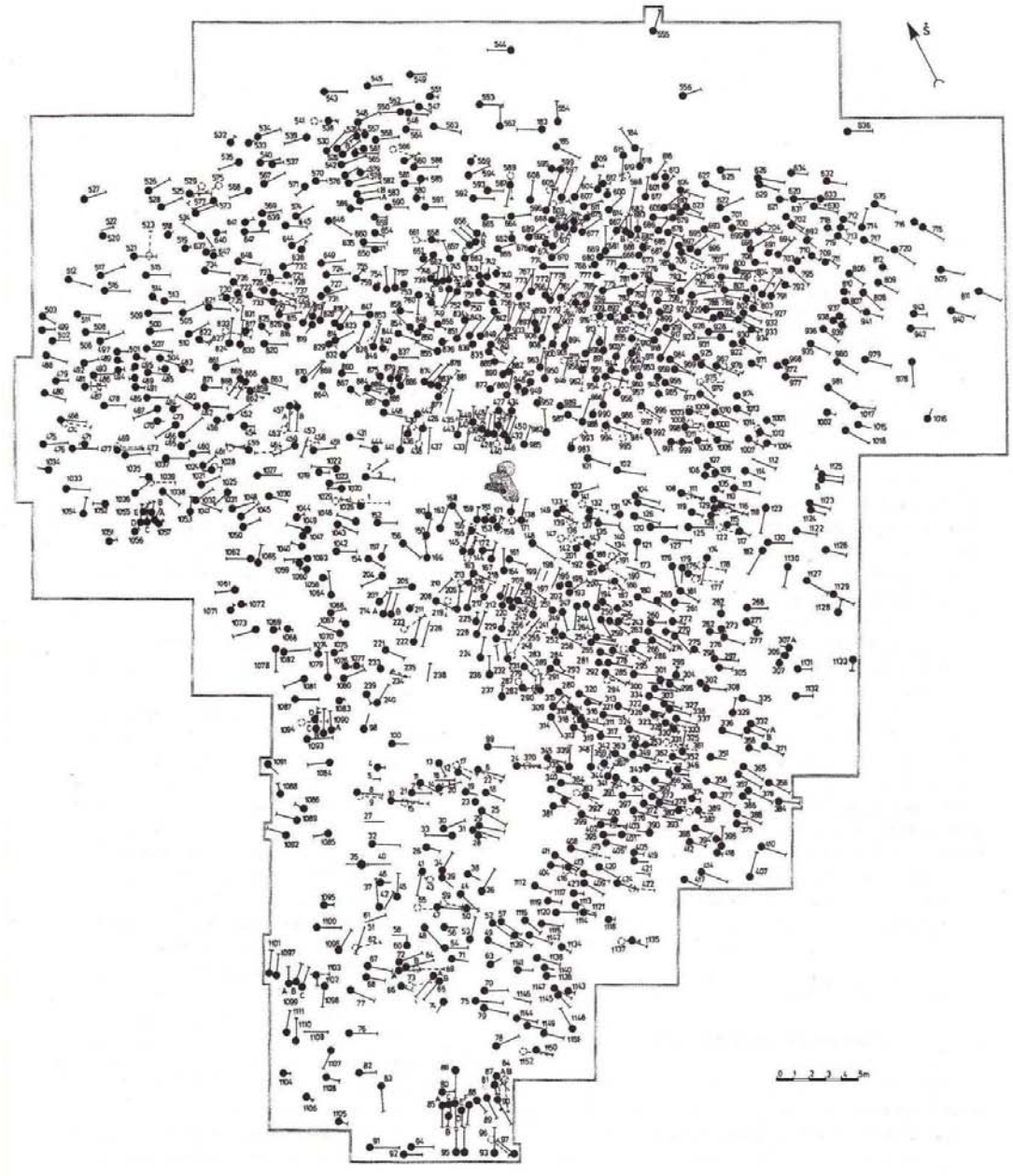

Figure 7. Planview map of Alytus cemetery and excavated adult and subadult burials.

prevented further attacks (Gudavičius, 1989). Though noblemen in the large urban centers quickly adopted the conversion to European Catholicism, other, traditional religious lifestyles in the countryside were maintained for nearly 130 years (Rowell, 2001; Beresnevičius, 2008). Illustrating this point, the first Catholic church was not constructed in Alytus until 1507 (Tyla, 1989; Navickas, 1988; Žepkaitė, 2001). This social history resulted in a complex mixture of burial traditions at the Alytus cemetery that involve the inclusion of pagan grave goods as well as Christian elements, including orientation in a particular direction (Paknys, 2001). This complexity makes it difficult to define social groups among the burials at Alytus; it is unclear whether grave goods are associated with the retention of Pagan traditions or reflect social status differences (Paknys, 2001).

The few historical documents about Alytus that remain describe a series of catastrophic events spanning centuries, which would have caused significant health stressors for the Alytus population. The first were the Teutonic Wars, mentioned above, and the Lithuanian Civil War, both of which occurred during the late fourteenth century A.D. Additionally, extensive population movements within the GDL occurred with Agrarian Reform in 1557, involving the elimination of older villages and isolated farmlands and subsequent migration into towns and villages. This reform resulted in increased population growth at Alytus by the 1581 census (1,150-1,200 people), but it also brought about diseases associated with increased population size, crowding, and poor sanitation (Jankauskas, 1998; Jankauskas and Schultz, 1999). Population size peaked during the early 17th century with 2,500 people occupying the town. By 1667, however, a series of fires, epidemics, and wars rapidly reduced the Alytus population to 450-700 (Kiaupa, 1989; Miškinis, 1989). By the early 18th century, the pressures of additional wars, plagues, and famine devastated Alytus.

In fact, during the existence of the GDL, there were at least 54 famine years (roughly every seventh year on average) due to multiple causes, including freezing weather conditions and crop failure (Grickevič, 1973). Famine years were especially harsh after the 16th century with the advent of the Little Ice Age, a period of climatic cooling that had significant effects on European agriculture (Baronas et al., 2011). The majority of the general populace, especially those of low socioeconomic status, was routinely on the verge of starvation (Jankauskas and Urbanavičius, 1998).

Following the depopulating events of the late 17th century, Alytus ceased to be a population settlement in the early 18th century. In 1706, the GDL was invaded by Sweden, and Alytus was attacked. This invasion was followed closely thereafter by an especially harsh, countrywide famine in 1708 (Navickas, 1988). The Big Plague (1709-1711), which devastated Lithuania, Poland, and Prussia, caused record high death tolls in the GDL. Under the burden of these conditions, by 1712 the town of Alytus was completely abandoned (Tyla, 1989).

Living Conditions and Sources of Health Stress

Living conditions in the GDL, and within Medieval Europe in general, presented nutritional challenges and were replete with substantial health stressors, including infection and other sources of disease. Based on historical records of the nearby GDL capital of Kernavė—an urban town with a similar population size to Alytus—the average life expectancy was significantly reduced relative to modern life expectancies in Lithuania [$e\chi$ = 21 years during the GDL; $e\chi$ = 69.6 years, averaged for both sexes in 1996, based on data in Kalediene and Petrauskiene (2000), though these values are biased on account of the high rates of subadult mortality that occurred during the time of the Grand Duchy]; over 30% of immature individuals

died before the age of five during the time of the GDL (Vėlius, 2003, 2005). A reduction in stature has also been demonstrated for Lithuanian populations during the Late Middle Ages, which indicates that there was a reduced growth rate in children between two to five years of age, as well as a delay in the adolescent growth spurt (Šereikienė and Jankauskas, 2002, 2004). Due to improvements in diet and health, modern Lithuanian adults are now ten to fifteen centimeters taller on average than medieval populations (Šereikienė and Jankauskas, 2004).

Highly disproportionate social hierarchy was a fundamental component of life in feudal societies like the GDL. Historical documents, for example, point to inequality in access to medical care. In the early 15th century, the first professional doctors entered the GDL from Western Europe; however, access to professional medical care was restricted to individuals of great political power, mostly noblemen, loyalty, and their families (Baronas, 2001; Andriušis, 2006). Peasants, villagers, and poor city dwellers resorted to magic and rudimentary forms of medicine to cure ailments, injuries, and illnesses (Siraisi, 1990; Baronas, 2001). Several GDL occupations (e.g., bath workers, barbers) provided medical services to townspeople in addition to their regular services. There were also self-taught folk doctors, herbalists, sorcerers, and healers who attempted to alleviate ailments of town dwellers on a daily basis. The majority of the Alytus population would have had limited access to the most advanced professional medical services available at the time, and were commonly the subjects of increased morbidity and mortality, in part due to infections, as well as reduced access to adequate nutrition.

Health stressors at Alytus were typical of those commonly present in other European towns during the Late Middle Ages. Some of these pathologies would be readily visible in cemetery samples, while others would not necessarily result in a skeletal response. Infectious disease was the most common cause of death (Jankauskas and Urbanavičius, 1998). Although

infectious disease does not necessarily result in metabolic disturbance, when present among subadults in conjunction with other nutritional health stressors, a synergistic relationship is created which often leads to malabsorption of nutrients (Lewis, 2007; Huss-Ashmore et al., 1982; Bennike et al., 2005). Tuberculosis, one of the main contributors to mortality in urban medieval Europe, was present in especially high frequency among the Alytus population (Jankauskas, 1998, 1999; Jankauskas and Urbanavičius, 1998).

In addition to skeletal lesions indicative of tuberculosis infection at Alytus, Faerman et al. (1999) confirmed the presence of *Mycobacterium tuberculosis* by the DNA analysis of Alytus skeletal remains. *M. tuberculosis* was found in individuals who both did and did not present with specific skeletal lesions. Thus, some individuals might have survived infection for a long enough period for, or experienced extended malnutrition that synergistically led to, the development of skeletal lesions. In contrast, other individuals succumbed to the infection or other causes of death before sufficient time elapsed to yield lesions. This difference has implications for the categorization of individuals with and without skeletal stress lesions, as discussed below in the *Methods* section. Tuberculosis infections in cattle (a significant factor in the transmission of the disease) could have also exacerbated nutritional deficiency at Alytus, as the bacteria can cause decreased milk supply (Johnson et al., 2001) and, therefore, calcium availability for human populations.

The Black Death and subsequent plague recurrences were also a significant cause of morbidity and death. In general, the plague affected the impoverished classes more acutely than the elite; with the introduction of the plague to the region, many of the aristocracy fled the crowded towns and secluded themselves in countryside homes (Ragauskienė, 2004). Records indicate that individuals between the ages of seven and thirteen were most susceptible to death

by bubonic plague. Plague had indirect effects; for example, it led to increased malnourishment, as families, and often whole communities, lost income or food production abilities when morbidity and mortality impacted individuals' productivity (Navickas, 1988; Ragauskienė, 2004). However, the epidemic spread of this disease coincides with rapid death prior to skeletal response, and thus, the plague leaves no bioarchaeological signature and was not likely to be a significant contributor to metabolic bone loss (which requires a particular duration of stress to induce skeletal response), though it would certainly have impacted cemetery composition.

Syphilis was another common infectious disease at Alytus (Jankauskas, 1994) that could have influenced subadult mortality, though identification of syphilitic individuals is difficult in skeletal samples (Ortner, 2003). Congenital syphilis typically develops with transmission of venereal syphilis from the mother to the fetus as early as 9 weeks gestation. While congenital syphilis most commonly results in spontaneous abortion within the first half of pregnancy, fetuses are not always stillborn and may even survive until puberty (late congenital syphilis) (Ortner, 2003). In such cases, skeletal indicators of the infection are visible after 2 years of age (Lewis, 2007).

Alytus subadults were also at high risk for developing anemia and other forms of malnutrition (e.g., scurvy, rickets) (Jankauskas and Schultz, 1999). Several factors contributed to this increased risk of metabolic disease, including intestinal parasites, poor sanitation, and prolonged breast-feeding coupled with protein-deficient weaning foods (Baronas et al., 2011). In medieval Europe, common weaning foods included a mixture of flour and bread cooked in water and cereal mixed with butter and broth or milk (Lewis, 2007). Additionally, bottles and spoons were often not cleaned between feedings or between infants, leading to increased infectious agent transmission (Thompson, 1984). Infantile diarrhea, associated with the factors above, was

the leading cause of infant death up until the 19th century (Jankauskas and Urbanavičius, 1998). Coupled with the underdeveloped immune system of children, these factors easily lead to malnutrition and increased mortality.

It was also common for adults and adolescents to continue to suffer from anemia as well, likely because of the general overreliance on cereals in the diet. Cereal grains (e.g., rye, wheat, oats, barley, millet, buckwheat) and legumes (e.g., lentils, beans, peas) made up a majority of the daily diet in the GDL; animal-based food was consumed in lower quantities (roughly 30% from meat and 10% from dairy products) (Baronas et al., 2011). Baked bread often constituted a significant portion of each meal, and domestic vegetables (e.g., turnips, radishes, cabbage, onions) were considerably lacking in essential nutrients. Only the more affluent aristocracy could afford to regularly consume high-quality foods, such as fish (e.g., perch, herring, cod, salmon) and imported items such as fruit (e.g., apples, cherries, plums, pears). For some individuals within the GDL, this kind of diet would have led to metabolic disturbances, primarily through the overreliance on cereals and lack of fresh vegetables (Baronas et al., 2011). As stated previously (see Chapter 3) phytates in cereals block calcium absorption, but the GDL diet also contains elements high in dietary acid load, which is linked to increased osteoclastic activity (Anderson, 1999; New, 2003).

Life for the peasants at Alytus would have been a daily struggle to grow enough food for the family while also paying high taxes; more affluent families could afford to avoid the most strenuous manual labor (Tyla, 1989). Physical activity at Alytus was similar to that of skilled craftsmen in other medieval towns. The most common occupation at Alytus was forestry—foresters, timber manufacturers, etc. Other specialized occupations included blacksmiths, woodworkers, bookbinders, millers, bakers, furriers, carpenters, cobblers, and butchers (Kiaupa,

1989; Urbanavičius, 2001). Townspeople, likely men, were also responsible for building and maintaining the town's bridges and roads (Baliulis, 2009). Other daily activities included agriculture, hunting, fishing, and animal husbandry (Baliulis and Meilus, 2001; Žepkaitė, 2001).

In summary, the environment in which most individuals who were interred at the Alytus cemetery lived would have contributed to high levels of metabolic stress. While individuals living in Alytus led physically active lives based on the historical evidence above, the feudal social system in which they pursued daily activities presented most of the population with limited options for advantageous nutritional and health conditions. It is from this general population, then, that the subadult sample used in this study was drawn.

The Dissertation Sample

As mentioned above, the complex mixture of burial traditions at Alytus makes it difficult to define status groups among individuals interred at the Alytus cemetery site, although historical documents point to status differences at Alytus. Therefore, burial goods and positions were not used to select Alytus skeletal remains for inclusion in the study. The study sample comprises 57 subadults, representing 42 burials, with an age range from birth to 14 years. Individuals below the age of one year were excluded because they have not made the transition from crawling to walking, and those above 14 years cannot be utilized due to the difficulty of estimating body mass from skeletal remains during this developmental period (see *Size Standardization*). In order for an individual to be included in the analysis, burials were *minimally* required to possess the following complete skeletal elements: one vertebrosternal rib (restricted to third through sixth ribs and minimally comprising the middle third of the rib), a complete right humerus, and a complete right femur. To ensure the most accurate age estimation and paleopathological analysis

possible, the most well-preserved and complete burials were targeted for data collection. Care was taken to include equal representation of all age cohorts and stress groups (presence/absence of stress markers); however, given that prior age estimations on the sample by others were limited and no previous researcher had performed a full paleopathological analysis on the Alytus subadult sample, it was not possible to target a sample during data collection that completely controlled for equal representation of age and pathology categories within the distribution of the final sample.

Specific criteria were used to determine which skeletal elements would be most appropriate for cross-sectional geometric and histomorphometric analyses. Only vertebrosternal ribs were included, because they are typically used in histomorphological assessment (Stout and Paine, 1992; Robling and Stout, 2008). Ideally, analysis would have been limited to a specific rib (e.g., the fifth or sixth rib) to eliminate potential morphological variation within the rib cage. It was not possible to implement such a requirement, because this would have reduced the sample size significantly; however, previous research has demonstrated similar cross-sectional properties (Cormier et al., 2005) and histomorphometry (Dudar, 1993) between vertebrosternal ribs. Ribs from the right side were preferred over the left when there was adequate preservation deemed appropriate for histological analysis; when none of the right third through sixth ribs was in good condition, a left rib was chosen for inclusion. Previous research has demonstrated no side asymmetries in rib cortical bone properties (Dudar, 1993). Proximal limb elements (humeri and femora) were used to evaluate environmental influences on the upper and lower limb, respectively, because proximal elements demonstrate greater variability in diaphyseal robusticity than distal elements (Stock and Pfeiffer, 2001; Stock, 2006; Shaw and Stock, 2009a) and are frequently evaluated in histomorphological analyses (Kerley, 1965; Tersigni, 2005; Crowder et

al., 2012; Crowder, 2013). Long bone elements from only the right side were utilized to minimize the effects of side asymmetry caused by activity differences (Auerbach and Ruff, 2006).

Caveats To Using An Archaeological Sample

There are multiple approaches and research designs that could potentially address the research questions posed in this dissertation. One such approach, which was not taken, would be to conduct experimental analyses on non-human animal models controlling for level, magnitude, and type of biomechanical loading as well as nutrition. Experimental studies on human analogues have been integral to understanding bone adaptation (Lanyon and Rubin, 1984; Biewener and Bertram, 1994; Bourrin et al., 2000; Bassett et al., 2007; see also Chapter 2), and, as reviewed in the background chapters, many have provided the framework and rationale for the hypotheses outlined in this study. However, the interaction between activity and metabolism in humans remains unresolved, because no animal model exactly mimics human bone dynamics and locomotor behavior (Turner, 2001; Leloyas et al., 2008).

Rats and mice have been the model of choice for exploring environmental influences on bone, but they are not ideal human analogues due to their differential timing and rates of growth, quadrupedal locomotor behavior, and a lack of cortical remodeling save for extreme loading conditions (Erben, 1996; Yao et al., 1999; Martin, 2007; Forwood, 2008). Although primates may demonstrate some advantages over rat models in having cortical remodeling and more human-like growth patterns (Mulhern and Ubelaker, 2003), loading patterns remain distinct from humans (Sockol et al., 2007; Pontzer et al., 2009). Additionally primate experimental research is expensive and ethically restrictive (Jee and Yao, 2001), and previous analyses of primate bone

have not yielded results significantly different from those of rat and mouse models (Jee and Yao, 2001). Results from primate studies, moreover, would not assist with behavioral interpretations from cortical bone morphology in past human skeletal samples, especially considering that most comparisons are made between long bones in the human upper and lower limb, due to their distinct utilization in humans, to assess differences in mobility and subsistence strategy. Furthermore, as experimentally induced metabolic stress cannot be ethically conducted on living humans, an archaeological skeletal sample is most appropriate.

As with any anthropological investigation using archaeological human remains, there are important limitations and caveats associated with testing scientific hypotheses with cemetery samples. The most notable is the challenging, yet unavoidable, osteological paradox (see discussion in Chapter 3). Although the effects of selective mortality and hidden health heterogeneity cannot be completely avoided, caution in interpretation can mitigate potentially false conclusions (Goodman, 1993; Goodman and Martin, 2002; Wright and Yoder, 2003). Therefore, in this study, individuals are not simply lumped into "stressed" and "non-stressed" groups based on lesion presence and absence. Rather, the presence of one or more lesions is indicative of *chronic* metabolic stress—the individual was healthy enough to recover, only to succumb to a subsequent stressor resulting in death. The lack of a lesion indicates either *acute* stress—an individual who succumbed quickly to stress before initiation of a skeletal response—or a *non-stressed* individual who died from other causes (Goodman et al., 1993). Unfortunately, the acutely stressed and non-stressed cannot be disentangled from one another in cemetery samples (Wood et al., 1992). However, given that chronic stress over a significant period of time is likely to cause alterations to bone mass and quality after attaining a certain threshold, it is an

assumption tested in this study that skeletal stress lesions will correlate with reduced bone mass; this is the basis of Hypotheses 1a and 1b as explained in Chapter 1.

Due to difficulties and inaccuracies in assigning sex to immature skeletal remains, the effects of biological sex on bone properties was not explored and no attempt was made to estimate sex in the subadult sample (Saunders, 1992). Sex differences in macroscopic cortical bone mass and distribution have been documented in adults, and these differences develop during growth, especially during and after puberty with the production of sex-specific hormone levels (Dupras and Pfeiffer, 1996; Ruff & Hayes, 1983; Ruff, 2003a). Less investigation has been conducted on histological variation between the sexes, but sources seem to indicate that rib microscopic structure shows no sex differences (Dupras and Pfeiffer, 1996; Streeter, 2005), while adult long bone microstructure does (Martin and Armelagos, 1979, 1985). However, without the ability to estimate sex in the subadult skeletons, the effect of sex differences on the results of this study will remain unknown. Yet, given that individuals over the age of 14 were excluded, and in light of previous studies of subadult skeletal remains, pooling males and females likely had a minimal effect on the variation in bone properties analyzed here.

METHODS

This section discusses the methodology used in this study to collect samples, obtain measurements, and perform all statistical analyses to address the proposed research hypotheses. Age estimation (as well as the age cohorts and terminology utilized in this study) and the procedures for assessing skeletal stress lesions are outlined below. Production and processing of bone histological sections to allow for cross-sectional geometry and histomorphology data

collection are explained in detail, and size standardization of bone properties is given special attention. Finally, this chapter concludes with an outline of the statistical analyses employed.

Age Terminology & Age Cohorts

The terminology used in the archaeological literature to refer to non-adults is often variable and at times inconsistent. For example, "juvenile" frequently refers to all skeletally immature individuals collectively, but some (e.g., Bogin, 1997) use it in reference to a particular developmental period during late childhood and prior to adolescence. The term "subadult" is a viable alternative for describing immature individuals, although it is associated with negative connotations (Lewis, 2007). The same terminological vagaries apply when choosing more specific age categories. The term "infant" can refer to individuals under the age of one as well as individuals up to five years of age (Lewis, 2007; Halcrow and Tayles, 2008). The specific research objectives posed often determine the choice of age terminology, further complicating the matter and making comparisons across studies difficult (Kamp, 2001). Therefore, it is important to carefully define age group terminology and categories and use it consistently within a study.

In this study, the term "subadult" refers to individuals of all developmental stages prior to the adult stage, and the terms "juvenile" and "child" refer to specific developmental periods specified by Bogin (1997). Like any classification system, age cohorts are often arbitrary, but necessary, divisions along a continuous developmental sequence that serve to organize information and aid in comparisons across studies. The distribution of individuals by stress group and age are presented following Bogin's (1997) evolutionary classification scheme and modified for the ages included in the study (1.0-1.99, 2.0-2.99, 3.0-6.99, 7.0-11.99, 12.0-13.99), as these

categories are commonly used in bioarchaeological analyses. Individuals were assigned to these categories based on mean dental and/or skeletal age estimates (see below). However, given the small sample sizes among stress groups within age cohorts, statistical analyses could not be performed separately for these groupings (see *Statistical Analysis* below). Thus, these age divisions are used in presenting summary statistics when necessary to allow for comparisons with other subadult studies, highlight the age distribution of the sample, and address potential age effects on statistical analyses performed on the entire sample. Because the questions posed in this study are biological in nature, the age terminology and cohorts used herein are based on biological age classifications that adequately represent biologically based developmental transitions. These terms are not based on social age or intended to reflect the complex social constructs and identities associated with immature individuals of the Alytus population (cf. Gottlieb, 2000; Kamp, 2001; Halcrow and Tayles, 2008).

Age Estimation

Age-at-death of each Alytus subadult was estimated using crown and root formation of the permanent (Smith, 1991) and deciduous dentition (Liversidge and Molleson, 2004). This method involved visual inspection of loose mandibular and maxillary teeth, as well as digital mandibular radiographs taken with an Aribex Nomad Pro X-ray gun, EVA dental digital X-ray film sensor, and EVAsoft software. The digital film sensor was held parallel to the X-ray beam using a custom built stand. Lateral mandibular X-rays were taken of all *in situ* unerupted tooth crowns and erupted tooth roots across the entire dental arcade, including anterior and posterior teeth from both left and right sides.

The use of crown and root formation from radiographs as an aging technique provides several advantages to other dental age estimation methods. First, although dental eruption has been used frequently in skeletal analyses to estimate subadult age, mandibular radiographs have been found to provide more accurate age estimates because dental formation is more robust to environmental perturbations (e.g., nutrition, tooth loss, caries, hormonal influences) than eruption (Ubelaker, 1989; Smith, 1991, Saunders, 1992; Conceição and Cardoso, 2011). Second, unlike dental eruption, dental formation is a continuous process rather than a discrete event, allowing for age estimates across a wider range within an ontogenetic sequence (i.e., perinates to late adolescents) (Demirjian, 1978). Third, radiographic assessment of dental formation captures developmental information from unerupted teeth, increasing accuracy in general but especially within one critical transition period for this study: between the cessation of deciduous dental eruption and onset of permanent dental eruption (3-6 years).

The calcification scores for Smith (1991) and Liversidge and Molleson (2004) were determined for each tooth that was observable via radiograph or loose from sockets. Each tooth was scored twice on two separate days; any inconsistencies between these two scores were resolved upon a third inspection. Each dental score was assigned a sex-averaged age estimate, and a mean of these age estimates was calculated to create a composite age estimate for each individual. Because of differences in burial preservation, these composite age estimates were based on variable numbers and types of teeth between individuals. Due to unexpected technical difficulties with the Nomad X-ray gun late into data collection, ten individuals could not be radiographed and were given age estimates based on traditional dental age estimation methods involving visible crown and root formation and tooth eruption (Buikstra and Ubelaker, 1994). All of the individuals in the Alytus sample were evaluated by these traditional dental age

methods and comparisons were made between radiographic age estimates and traditional age estimates. These comparisons demonstrate a small average absolute error between the two methods ($\bar{x}$ = 0.9 years, standard deviation = 0.9 years, range = 0.1-3.7 years, n = 33), possibly due to the high frequency with which unerupted teeth were visible in their crypts and erupted teeth could be removed from the alveolus for visual inspection. The age estimates for each individual, by present teeth and their mean age, are presented in Appendix I.

When using dental age estimation methods, subadult growth rates are thought to be equivalent to those of the reference population, which are typically modern, healthy North American or European populations (Hoppa and Vaupel, 2002). In this case, Alytus developmental dental rates are assumed to be similar to those of medieval Scottish and British subadults of known age (Smith, 1991; Liversidge and Molleson, 2004). Ideally, a reference standard from the same region would be used; unfortunately, no aging standard currently exists for Lithuanian populations. Being a European population, Alytus subadults are assumed to not significantly differ in dental formation rates from the Western European reference populations. Furthermore, as noted above, dental development is robust to environmental perturbations compared to other skeletal indicators of age (Saunders et al., 1993; Konigsberg and Holman, 1999; Saunders, 2000); therefore, given the possible age indicators, the use of tooth root development as the basis for age estimates is the most resistant to the effects of variable development rates due to metabolic stress in individuals from Alytus.

When a significant portion of the dentition was missing (unless the teeth were diagnostic of a particular age range), age was predicted from the appearance and fusion of primary ossification centers, epiphyseal closure (Scheuer and Black, 2000; Baker et al., 2005), and/or regression formulae for femoral diaphyseal length (Scheuer et al., 1980; Scheuer and Black,

2000). This method was used on seven individuals (12% of the total sample). Individual age estimates based on these two alternative methods are presented in Appendix I. When the age estimates differed between the above methods, the individual was assigned the femoral diaphyseal length estimate, mainly because of pronounced delay in skeletal ossification and fusion rates in the Alytus sample. The final distribution of sample ages is presented below in the context of defining stress group categories.

Assessment of Pathological Skeletal Lesions

Despite the limitations associated with the osteological paradox (see Chapter 3), skeletal lesion presence was observed and recorded as the criterion for assigning individuals to two stress groups: lesion group and no lesion group. Each skeleton was assessed for the presence of three skeletal lesions: porotic hyperostosis, dental enamel hypoplasia, and osteoperiostitis. These were categorized and recorded according to the techniques specified below. Severity scores were not assigned to these pathologies, as lesion severity is not hypothesized to correlate with metabolic bone loss. Individuals with skeletal evidence of congenital disorders and/or trauma were excluded from analyses to avoid as much as possible the inclusion of individuals who died from non-metabolic and accidental deaths. Lesion data for each individual are presented in Appendix II. Representative photographs of each type of stress lesion are presented in Appendix III; digital photographs of all stress lesions are available upon request.

Porotic Hyperostosis

Porotic hyperostosis was considered present when porosity with coalescing foramina and expansion of the diplöe was evident on the ectocranial surface of the cranial vault and/or the

superior surface of the orbit. These lesions are considered a robust indicator of metabolic stress in skeletal samples and have been associated with iron-deficiency anemia, poor nutrition, scurvy, rickets, infectious disease, and chronic diarrhea (Stuart-Macadam, 1992; Schultz, 2001; Blom et al., 2005; Ortner, 2003; Walker et al., 2009). The presence of porosity on the latter surface is referred to as cribra orbitalia but is considered here along with cranial lesions because both types of lesions likely share a similar etiology and often manifest in the same individuals (Stuart-Macadam, 1989; Schultz, 2001; but see Walker et al., 2009). Care was taken to exclude cases of non-pathological porosity caused by localized osteitis or postmortem erosion (Wapler et al., 2004). Porotic hyperostosis was observed under natural light with the aid of a magnifying hand lens (10x).

Dental Enamel Hypoplasia

Dental enamel hypoplasias (DEH) are linear grooves or pit defects that form when ameleogenesis is temporarily halted; the defect appears once the individual recovers and ameleogenesis resumes. Because teeth do not remodel like bone, these defects represent a permanent record of past developmental disruptions from the fetal period to about 10 years old (Hillson, 2000; Goodman and Rose, 1990). DEH presence has been linked to frequencies of skeletal lesions and archaeological evidence of dietary deficiency (Goodman and Armelagos, 1989; Goodman and Rose, 1991; Blakey and Armelagos, 1985; Temple, 2007; Klaus and Tam, 2009), although physical trauma also leads to DEH formation (Yaeger and Sharawy, 1986). DEH were observed and recorded in all teeth following protocols set out in Goodman and Armelagos (1990).

To differentiate normal perikymata variations from enamel defects, the presence/absence of DEH was recorded for each tooth under natural light with a magnifying hand lens (10x). The developmental stage of each enamel defect was estimated by measuring from the midline of the defect to the cemento-enamel junction with digital calipers to the nearest hundredth of a millimeter (Goodman and Rose, 1990). Due to lack of access to a high-powered microscope at the skeletal collection, perikymata could not be counted (Hillson, 1992) and, therefore, enamel defects reported in this study represent a minimum estimate of those potentially present. However, given the nature and purpose of the analysis—to identify individuals under chronic metabolic stress and estimate periodicity of stressful episodes in the Alytus sample—the method described above is sufficient for the task.

In order to avoid inclusion of enamel defects caused by localized trauma rather than physiological stress, DEH was recorded as a true disruptive event only when it was present in at least two teeth at the same developmental stage; a defect was not counted as a disruptive event if fewer than four enamel sections (i.e., teeth) at a particular developmental stage were present (Goodman and Rose, 1990). In other words, a disruptive event must manifest as an enamel defect in at least two out of four or more separate teeth at the same developmental stage.

Osteoperiostitis

Osteoperiostitis is new bone formation following periosteal reaction to a physiological stressor, including malnutrition, injury, or infection. Osteoperiostitis must be differentiated from normal porosity that occurs during growth processes and can mimic pathological lesions (Lewis, 2007; Ortner et al., 2001). Osteoperiostitis has been linked to malnutrition and other metabolic disorders, as well as infectious diseases (e.g., tuberculosis, leprosy, treponemal disease); and

thus, the presence of these lesions in high frequency within a population is indicative of high disease load and malnutrition (Mensforth et al., 1978; Ortner, 2003). Signs of *specific* infectious disease (i.e., tuberculosis) were not present in the Alytus individuals sampled and were, therefore, not utilized for the purposes of this study. The presence and distribution of osteoperiostitis were assessed throughout the entire skeleton of each burial, including the cranium, under natural light with a magnifying hand lens (10x) following Buikstra and Ubelaker (1994). Localized periosteal reactions are more likely caused by trauma or infection of the surrounding tissue (Ortner and Putschar, 1985); and, therefore, individuals with osteoperiostitis that was limited to a single element were not recorded as having osteoperiostitis present, although the condition was noted.

Specific Diseases of Malnutrition

To account for specific diseases of malnutrition (i.e., scurvy, rickets) that affect the skeleton during late stages of the disease, each skeleton was assessed for the particular distribution of non-specific lesions and additional phenotypic characteristics that are diagnostic of each of the two specific diseases, following Lewis (2007). Within the Alytus sample utilized for this study, no subadult individuals with the specific patterns of stress markers associated with rickets and scurvy were identified. All of the pathological lesions used to separate Alytus skeletal remains into stress groups, therefore, are indicative of non-specific physiological stress.

Determination of Stress Groups

Table 1 provides the frequencies of dental and skeletal stress lesions by type and their general location within the skeleton (i.e., postcranial or cranial). These frequencies are presented

within age cohorts and across the entire subadult sample to demonstrate the distribution of pathological lesions with age. These summary statistics are provided to show the types of pathologies present at the Alytus site; however, these categories are not used in statistical comparisons, which are made between lesion and no lesion groups based on lesion presence and absence (see below). In the Alytus sample, DEH was present only in individuals above the age of seven, and this anomaly is further discussed in Chapters 5 and 6.

Table 1. Frequencies of pathological dental and skeletal lesions by age and skeletal location.

	Cranial										**Postcranial**				**Total**
	PH (Vault)		PH (Orbital)		Total PH		Other Lesions		DEH		Osteo-periostitis		Other Lesions		
Age	n	%	n	%	n	%	n	%	n	%	n	%	n	%	n
1.0-1.99	2	33.3	0	0.0	2	33.3	0	0.0	0	0.0	2	33.3	0	0.0	6
2.0-2.99	1	14.3	2	28.6	6	85.7	2	33.3	0	0.0	3	42.9	0	0.0	7
3.0-6.99	1	5.9	2	11.8	3	17.6	2	33.3	0	0.0	5	29.4	0	0.0	17
7.0-11.99	2	10.5	3	15.8	6	31.6	1	16.7	11	57.9	8	42.1	2	10.5	19
12.0-13.99	1	12.5	2	25.0	3	37.5	1	16.7	6	75.0	3	37.5	2	25.0	8
Total	**7**	**12.3**	**9**	**15.8**	**20**	**35.1**	**6**	**10.5**	**17**	**29.8**	**21**	**36.8**	**4**	**7.0**	**57**

PH=porotic hyperostosis, DEH-dental enamel hypoplasia

Table 2 displays the distribution of the skeletal sample by age cohort and stress group. Individuals who possessed one or more of the three stress lesions described above were classified in the lesion group, while those without visible lesions were classified in the no lesion group. Due to the presence of significant health stressors at Alytus and the circumstances involved with increased mortality hazards and cemetery composition, there are few individuals above the age of seven in the acute stress group. The effects of this sampling bias on statistical analyses are discussed in Chapter 5.

Table 2. Age distribution of the Alytus skeletal sample by stress group.

	Lesion Group		No Lesion Group		Total
Age Category	n	%	n	%	n
1.0-1.99	3	50.0	3	50.0	6
2.0-2.99	6	85.7	1	14.3	7
3.0-6.99	7	41.2	10	58.8	17
7.0-11.99	17	89.5	2	10.5	19
12.0-13.99	8	100.0	0	0.0	8
Total	**41**	**71.9**	**16**	**28.1**	**57**

Data Loss Mitigation

After examining indicators of metabolic stress and aging criteria, the three elements from each individual were measured and prepared for histological sectioning. Given the destructive methods required for this study, it was critical to minimize the impact of bone sectioning on future research that uses the sampled subadults in the Alytus skeletal collection. Therefore, a data loss mitigation plan was implemented prior to histological sectioning to collect as many measurements as possible from the sampled elements (Table 3), though most of these data are not utilized in this study. The data loss mitigation plan, in addition to the data collected for the dissertation analysis (Tables 4 and 5), entails all measurements typically collected on subadult skeletal remains, namely limb bones (Ruff, 2007; Cowgill, 2010; Garofalo, 2012). This plan included full digital photographic documentation of each skeletal element that was sampled and the collection of diaphyseal and articular dimensions of the humerus and femur, as well as femoral neck-shaft angle. These data will be publicly available to researchers upon request after publication of the dissertation analyses.

Table 3. Additional data collected to minimize data loss prior to destructive histological sampling.

Bone Element	Measurement Type	Measurement[1]	Instrument	Reference	% Measurement error[2]
Femur and Humerus	Diaphyseal dimensions[3]	ML diameter at midshaft	Digital calipers	Buikstra and Ubelaker (1994)	0.66 (F) 1.34 (H)
		AP diameter at midshaft	Digital calipers	Buikstra and Ubelaker (1994)	0.41 (F) 0.62 (H)
Humerus only	Diaphyseal dimensions[4]	ML diameter at distal shaft	Digital calipers	Ruff (2003a)	0.73
		AP diameter at distal shaft	Digital Calipers	Ruff (2003a)	0.62
	Metaphyseal dimensions	Distal metaphyseal breadth	Digital calipers	Buikstra and Ubelaker (1994)	0.53
Femur only	Angle	Neck-shaft angle	Image J	Martin (1928)	

[1] Planes are abbreviated: AP, anterior-posterior; ML, medio-lateral.
[2] Average difference of three measurement trials from their mean, divided by the mean and multiplied by 100 (following White, 2000). Elements are abbreviated: F, femur; H, humerus.
[3] Taken at 45.5% diaphyseal length (following Ruff, 2003a).
[4] Taken at 41% diaphyseal length (following Ruff, 2003a).

Bone Locations And Orientation for Histological Sampling

The locations for macromorphological and histomorphological analysis were chosen based on their mechanical significance; these locations are typically the sites where cross-sectional properties are measured using radiographs and/or periosteal casts. Given the unique morphology of immature remains relative to adult remains, the sampled bone locations, especially in the humerus and femur, were taken to best compare with the locations typically measured in adult individuals (e.g., Ruff, 2008a). Due to delayed epiphyseal fusion at Alytus, total bone length was not used in locating the histological samples. Data were instead collected at 45.5% femoral diaphyseal length and 41% humeral diaphyseal length, both determined from the distal ends of the bones (Figures 8a and 8b). These locations correlate with 50% and 40% of total bone length, respectively, due to differential rates of growth between the proximal and distal portions of the diaphysis (Ruff, 2003a).

Researchers have not typically examined the cross-sectional geometric properties of ribs (cf. Cormier et al., 2005). Thus, unlike the long bones of the limbs, standard sampling locations from ribs are not defined. In this study, complete ribs were sampled at the point of greatest bending, as it is a consistently identifiable location. This location was determined by placing the rib on a gridded surface, aligning the vertebral and sternal ends, and using a tangent line to mark the furthest projecting point on the cutaneous cortex (Figure 8c). When rib elements were not complete, the location of interest was restricted to the middle third of the rib, without metric assessment of the location, as is customary in rib histological methods (Crowder et al., 2012). A total of 13 individuals' ribs (23% of the total sample) were sampled using the latter method.

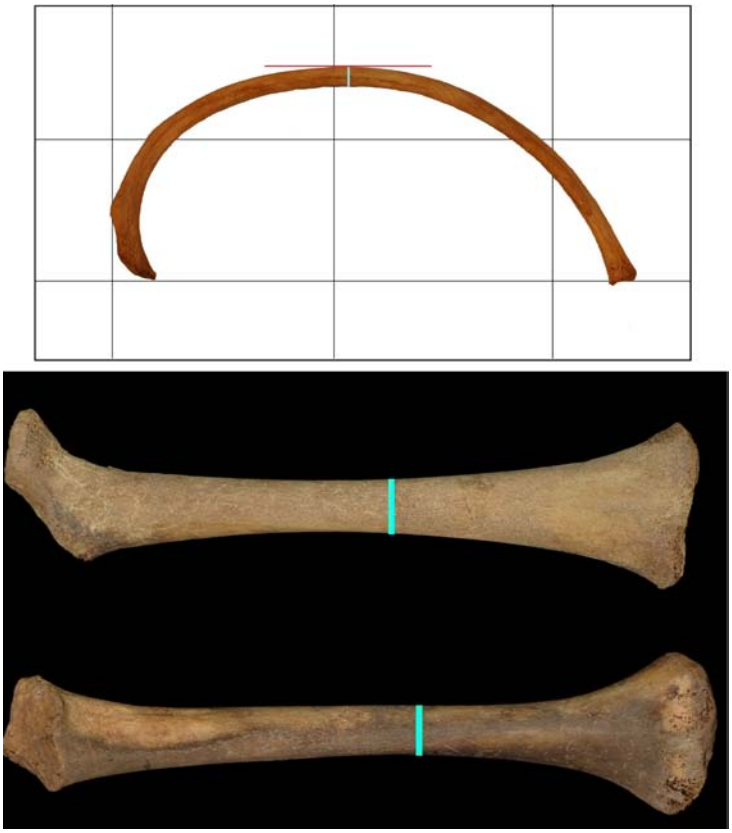

Figure 8. Histological sampling locations for femora, humeri, and complete rib elements. (Elements are not to scale)

In order to ensure that cross-sections obtained from the bones were perpendicular to the long axis ("neutral axis") of the elements, and therefore were not oblique or otherwise distorted, an explicit orientation protocol was followed to align elements before they were histologically sectioned (Figure 9). In addition, the orientation of each section needed to be maintained after removal from the diaphysis of the element; anatomical reference axes (anteroposterior and mediolateral planes) were marked on each element before sectioning to maintain anatomical orientation of the histological thin sections after sampling. Procedures for determining reference axes for adult long bones (Ruff and Hayes, 1983) could not be performed on the subadult remains, due to the absence of fused epiphyses. Therefore, a new method for locating reference axes in subadults was developed to be comparable with that of the adults.

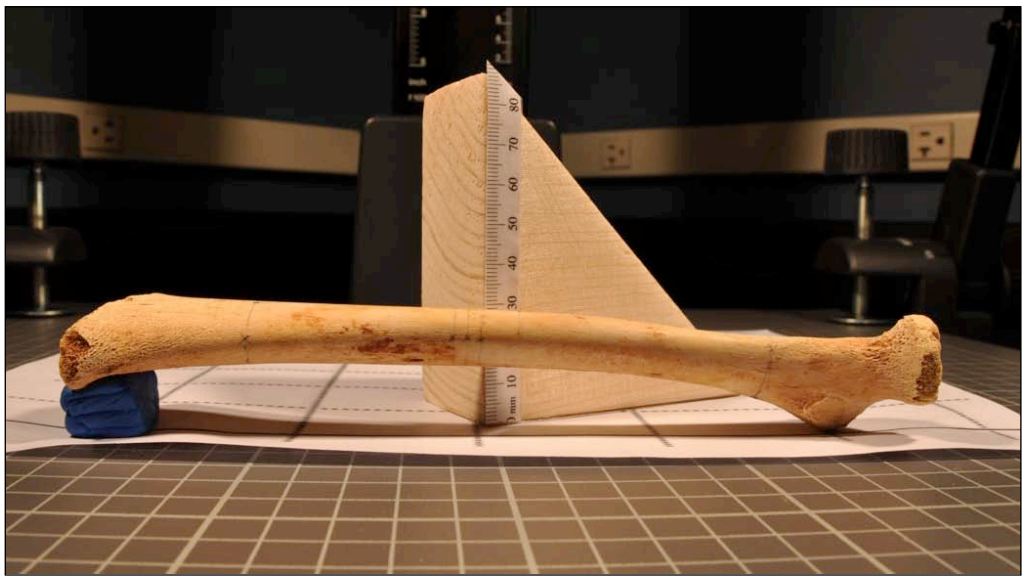

Figure 9. Anatomical alignment of long bones to maintain orientation of histological samples after sectioning.

For long bones, this method involved making two marks where calipers touch the maximum medio-lateral (ML) diameter at the proximal and distal portions of the diaphysis. To avoid including the metaphyses, these marks were made at 80% and 20% of diaphyseal bone length, respectively, measured from the distal ends of the bones. The plane that includes all four ML marks is the frontal plane. Next, the midpoint between each set of ML marks was delineated on the anterior and posterior surfaces of both the proximal and distal portions. The plane that includes all four AP marks is the sagittal plane.

To ensure proper orientation in the frontal plane, each element was placed in anatomical position on a grid so that the longitudinal axis of the diaphysis was parallel to the grid. The longitudinal axis was defined as the line within the sagittal plane connecting the midpoints of the proximal and distal AP marks. Orientation in the sagittal and transverse planes was maintained by using clay to support the position of the element so that that all four ML marks were parallel to the substrate. This task was accomplished by using a measuring triangle block, as depicted in Figure 9, to align each ML mark equidistant from the grid. Last, the appropriate AP and ML marks were extended onto the section of bone to be removed for histological sampling, using the triangular block to ensure the axes did not deviate from those marked on the diaphyseal ends. The sagittal plane at the sampling location was defined by marking anterior and posterior points that fall on the lines connecting the proximal and distal AP points. Likewise, the coronal plane for the sampling location was delineated by identifying the medial and lateral points that fell on lines connecting proximal and distal ML points.

Histological Sectioning

The procedures outlined below for the production of histological thin sections are based on the author's previous experience with human fetal and subadult macaque bone histology (Eleazer, 2007), as well as the literature on histological analysis of ancient tissues (Grupe and Peters, 2006). This methodology involves the careful removal of bone wafers without damage to the remaining element. The majority of these procedures are identical to those performed on adult human archaeological bone (Grupe and Garland, 1993; Paine, 2007). Though, in certain instances, the fragile condition of subadult archaeological bone requires modifications to established methods (e.g., use of Dremel tool and thicker histological sections; see below) to prevent macro- and micro-fractures on both the sampled section and the element as a whole.

Bone wafers of seven to ten millimeters in length were cut from each element at the locations of interest specified above using a Dremel rotary tool equipped with a fiber-reinforced cutting wheel for the more robust specimens and a diamond cutting wheel for the more fragile bones, such as ribs and the long bones of younger children. These wafers contained the cross-sectional location of interest at their midpoint. These wafers were removed precisely perpendicular to the long axis of the diaphysis, using the anatomical axes determined using the protocol discussed above. Seven to ten millimeter wafers maximize cutting accuracy while not compromising the area to be observed histologically, preventing cracking on both the wafer itself and the remaining skeletal element.

After extraction, the wafers were embedded in epoxy resin to stabilize them for thin sectioning following mixture ratios established by Paine (2007). A vacuum pump and dessicator were used to remove air bubbles and impregnate the entire specimen with epoxy. Thin sections were cut from these embedded wafers using a TechCut 4 precision low speed saw (Allied, Inc.)

equipped with a diamond wafer blade and mounted to petrographic slides using Permount™ mounting medium. Biomechanical axes of orientation were preserved by marking each thin section with permanent marker on the side that was mounted to the glass slide, preventing the removal of such marks during grinding. The mounted sections were ground to a thickness of 100-200 micrometers, depending on the fragility of the sample, using a Metaserv 2000 polisher machine. Histological protocol for adult cortical bone calls for thin sections less than 100 micrometers (Stout and Pain, 1992); however, the porosity and fragility of subadult bone prevents the ability to produce such thin sections without damage to the specimen.

Scratches produced during the grinding process were removed with a series of fine-grained buffing papers of increasing grit (400, 600, 1500 grit). Chemical staining (e.g., toluidine blue) of the specimens was not performed, as taphonomic changes to ancient bone tissue prevent adequate absorption of these chemicals. Such staining techniques are typically used in fresh, modern bone to detect recent remodeling events (Grupe and Peters, 2006); however, all the microscopic structures of interest to this study are clearly visible under transmitted light microscopy without bone stains, described below. Cover slips were used to increase visibility of microscopic structures under light microscopy.

Data Collection

The following section describes the methodology employed when measuring the macroscopic and microscopic bone properties of the Alytus subadult individuals. All measurements were collected without prior knowledge of skeletal and dental pathology in order to prevent bias in measuring cross-sectional properties and histomorphology. Though the pathological assessments were conducted while collecting data in Lithuania, the metabolic stress

categories for each individual were not determined until *after* cross-sectional geometric properties and histomorphometric measurements were taken. Thus, several months had elapsed between initial pathological analysis and data collection from the histological thin sections.

Macromorphological Measurements

Cross-sectional measurements used in this study are listed in Table 4. These measurements were chosen based on previous research demonstrating their relevance to both health status and mechanical strength (see Chapters 2 and 3). Strength properties typically analyzed in long bones (e.g., I_{max}, I_{min}, J, Z_p) were not performed on rib elements, because ribs are not loaded as beams in compression along the longitudinal axis (Cormier et al., 2005). Therefore, only estimates of rib macroscopic bone mass (i.e., CA, TA, MA) were employed.

As histological sampling allows for direct measurement of both the periosteal and endosteal surfaces, traditional methods (e.g., O'Neill and Ruff, 2004) utilizing casting material, such as putty and radiographs were not necessary. Digital images of the entire cross-section of each bone section were captured at 40x magnification and 853.33 pixels/mm resolution with a Leica DMLS microscope and Olympus BH-2 digital microscope camera. Care was taken to ensure that each image contained areas of the bone that overlapped with adjacent images in the slide. These images were then stitched together on an Apple iMac (late 2011 model) using the auto-stitch feature in Adobe Photoshop CS5, which stacks overlapping images to create a high-resolution composite image of the entire cross-section (Figure 10). Because the resolution of the image and calibration of the microscope is known (i.e., 853.33 pixels per mm), direct macroscopic and microscopic measurements of the composite images can be made that correspond to the true dimensions. The auto-stitch feature frequently has trouble stitching

Table 4. Cross-sectional properties used to quantify macroscopic bone mass and bone strength.

Bone Element	Measurement Type	Measurement	Unit	Description
Femur, Humerus, Rib	Cross-sectional properties of mass[1]	Total Subperiosteal Area (TA)	mm^2	Area within periosteal surface
		Medullary Area (MA)	mm^2	Area within medullary cavity
		Cortical Area (CA)	mm^2	Strength in compression and tension (TA-MA)
		Percent Cortical Area (%CA)		Cortical area relative to total area (CA/TA) x 100
Femur, Humerus	Cross-sectional properties of strength[2]	Maximum Second Moment of Area (I_{max})	mm^4	Maximum bending rigidity
		Minimum Second Moment of Area (I_{min})	mm^4	Minimum bending rigidity
		Circularity (I_{max}: I_{min})		Ratio of maximum and minimum bending rigidities
		Polar Second Moment of Area (J)	mm^4	Torsional and twice average bending rigidity
		Polar Section Modulus (Z_p)	mm^3	Torsional and twice average bending strength

[1] Humerus and femur standardized by body mass estimated from distal femoral metaphyseal ML breadth. Ribs standardized by estimated stature as a body size approximation (following Ruff, 2007).
[2] Second moments of area (I and J) standardized by body mass × bone length^2. Section moduli (Z) standardized by body mass × bone length (Ruff, 2008a).

together individual images with precise accuracy, although it usually recognizes which images should be adjacent. Therefore, the individual images had to be shifted manually in Adobe Photoshop to ensure precise overlap at the microscopic level. High precision in this task is necessary because small amounts of error in the placement of successive images will compound into inaccurate cross-sectional areas and distorted microscopic features.

The files generated by this method are very large and require a computer with a significant amount of memory and processing power. Due to these constraints, the images were taken at 40x magnification to minimize composite file size while maximizing visibility of

histomorphology. At this magnification, all microscopic features were clearly visible. Once completed, each composite image was manipulated in Photoshop to prepare it for cross-sectional geometric analysis. For the humeri and femora, anteroposterior and mediolateral planes were delineated on the composite images with the line tool and followed the marks made on the section with permanent marker. The images were then rotated into anatomical position with the AP dimension vertical and the ML dimension horizontal. For all skeletal elements, the background was manually replaced with white pixels (pixel value=0) and cortical bone with black pixels (pixel value=255) in Photoshop (Figure 10). Trabecular bone was digitally erased from the images, as it is not taken into account when calculating cortical bone areas and strength properties (Agnew and Stout, 2012; Crowder, 2013).

It is acknowledged in histological studies that the removal of trabecular bone from cross-sections is inherently subjective, as the margin between trabecular bone and cortical bone is generally continuous (Agnew and Stout, 2012). In radiographic images of fresh bone, trabecular bone is removed based on a density threshold. Such methods, however, are not applicable to taphonomically altered, ancient bone. For these reasons, observer consistency in the removal of trabecular bone from cross-sections is essential.

Cross-sectional geometric properties were calculated from the processed images using a program written for MATLAB (see Appendix IV for the code), provided by Benjamin Auerbach. This program converts the binary image files into a two-dimensional matrix, and calculates the geometric properties of that matrix in order to determine the bone cross-sectional properties. A test of a washer with known geometric properties (available at http://www.hopkinsmedicine.org/fae/mmacro.htm) verified the accuracy of this program. The MATLAB code was used in lieu of other programs for calculating cross-sectional properties

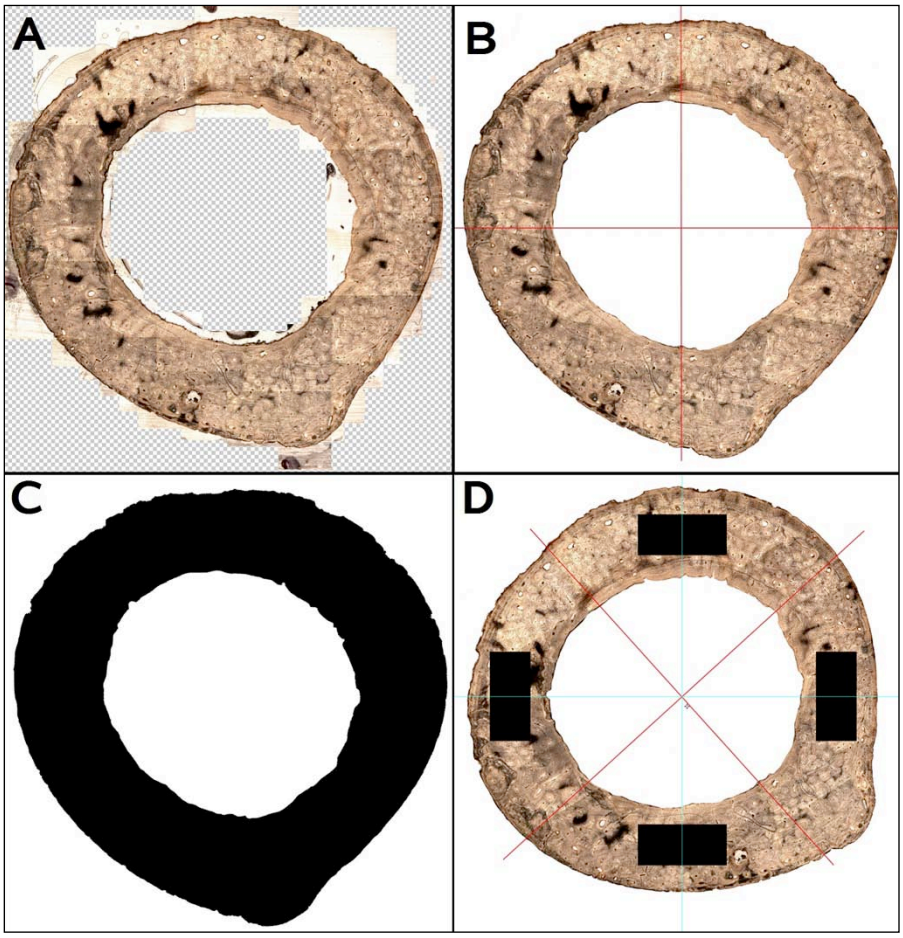

Figure 10. Methodology for processing images of bone cross-sections and defining histological regions of interest. A. Stitched composite image of individual histological images overlapped to recreate entire cross-section; B. Rotation of composite image into anatomical orientation and delineation of anteroposterior and mediolateral axes; C. Image processing for calculation of cross-sectional properties; D. Rotation of composite image by theta for location of histological regions of interest (ROI), which are designated by the black boxes.

(e.g., MomentMacro; Ruff, 2008a), as those moment calculators are optimally designed for use on radiographic images. In addition to calculating the geometric cross-sectional properties listed in Table 4, the MATLAB program also produced an output image of each cross-section rotated into an orientation reflecting I_{max} and I_{min} (x-axis = I_{max}, y-axis = I_{min}), which in turn was used to visually aid the manual rotation of the long bone composite images in Photoshop by the degrees

specified by theta. The long bone composite images were rotated by the value of theta, which was output by the MATLAB code and was used to assist in the location of the histological regions of interest along I_{max} and I_{min}, described below. Once rotated, horizontal and vertical guide lines placed in Photoshop corresponded to I_{max} and I_{min}, respectively. Due to technical difficulties with the large file sizes and imaging software, 13 cross-sections could not be analyzed for geometric properties. The age and stress group distribution of the final sample used in macromorphic assessment is presented in Table 5. Therefore, not all of the Alytus individuals were represented in statistical comparisons by all three skeletal elements.

Table 5. Age distribution of the final sample utilized for cross-sectional geometric analyses by stress group and bone element.

	Femur			**Humerus**			**Rib**		
Age Categories	Lesion Group	No Lesion Group	Total	Lesion Group	No Lesion Group	Total	Lesion Group	No Lesion Group	Total
1.0-1.99	3	3	6	3	3	6	3	3	6
2.0-2.99	5	1	6	5	1	6	6	1	7
3.0-6.99	5	9	14	6	10	16	7	10	17
7.0-11.99	15	1	16	14	2	16	17	2	19
12.0-13.99	6	0	6	7	0	7	8	0	8
Total	**34**	**14**	**48**	**35**	**16**	**51**	**41**	**16**	**57**

Histomorphological Measurements

The histomorphological properties measured for this project are listed in Table 6. These measurements were selected to best reflect microscopic bone mass and remodeling rates and their validity in representing histomorphological variation (Crowder, 2013). Some measurements frequently collected in histomorphometric studies to infer remodeling rates, such as the number

of certain osteon types (i.e., intact, fragmented, zonal, Type II) and osteon population density, were not analyzed here because frequency data are likely to differ based on the amount of cortical bone present within the cross-section. Utilization of such data may lead to spurious results when compared across skeletal elements with different absolute and relative cortical areas and between individuals of varying metabolic status. In this study, the average size and total area of histological structures are analyzed relative to the area of bone investigated to represent microscopic bone mass within each bone. All measurements were taken from the digital composite images of the histological sections, described above, using ImageJ software. The entire bone cross-section was measured for rib sections; however, regions of interest were selected on humeri and femora to strategically sample specific locations in the cross-sections that correspond with axes of mechanical loading. The specific methodology employed in analyzing the regions of interest is outlined below.

Humeri and Femora. Within the long bone elements, measurements were taken at four regions of interest (ROI), two each along the maximum (I_{max}) and minimum (I_{min}) axes of bending, respectively (Figure 10). Each rectangular ROI represents 3% of cortical area for the particular cross-section, maintains an aspect ratio of 2.18:1 across all elements, and was placed in the center of each cortex so that the I_{max} or I_{min} axis bisected the ROI. Previous research has demonstrated that ROIs containing 3% of cortical area in the anterior cortex of adult femora contained 95% of variation in histomorphometry (Iwaniec et al., 1998). A large rectangular ROI was chosen for subadult long bones over previously established adult ROIs (see Robling and Stout, 2000 for discussion) due to the unique distribution of intracortical osteonal structures during growth. The shape and size of the rectangular ROIs, and its location in the center of the

Table 6. Histomorphometric measurements used to quantify microscopic bone mass and remodeling.

Measurement	Description	Reference
Mean Intact Osteon Size (Avg On.Ar)	The average area of intact secondary osteons, excluding fragmented osteons.	Pfeiffer et al. (2006)
Mean Fragmented Osteon Size (Avg On.Fg)	The average area of osteons fragmented by the creation of additional osteons (less than 90% of the Haversian canal remains intact).	Stout (1989)
Mean Haversian Canal Size (Avg HC.Ar)	The average area of Haversian canals contained within intact osteons.	Pfeiffer et al. (2006)
Mean Osteon Cortical Size (Avg On.C.Ar)	The average area of cortical bone contained within intact osteons (On.Ar-HC.Ar).	Pfeiffer et al. (2006)
Mean Resorption Space Size (Avg RS.Ar)	The average area of resorption spaces.	Lazenby (1986)
Mean Pore Size (Avg Por.Ar)	The average area of porous structures (e.g., resorption spaces, Haversian canals) present within the cross-section.	Streeter (2005)
Intact Osteon Area (Total On.Ar)	The total area of intact secondary osteons, excluding fragmented osteons, within the cross-section.	Pfeiffer et al. (2006)
Fragmented Osteon Area (Total On.Fg)	The total area of osteons fragmented by the creation of additional osteons (less than 90% of the Haversian canal remains intact) within the cross-section.	Stout (1989)
Haversian Canal Area (Total HC.Ar)	The total area of Haversian canals contained within intact osteons within the cross-section.	Pfeiffer et al. (2006)
Osteon Cortical Area (Total On.C.Ar)	The total area of cortical bone contained within intact osteons (On.Ar-HC.Ar) within the cross-section.	Pfeiffer et al. (2006)
Resorption Space Area (Total RS.Ar)	The total area of resorption spaces within the cross-section.	Lazenby (1986)
Porosity (Total Por.Ar)	The total area of porous structures (e.g., resorption spaces, Haversian canals) present within the cross-section.	Streeter (2005)
Osteonal Bone Area (Total On.B.Ar)	The total area of osteonal bone, including intact and fragmented osteons (Total On.Ar + Total On.Fg.Ar)	Ahlqvist and Damsten (1969)

cortex, avoids inclusion of the endosteal and periosteal portions of the cortex that frequently contain unremodelled interstial lamellae in immature individuals, especially the youngest ones (Lazenby, 1986; Goldman et al., 2009). Inclusion of these areas would have potentially diminished the amount of histological data for younger subadults and introduced age bias in the amount of osteonal bone included in the region of interest.

Images of the ROIs were captured from the stitched composite images and analyzed in ImageJ. ROIs containing significant diagenetic change that obliterated osteonal structures were eliminated from analysis; this constituted 2% of the total femoral regions of interest (n = 2) and 4% of the total humeral regions of interest (n = 5). In some cases, entire long bone elements were eliminated from analysis, and in other cases only portions of the cross-section could be measured. When only portions of ROIs could be measured, measurements were standardized by the area occupied by non-diagenetic bone (see *Size Standardization*).

When a histological feature was only partially included in the ROI, it was measured and labeled as an incomplete feature. Mean size histological variables (e.g., Avg. On.Ar, Avg. Por.Ar) represent measurements on complete features only; these variables lend information on the average size of remodeling events. Total area measurements involve the area encompassed by all features within the ROI—both complete and incomplete—and provide information about both the size and frequency of remodeling events within the ROI.

Ribs. Because ribs are not modeled as beams loaded in compression like long bones are, ROIs along I_{max} and I_{min} could not be utilized; and thus, the entire cross-section of each rib was analyzed for histological properties. This method is typically employed when estimating age and

investigating metabolic effects from rib cortical histomorphometry (Robling and Stout, 2008; Crowder et al., 2012).

In this study, histological structures were measured in one section of each rib element. Frost (1969) recommended measuring osteonal structures in at least 50 mm^2 of adult rib cortical bone, often requiring multiple thin sections from the same rib element, especially if the sample contains diagenesis (Stout and Paine, 1992). This methodology cannot be readily applied to younger individuals, as their rib cortical thicknesses and areas are typically smaller than in adults, and it would take increasingly more rib sections in the youngest individuals to meet the protocols set out by Frost. Moreover, such an analysis would include a disproportionately larger percentage of rib sections along the rib's length for younger individuals (as they have smaller ribs) relative to older individuals, causing potential variation in histomorphometric properties along the rib's length to affect comparisons across individuals (see Cormier et al., 2005, for discussion about variation in rib material properties). Thus, this method had to be modified to account for these discrepancies.

In some cases, extensive diagenetic change prevented measurement of any portion of the rib cross-section, and these sections were excluded from analyses. Diagenesis is more common in adult rib elements relative to other adult skeletal elements, due to their thin cortical shell. Diagenesis is also more frequent in subadult bone, in general, relative to adult bone, due to increased fragility and porosity (Hanson and Buikstra, 1987). The Alytus subadult rib elements contained significant obliteration of microscopic structure due to diagenetic change, and 22 sections (39%) had to be excluded from analyses. Of the remaining elements, 25 ribs (71%) were found to have good to excellent preservation, and 10 (29%) were unaffected by taphonomy. To include the maximum amount of information possible, the portions of each rib section that were

free from diagenesis were measured and analyzed as a percentage of non-diagenetic rib cortical area. For ribs containing portions of diagenesis, these regions were measured with ImageJ and subtracted from total rib cortical area when standardizing histological measurements (see *Size Standardization*). While this technique involves analysis of different proportions of cortical bone across individuals, it mimics current methods for adult ribs, which also account for taphonomic effects (Crowder et al., 2012). On average, 7% of rib cortical area was excluded on the basis of diagenetic change. The age and stress group distribution of the final sample utilized in histological analyses is presented in Table 7.

Table 7. Age distribution of the final sample utilized for histomorphometric analyses by stress group and bone element.

	Femur			**Humerus**			**Rib**		
Age Categories	Lesion Group	No Lesion Group	Total	Lesion Group	No Lesion Group	Total	Lesion Group	No Lesion Group	Total
1.0-1.99	3	2	5	3	3	6	3	2	5
2.0-2.99	3	0	3	3	0	3	3	0	3
3.0-6.99	4	5	9	4	9	13	5	9	14
7.0-11.99	8	0	8	6	1	7	10	1	11
12.0-13.99	0	0	0	0	0	0	2	0	2
Total	**18**	**7**	**25**	**16**	**13**	**29**	**23**	**12**	**35**

Analyses and Statistical Methods

Size Standardization

Cross-sectional Geometric Properties. Three dimensions were taken for size standardization of cross-sectional geometric properties (Table 8). Standardization of adult long bone cross-sectional properties is required to account for size differences (i.e., body mass and

mechanical length of an element) that in turn will affect mechanical loading independent of behavioral activity. Size standardization is even more important for comparing immature individuals who vary significantly in size with age. Depending on the bone and the measurement being quantified, cross-sectional properties were size-standardized by body mass, bone length, or a combination of the two. Following Ruff (2007), body mass was estimated for each individual from distal femoral metaphyseal breadth. In long bones, cross-sectional geometric properties of bone mass (i.e., TA and CA) were standardized by body mass, second moments of area (i.e., I_x, I_y, I_{max}, I_{min}) were standardized by body mass x bone length^2, and section moduli (e.g., Z_p) were standardized by body mass x bone length (Ruff, 2008a).

Table 8. Measurements used in size standardization of cross-sectional properties.

Bone Element	Measurement Type	Measurement[1]	Instrument	Reference	% Measurement error[2]
Femur and Humerus	Bone length	Biomechanical diaphyseal length	Subadult osteometric board	Trinkaus et al. (2002)	0.17 (F) 0.19 (H)
	Metaphyseal dimensions	Distal ML metaphyseal breadth	Digital Calipers	Buikstra and Ubelaker (1994)	0.27 (F) 0.39 (H)
Rib	Bone length	Cord length	Digital Calipers	Fazekas and Kósa (1978)	0.31

[1] Planes are abbreviated: AP, anterior-posterior; ML, medio-lateral.
[2] Average difference of three measurement trials from their mean, divided by the mean and multiplied by 100 (following White, 2000). Elements are abbreviated: F, femur; H, humerus.

Because Alytus subadults exhibit delayed epiphyseal fusion relative to the Ruff (2007) reference population (the Denver growth sample), Alytus individuals at or above 13 years of age could not be size-standardized directly using the Ruff regression equations without first converting diaphyseal lengths to total bone lengths. The conversion equation [Diaphyseal length

× (Femoral ratio=1.097) or (Humeral ratio=1.079) = Total bone length] was applied to these individuals prior to stature estimation and size standardizations using bone length.

Whether humeral cross-sectional properties should be standardized by bone length alone or with estimates of body mass as well has been debated (Ruff, 2008a; Cowgill, 2010). Although the upper limb is not weight bearing, the relationship between upper limb strength and body mass is apparent (Churchill, 1994); and when it is possible to adequately estimate body mass from well-preserved skeletal remains (as is the case in the Alytus sample) it is advisable to incorporate body mass into humeral size-standardizations (Ruff, 2008a). For these reasons, all humeral cross-sectional properties were size-standardized by body mass when appropriate.

Because it utilizes a European American reference population, Ruff's (2007) body mass estimation method involves similar caveats as age-at-death estimation methods using skeletal age indicators. Subadult body mass in an ancient population such as Alytus likely differed from that of a modern population due to differences in diet, body proportions, and rates of growth. However, this method is the only one currently available for estimating body mass from subadult skeletal remains and was therefore used in this study.

Size standardization is not typically performed on adult ribs but is necessary in this study due to significant variation in body size over the course of ontogeny. As not all rib elements were complete enough to be measured, rib chord length (referenced in Table 8) could not be used. Therefore, estimates of rib cortical area were standardized by stature estimates as a body size approximation. Such methodology must assume isometry between rib dimensions and stature during growth, which has not been established. However, stature is the only body size estimate other than rib chord length that would be appropriate for standardization without incurring additional isometric assumptions in using another scaling factor (Auerbach and Sylvester, 2011).

Stature was estimated following regression equations outlined in Ruff (2007) using femoral diaphyseal length in individuals less than 13 years of age and femoral total bone length (estimated from femoral diaphyseal length) in those 13 to 14 years of age.

Histomorphometry. Osteon size in adults does not appear to vary significantly between the sexes or with age, although it does differ depending on the skeletal element being investigated (Pfeiffer, 1998; Pfeiffer et al., 2006). Osteon population density, however, does increase steadily with age (Kerley, 1965; Stout and Paine, 1992; Streeter, 2005; Doppler et al., 2006). It is possible that changes in osteon size occur during ontogeny and that these size differences could affect comparisons across groups with different age compositions. However, previous research on secondary osteon size in subadult ribs showed no significant differences with age (Streeter, 2005), further supporting analyses in adults and suggesting that osteon size is relatively conserved across the human lifespan in non-pathological cases. Thus, size standardization of histological measurements to remove size-related age effects was not performed in this study.

Similarly, age-related increases in the number of osteons are liable to bias estimates of remodeling rates, total areas of osteonal bone, and porosity between stress groups with differing age distributions. This issue is partially avoided in this research by the exclusion of histological frequency data (e.g., osteon population density) from analyses (as discussed above). Additionally, total areas for each histological measurement are standardized by the area of the ROI to eliminate bias towards measuring more histological structures in larger (i.e., older) elements. For long bones, this involves dividing each variable by the combined areas of the ROIs to be included in each comparison. Because ROIs were consistently 3% of cortical area for both

the humerus and femur, these standardizations make comparisons between these elements analogous. However, because the entire rib cross-section had to be measured and diagenesis was more frequent in rib bones, histological variables in these elements were treated differently from long bones. Standardization by observable rib cortical area (rib CA-total diagenetic bone area) was performed for each element. For both long bones and ribs, area standardizations were only conducted on histological variables assessing total areas summed across the ROI (e.g., osteonal bone area, porosity) and not average size variables (e.g., mean intact osteon size).

Despite these standardizations, differences in osteon population density and remodeling could nevertheless affect statistical comparisons, especially those assessing total area measurements. Older individuals may have higher porosities and percentages of osteonal bone relative to younger individuals. In the Alytus sample, the lesion group contains almost all of the older children and adolescents, and age differences between the stress groups may affect statistical comparisons for histological variables (see Chapter 6 for full discussion).

Statistical Analysis

To address the hypotheses and research questions presented in Chapter 1, a variety of statistical methods were employed. Before comparing bone properties indicative of bone mass and distribution, basic size variables (i.e., body mass, stature, bone length) were compared between the stress groups to identify possible metabolic effects on chronically stressed subadults relative to acutely stressed/non-stressed subadults. Comparisons between the lesion and no lesion groups were made for both macroscopic and microscopic measurements using analysis of covariance (ANCOVA) with age as a covariate to partially account for variance among groups due to age differences. These tests were conducted on the entire sample rather than individual

age cohorts (e.g., Bogin's age classifications) because of limited sample sizes, especially for histological measurements, in these groups (see Tables 5 and 7).

Parametric statistics were favored for comparisons including the entire sample; nonparametric statistics (i.e., Mann-Whitney) lack the statistical power of ANCOVAs, and their application in this study to the entire sample would require z-score transformation to minimize age effects caused by differential age distribution between the stress groups. Such practice would result in several computational steps away from the original data and thus less easily interpretable results. Furthermore, ANCOVA is robust to violations of statistical assumptions (namely, normality), and corrected *F* tables have been constructed to address unequal variances (Wildt and Ahtola, 1978). This stated, most of the data do not violate normality when analyzed as a whole but do violate this assumption when restricted to smaller sample sizes, such as age cohort groupings. Therefore, when analyses were conducted on a subset of the sample (individuals between one and seven years of age; see Chapter 5) nonparametric statistics (i.e., Mann-Whitney and Kruskal-Wallis test) were utilized rather than ANCOVA due to small sample sizes in this sample subset. These nonparametric statistics are more robust in the case of small sample sizes than ANCOVA. As all dimensions examined in these analyses are size-standardized, while age is not accounted as a covariate in these age-group restricted nonparametric analyses, the results between nonparametric and parametric analyses are still comparable in this study with some caution.

ANCOVAs and nonparametric analyses were used to evaluate three sets of comparisons. First, for both cross-sectional and histomorphometric properties, comparisons were made between single skeletal elements among the stress groups (e.g., femoral %CA in lesion group versus femoral %CA in no lesion group). These statistics test whether cross-sectional properties

and microscopic bone mass are reduced in individuals with lesions relative to those without lesions for each element separately (Hypotheses 1a, 1b, 2a). Second, similar comparisons were made across the three skeletal elements *within* each stress group (e.g., femoral %CA versus humeral %CA versus rib %CA within the lesion group) to identify differences in the *pattern* of macroscopic and microscopic variables among elements in these groups (Hypotheses 2a, 2b). Third, ANCOVA was used to test for differences between the stress groups in microscopic bone mass and remodeling along the axes of bending within the femur and humerus (Hypothesis 2c). These comparisons were made separately for each long bone and involved the calculation of variables that reflect the magnitude of difference between I_{max} and I_{min} by subtracting the latter from the former (e.g., femoral I_{max} porosity – femoral I_{min} porosity).

For each of the three sets of analyses outlined above, chi-square tests were conducted to compare frequencies of patterns across elements for each of the variables and between the stress groups (Hypotheses 1a, 1b, 2a, 2b, 2c). These analyses involved only individuals within the Alytus sample who possessed data for all three skeletal elements and explore the variation in macroscopic and microscopic patterns *within* individuals, using an approach similar to the test for crossed-symmetry devised in Auerbach and Ruff (2006). For each variable, the frequencies of individuals displaying specific patterns of relative magnitudes across bone elements were determined (e.g., Femur %CA > Humerus %CA > Rib %CA versus Humerus %CA > Femur %CA > Rib %CA). Then the frequencies of individuals displaying each pattern for a certain variable were analyzed against the null hypothesis that frequencies are equal between the stress groups. When no significant differences were found between the stress groups, the analysis was conducted again on the full sample (including both lesion and no lesion groups) to determine the overall frequencies of patterns for Alytus subadults. Such analyses supplement those conducted

with ANCOVA by testing whether comparisons of means across elements and between groups is representative of actual individual patterns. Chi-square tests were not performed on the subset of Alytus subadults between the ages of one and seven years due to the small number of individuals possessing data for all three elements.

In all statistical comparisons, no attempt was made to correct for multiple comparisons, despite the potential for increased likelihood of Type I errors as the number of comparisons increases. Such corrections (i.e., sequential Bonferroni corrections) decrease the level of alpha by dividing it by the number of comparisons; however, this practice is associated with reductions in statistical power, which is already an issue with the present data set, as noted above. Recently, researchers have begun to question the use of Bonferroni corrections (Perneger, 1998; Cabin and Mitchel, 2000; Moran, 2003; Nakagawa, 2004). Although falsely rejecting the null hypothesis (i.e., Type I error) is a serious concern, so is restricting the ability to find any statistical significance whatsoever. It has also been argued that Bonferroni corrections discourage intricate and extensive analyses; the more statistical exploration conducted, the more corrections must be performed to correct for multiple tests, and therefore the probability of finding any significant patterns is hindered (Moran, 2003). This paradox leads to potential bias in publications. Multiple comparison corrections create scenarios where extensive analyses result in lack of significant findings, and thus, arguably less inclination by authors to publish statistically limited results. However, less thorough analyses will more often lead to significance and publishable scientific work (Nakagawa, 2004).

Along these lines, as well, the results presented in the following chapters are interpreted in light of the knowledge that lack of statistical significance is not evidence of lack of *biological* significance. Similarly, statistically significant results may not be biologically significant; if the

difference between two groups were of small magnitude (e.g., one millimeter for a long bone measuring twenty centimeters), yet had statistical significance, the biological consequence of this difference would likely be minimal. These interpretative strategies are especially true of studies such as this one, where expected magnitudes of difference in geometric and histological properties among subadults are unknown. For these reasons, and due to limited sample sizes in the Alytus archaeological sample for some comparisons, non-significant trends are also explored within the data to investigate biological patterns within and across individuals. Whether comparisons resulted in statistical significance is noted for each comparison as it is discussed.

Data were recorded and size standardizations were calculated in Microsoft Excel 2011. All further calculations were also performed using Excel. Statistical analyses were conducted using IBM SPSS version 20.1.

CHAPTER 5: RESULTS

This chapter presents the results of the statistical analyses of all bone properties described in Chapter 4. Special consideration is given initially to limitations imposed on these analyses due to the sample composition for each stress group category (lesion and no lesion). This is followed by comparisons of scaling factors (i.e., body mass, stature, and long bone length) between the two stress group categories, as well as comparisons of growth based on age estimations using skeletal and dental criteria. Subsequently, the chapter presents results of ANCOVAs and chi-square tests described under the "Statistical Analysis" section of Chapter 4. Some limited discussion of result implications is included when necessary in this chapter, but interpretations of results are reserved for the Discussion in Chapter 6.

Weighted means and standard deviations, using age as a weight, are reported for each osteological, cross-sectional geometric, and histomorphometric dimension examined for the entire sample as a whole. Unweighted means and standard deviations are not reported because ANCOVAs compare all ages using age as a continuous covariate variable, and comparison of unweighted means does not accurately reflect the nature of the analyses. Because many of this chapter's analyses compare all ages simultaneously between the two stress categories, the results in this chapter do not report means and standard deviations for each of the Bogin age cohorts. These descriptive statistics may be found for each bone property in Appendices V-VII. To improve readability of this chapter, all cross-sectional geometric and histomorphometric summary data are reported in the appendices. For analyses conducted on the entire sample, weighted means and standard deviations are reported in Appendices VIII-X. For nonparametric

analyses, medians for cross-sectional and histomorphometric dimensions are presented in Appendices XI-XIII.

Statistical Approach to Age Differences Between Stress Groups

As discussed in Chapter 4, there are differences in age distribution between the lesion and no lesion groups, largely caused by differences in the presence of dental enamel hypoplasia (DEH) among the Alytus sample. DEH was present only in individuals above the age of seven years old (see Table 1, page 126). This discrepancy affects comparisons of all bone properties between the groups. Solutions for this difference in the age distributions between stress groups are discussed below.

The difference in the presence of pathological lesions for subadults younger and older than seven years is due to multiple reasons. The onset of permanent dental eruption in subadults (around seven years in the Alytus sample), combined with the well preserved dental arcades and intact alveolar bone, prevented the examination of DEH in the unerupted permanent dentition of the youngest individuals; no DEH was observed in the deciduous dentition. Some of the individuals under the age of seven could have possessed DEH following recovery from a stress event, but could not be observed. Thus, some chronically stressed individuals under the age of seven may have been miscategorized into the no lesion group. Yet, without direct observation, it is unknown whether such a scenario exists in this sample.

DEH was observable in older Alytus subadults with erupted permanent dentition, and its presence suggests recovery from stress events that occurred between birth and ten years of age, after which permanent teeth become fully mineralized. In the Alytus sample, 28 individuals could be assessed for DEH presence in the permanent dentition, and 61% of these individuals

possessed one or more enamel growth disruptions. The estimated ages of dental hypoplasia occurrence ranged from roughly nine months to six years of age, with the highest frequencies of DEH occurring between the ages of two and four (Appendix XIV), a pattern typical of other archaeological populations and likely caused by weaning stress. The deciduous dentition has already erupted by these ages, and crown formation of those deciduous teeth ceased within two years of birth. Weaning stress, or any stress encountered thereafter, would thus not be recorded as hypoplasias on the deciduous teeth. This is a possible explanation for the lack of DEH within the deciduous dentition in the Alytus sample.

The age discrepancy in DEH presence at Alytus, in part, contributes to the low number of individuals in the no lesion group (n = 2) who are over seven years of age. By older childhood and adolescence, the majority of Alytus individuals older than seven years (n = 24, 92%) possess some pathological indicator of metabolic stress (whether skeletal or dental), most likely because they have recovered from one or more metabolic stress events commonly experienced by younger subadults. One could argue that older subadults who possess DEH but lack other pathological lesions are not necessarily individuals who died from recent chronic stress events but those who survived metabolic stress as a young child only to succumb to acute illness or accidental death as an older child or adolescent.

This scenario is certainly plausible and cannot be ruled out as an explanation for the demographics of the Alytus sample. However, there remain justifiable reasons for categorizing individuals into the lesion group when the individual's only observable pathological lesion is DEH. As discussed in Chapter 4, DEH in older subadult and adult skeletal remains is traditionally used to indicate chronic stress in a population, because its presence suggests increased risk of frailty and reduced health status. These changes in morbidity have lasting

effects throughout growth. DEH in adults (Paine and Brenton, 2006) and subadults (Seow et al., 1989) has previously been linked to reduced bone mass, and as discussed in Chapters 2 and 3, bone loss during growth has lasting influences on strength throughout ontogeny and adulthood. For these reasons, analyses were initially conducted on the entire age range and employed the presence and absence of DEH in the categorization of individuals into lesion and no lesion groups, respectively (in addition to other skeletal lesions). Where appropriate, analyses on the entire sample utilized age as a covariate in ANCOVAs to account for variance due to age differences among the stress groups.

Because ANCOVA can only account for variance due to age and will not necessarily eliminate all statistical differences caused by age effects, analyses were also performed on a subset of the Alytus sample: individuals between the ages of one and seven years (1.0-6.99 years old). This subset was chosen for several reasons. First, Alytus individuals below the age of seven years have not experienced full permanent dental eruption; thus, by focusing on younger subadults, the confounding factors associated with differential DEH presence between the two stress groups are avoided. This procedure effectively eliminates DEH from consideration in stress categories, because DEH was not visible in individuals between one and seven years of age, though it is likely present in the unobservable permanent dentition. Second, although metabolic stress can affect individuals in late childhood and adolescence, its effects are most pronounced in infants and younger children. Therefore, differences in bone properties between the stress groups may be greater and/or more prevalent in this younger age range.

Third, and perhaps most importantly, this subset incorporates almost equal numbers of individuals from both stress groups, removing the large number of older, chronically stressed subadults from analyses. Older subadults are likely to have greater cortical bone and stronger

cross-sections relative to their size than younger subadults, as well as different relative strength proportions in their humeri and femora due to alterations in mechanical loading between the upper and lower limb. Additionally, older subadults will have higher rates of intracortical remodeling per unit area of cortical bone. Therefore, when using the entire Alytus sample, differences present between the lesion and no lesion groups could be partially driven by age differences in bone properties rather than simply metabolic influences.

Body Mass and Size in the Alytus Sample

ANCOVA comparisons of body mass, stature, femoral length, and humeral length show no significant differences between the lesion and no lesion groups (Table 9, Figure 11). When comparisons are restricted to individuals below the age of seven years, there remain no statistically significant differences between the stress groups, although individuals with lesions do possess lower median values for all variables (Table 10). These results suggest that, within the Alytus sample, subadults with lesions do not have significantly reduced body mass or restricted growth in body size (i.e., long bone growth and stature) relative to those without lesions. Alternatively, it is possible that the long bone linear dimensions that estimate these properties do not reflect effects of the metabolic stressors that led to pathological lesions. The lack of congruence between measurements of size and the presence of skeletal lesions—and thus differences in stress categories—is unexpected.

Although body size is not significantly smaller in individuals presenting pathological lesions, skeletal age estimates based on femoral length are younger relative to dental age estimates in *almost all* individuals at Alytus, indicating that some sort of metabolic disturbance may be affecting growth in this population as a whole (Figure 12). Generally, individuals in both

the lesion group and no lesion group have short femur lengths for their dental age based on the dental and skeletal age estimates of European reference populations. An ANOVA demonstrates no significant differences between the stress groups in the magnitude of delay in skeletal growth relative to dental growth (p = 0.099; lesion group $\overline{\chi}$ = 2.43 years; no lesion group $\overline{\chi}$ = 1.59 years), though the lesion group is non-significantly more delayed. These data confirm reports discussed in Chapter 4 of restricted growth in height in medieval Lithuanian populations relative to modern Lithuanian populations.

Table 9. Results of ANCOVA comparing estimated body mass, stature, femoral length, and humeral length between stress groups.

Dimension	$\text{Mean}_{\text{weighted}}$ (Std. Dev.)		ANCOVA *p*-value
	No Lesion Group	Lesion Group	
Estimated Body Mass (kg)	13.34 (3.77)	22.98 (12.96)	0.776
Estimated Stature (cm)	92.23 (13.36)	109.00 (23.08)	0.822
Femur Length (mm)	188.00 (39.55)	243.09 (74.88)	0.803
Humerus Length (mm)	142.85 (26.27)	180.70 (51.20)	0.934

Table 10. Results of Mann-Whitney U-tests comparing estimated body mass, stature, femoral length, and humeral length between stress groups (1.0-6.99 years).

Dimension	Medians		Mann-Whitney *p*-value
	No Lesion Group	Lesion Group	
Estimated Body Mass (kg)	12.27	10.74	0.177
Estimated Stature (cm)	91.46	81.96	0.179
Femur Length (mm)	183.75	157.35	0.193
Humerus Length (mm)	139.72	122.54	0.192

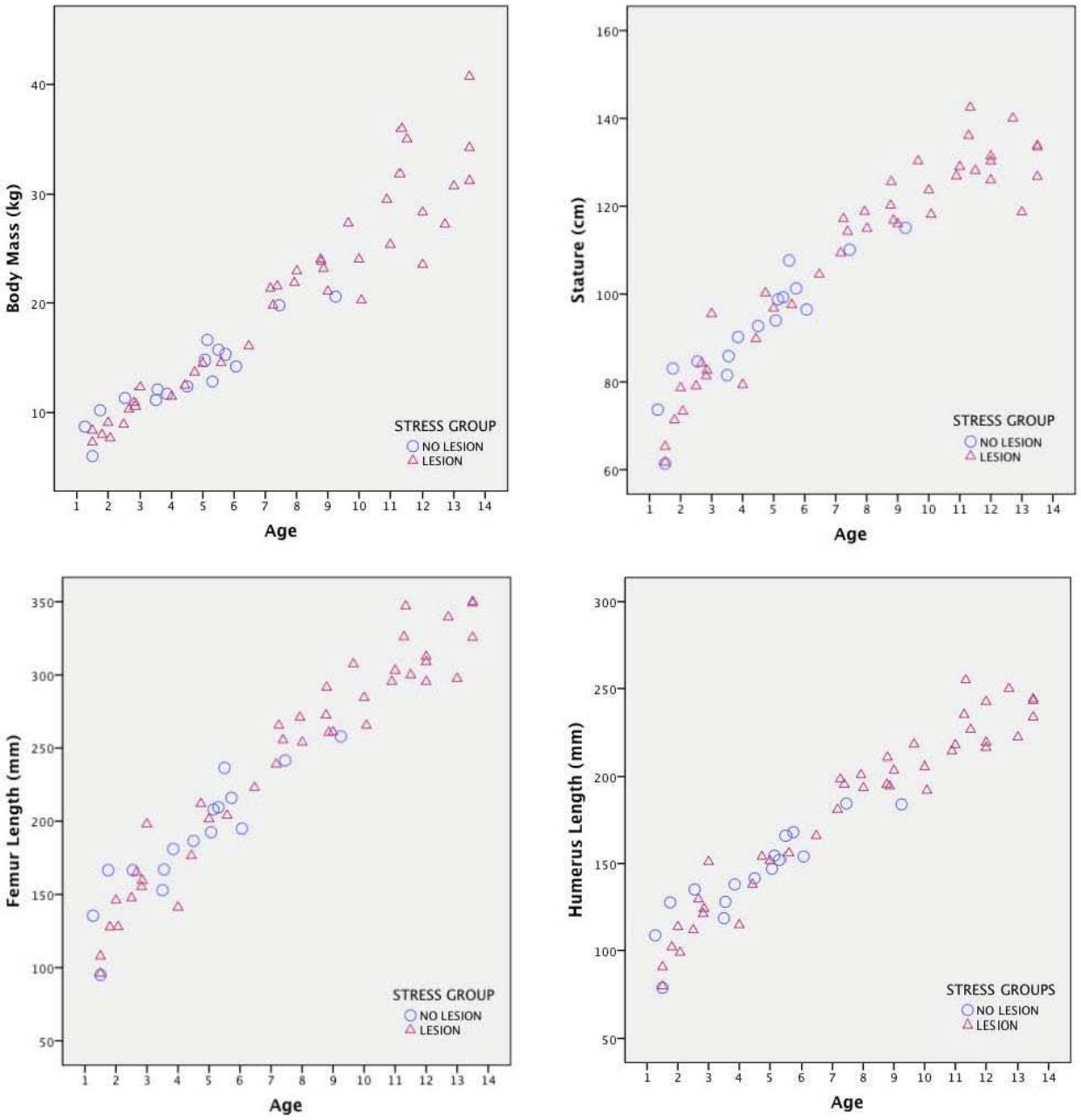

Figure 11. Scatterplots of estimated body mass, stature, femoral length, and humeral length by age and stress group.

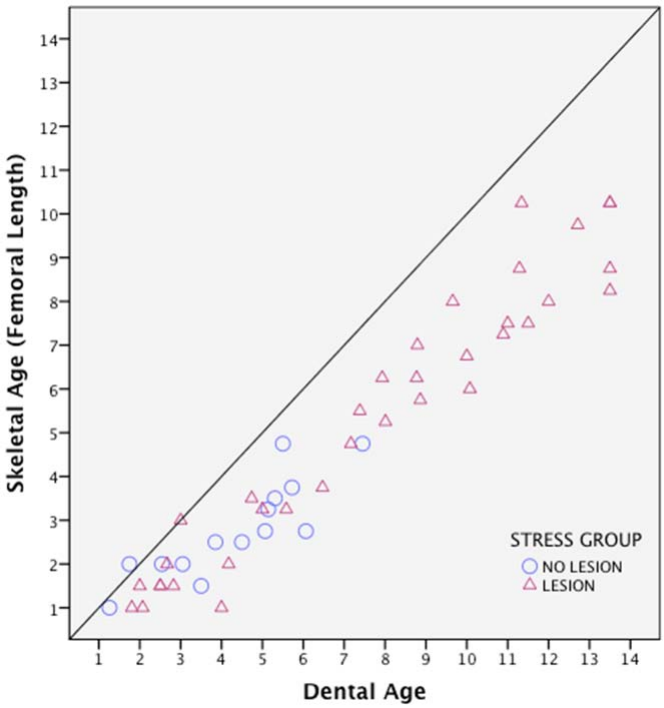

Figure 12. Scatterplot of skeletal age estimated from femoral length versus dental age estimates for each individual.

Cross-sectional Geometric Properties

This section presents the results of analyses comparing the cross-sectional geometric properties described in Chapter 4. Initial analyses contrast cross-sectional properties of the same element between stress groups. Further statistical analyses compare the properties across the three elements (rib, humerus, and femur) within each stress category. Finally, comparisons of cross-sectional geometric properties among the three elements and between the two stress groups are presented. The analyses are first reported for the entire sample and then for the age-restricted one-to-seven-year-old subset of the total sample.

Comparisons Between Stress Groups Within Each Skeletal Element (Hypotheses 1a and 2a)

All Ages. ANCOVA results comparing means for cross-sectional properties within each skeletal element and between the two stress groups are presented in Table 11. Boxplots of significantly different mean values and non-significant trends are presented in Figure 13. As explained in Chapter 4, no second moments of area or section moduli are calculated for the ribs, given their varied and difficult-to-model mechanical loading patterns with respect to long bones.

No significant differences are found in size-standardized measures of femoral cross-sectional areas, second moments of area, or polar section modulus between the lesion and no lesion groups. The only significant differences in femoral geometric properties lie in non-standardized variables (i.e., %CA and I_{max}:I_{min}); the femora of individuals in the lesion group have higher values than femora from individuals in the no lesion group for both measurements. Thus, subadults with lesions have higher amounts of femoral cortical bone relative to the total area of the cross-section and less circular femoral diaphyses.

Table 11. Results of ANCOVA comparing cross-sectional geometric properties within bone elements between stress groups.

Cross-sectional dimension	Femur *p*-value	Humerus *p*-value	Rib *p*-value
TA	0.865	0.399	0.007*
CA	0.271	0.423	0.071
MA	0.150	0.623	0.008*
%CA	0.021*	0.570	0.119
I_{max}	0.516	0.031*	
I_{min}	0.967	0.023*	
I_{max}:I_{min}	0.024*	0.701	
J	0.738	0.023*	
Z_p	0.956	0.053	

* Asterisks denote significant differences between the stress groups for the given dimension.

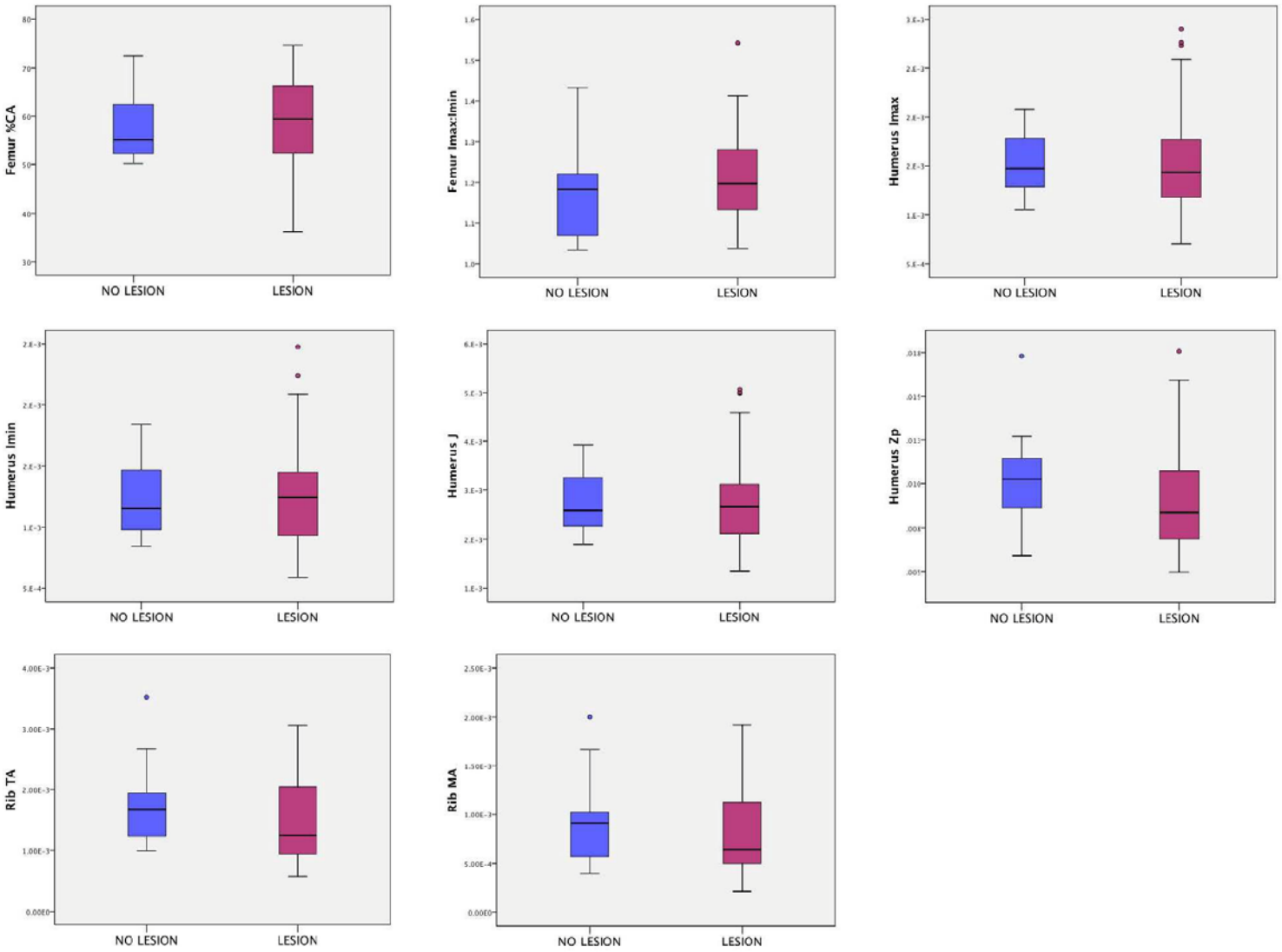

Figure 13. Boxplots of cross-sectional geometric properties between stress groups.

In the humerus, no significant differences exist in any of the cross-sectional areas, including %CA. For second moments of area, however, bending rigidities (I_{max}, I_{min}) and J are significantly greater in the humeri of the lesion group. These patterns suggest that chronic stress is associated with redistribution of the same amount of cortical area to result in stronger humeri relative to acute stress and non-stress. Despite these differences, humeral circularity and humeral Z_p are not statistically divergent between the stress groups, though individuals without lesions have non-significantly higher values of humeral Z_p ($p = 0.053$).

Rib cross-sectional areas also vary between the stress categories. Rib TA and MA are significantly higher in the no lesion group, indicating expanded periosteal and endosteal dimensions in these individuals in comparison to the lesion group. However, rib CA and %CA are unaffected by these differences in cortical bone distribution, and these variables exhibit no statistical differences between the stress categories. Therefore, much like alterations in the lesion group's humeri, the no lesion group's ribs have similar amounts of cortical bone present relative to the lesion group's ribs, but this bone has been redistributed away from the sectional centroid.

Relative strength proportions in the humerus and femur were also explored to ascertain if the alterations in long bone strength properties result in changes to relative strength proportions between stress groups. Figure 14 depicts natural logged humeral J graphed on natural logged femoral J along with a line of isometry between the two strength properties. (Note that, as these values are size standardized, the raw values for J are less than one, resulting in negative logged values; this has no effect on the distribution of the data in the scatterplot.) Only individuals represented by both a humerus and femur were included in this analysis ($n = 43$).

Except for two individuals from the lesion group who fall above the isometric line (indicating higher humeral strength relative to femoral strength), the remaining Alytus

individuals fall below the line and demonstrate stronger femora relative to humeri. This pattern within individuals is expected regardless of metabolic status; therefore, the magnitude of difference in relative strength proportions was compared between the stress groups. An ANCOVA performed on the logged ratio of humeral torsional strength to femoral torsional strength [ln (Humerus J/Femur J)] for each individual indicates significant differences between the stress groups (p = 0.024; lesion group $\overline{\chi}$ = -0.34; no lesion group $\overline{\chi}$ = -0.48; Figure 15). Individuals with lesions have higher values (i.e., closer to zero) on average than those without lesions, indicating that their humeri and femora are more similar in strength. Individuals without

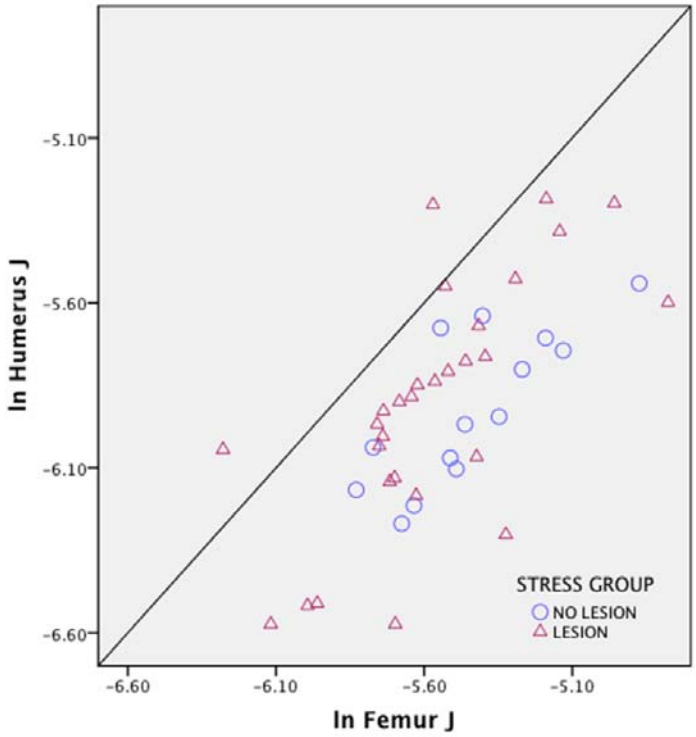

Figure 14. Scatterplot of logged humeral torsional strength on logged femoral torsional strength.

lesions have lower values, demonstrating stronger femora relative to humeri in comparison to individuals with lesions. These differences mirror those present in the ANCOVA results described above for each element separately. With chronic stress, alterations to humeral J and no alterations to femoral J lead to more similar upper to lower limb strength proportions.

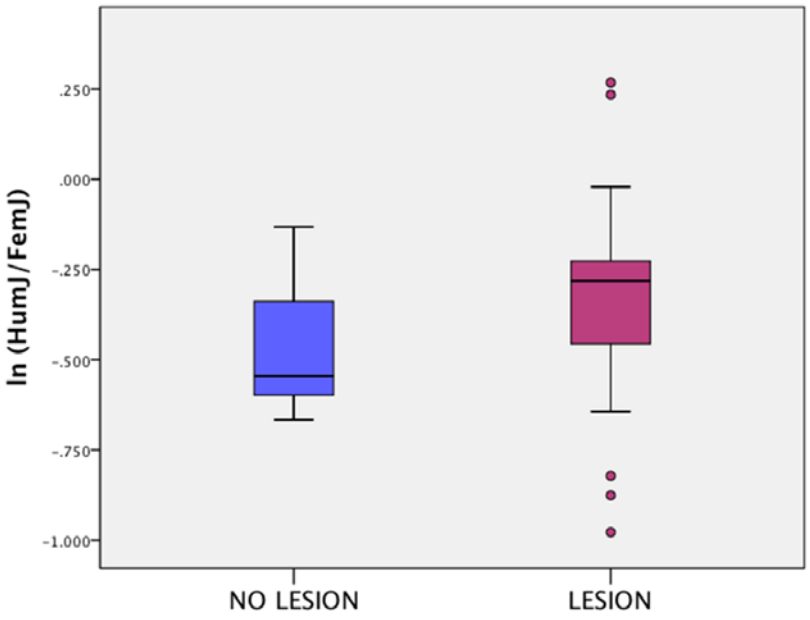

Figure 15. Boxplot of logged ratio of humeral torsional strength to femoral torsional strength.

Under Seven Years. The larger proportion of older individuals in the lesion category could plausibly cause some of the differences in cross-sectional properties, outlined above, that were reported between the stress groups. Mann-Whitney *U*-test results comparing cross-sectional properties between stress groups in the younger subadult subset (1.0-6.99 years) are presented in Table 12. Boxplots of significantly different mean values and statistically nonsignificant, but notable, trends among means are presented in Figure 16.

Table 12. Results of Mann-Whitney *U*-tests comparing cross-sectional geometric properties within bone elements between stress groups (1.0-6.99 years).

Cross-sectional dimension	Femur *p*-value	Humerus *p*-value	Rib *p*-value
TA	0.990	0.329	0.017*
CA	0.169	0.734	0.028*
MA	0.153	0.376	0.047*
%CA	0.064	0.701	0.423
I_{max}	0.479	0.210	
I_{min}	0.960	0.056	
I_{max}:I_{min}	0.064	0.571	
J	0.153	0.104	
Z_p	0.418	0.125	

* Asterisks denote significant differences between the stress groups for the given dimension.

All significant differences in long bone cross-sectional properties between the stress groups are no longer present when considering only younger subadults, though Humeral I_{min} is non-significantly greater in the lesion group ($p = 0.056$). In the rib, TA and MA are still significantly higher in the lesion group; however, rib CA is now also significantly higher in this group, though %CA remains similar between the stress groups. These results point to macroscopic bone loss in young, chronically stressed subadults (i.e., endosteal loss resulting in increased MA) but periosteal compensation for this bone loss (i.e., increased TA). This difference in rib TA is greater than that for MA, resulting in increased CA in subadults with lesions; however, the amount of rib CA relative to the total cross-sectional area (i.e., rib %CA) is not different between the groups.

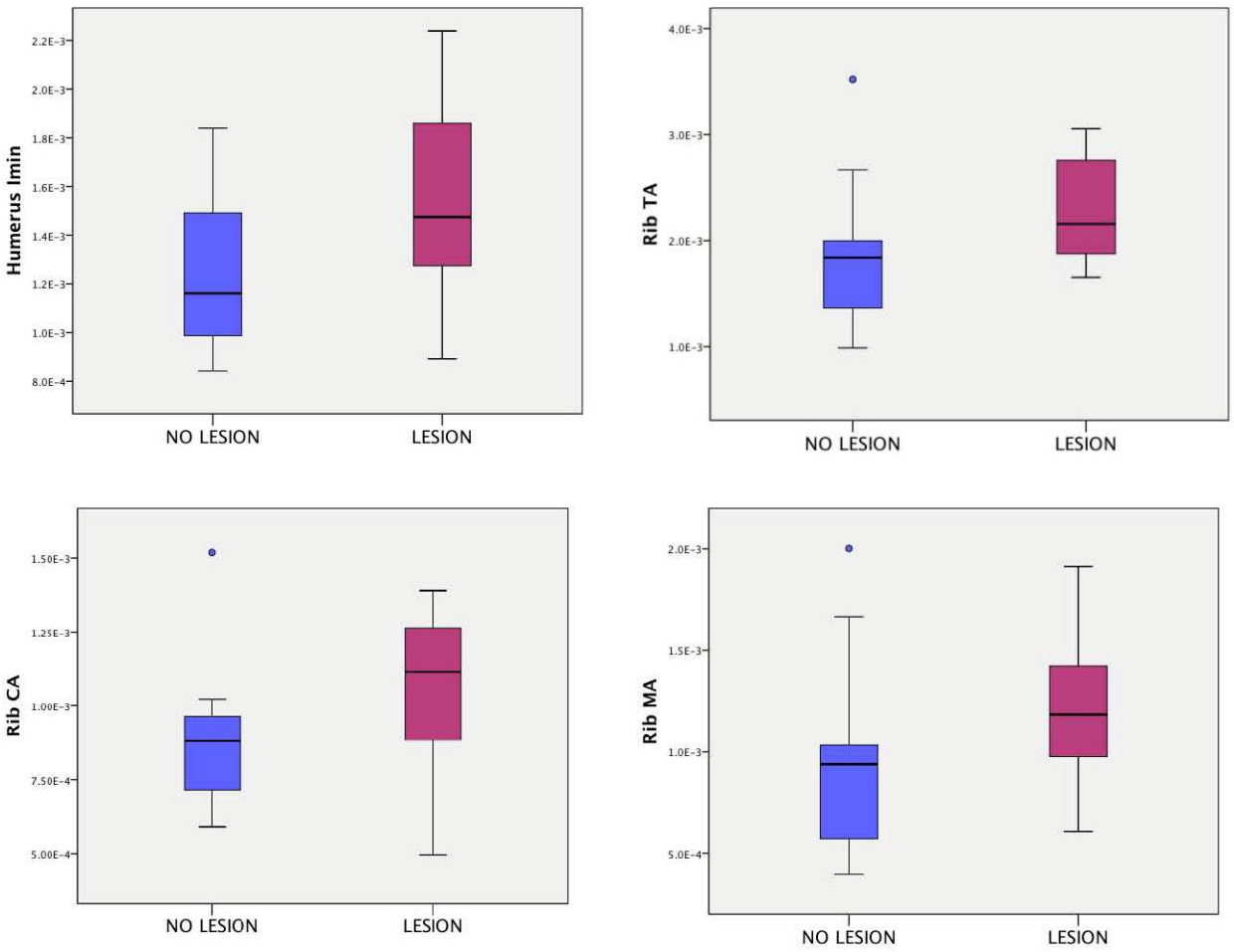

Figure 16. Boxplots of cross-sectional geometric properties between stress groups (1.0-6.99 years).

When comparing relative strength proportions between the humerus and femur in the younger subadult sample, the difference in strength found previously between the stress groups does not exist. Figure 17 shows the relationship between natural logged humeral J and femoral J for each individual possessing both long bone elements (lesion group n = 12, no lesion group n = 13). Except for one individual from the lesion group who has higher humeral strength relative to femoral strength, the younger subset generally has higher femoral strength relative to humeral strength, as was found previously for the entire sample. A Mann-Whitney U-test showed no statistically significant differences in ln (Humeral J/Femoral J) between the lesion and no lesion groups (p = 0.110; lesion group $\tilde{x}$= -0.26; no lesion group $\tilde{x}$= -0.53). As is the case

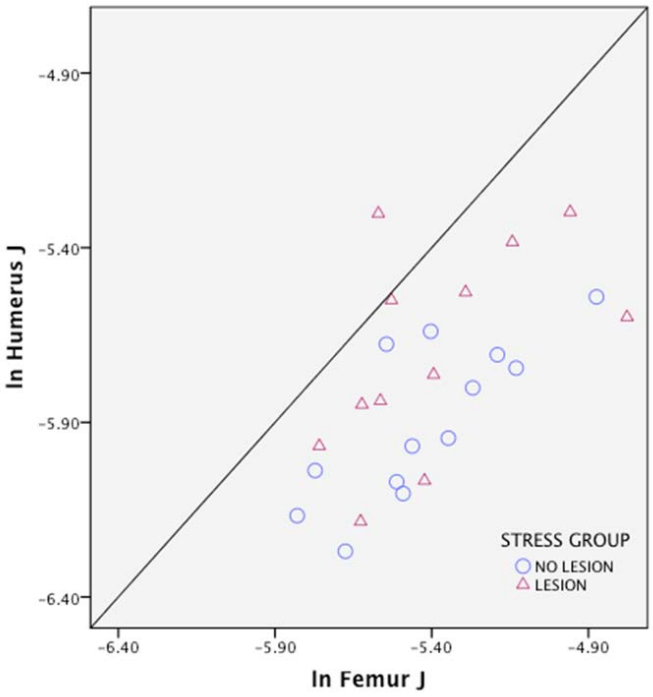

Figure 17. Scatterplot of logged humeral torsional strength on logged femoral torsional strength (1.0-6.99 years).

with the entire sample, individuals with lesions have higher values (i.e., closer to zero) on average than those without lesions (Figure 18); however, unlike before, this difference is not statistically significant. Figure 18 indicates that some of the individuals with high and low values for ln (Humeral J/Femoral J) have been eliminated with the removal of older chronically stressed subadults.

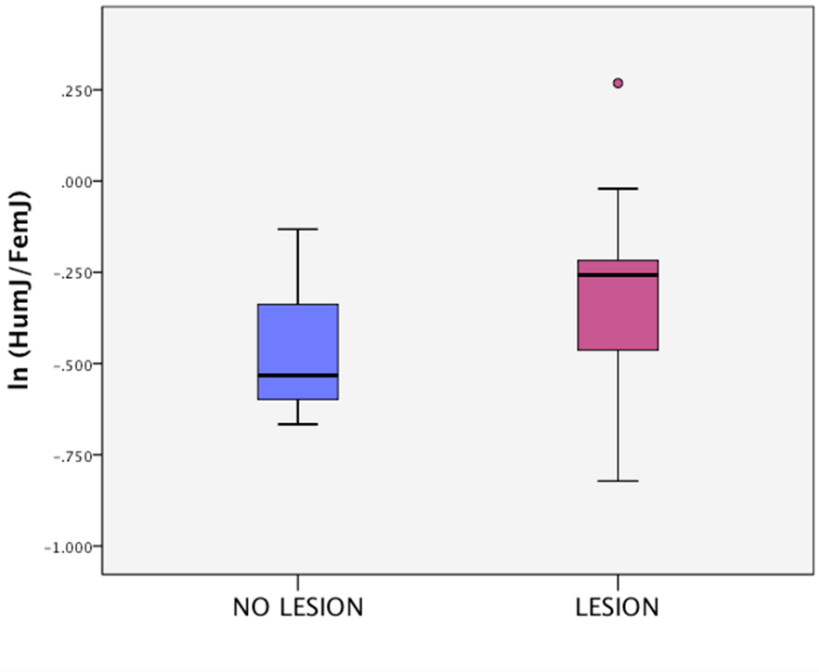

Figure 18. Boxplot of logged ratio of humeral torsional strength to femoral torsional strength (1.0-6.99 years).

Comparisons Within Stress Groups Across Three Elements (Hypotheses 1a and 2a)

All Ages. ANCOVA results comparing cross-sectional geometric properties among the three bones and within stress categories separately are presented in Table 13. These comparisons were conducted to reveal statistical patterns in macroscopic bone properties across the skeleton

and to contrast these patterns among the stress groups. Rib strength properties were not assessed for reasons outlined in Chapter 4; and, thus, only cross-sectional areas (TA, CA, MA, %CA) were evaluated across all three elements, while strength properties were assessed between the two long bones. In analyses presented in the subsequent sections, line graphs of means for each element are used as visual aids to reveal the underlying patterns both within and between stress groups. This method is not used for the current comparison, because age effects in cross-sectional properties between the lesion and no lesion groups distort the relationships among these properties and make interpretation of graphical depictions spurious. In presenting differences within stress groups for the entire sample, reference is made to the weighted means presented in Appendix VIII. These means are directly comparable to the ANCOVA results presented in Table 13, because they account for differential age distribution among the stress groups.

Although the no lesion group has a smaller sample size than the lesion group, both possess similar patterns in mean cross-sectional areas across the femur, humerus, and rib. For both groups, cortical area declines with decreased loading across the skeletal elements (Femur > Humerus > Rib) and differences between each bone are statistically significant. The same pattern of mean values and statistical significance across the bones is present for TA and MA. This pattern is, of course, logical—femora, standardized by body mass, are larger bones in cross-section than humeri, and both are much larger than ribs—but it is important to examine the raw differences before assessing the relative amount of total cross-sectional area in each element.

The only measurement that demonstrates a different pattern between the stress groups is %CA. For both stress groups, significant differences exist between each long bone and the rib for %CA but not between the long bones. Additionally, in individuals without lesions, this variable

Table 13. Results of ANCOVA comparing cross-sectional geometric properties between skeletal elements within stress groups.

Element	Cross-sectional dimension	Humerus		Rib	
		Lesion group *p*	No lesion group *p*	Lesion group *p*	No lesion group *p*
Femur	TA	<0.001*	<0.001*	<0.001*	<0.001*
	CA	<0.001*	<0.001*	<0.001*	<0.001*
	MA	<0.001*	<0.001*	<0.001*	<0.001*
	%CA	0.327	0.429	<0.001*	0.004*
	Imax	<0.001*	<0.001*		
	Imin	<0.001*	<0.001*		
	J	<0.001*	<0.001*		
	Zp	0.001*	<0.001*		
Humerus	TA			<0.001*	<0.001*
	CA			<0.001*	<0.001*
	MA			<0.001*	<0.001*
	%CA			<0.001*	0.027*
	Imax				
	Imin				
	J				
	Zp				

* Asterisks denote significant differences between the skeletal elements within stress group for the given dimension.

declines with decreased loading across the elements (Femur > Humerus > Rib), whereas in individuals with lesions the humerus has the highest %CA, the femur is intermediate, and the rib has the lowest values.

The lesion and no lesion groups also share the same patterns in strength properties between their long bones. For both groups, second moments of area and polar section modulus are significantly higher in the femur than in the humerus, which supports mechanical expectations for human subadults who have transitioned from crawling to walking.

The similarity in these macroscopic relationships within both stress categories indicates a biological pattern that is mostly conserved in individuals despite the cross-sectional geometric alterations associated with pathological lesion presence outlined in the previous analysis. Therefore, regardless of inferred metabolic status and body size (all measures are size-standardized), cortical envelopes (i.e., periosteal, endosteal) expand, body mass standardized cortical area increases, and strength properties increase with increased loading across the skeleton. Relative to total area, however, cortical area follows this pattern only in individuals without lesions.

Under Seven Years. The analyses performed above were reexamined in the younger subsample. Kruskal-Wallis test results comparing cross-sectional geometric properties among the three bones and within stress categories separately are presented in Table 14. Line graphs depicting patterns among the elements are provided in Figure 19. Because the rib elements are standardized by stature rather than body mass, values for rib cross-sectional areas were multiplied by a factor of 1000 when presenting the line graphs in Figure 19. This rescaling was performed only to assist with visual detection of patterns across elements in these graphs, as greater differences in size-standardized values between the long bone elements and the ribs precluded adequate graphical depiction of elemental patterns. This rescaling was not performed in the ANCOVA analysis and does not affect the assessment of differences in *patterns* among the bone elements, although it does visibly reduce the magnitude of differences in variables between long bones and ribs in Figure 19.

TA, CA, and MA in subadults between the ages of one and seven generally follow the same patterns as in the entire Alytus sample, with mean values decreasing among skeletal

elements in concert with mechanical loading decreases. These differences remain statistically significant between all three bones. Though the patterns within the stress groups are the same, a few of the trends between the stress groups have shifted compared to trends for individuals of all ages. Whereas TA was almost identical in all elements between the stress groups previously, TA in younger subadults is slightly elevated in all three of the lesion group's elements relative to elements in the no lesion group; this difference is greatest in the rib. This trend supports the significant differences between the stress groups in the Mann-Whitney test for rib TA.

Table 14. Results of Kruskal-Wallis tests comparing cross-sectional geometric properties between elements within stress groups (1.0-6.99 years).

Element	Cross-sectional dimension	Humerus		Rib	
		Lesion group *p*	No lesion group *p*	Lesion group *p*	No lesion group *p*
Femur	TA	<0.001*	<0.001*	<0.001*	<0.001*
	CA	0.002*	<0.001*	<0.001*	<0.001*
	MA	<0.001*	0.002*	<0.001*	<0.001*
	%CA	0.382	0.528	0.114	0.023*
	Imax	0.008*	<0.001*		
	Imin	0.012*	<0.001*		
	J	0.010*	<0.001*		
	Zp	0.052	0.002*		
Humerus	TA			<0.001*	<0.001*
	CA			<0.001*	<0.001*
	MA			<0.001*	<0.001*
	%CA			0.254	0.251
	Imax				
	Imin				
	J				
	Zp				

* Asterisks denote significant differences between the skeletal elements within each stress group for the given dimension.

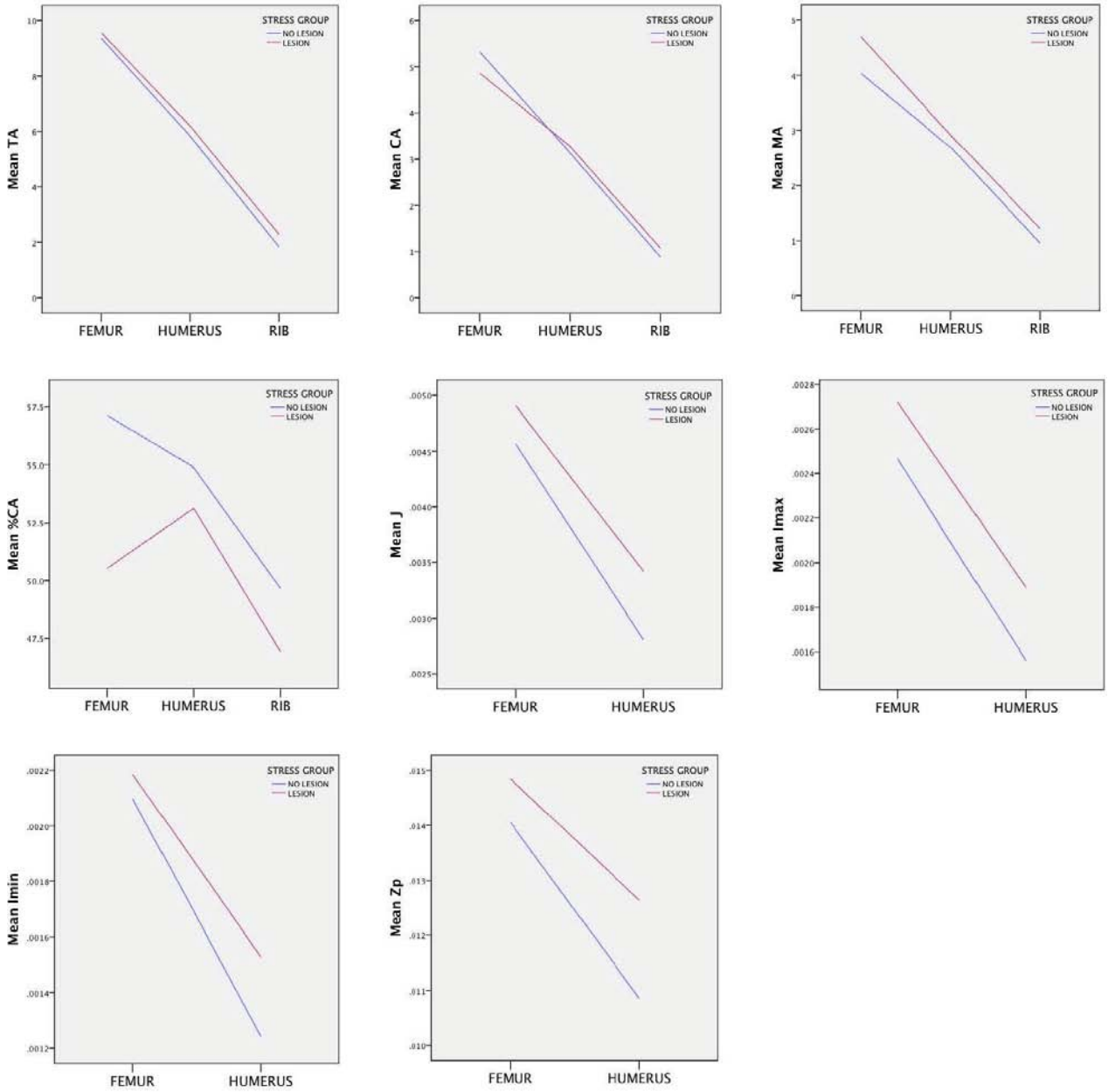

Figure 19. Graphs of cross-sectional geometric properties across skeletal elements (1.0-6.99 years).

Furthermore, while mean MA in the entire Alytus sample was unexpectedly lower in all three of the lesion group's elements, in younger subadults lesion presence is associated with non-significantly *increased* MA in all three elements. This pattern is expected given hypothesized systemic bone loss with metabolic stress; however, unexpectedly, the greatest difference in MA between the groups is in the most heavily loaded element, the femur. CA is also reduced in the lesion group's femora relative to those of the no lesion group, a difference that was not present previously and can be explained by the higher relative MA in the femora of individuals with stress lesions.

Significant differences present in the entire Alytus sample between long bone %CA and rib %CA are not significant in the younger subsample, except for the difference between femoral and rib %CA in the no lesion group. Non-significant trends within the stress groups remain the same; individuals with stress lesions have the highest %CA in the humerus, while individuals without lesions show decreased %CA with decreased loading. Patterns in %CA *between* the stress groups in the younger subadults, however, vary from those reported among all ages. The lesion group possesses lower %CA in all three skeletal elements compared to the no lesion group, which indicates systemic metabolic bone loss. This difference in %CA is greatest in the femur and similar for the humerus and rib. Thus, although bone loss occurs throughout the skeletons of chronically stressed individuals, the magnitude of this bone loss relative to the total area of the cross-section is not equivalent in all bones. Moreover, this pattern does not follow that expected given mechanical loading demands placed on these elements; the element under the highest mechanical loading demands exhibits the greatest loss in association with chronic metabolic stress.

Long bone strength relationships within stress groups are similar for both younger subadults and the entire Alytus sample. As before, both groups demonstrate significantly higher second moments of area and section modulus in the femur compared to the humerus. However, again, patterns *between* the stress groups for the younger subadult sample are quite different from those for the entire sample. The lesion group has higher values of femoral I_{max}, I_{min}, J, and Z_p compared to the no lesion group, a pattern opposite of that found when older subadults were included. Likewise, the younger subset demonstrates higher mean values in these variables for the humerus, whereas, when including the older individuals, the stress groups had very similar humeral strength properties. For all measurements, the magnitude of difference between the stress groups is greater in the humerus than in the femur. This pattern is caused by smaller differences between femoral and humeral strength properties in subadults with lesions than in subadults without lesions. In other words, long bone strength properties in chronic metabolic stress are enhanced compared to acute stress/non-stress but especially so in the humerus.

Overall, these non-significant trends indicate systemic metabolic bone loss in association with skeletal indicators for chronic stress, especially in the femur. Although systemic bone loss supports Hypothesis 1a, the fact that bone loss is greatest in the femur is unexpected. This systemic bone loss appears to be somewhat compensated by minor periosteal expansion in all three elements and increased strength properties in the long bones. However, compensation is greater in the humerus and rib than in the femur. Femoral TA is almost identical between the stress groups, and femoral CA and %CA are more reduced in the lesion group relative to the no lesion group when compared to other elements. As discussed previously, rib dimensions are all significantly expanded in the lesion group and %CA is similar between the stress groups, which is evidence of compensation for medullary bone loss. In the lesion group, greater increases in TA

and smaller reductions in %CA in humeri relative to femora may be responsible for the increased humeral strength properties in this stress group.

Comparisons Between Stress Groups Across Three Elements (Hypothesis 1a)

All Ages. To illuminate whether the patterns for mean variables are reflective of actual patterns across elements *within* individuals, a chi-square analysis was conducted on patterns among elements between the stress groups. This analysis employed 42 individuals (lesion group *n*=28, no lesion group *n* =14) with all three elements analyzed. Results of a chi-square analysis on the patterns of %CA among the three skeletal elements and between the stress groups are presented in Table 15. The other cross-sectional areas measured for these three elements (i.e., TA, MA, CA) demonstrated the same pattern in all Alytus subadult individuals included in the analysis (decreased area as hypothesized local loading demands decrease; Femur > Humerus > Rib), and thus a chi-square test was not performed on these variables.

Table 15. Counts of individuals with patterns of relative magnitudes in percent cortical area (%CA) among elements between stress groups.

Relative magnitude of %CA among elements[1]	Lesion group		No lesion group	
	Count	%	Count	%
F > H > R	8	29	3	11
H > F> R	14	50	6	21
H > R > F	1	4	0	0
F > R > H	2	7	5	18
R > H > F	2	7	0	0
R > F > H	1	4	0	0
Total	**28**		**14**	

[1] F = femur; H = humerus; R = rib.

Table 15 shows several patterns in relative %CA among the bones that are unexpected based on both mechanical and metabolic hypothesized relationships. A Fisher's exact test indicates no differences between the stress groups in the frequencies of individual elemental patterns for %CA ($p = 0.291$). These results confirm findings in the previous analysis; however, they additionally demonstrate the variation in patterns present among the Alytus subadults that contribute to the mean values compared above with ANCOVA.

Because no significant differences exist between the lesion and no lesion groups in frequencies of relative %CA patterns among elements, these two groups were combined to increase sample size (and thus statistical power) and a chi-square test was performed on the overall pattern of %CA among the bones, testing the null hypothesis that the frequencies for each pattern are equal (Table 16). This analysis demonstrates the patterns present among all Alytus subadults. As a reminder, it is expected that both the femur and humerus have greater %CA relative to ribs, given higher mechanical loading on those elements, and femora are expected to have higher values than humeri to reflect differences in supporting body mass.

Table 16. Counts of individuals with patterns of relative magnitudes in percent cortical area (%CA) among elements across stress groups.

Relative magnitude of %CA among elements[1]	Count	%	Std. Resid[2]
F > H > R	11	26%	3.8
H > F > R	20	48%	13.8
H > R > F	1	2%	-6.2
F > R > H	7	17%	-.2
R > H > F	2	5%	-5.2
R > F > H	1	2%	-6.2
Total	**42**		

[1] F = femur; H = humerus; R = rib.
[2] Standardized residuals reflect the deviation of the observed frequency from the expected frequency based on the chi-square test.

Results support the hypothesis that femora and humeri will have greater %CA than ribs, though which of those two elements has greater %CA varies ($p = 0.000$). Assessment of standardized residuals shows that more individuals possess decreasing %CA as loading demands decrease (Femur > Humerus > Rib) and more individuals with higher humeral %CA relative to femoral %CA and higher femoral %CA relative to ribs (Humerus > Femur > Rib) than expected based on the null hypothesis of equal frequencies among patterns. The majority of individuals demonstrate the latter pattern. Significantly fewer individuals demonstrate other potential patterns, but they nevertheless are present in several subadults.

Under Seven Years. As discussed in Chapter 4, all three skeletal elements were preserved in very few individuals ($n = 23$) in the younger age subset. Therefore, individual patterns in relative magnitudes of cross-sectional geometric properties among elements were not evaluated for individuals with age estimates under seven.

Histomorphometric Properties

This section presents the results of analyses comparing the histomorphometric properties described in Chapter 4. Analyses in this section follow the same pattern as those conducted for cross-sectional properties above: comparisons of histomorphometric properties of the same element between stress groups, followed by comparisons of the properties of all three elements (rib, humerus, and femur) within stress categories. Analyses of differences in patterns of histomorphometric properties among the three elements within individuals and between the two stress groups are presented. Finally, this section concludes with an analysis of differences in long bone histological measurements in relation to the cross-sectional geometric properties analyzed

above. Analyses again are conducted first within the complete sample and then in the sample subset of individuals younger than seven years.

Comparisons Between Stress Groups Within Each Skeletal Element (Hypothesis 1b)

All Ages. ANCOVA comparisons of histological variables between lesion and no lesion groups are presented separately for each bone element in Table 17. For both mean size variables (e.g., average osteon size, average pore size) and total area measurements there are no significant differences between the stress groups. This lack of significance is unexpected based on hypothesized microscopic bone loss with metabolic stress inferred from pathological lesions. Because no differences in histological properties exist between the groups, the remaining analyses focus on patterns across elements within the groups, as well as frequency distributions of patterns across the three elements.

Table 17. Results of ANCOVA comparing histomorphometric properties within bone elements between stress groups.

Histomorphometric property	Femur *p*-value	Humerus *p*-value	Rib *p*-value
Avg. On.Ar	0.760	0.196	0.326
Avg. On.Fg.Ar	0.558	0.655	0.456
Avg. On.C.Ar	0.709	0.108	0.282
Avg. Por.Ar	0.954	0.192	0.415
Avg. RS.Ar	0.638	0.617	0.672
Avg. HC.Ar	0.935	0.500	0.342
Total On.Ar	0.680	0.113	0.711
Total On.Fg.Ar	0.695	0.787	0.549
Total On.C.Ar	0.984	0.450	0.461
Total Por.Ar	0.699	0.277	0.877
Total RS.Ar	0.535	0.400	0.760
Total HC.Ar	0.772	0.340	0.461
Total On.B.Ar	0.663	0.836	0.626

* Asterisks denote significant differences between the stress groups for the given property.

Under Seven Years. Mann-Whitney *U*-test comparisons for histological variables in Alytus subadults between the ages of one and seven are presented in Table 18. Like the results reported for the full sample (Table 17), these results also indicate no significant differences between the stress groups in any histomorphometric variable. Thus, elimination of older, chronically stressed subadults from the analyses does not affect the lack of statistically significant differences in histomorphometric properties between the lesion and no lesion groups.

Table 18. Results of Mann-Whitney *U*-tests comparing histomorphometric properties within bone elements between stress groups (1.0-6.99 years).

Histomorphometric property	Femur *p*-value	Humerus *p*-value	Rib *p*-value
Avg. On.Ar	0.740	0.180	0.133
Avg. On.Fg.Ar	0.813	0.771	0.193
Avg. On.C.Ar	0.669	0.107	0.171
Avg. Por.Ar	0.270	0.180	0.438
Avg. RS.Ar	0.133	0.381	0.151
Avg. HC.Ar	0.364	0.999	0.171
Total On.Ar	0.601	0.314	0.101
Total On.Fg.Ar	0.601	0.314	0.133
Total On.C.Ar	0.887	0.381	0.133
Total Por.Ar	0.740	0.381	0.478
Total RS.Ar	0.740	0.722	0.652
Total HC.Ar	0.887	0.872	0.243
Total On.B.Ar	0.887	0.821	0.116

* Asterisks denote significant differences between the stress groups for the given property.

Comparisons Within Stress Groups Across Three Skeletal Elements (Hypothesis 2b)

All Ages. ANCOVA results addressing differences across the three bones are presented separately for each stress group in Table 19. The subsequent figures present the means for these comparisons graphically. Figure 20 presents stress group means of histological mean size

variables. The means for total area variables for each group are presented in Figure 21. When comparing mean size histological variables across elements, the two stress groups show similar patterns, though significant differences are more frequent between the humerus and rib in individuals without lesions and more common between the femur and rib in individuals with lesions (Table 19).

Table 19. Results of ANCOVA comparing histomorphometric properties between elements within stress groups.

Element	Histomorphometric property	Humerus		Rib	
		Lesion group	No lesion group	Lesion group	No lesion group
		p	*p*	*p*	*p*
Femur	Avg. On.Ar	0.157	0.986	0.001*	0.016*
	Avg. On.Fg.Ar	0.280	0.870	0.005*	0.390
	Avg. On.C.Ar	0.137	0.733	0.001*	0.021*
	Avg. HC.Ar	0.416	0.077	0.033*	0.007*
	Avg. RS.Ar	0.778	0.459	0.085	0.257
	Avg. Por.Ar	0.899	0.565	0.020*	0.046*
	Total On.Ar	0.004*	0.002*	<0.001*	<0.001*
	Total On.Fg.Ar	0.036*	0.953	0.012*	0.034*
	Total On.C.Ar	0.209	0.985	<0.001*	<0.001*
	Total HC.Ar	0.323	0.084	<0.001*	<0.001*
	Total RS.Ar	0.236	0.843	0.744	<0.001*
	Total Por.Ar	0.323	0.556	0.637	0.319
	Total On.B.Ar	0.378	0.909	<0.001*	<0.001*
Humerus	Avg. On.Ar			0.080	0.005*
	Avg. On.Fg.Ar			0.101	0.402
	Avg. On.C.Ar			0.074	0.002*
	Avg. HC.Ar			0.215	0.204
	Avg. RS.Ar			0.168	0.619
	Avg. Por.Ar			0.018*	0.080
	Total On.Ar			0.299	0.201
	Total On.Fg.Ar			<0.001*	0.011*
	Total On.C.Ar			<0.001*	<0.001*
	Total HC.Ar			0.002*	0.001*
	Total RS.Ar			0.352	0.884
	Total Por.Ar			0.139	0.611
	Total On.B.Ar			<0.001*	<0.001*

* Asterisks denote significant differences between the skeletal elements within each stress group for the given property.

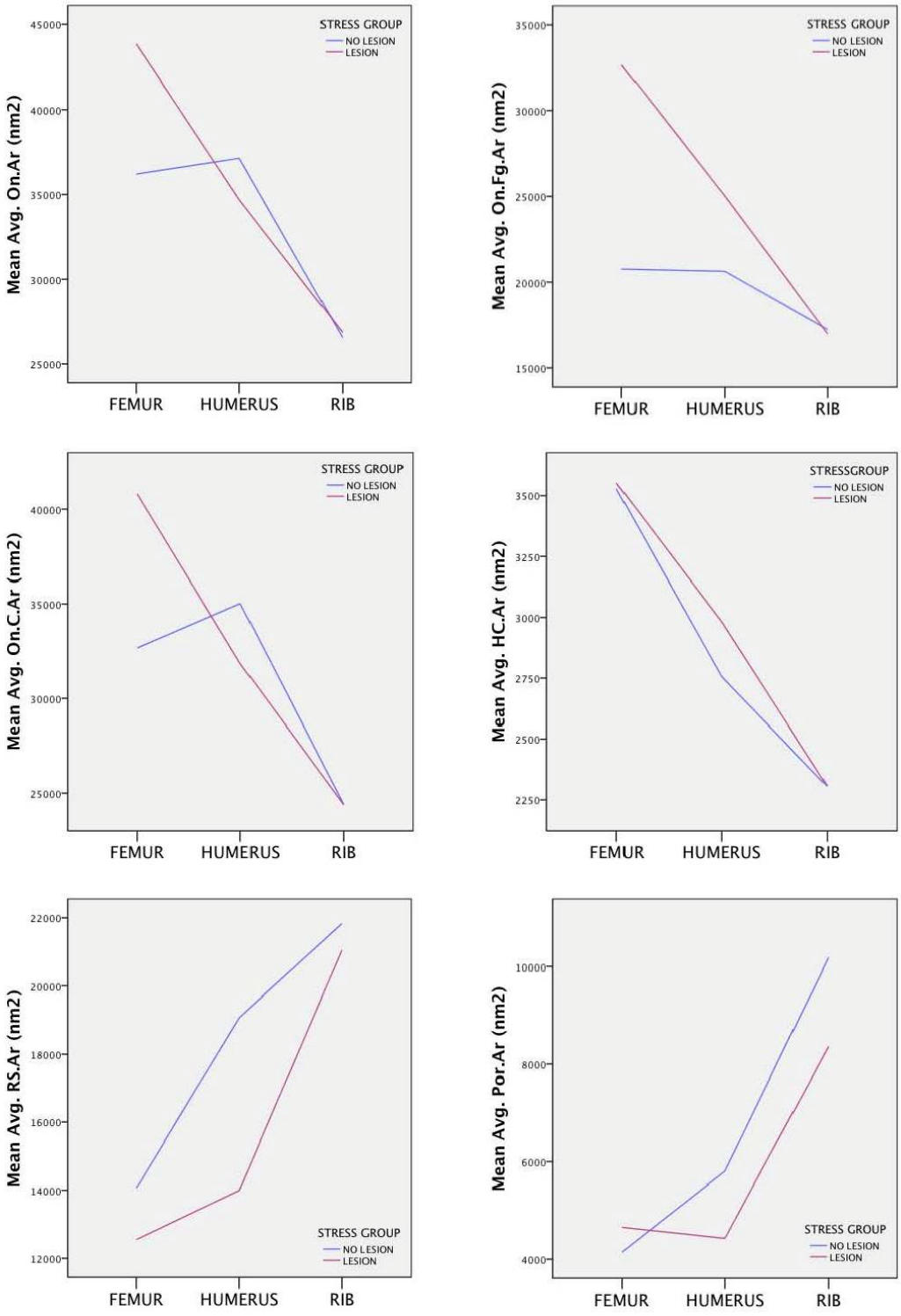

Figure 20. Graphs of mean size histomorphometric variables compared among skeletal elements between stress groups.

The lesion group demonstrates a trend towards decreased osteon size as loading demands decrease across the elements, with significant differences present only between femoral osteons and rib osteons (Figure 20). In the no lesion group, both femoral and humeral osteons are significantly larger than rib osteons, though no significant differences exist between the two long bones. Unlike in the lesion group, osteon size in the no lesion group does not decrease linearly with loading, and humeral osteons are non-significantly larger than femoral osteons in this group.

Fragmented osteon size follows the same exact pattern as intact osteon size in subadults with lesions, demonstrating a linear decrease in size with decreased loading and significant differences between femora and ribs. Subadults in the no lesion group exhibit no significant differences among the elements for fragmented osteon size. Taking these variables of osteon size into consideration, in both groups this pattern indicates increased removal of bone with each remodeling event in cases of high mechanical loading. However, it is unexpected that *only* individuals with lesions would show such strong differences among their elements, and this discrepancy may be caused by the larger number of older subadults in the lesion group (see Chapter 6).

As with mean intact and fragmented osteon size, lesion presence is associated with decreased osteon cortical area and Haversian canal size as loading decreases; again, only the femur and rib significantly differ in these dimensions. Individuals without lesions show this same pattern in Haversian canal area. For average osteon cortical area, though, individuals in the no lesion group show a different pattern: humeral values are highest, while the femur is intermediate and the rib has the lowest osteon cortical areas. The two long bones in the no lesion group are not significantly different from one another, while the humerus has significantly more osteonal

cortical area than the rib. This difference in pattern between the two stress groups is likely caused by the non-significant tendency for humeri in the no lesion group to have larger osteons, continued osteon filling (evidenced by high osteonal cortical area) and smaller Haversian canals than both the femora of the no lesion group and the humeri of the lesion group. Thus, it appears more bone is being remodeled in the humeri of individuals without lesions, but remodeling is not unbalanced, and resorbed bone is being adequately replaced. Overall, these patterns along with patterns for osteon size among the elements suggest more resorption by BMUs in highly loaded skeletal elements, but balanced replacement with bone formation.

There are no significant differences in either stress group for resorption space size among the elements. Both stress groups demonstrate the same trend across the elements, with resorption space size increasing as loading decreases; this supports mechanical models of bone mass conservation in elements experiencing high loading. When both Haversian canal size and resorption space size are considered together, a slightly different pattern is evident in pore size between the stress groups than for either pore type alone. For both lesion and no lesion groups, pore size is significantly higher in the rib relative to the humerus and femur. No significant differences in pore size were found between the two long bone elements for either stress group. Like the patterns for resorption space size, these findings support hypothesized removal of microscopic bone mass preferentially from the least loaded elements, even though these patterns are present in all Alytus subadults rather than just subadults in the lesion group. The pattern across the elements does differ between stress groups; though not statistically significant, subadults in the no lesion group have larger pores in their humeri relative to their femora, while those with lesions possess the opposite pattern.

Despite the lack of significant differences in ANCOVA analyses in mean size histological properties between the lesion and no lesion groups, non-significant differences between mean values for bone elements *between* the stress groups reveal some noteworthy observations. For example, average osteon size and osteon cortical area both are greater in the lesion group's femora than in the no lesion group's femora, but the opposite pattern is present in the humerus for these variables. In contrast, rib osteon size and osteon cortical area are more similar among the groups. Thus, based only on these variables, one may conclude that chronic stress results in more bone resorption during each remodeling event in the femur and less resorption in the humerus relative to acute stress and non-stress.

Also, individuals in the lesion group show larger fragmented osteons in both the femur and humerus relative to those in the no lesion group, though values in the rib are similar between the two groups. For Haversian canal size, values for femora and rib elements are similar between the stress groups, but humeral Haversian canal size is non-significantly lower in the no lesion group relative to the lesion group. This pattern, combined with the fact that individuals with lesions have smaller osteons in their humeri, indicates arrested osteon filling in this element. Most interestingly and unexpectedly, resorption spaces in the lesion group are smaller in all elements relative to the no lesion group, especially in the humerus. When considering all porous structures together, average pore size tends to be larger in individuals without lesions for both the humerus and rib but smaller for the femur. This pattern points to *reduced* pore size in the humeri and ribs of chronically stressed individuals and increased size only in the femora of these individuals, a pattern not in congruence with mechanical expectations.

When assessing microscopic total area measurements (figure 21), the significant differences present within groups, as well as non-significant differences, are similar in both

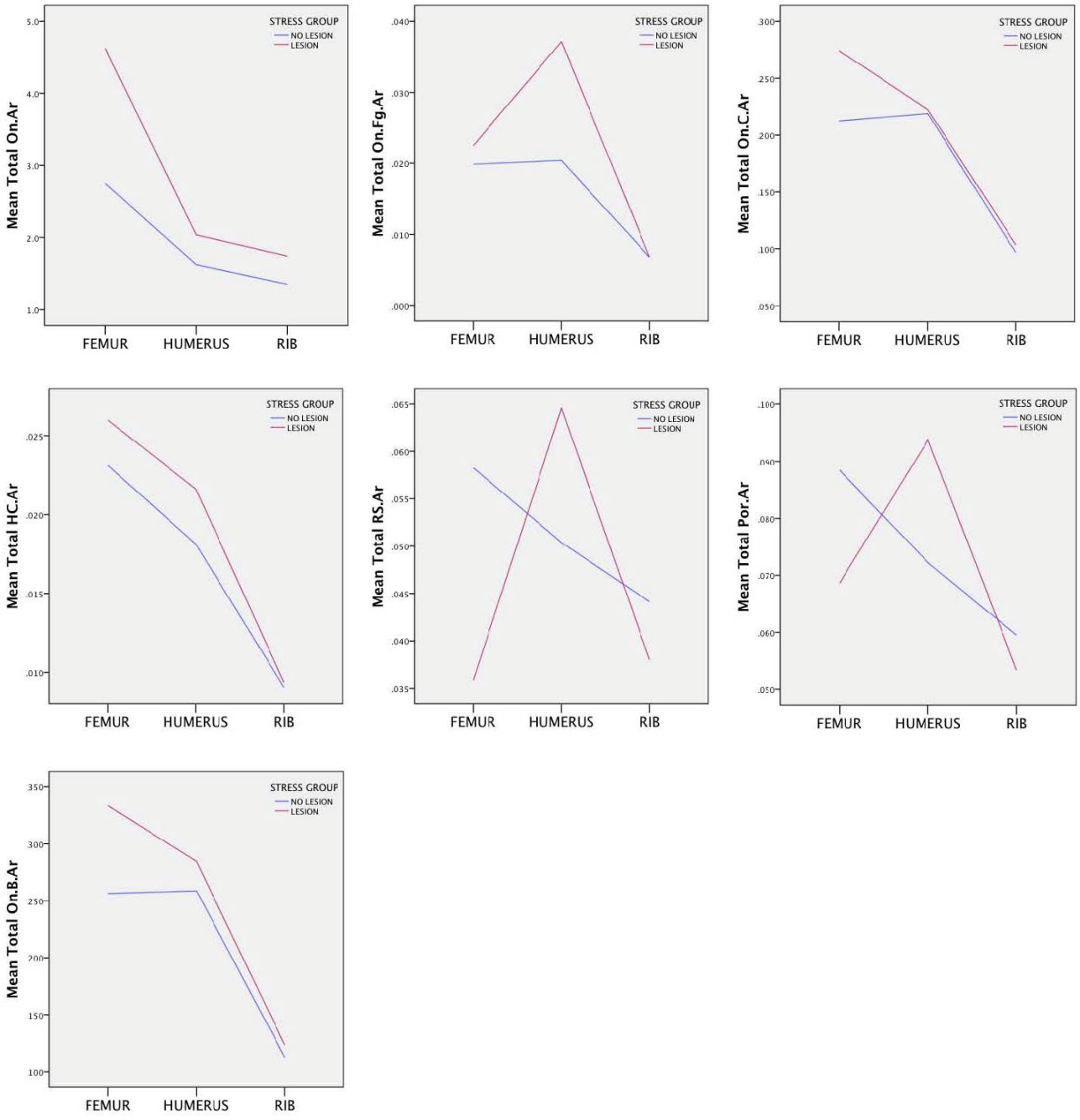

Figure 21. Graphs of total area histomorphometric variables compared among skeletal elements between stress groups.

lesion and no lesion groups with a few exceptions. Subadults in both groups demonstrate reduced intact osteonal bone per unit area as loading demands decrease across the skeleton; in both groups femoral intact osteonal bone is significantly higher than in the humeri and ribs. No significant differences for this variable exist in either stress group between the humerus and rib. For both groups, this pattern reflects hypothesized increased remodeling rates with increased loading.

For both total osteonal cortical area and total Haversian canal area, the lesion and no lesion groups have significantly higher values in their femora and humeri relative to their rib elements but no significant differences between the long bone elements. In the lesion group, these variables decrease with decreased loading across the bones. Within the no lesion group, the same is true of total Haversian canal area, whereas total osteonal cortical area is more similar between the two long bones (i.e., non-significantly higher in humeri than femora) and significantly lower in the rib.

In subadults with lesions, total resorption space area is not significantly different among the three skeletal elements, whereas in individuals without lesions femoral resorption is significantly higher than rib resorption. The non-significant patterns among the stress groups are also notably dissimilar. In the lesion group, humeral resorption is the highest, whereas resorption in the femur and rib are quite low, with rib resorption only slightly higher than femoral resorption. However, resorption area declines steadily with decreased loading across the elements of individuals in the no lesion group. Total porosity demonstrates similar trends, though no significant differences are evident among the elements for either stress group. Non-significant trends are the same as for resorption, although subadults with lesions actually have less porosity in their ribs than in their femora. These variables show unexpected patterns in both stress groups

based on metabolic bone loss hypotheses alone (more bone is resorbed from heavily loaded elements) and, again, mirror the patterns that indicate increased remodeling rates with increased mechanical demands.

Despite the lack of significant differences in total area histological properties between the stress groups in ANCOVA analyses, non-significant differences for each element between stress groups reveal some expected and unexpected patterns. Subadults in the lesion group have higher values of total intact osteonal bone in all three elements relative to those in the no lesion group, especially in the femur. Additionally, subadults in the lesion group have higher total fragmented osteon area in their long bones; however, mean values for the rib are similar between the stress groups. Taken together, these differences indicate that individuals in the lesion group have higher amounts of total remodeled bone per unit area compared with the no lesion group. These findings are indicative of increased *systemic* remodeling with chronic stress, which is more marked in the femur and least marked in the rib.

Total osteonal cortical area tends to be similar between the lesion and no lesion groups for the humerus and rib, but for the femur, osteonal cortical area in the no lesion group is reduced relative to the lesion group. Total Haversian canal area is generally non-significantly higher in the lesion group's femora and humeri compared to the no lesion group's femora and humeri, though mean values for the rib are similar between the stress groups. Finally, total resorption space area and porosity are greater in the femora and ribs of individuals without lesions, but individuals with lesions have humeri that possess higher resorption and porosity. This pattern is unexpected based on both mechanical and metabolic hypotheses and will be considered further in the Discussion (see Chapter 6).

Under Seven Years. Kruskal-Wallis test comparisons across the three bones are presented separately for each stress group in Table 20. The subsequent figures present the means for these comparisons graphically: Figure 22 presents stress group means of histological mean size variables; the means for total area variables for each group are presented in Figure 23. Compared to the ANCOVA results on the entire Alytus subadult sample, significant differences within the stress groups and across elements are not the same in the subsample, some of the non-significant trends within groups have been altered, and relationships between the stress groups are mostly different.

The patterns within stress groups for average intact osteon size, fragmented osteon size, osteon cortical area, and Haversian canal size are the same as those detected for the entire sample, though which elemental comparisons exhibit significant differences has changed. For example, individuals from the lesion group still demonstrate a trend towards decreased intact osteon size as loading demands decrease, while individuals from the no lesion group have similar intact osteon size in their long bones and decreased intact osteon size in their ribs. These shifts in significance levels within the groups appear to be caused by more similar values for histological mean size variables between femora and humeri in the lesion group. The removal of the older, chronically stressed subadults decreased the magnitude of difference in the average size of osteonal structures between the two long bones. Even so, in the younger subadults from both stress groups, osteonal dimensions in both long bones tend to be larger than those in the rib, as was reported for the entire Alytus sample.

Table 20. Results of Kruskal-Wallis tests comparing histomorphometric properties between elements within stress groups (1.0-6.99 years).

Element	Histomorphometric property	Humerus		Rib	
		Lesion group	No lesion group	Lesion group	No lesion group
		p	*p*	*p*	*p*
Femur	Avg. On.Ar	0.545	0.933	0.011*	0.113
	Avg. On.Fg.Ar	0.324	0.673	0.128	0.892
	Avg. On.C.Ar	0.545	0.673	0.105	0.160
	Avg. HC.Ar	0.597	0.108	0.011*	0.016*
	Avg. RS.Ar	0.450	0.735	0.481	0.390
	Avg. Por.Ar	0.999	0.612	0.573	0.160
	Total On.Ar	0.059	0.524	0.011*	0.389
	Total On.Fg.Ar	0.130	0.076	0.020*	0.033*
	Total On.C.Ar	0.406	0.933	0.001*	0.013*
	Total HC.Ar	0.496	0.673	0.001*	0.008*
	Total RS.Ar	0.597	0.612	0.944	0.556
	Total Por.Ar	0.364	0.554	0.011*	0.033*
	Total On.B.Ar	0.546	0.866	0.002*	0.004*
Humerus	Avg. On.Ar			0.057	0.074
	Avg. On.Fg.Ar			0.031*	0.805
	Avg. On.C.Ar			0.049*	0.027*
	Avg. HC.Ar			0.024*	0.085
	Avg. RS.Ar			0.944	0.389
	Avg. Por.Ar			0.833	0.110
	Total On.Ar			0.439	0.387
	Total On.Fg.Ar			0.001*	0.538
	Total On.C.Ar			0.001*	0.023*
	Total HC.Ar			0.001*	0.001*
	Total RS.Ar			0.725	0.498
	Total Por.Ar			0.007*	0.036*
	Total On.B.Ar			<0.001*	0.001*

* Asterisks denote significant differences between skeletal elements within stress groups for the given property.

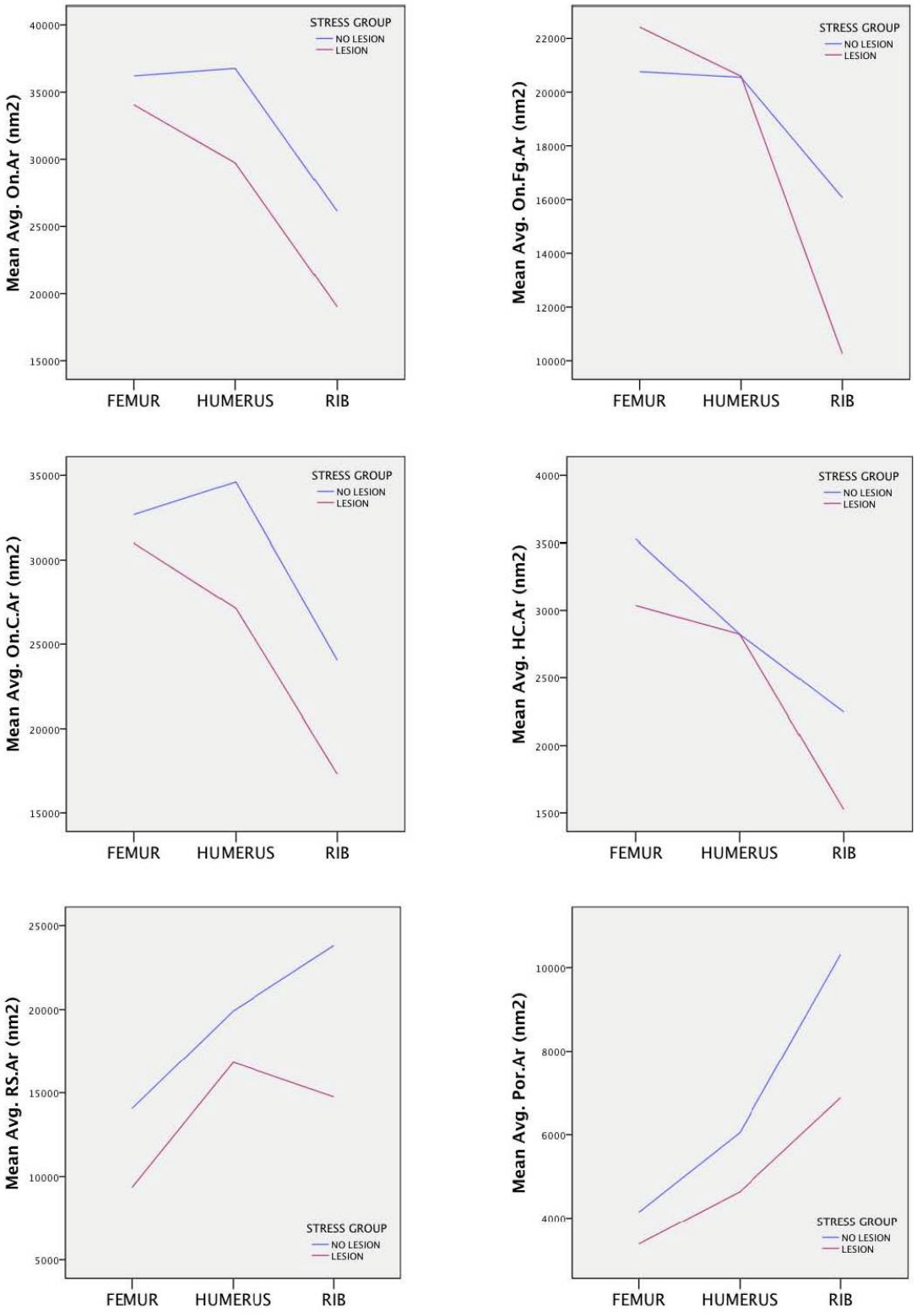

Figure 22. Graphs of mean size histomorphometric variables compared among skeletal elements between stress groups (1.0-6.99 years).

For resorption space size and pore size, the relationships among the elements within the lesion group have now been altered with removal of the older subadults, while patterns within the no lesion group are the same. Resorption space size no longer increases with decreased loading in the lesion group; individuals with lesions tend to have the largest resorption spaces in their humeri, the smallest ones in their femora, and intermediate ones in their ribs. Likewise, the pattern in pore size among long bones in the lesion group is altered; average pore size is now higher in humeri relative to femora, though rib elements maintain the highest average pore size.

The most notable discrepancies between the present analyses and those performed on the entire Alytus sample are found in the non-significant differences *between* the stress groups in histological mean size variables for each bone element. With only one exception (humeral HC.Ar), intact osteonal dimensions (Avg. On.Ar, Avg. On.C.Ar, Avg. HC.Ar) are non-significantly higher in all three elements of the no lesion group compared to the lesion group, indicating increased resorption during remodeling. For Avg. On.Ar and Avg. On.C.Ar, values are more similar between the stress groups in the femur than they are in either the humerus or rib, which may indicate conservation of microscopic bone mass in the femur. Specifically, because the magnitude of difference in osteonal size dimensions is now smaller between femora and humeri of the lesion group, femora in this group possess non-significantly smaller intact osteonal dimensions than femora in the no lesion group. This pattern is opposite of that found previously.

In addition, the lesion group's humeri have smaller average intact osteons and osteonal cortical area than the no lesion group's humeri; however, Haversian canal size is more similar between the groups. Based on intact osteons alone, this suggests that although more bone is being resorbed during remodeling in the humeri of the no lesion group, bone balance is

maintained and osteon refilling is not disrupted. Moreover, rib osteonal dimensions are no longer similar between the stress groups, as they were previously for the entire sample. Chronic stress is associated with much reduced dimensions for all rib intact osteonal variables.

As found previously, the lesion group has non-significantly lower resorption space size and pore size in all three skeletal elements compared to the no lesion group. However, because of the shifts described above among elements in the lesion group, the greatest difference in resorption space size between the groups now lies in the rib, not the humerus. The humerus actually possesses the smallest difference in resorption space size among the stress groups. For average pore size, differences are greatest between the stress groups in the ribs, smallest in the femur, and intermediate in the humerus, a pattern that was not present previously. Taken together, these results suggest systemic metabolic bone loss in individuals without lesions that occurs preferentially in the least loaded element (i.e., the rib).

Mean values for total area measurements in younger Alytus subadults demonstrate the same patterns within stress groups as those revealed in analyses on individuals of all ages (Figure 23). Though, the patterns of significant differences across elements and within the stress groups have changed. Additionally, the non-significant relationships *between* the stress groups have been altered by the removal of older, chronically stressed subadults.

Subadults with lesions have non-significantly lower values of Total On.Ar and Total On.C.Ar in all three elements relative to subadults without lesions. This pattern is the opposite of that present in the comparisons employing individuals of all ages and is unexpected given hypothesized increased remodeling with metabolic stress. In addition, previously, the magnitude of difference in Total On.Ar and Total On.C.Ar between femora and humeri in the lesion group caused the greatest differences between the stress groups to be present in the femur. In younger

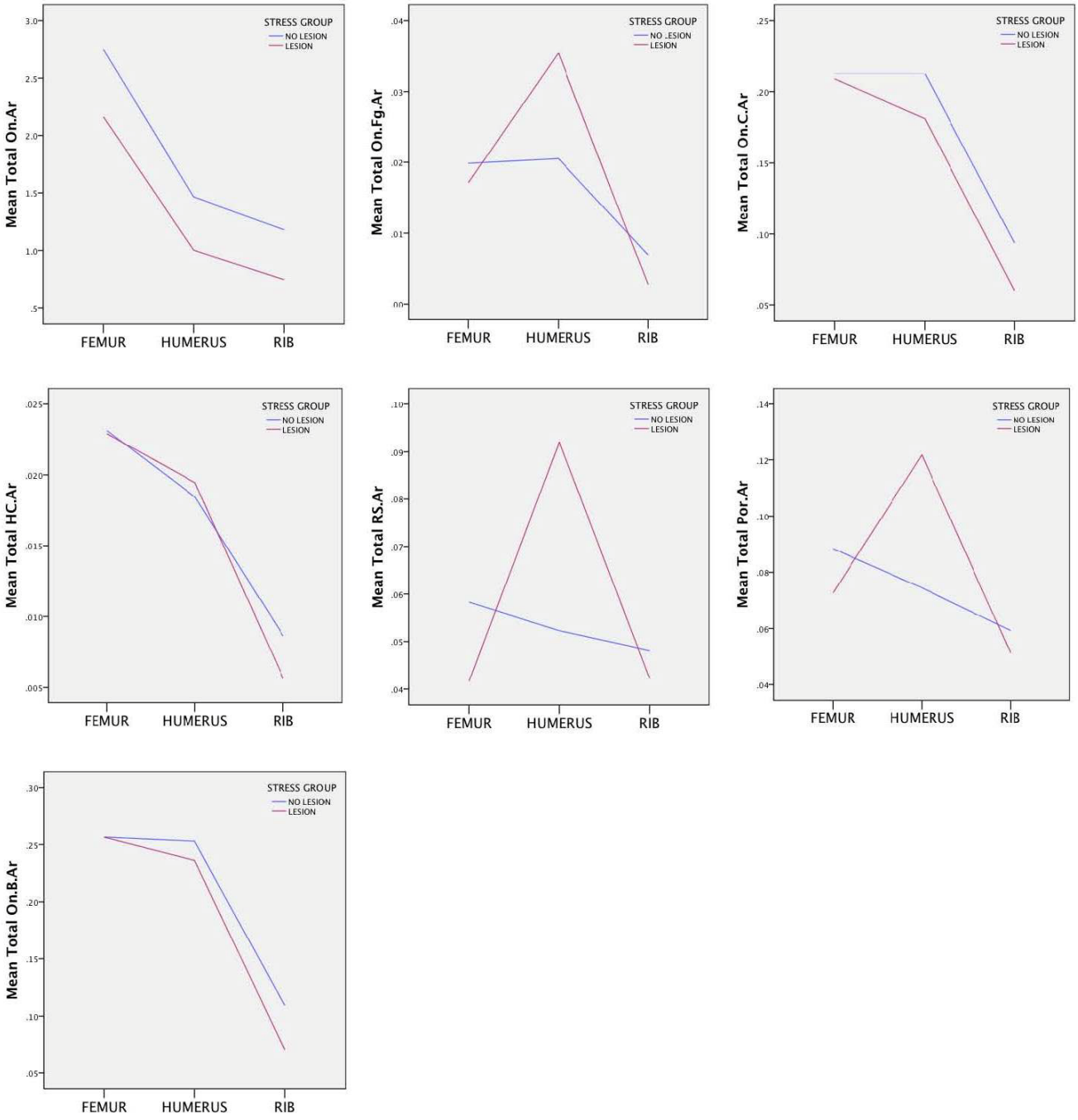

Figure 23. Graphs of total area histomorphometric variables compared among skeletal elements between stress groups (1.0-6.99 years).

subadults, however, Total On.Ar is reduced in the lesion group's elements in roughly equal amounts relative to the no lesion group, and femoral Total On.C.Ar is very similar between the groups.

Total HC.Ar is also quite different among the stress groups. Interestingly, chronic stress is not associated with reduced femoral and humeral Total HC.Ar, as would be expected given the reduced Total On.Ar and Total On.C.Ar in these elements. Femora in the lesion group have almost identical Total HC.Ar compared to femora in the no lesion group, and humeri in the lesion group actually have slightly higher proportions of Haversian canal area than humeri in the no lesion group. Whereas rib Total HC.Ar was almost identical in comparisons incorporating all ages, it is non-significantly reduced in the lesion group. Therefore, based on intact osteons, there is more remodeled bone systemically in acute stress/non-stress relative to chronic stress, and *proportional* to this amount of intact osteonal bone, individuals with lesions tend to demonstrate reduced femoral osteon filling (e.g., greater total femoral Total HC.Ar) and enhanced humeral osteon filling (i.e., less total humeral Total HC.Ar).

Unlike results for Total On.Fg.Ar in the entire sample, this variable is slightly non-significantly higher in the no lesion group's femora and ribs than in the lesion group's femora and ribs. However, humeri in the lesion group have a much higher mean value than humeri in the no lesion group. Likewise, Total On.B.Ar does not exhibit the same pattern in younger subadults as before. Total relative amounts of remodeled bone are practically identical between groups in the femur, whereas humeri and ribs in the no lesion group possess non-significantly higher amounts of remodeled bone. This suggests that the increased remodeling that occurs in acute

stress/non-stress relative to chronic stress happens preferentially in elements not under the highest loading demands (i.e., humeri and ribs).

Patterns between the stress groups for Total RS.Ar and Total Por.Ar are the same as those found in previous analyses on the entire sample. Although removal of older individuals does change the magnitude of differences between the elements for both groups, the results are the same. Subadults with lesions have less porosity in the femur and rib and more porosity in the humerus than subadults without lesions.

Comparisons Between Stress Groups Across Three Skeletal Elements (Hypothesis 2b)

All Ages. To determine if patterns in mean values for histomorphometric variables are representative of patterns *within* individuals, a chi-square test was performed on elemental patterns between the stress groups. This analysis employed the 18 individuals (lesion group $n = 11$, no lesion group $n = 7$) who had histomorphometric data completed on all three elements. Chi-square results among the three skeletal elements and between the two stress groups are presented in Table 21. Sample sizes within these groups are quite low, and where appropriate, a Fisher's exact test was conducted to account for cell counts less than five.

No significant differences between the stress groups in frequency distributions of elemental patterns were found for any of the histomorphometric variables, and this lack of significance may be attributable to small sample sizes among groups for histological data. However, what Table 21 does show is the variation in patterns present among the Alytus subadults that contribute to the mean values compared above with ANCOVA for the full sample. Not all individuals within the stress categories demonstrate the same pattern in remodeling and microscopic bone mass among their skeletal elements.

Table 21. Results of chi-square tests comparing frequencies of patterns in histomorphometric properties among bone elements between stress groups.

Dimension	Group		F >H >R	F <H <R	R >F >H	F >R >H	H >F >R	H >R >F	*p*
Avg. On.Ar	Lesion	Count	3	0	1	2	5	0	0.894
		%	27%	0%	9%	18%	45%	0%	
	No lesion	Count	2	0	1	0	4	0	
		%	18%	0%	9%	0%	36%	0%	
Avg. On.Fg.Ar	Lesion	Count	4	1	0	1	4	1	0.736
		%	36%	9%	0%	9%	36%	9%	
	No lesion	Count	2	2	1	0	2	0	
		%	18%	18%	9%	0%	18%	0%	
Avg. On.C.Ar	Lesion	Count	4	0	1	1	5	0	0.657
		%	36%	0%	9%	9%	45%	0%	
	No lesion	Count	1	1	0	0	5	0	
		%	9%	9%	0%	0%	45%	0%	
Avg. HC.Ar	Lesion	Count	4	1	0	1	4	1	0.930
		%	36%	9%	0%	9%	36%	9%	
	No lesion	Count	4	0	0	1	2	0	
		%	36%	0%	0%	9%	18%	0%	
Avg. RS.Ar	Lesion	Count	1	2	3	2	2	1	0.675
		%	9%	18%	27%	18%	18%	9%	
	No lesion	Count	0	4	1	0	1	1	
		%	0%	36%	9%	0%	9%	9%	
Avg. Por.Ar	Lesion	Count	2	3	2	1	3	0	0.893
		%	18%	27%	18%	9%	27%	0%	
	No lesion	Count	0	3	2	0	2	0	
		%	0%	27%	18%	0%	18%	0%	
Total On.Ar	Lesion	Count	4	1	2	3	1	0	0.815
		%	36%	9%	18%	27%	9%	0%	
	No lesion	Count	4	0	0	2	0	1	
		%	36%	0%	0%	18%	0%	9%	
Total On.Fg.Ar	Lesion	Count	1	0	0	0	8	2	0.461
		%	9%	0%	0%	0%	73%	18%	
	No lesion	Count	1	0	1	1	4	0	
		%	9%	0%	9%	9%	36%	0%	
Total On.C.Ar	Lesion	Count	5	0	0	0	5	1	0.815
		%	45%	0%	0%	0%	45%	45%	
	No lesion	Count	4	0	0	0	2	1	
		%	36%	0%	0%	0%	18%	9%	
Total HC.Ar	Lesion	Count	3	0	0	1	6	1	0.310
		%	27%	0%	0%	9%	55%	9%	
	No lesion	Count	5	0	0	0	2	0	
		%	45%	0%	0%	0%	18%	0%	
Total RS.Ar	Lesion	Count	0	5	1	1	3	1	0.730
		%	0%	45%	9%	9%	27%	9%	
	No lesion	Count	1	1	1	1	2	1	
		%	9%	9%	9%	9%	18%	9%	
Total Por.Ar	Lesion	Count	3	2	0	1	4	1	0.962
		%	27%	18%	0%	9%	36%	9%	
	No lesion	Count	2	1	1	1	2	0	
		%	18%	9%	9%	9%	18%	0%	
Total On.B.Ar	Lesion	Count	4	0	0	0	5	2	0.465
		%	36%	0%	0%	0%	45%	18%	
	No lesion	Count	5	0	0	0	1	1	
		%	45%	0%	0%	0%	9%	9%	

Because no significant differences exist between subadults with and without lesions, these two stress categories were grouped to increase sample size and a chi-square test was performed to compare frequencies of the overall pattern of histomorphometry among the bones, testing the null hypothesis that the frequencies for each pattern are equal (Table 22). In this analysis, five histomorphometric variables (i.e., Avg. On.C.Ar, Avg. HC.Ar, Total On.Ar, Total On.Fg.Ar, Total HC.Ar) have significantly different frequencies among the six possible elemental patterns.

Assessment of standardized residuals shows that there are more individuals who possess decreasing osteonal cortical area as loading demands decrease (Femur > Humerus > Rib) and more individuals with higher humeral Avg. On.C.Ar relative to femoral Avg. On.C.Ar and femoral Avg. On.C.Ar relative to rib Avg. On.C.Ar (Humerus > Femur > Rib) than expected based on the null hypothesis. The majority of individuals demonstrate the latter pattern. The same situation is evident for Avg. HC.Ar, although more individuals demonstrate the former pattern. This finding is interesting because the latter pattern for Haversian canal size is not evident in the ANCOVA analysis comparing mean values for this dimension.

For total osteonal area, significantly more individuals demonstrate decreased remodeling with decreased loading (Femur > Humerus > Rib), but significantly more individuals also present the reverse for the rib and humerus (Femur > Rib > Humerus). This latter pattern was also not visible in the previous analysis. Total fragmented osteon area has significantly more individuals with the Humerus > Femur > Rib pattern, while all other patterns possessed lower frequencies than expected, and these results mirror those detected with ANCOVA. For total Haversian canal area, however, more individuals possessing decreasing values with decreased loading (Femur > Humerus> Rib) and those with the reverse for the humerus and femur

Table 22. Results of chi-square tests comparing frequencies of patterns in histomorphometric properties among bone elements, stress groups combined.

Dimension		F >H >R	F <H <R	R >F >H	F >R >H	H >F >R	H >R >F	*p*
	Count	5	0	2	2	9	0	0.066
Avg. On.Ar	%	28%	0%	11%	11%	50%	0%	
	Std. Resid	0.5		-2.5	-2.5	4.5		
	Count	6	3	1	1	6	1	0.077
Avg. On.Fg.Ar	%	33%	17%	6%	6%	33%	6%	
	Std. Resid	3.0	0	-2.0	-2.0	3.0	-2.0	
	Count	5	1	1	1	10	0	0.000*
Avg. On.C.Ar	%	28%	6%	6%	6%	56%	0%	
	Std. Resid	1.4	-2.6	-2.6	-2.6	6.4		
	Count	8	1	0	2	6	1	0.024*
Avg. HC.Ar	%	44%	6%	11%	33%	6%	6%	
	Std. Resid	4.4	-2.6		-1.6	2.4	-2.6	
	Count	1	6	4	2	3	2	0.419
Avg. RS.Ar	%	6%	33%	22%	11%	17%	11%	
	Std. Resid	-2.0	3.0	1.0	-1.0	0	-1.0	
	Count	2	6	4	1	5	0	0.358
Avg. Por.Ar	%	11%	33%	22%	6%	28%	0%	
	Std. Resid	-1.6	2.4	.4	-2.6	1.4		
	Count	8	1	2	5	1	1	0.015*
Total On.Ar	%	44%	6%	11%	28%	6%	6%	
	Std. Resid	5.0	-2.0	-1.0	2.0	-2.0	-2.0	
	Count	2	0	1	1	12	2	<0.001*
Total On.Fg.Ar	%	11%	0%	6%	6%	67%	11%	
	Std. Resid	-1.6		-2.6	-2.6	8.4	-1.6	
	Count	9	0	0	0	7	2	0.141
Total On.C.Ar	%	50%	0%	0%	0%	39%	11%	
	Std. Resid	3.0				1.0	-4.0	
	Count	8	0	0	1	8	1	0.012*
Total HC.Ar	%	44%	0%	0%	6%	44%	6%	
	Std. Resid	3.0			-3.5	3.5	-3.5	
	Count	8	0	0	1	8	1	0.279
Total RS.Ar	%	44%	0%	0%	6%	44%	6%	
	Std. Resid	-2.0	3.0	-1.0	-1.0	2.0	-1.0	
	Count	2	6	2	2	5	1	0.219
Total Por.Ar	%	11%	33%	11%	11%	28%	6%	
	Std. Resid	2.0	0	-2.0	1.0	3.0	-2.0	
	Count	9	0	0	0	6	3	0.243
Total On.B.Ar	%	50%	0%	0%	0%	33%	17%	
	Std. Resid	3.0				0	-3.0	

* Asterisks denote significant differences between the frequencies of relative magnitude among elements for each given property.

(Humerus > Femur > Rib) were found relative to other patterns. While the former pattern was detected in the ANCOVA analyses, the latter was not evident. Overall, these chi-square results demonstrate patterns within individuals that are not visible when bone property values are averaged across individuals.

Under Seven Years. As discussed in Chapter 4, individual patterns in relative magnitudes of histomorphometric properties among elements were not evaluated on the younger subadult subset due to very few individuals (n = 14) with all three elements analyzed.

Comparisons Between Stress Groups Within Long Bone Cross-sections (Hypothesis 2c)

All Ages. ANCOVA results comparing histomorphometric properties between I_{max} and I_{min} (i.e., $I_{max} - I_{min}$) between the stress groups are presented for both the femur and humerus in Table 23. No statistically significant differences exist between the lesion and no lesion groups for any of the total area measurements. The only significant difference for mean size variables occurs in humeral Haversian canal size. Subadults without lesions have larger Haversian canals, on average, along humeral I_{max} compared to humeral I_{min}, while the mean for individuals with lesions is closer to zero, indicating similarity between the axes in this variable under chronic stress (Figure 24).

Table 23. Results of ANCOVA comparing histomorphometric properties for maximum (I_{max}) versus minimum (I_{min}) long bone second moments of area between stress groups.

Histomorphometric property	Femur *p*-value	Humerus *p*-value
Avg. On.Ar	0.502	0.150
Avg. On.Fg.Ar	0.761	0.514
Avg. On.C.Ar	0.428	0.178
Avg. HC.Ar	0.861	0.038*
Avg. RS.Ar	0.242	0.990
Avg. Por.Ar	0.990	0.343
Total On.Ar	0.398	0.701
Total On.Fg.Ar	0.767	0.392
Total On.C.Ar	0.363	0.786
Total HC.Ar	0.674	0.445
Total RS.Ar	0.474	0.331
Total Por.Ar	0.524	0.417
Total On.B.Ar	0.449	0.600

* Asterisks denote significant differences between the stress groups for I_{max} - I_{min}.

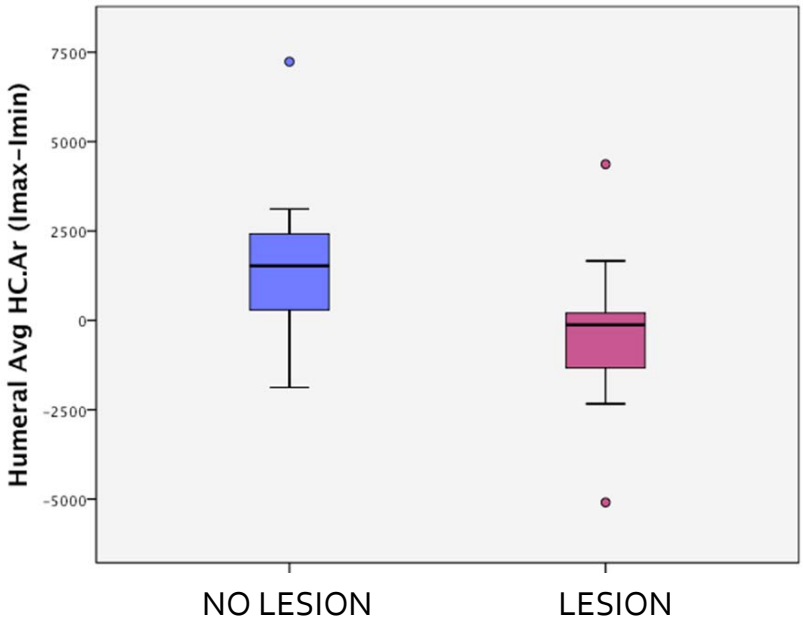

Figure 24. Boxplot of Haversian canal size differences between humeral I_{max} and I_{min}.

Results of chi-square tests to assess the frequencies of patterns within individuals possessing histological data for both a humerus and femur are presented in Table 24. This analysis employed 28 Alytus subadults (lesion group n = 17, no lesion group n = 7). In the femur, there are no significant differences between the stress groups for any histological variable comparison between I_{max} and I_{min}. In the humerus, however, there are several significant differences between the lesion and no lesion groups in the maximum and minimum axes of bending. There are significantly more individuals with lesions demonstrating larger Haversian canals along I_{min} compared to I_{max} than would be expected based on the null hypothesis (std. residual=1.2). More subadults without lesions possess the opposite pattern than expected (std. residual=1.2). Similarly, comparing the stress groups, there are significant differences in the

Table 24. Results of chi-square tests comparing the frequencies of histomorphometric properties for maximum (I_{max}) versus minimum (I_{min}) long bone second moments of area between stress groups.

Histomorphometric property	Femur					Humerus				
	Imax > Imin		Imin > Imax		*p*-value	Imax > Imin		Imin > Imax		*p*-value
	Lesion	No lesion	Lesion	No lesion		Lesion	No lesion	Lesion	No lesion	
Avg. On.Ar	12	4	5	3	0.428	6	9	10	3	0.055
Avg. On.Fg.Ar	8	3	9	4	0.605	7	4	9	8	0.435
Avg. On.C.Ar	11	3	6	4	0.296	6	9	10	3	0.055
Avg. HC.Ar	12	5	5	2	0.682	6	10	10	2	0.019*
Avg. RS.Ar	7	4	10	3	0.395	13	7	3	5	0.183
Avg. Por.Ar	7	5	10	2	0.185	12	7	4	5	0.299
Total On.Ar	10	2	7	5	0.185	5	8	11	5	0.105
Total On.Fg.Ar	8	2	9	5	0.357	6	10	7	6	0.307
Total On.C.Ar	12	2	5	5	0.075	4	7	12	6	0.114
Total HC.Ar	10	4	7	3	0.643	5	8	11	5	0.105
Total RS.Ar	8	3	9	4	0.605	13	5	3	8	0.023*
Total Por.Ar	11	3	6	4	0.296	12	6	4	7	0.114
Total On.B.Ar	10	3	7	4	0.395	5	9	11	4	0.048*

* Asterisks denote significant differences between the stress groups in the frequencies of greater magnitudes in I_{max} versus I_{min} for the given property.

distribution of total resorption and osteonal bone areas between the humeral axes of bending. The no lesion group's humeri have greater bone resorption along the I_{min} relative to the I_{max} axis than expected (std. residual=1.4), while humeri in the lesion group show the opposite pattern (std. residual=1.0). It is important to note, however, that once Haversian canal area and resorption space area are combined, there are no differences between the groups in porosity distribution between the two axes. The humeri of individuals without lesions more often demonstrate greater amounts of osteonal bone along the I_{max} axis compared to the I_{min} axis than expected (std. residual=1.1), while individuals with lesions have greater amounts of osteonal bone along the I_{min} axis than the I_{max} axis (std. residual=0.9).

Overall, these results suggest conservation of bone mass within the femur between the axes of bending and more potential for variation between these axes in the humerus. Given the difference in age distribution between the stress groups, one may be led to conclude that the divergent pattern between the stress groups in humeral histomorphometric properties relative to bending axes is a reflection of stress-dependent differences in relative loading between these axes. In other words, the humeri of individuals without lesions could be more strongly reinforced along the I_{max} axis than the humeri of individuals with lesions, causing increased remodeling in this dimension. Yet, ANCOVA results showed no significant differences in humeral I_{max}:I_{min} between the stress groups, and non-significant trends also do not demonstrate enhanced I_{max} relative to I_{min} in the no lesion group. Therefore, these disparate patterns are not likely caused by differences between the stress groups in bending loads within the humerus. The implications of these patterns are further discussed in Chapter 6.

Under Seven Years. Table 25 presents the Mann-Whitney *U*-test results comparing histomorphometric properties between I_{max} and I_{min} for the younger subsample. Results are the same as those found in the entire Alytus subadult sample. Humeral Avg. HC.Ar is the only histological property that is significantly different between the stress groups. Figure 25 demonstrates that younger subadults in the no lesion group also have larger Haversian canals on average along humeral I_{max} compared to humeral I_{min}. Removal of the older chronically stressed individuals did not shift the mean value of Avg. HC.Ar away from zero (i.e., similarity between the axes); however, it did reduce the variance within the lesion group for this variable, as would be expected. These results are further discussed in Chapter 6.

Table 25. Results of Mann-Whitney *U*-tests comparing histomorphometric properties for maximum (I_{max}) versus minimum (I_{min}) long bone second moments of area between stress groups (1.0-6.99 years).

Histomorphometric property	Femur *p*-value	Humerus *p*-value
Avg. On.Ar	0.601	0.080
Avg. On.Fg.Ar	0.887	0.771
Avg. On.C.Ar	0.364	0.123
Avg. HC.Ar	0.536	0.025*
Avg. RS.Ar	0.364	0.159
Avg. Por.Ar	0.364	0.418
Total On.Ar	0.133	0.254
Total On.Fg.Ar	0.475	0.418
Total On.C.Ar	0.109	0.228
Total HC.Ar	0.813	0.093
Total RS.Ar	0.999	0.123
Total Por.Ar	0.999	0.381
Total On.B.Ar	0.315	0.346

* Asterisks denote significant differences between the stress groups for I_{max} - I_{min}.

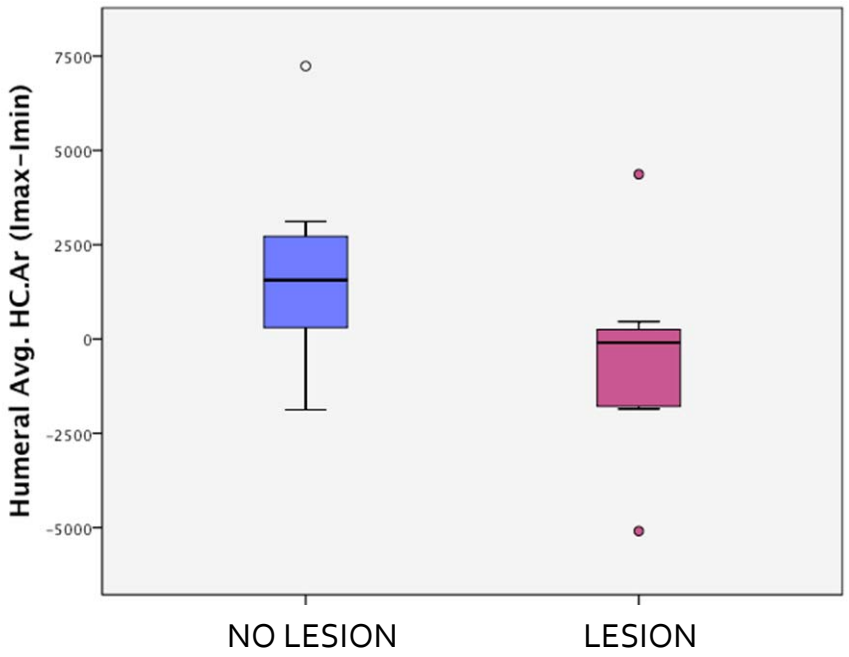

Figure 25. Boxplot of Haversian canal size differences between humeral I_{max} and I_{min} (1.0-6.99 years).

CHAPTER 6: DISCUSSION AND CONCLUSIONS

This study set out to examine the influence of metabolic stress on variation in histomorphometric properties and cross-sectional diaphyseal geometry of elements under different loading effects (the rib, humerus, and femur). The study's results have important implications concerning the interrelationship of macromorphology and micromorphology in shaping skeletal elements, as well as their independent variation among the three elements measured. While the study focuses on local and systemic bone responses to mechanical loading and metabolic insults, it also has broader implications for research on archaeological human skeletal remains. Results argue for some caution in the interpretation of signs of metabolic stress and impaired health in past populations, as well as the different ways in which cortical bone responds to these phenomena.

This chapter synthesizes the main results from the statistical analyses presented in Chapter 5 and discusses their implications for the hypotheses set out in the Introduction. To remind the reader, these hypotheses were derived from three broader questions (see Chapter 1), but the study fundamentally focuses on one central query: What changes manifest in cortical bone in relation to metabolic stress across skeletal elements that experience different mechanical loads? The analyses were performed to assess these effects on a macroscopic scale through comparisons of cross-sectional geometry, and then on a microscopic scale through comparisons of histomorphometry, examining these scales both independently and in concert. The Introduction set out five specific hypotheses. These hypotheses generally expected individuals categorized in the lesion group to show compensation at a macroscopic scale for bone loss due to the effects of long-term stressors, while compensating for chronic stress microscopically in ways

that minimally impacted the mechanical strength of the bone. In the long bones, the hypotheses further stated that any microscopic bone loss associated with chronic stress would occur in the diaphyseal anatomical planes that experienced the lowest mechanical loads, as bone loss in these locations would have less of an impact on each bone's bending strength.

As with any research like this study, there are caveats and limitations that should be considered, and these are discussed in detail below. The complexities inherent in studying the osteological patterns assessed herein, especially in an archaeological subadult sample, introduce both anticipated and unanticipated restrictions. Many of these limits and cautions were discussed in the background chapters (Chapters 2 and 3), as well as the "Materials" section of Chapter 4, but are considered below in relation to the outcomes of the statistical analyses.

From the exploration of the hypotheses, a few conclusions emerge:

1) Chronic metabolic stress is associated with reduced macroscopic bone mass in all three skeletal elements, and mechanical compensation for this bone loss results in increased strength properties. However, the *relative* relationships in cross-sectional properties among the elements, and thus mechanical loading demands, are not markedly disrupted.

2) Chronic metabolic stress is associated with reduced microscopic bone mass, but this bone loss does not occur in all three skeletal elements, nor does it occur preferentially in the least loaded element (i.e., the rib) as was expected. Thus, chronic metabolic stress disrupts the relationship between microscopic bone mass and the effects of mechanical loading on cortical bone.

3) In both individuals with and without pathological stress lesions, a negative relationship exists between macroscopic and microscopic bone mass, which indicates that considerable reductions in cortical area due to metabolic effects may remove evidence for microscopic bone loss. This relationship highlights the complex interaction of macroscopic and microscopic cortical morphology.

The following sections discuss how the evidence for or against the hypotheses collectively develops these conclusions. Prior to the review of these conclusions, general differences between the two stress groups are discussed in light of the hypotheses. Because of the need to separate analyses between the complete sample, including individuals of all ages, and the subsample of subadults under the age of seven, the results are synthesized below for each of these sets of results separately. These brief syntheses are then united for a more complete discussion of the main results that address each hypothesis.

Comparison of Body Mass and Size in the Two Stress Groups

Before evaluating differences between the stress groups in cortical bone properties, comparisons were made to establish whether individuals with pathological lesions also possess other skeletal indicators of metabolic disturbance relative to individuals without lesions. Results indicate an unexpected lack of significant differences between the groups in estimated body mass, estimated stature, and long bone lengths; although, in the younger subset of individuals, all these variables were non-significantly lower in individuals possessing stress lesions. Further assessment also demonstrated that all Alytus subadults with dental age estimates possess reduced femoral lengths for their dental age, and this trend is consistent with previous findings of

reductions in stature for age in medieval relative to modern Lithuanian populations (see the "Materials" section in Chapter 4). These results suggest two potential explanations: first, pathological lesions indicative of chronic metabolic stress may not necessarily be associated with other skeletal indicators of stress at the *individual* level, and second, all Alytus subadults may have experienced some form of metabolic stress or other factors that affected growth in this population. It is possible that part of this discrepancy is due to the general inability to identify dental enamel hypoplasia (DEH) in the younger subadults (< seven years old), and, thus, some of the individuals categorized in the no lesion group may have been misassigned into this category. Even if this were the case, the stress groups may still be compared to address the research hypotheses, because they demonstrate relative magnitudes of metabolic stress. Individuals with stress lesions show evidence of prolonged, chronic metabolic stress compared to individuals who have not developed such lesions: younger individuals in the lesion group who have unobservable DEH still have other additional pathological lesions compared to the no lesion group, and most of the older individuals in the lesion group also possess these additional lesions (see Appendix II).

Addressing Research Hypotheses: Comparisons Between Stress Groups

Five hypotheses set out in the Introduction focused on expected differences in cortical bone structure between the two stress groups. Hypotheses 1a and 2a were concerned with cross-sectional geometric properties: 1a set out the expectation that individuals with lesions would exhibit reduced cortical bone compared to individuals without lesions, and 2a followed up on this hypothesis by anticipating that the bones of individuals in the lesion group would compensate for this cortical bone loss through expansion of the periosteal surface. These effects

were thought to occur with decreasing magnitude from the femur, to the humerus, and then the rib. Mirroring those two hypotheses, Hypotheses 1b and 2b set out predictions that individuals with lesions would also show reduced cortical bone on a histomorphometric scale: the bones of individuals in the lesion group would have increased resorption, increased bone turnover rates, and/or disrupted replacement of bone during remodeling compared with the bones of the no lesion group. These microscopic bone changes were anticipated to be least visible in the femur, then increasingly in the humerus, and highest in the rib. Hypothesis 2c concerned the interaction between cross-sectional and histomorphometric properties and predicted that microscopic bone loss in individuals with stress lesions would be concentrated within regions of long bone cross-sections in such a way that reductions to bone strength are minimized. This targeted removal of microscopic bone mass would occur along the axis of minimum bending rigidity (I_{min}) and would be more apparent in the femur relative to the humerus.

If only the second set of hypotheses (2a, 2b, and 2c) were upheld, this would suggest evidence of a direct and predictable interaction between mechanics and metabolism that may be accounted for in bioanthropological analyses by careful selection of appropriate skeletal elements for study. If only the first set of hypotheses (1a and 1b) is supported, metabolic stress can be said to have a strong effect on cortical morphology despite effects of mechanical loading; thus, metabolic stress may, in some cases, limit interpretations of behavioral activity from skeletal remains. Likewise, if neither set of hypotheses is supported, it could be concluded that mechanical loading has a considerable influence on morphology despite metabolic disturbance; paleopathological analyses concerned with bone loss would, thus, require reevaluation to determine whether metabolic stress can be inferred from archaeological samples. Below are syntheses of the results in relation to these hypotheses.

Cross-sectional Geometric Properties (Hypotheses 1a and 2a)

All Ages. Overall, results of comparisons between the stress groups in cross-sectional geometric properties do not support Hypothesis 1a and Hypothesis 2a with some important exceptions and caveats. Chronic stress is not correlated with systemic bone loss in all three skeletal elements (contrary to Hypothesis 1a). In fact, including the older (≥ seven-year-old) individuals, subadults with lesions have significantly higher %CA in their femora and statistically similar %CA in their humeri and ribs compared to subadults without lesions. Comparing the means among the skeletal elements in Table 11, though, shows that individuals in the lesion group have lower macroscopic bone mass in their ribs compared to individuals in the no lesion group (indicating preferential bone loss in the least loaded bone analyzed).

Patterns in humeral cortical bone distribution and shape could suggest potential compensation for *previous* reductions in humeral bone mass, however (following the arguments behind Hypothesis 2a, which were explored in the discussion of mechanical effects on cortical bone in Chapter 2). In the full sample, subadults in the lesion group have significantly greater polar second moments of area (J) and bending rigidity along I_{min}, shape changes that could have been brought about by periosteal compensation following endosteal bone loss. These increases in humeral strength seem to be the cause of more similar strength proportions between the humerus and femur in subadults with lesions relative to subadults without lesions. Interestingly, while chronic stress is associated with significant shifts in humeral strength and shape, femoral strength properties and rib cross-sectional areas are not significantly different between the stress groups.

The effect of different age compositions of the two stress groups is a crucial caveat to the interpretation of the differences in elemental patterns between the stress groups described above.

Because all cross-sectional measurements have been size-standardized, differences found between the stress groups are due to differences in cross-sectional areas and shape distributions outside of differences in body size among the individuals. However, previous research has demonstrated that with increased age during growth, long bone diaphyses become stronger and contain more cortical bone *relative to their size* (Ruff, 2003a; Cowgill, 2010). In addition, femoral and humeral diaphyseal shape (e.g., I_{max}:I_{min}) is known to change during growth with alterations in behavioral activity (Ruff, 2003a; Cowgill et al., 2010). Because of these effects, one may conclude that the values for cross-sectional geometric properties in the lesion group will be skewed. Specifically, femoral second moments of area and polar section modulus both increase relative to the humerus with age, femoral midshaft values of I_{max}:I_{min} increase with age (while humeri remain more similar), and all long bones have positive allometry through growth in bone cross-sectional geometric properties. Thus, the results for the full sample synthesized above require additional consideration using the young (< seven-year-old) subsample.

Under Seven Years. As explained above, it was important to analyze the younger subset of subadult individuals, aged one to seven years, which contained relatively equal age composition between the stress groups. As discussed in Chapter 5, this methodology eliminates a large portion of available data from the Alytus sample, specifically the individuals who are likely to have been under chronic stress for the longest periods of time, but also makes comparisons between stress categories more consistent and interpretable. Given the nature of the data available, this statistical approach improves the interpretation of results to address the research hypotheses.

Comparisons of cross-sectional properties in the younger Alytus subadults indicate that age effects due to including older (≥ seven years) chronically stressed individuals were likely driving the differences observed in long bone cross-sectional geometric properties between stress groups in the full Alytus sample. This conclusion is supported by the lack of significant differences between stress groups in the younger subadult sample for any of the long bone cross-sectional properties, and in relative long bone strength proportions between the humerus and femur. This discrepancy undoubtedly was affected by lower statistical power associated with the smaller sample size for the restricted younger subsample. To this point, comparisons of trends in cross-sectional geometric properties between stress groups (Figure 19), not accounting for statistical significance, support Hypothesis 1a and reject Hypothesis 2a. While these results at first appear to disagree with those reported for the full sample, closer examination reconciles the two sets of analyses.

In the younger subsample, the presence of pathological lesions is not associated with statistically significant macroscopic bone loss in any of the three skeletal elements; however, each element does possess less %CA in individuals with stress lesions, which is support for Hypothesis 1a. The reason for the difference of this conclusion with the one drawn for the total sample is due to the inclusion of older individuals and the associated positive allometry in cortical bone, especially of femora. These reductions in cortical bone indicate the presence of some systemic metabolic disturbance in association with indicators for chronic stress. Relative to individuals without lesions, those with lesions do tend to demonstrate systemic endosteal bone loss (i.e., greater MA) and slight periosteal compensation for said bone loss (i.e., greater TA), as expected according to Hypothesis 2a. Nevertheless, although the amount of bone loss and inferred subsequent compensation is not equivalent across the skeleton (support for Hypothesis

2a), the proposed pattern of relative compensation among elements (i.e., Femur > Humerus > Rib) is not present (rejection of Hypothesis 2a *sensu stricto*). A significant majority of the subsample, however, shows more cortical bone in the humeri and femora relative to the rib in both stress groups.

The greatest difference in percent cortical area between the stress groups occurs in the femur. As the femur experiences the greatest mechanical loads of the elements analyzed in this study, it is unexpected that chronic metabolic stress would result in preferential bone loss in this element rather than the rib or humerus. Furthermore, the difference between the stress groups in %CA is lowest in the humerus, which one may interpret as conservation of macroscopic bone mass in the upper limb relative to the lower limb and axial skeleton. This conservation is also evident in comparisons of patterns between the stress groups in TA; although increases in TA in the elements of the lesion group are small and not significant, periosteal dimensions are relatively more expanded in the humerus and rib than in the femur, in contrast with the no lesion group. This periosteal expansion with chronic stress is statistically significant in the rib and appears to cause the non-significantly greater increases in strength properties in humeri relative to femora. These results do not indicate as much compensation for macroscopic bone loss in the femur relative to other elements, although the femora of individuals with lesions are non-significantly stronger in bending and torsion relative to individuals without lesions. It may be presumed that this increase in resistance to loading in the femur is adequate enough to meet mechanical demands, though this cannot be determined from the data and would depend on the activity level of the individual.

Therefore, by examination of the younger subsample, lower average amounts of cortical bone (regardless of magnitude) in individuals with lesions does not result in decreased bone

rigidity, but rather results in increased bone rigidity relative to individuals without lesions. The differences observed in the elements of the younger individuals categorized in the lesion group are due to redistributions of cortical bone further away from the cross-sectional centroid. This pattern is true of all three skeletal elements, not just the long bones, which experience comparatively greater mechanical loading.

Histomorphometric Properties (Hypotheses 1b and 2b)

All Ages. Overall, results of histological comparisons between the stress groups for the entire Alytus sample do not support Hypotheses 1b and 2b. In contrast to expectations of systemic microscopic bone loss in chronically stressed subadults, there are no significant differences between the stress groups in the average size or total area composed of microscopic indicators of intracortical resorption and remodeling. This fails to support Hypothesis 1b. Even considering non-significant trends, individuals with stress lesions do not have larger average remodeling events (evidenced by Avg. On.Ar, Avg. RS.Ar, and Avg. Por.Ar) across all three elements. This indicates that each BMU does not tend to remove more bone systemically with chronic metabolic stress. In fact, osteon size and pore size are only greater in the femora of individuals from the lesion group, and resorption spaces are smaller on average for all three skeletal elements relative to individuals in the no lesion group. Thus, although intact osteons in the humeri of chronically stressed individuals do have larger average Haversian canals (arrested osteon filling in this element only), overall pore size is not systemically larger in these individuals.

However, these data reflect the average amount of bone being resorbed and replaced with each BMU event; total area measurements take into account the size as well as the rate of

remodeling events. Although individuals with lesions have greater amounts of intact, fragmented, and total osteonal bone (i.e., indicators associated with increased remodeling) in all three elements, suggesting removal of more bone than individuals without lesions, this discrepancy does not result in systemically increased porosity. These findings are indicative of increased *systemic* remodeling with chronic stress, but suggests bone balance rather than arrested bone deposition in chronically stressed subadults. Therefore, these results reject Hypothesis 1b.

Similarly, Hypothesis 2b is not supported by the analyses on the entire sample. Both individuals with and without stress lesions have increased average resorption space size and pore size with decreased loading demands; thus, heavily loaded elements demonstrate smaller average pore size. However, total amounts of resorption and porosity per unit area do not increase with decreased loading (i.e., Rib > Humerus > Femur), rejecting Hypothesis 2b. These findings are also present in the younger subadult sample and are discussed further with specific reference to that subset of the sample.

Like the analyses of cross-sectional geometric patterns when the entire Alytus sample was analyzed, there are potential age effects that bias the histomorphometric results. Compared to individuals without lesions, those possessing lesions tend to demonstrate more divergence between their long bone elements in many of the mean size and total area histological measurements. Remodeling rates are known to increase over the course of ontogeny and with increased mechanical loading. Comparisons of the younger subadult sample eliminate this bias by removing the older subadults, who possess increased intracortical remodeling and are likely to have had different behavioral activity patterns in their limbs relative to younger subadults.

Under Seven Years. Results of histomorphometric comparisons between the stress groups for individuals below the age of seven suggest the rejection of Hypotheses 1b and 2b. As is the case with the entire Alytus sample, younger subadults with lesions do not demonstrate significantly higher remodeling or enhanced microscopic bone loss in all three bones relative to subadults without lesions (rejection of Hypothesis 1b). In fact, when compared to the no lesion group, each BMU in the lesion group tends to remove *smaller* amounts of bone (based on Avg. On.Ar, Avg. RS.Ar, Avg. Por.Ar) in all three skeletal elements. Individuals with stress lesions also tend to possess reduced total amounts of osteonal bone in their humeri and ribs. Total resorption space area and total porosity are also not systemically higher in elements of individuals from the lesion group, although the humerus does show increased microscopic bone loss relative to all elements in the no lesion group.

Thus, chronically stressed subadults are losing microscopic bone mass, yet this loss is occurring preferentially in the humerus but not the rib, a rejection of Hypothesis 2b. This bone loss takes the form of increased total resorption space area, as well as slightly increased total Haversian canal area. Why chronic stress would preferentially remove bone intracortically from humeri and conserve microscopic bone mass in femora and ribs remains unknown. The humeri of chronically stressed individuals have the highest %CA and greatest relative compensation in second moments of area and polar section modulus, which would suggest that intracortical bone loss associated with metabolic stress may occur in elements that are structurally reinforced macroscopically (see below for further discussion).

Interaction of Macroscopic and Microscopic Properties (Hypothesis 2c)

A final hypothesis (2c) directly correlates the results obtained from analyses of cross-sectional properties with histomorphometric properties. The final set of analyses synthesized below assesses whether the microscopic bone loss in the humeri of chronically stressed individuals, discussed above, occurred preferentially along the axis of least resistance to bending (I_{min}) and whether evidence for differences in remodeling occurred between that axis and I_{max} in both the humerus and femur.

All Ages. The findings for distribution of microscopic bone mass in relation to macroscopic cortical bone properties generally support Hypothesis 2c. ANCOVA results indicate histological variables are mostly similar among the bending axes in both stress groups; thus, chronic stress does not appear to be linked with significant preferential microscopic bone loss along I_{min}. These results support the ANCOVA comparisons that found no significant differences in histomorphometric properties between the stress groups. The humeri of individuals without lesions have significantly larger average Haversian canal sizes along I_{max} relative to I_{min} in comparison to individuals with lesions. Subadults in the lesion group have more similar average Haversian canal sizes between the axes, either because they possess reduced average values along I_{max} or increased values along I_{min}. In either case, these morphological shifts do not result in different *total* Haversian canal area or porosity between the axes in these individuals. Thus, the relative distribution of microscopic bone mass between long bone bending axes does not differ between the stress groups based on these analyses.

Different conclusions are drawn from comparing patterns within individuals with chi-square tests (as opposed to the comparisons between groups by element). In these comparisons,

chronic stress appears to be linked to larger average Haversian canal size along humeral I_{min} relative to humeral I_{max}. Compared to individuals without lesions, who demonstrate larger average Haversian canals along I_{max}, this shift suggests conservation of bone mass in the humerus along I_{max} in cases of chronic metabolic bone loss. This pattern is not evident in total Haversian canal area or total area of porous structures, which means that individuals with lesions do not have more porous bone along I_{min} compared to I_{max}. However, there is a tendency for osteon filling to be arrested, and future research is necessary to determine if these patterns exist in comparisons with larger sample sizes. Thus, bone loss in the form of arrested osteon filling occurs preferentially in the axis of minimum bending rigidity, a scenario that would minimize reductions in whole bone strength and thus tentatively supports Hypothesis 2c.

Also in support of Hypothesis 2c, the femora of individuals in the lesion group do not demonstrate evidence of microscopic bone loss in either the ANCOVA or chi-square comparisons. Differences between the stress groups in relative distribution of bone mass along bending axes, therefore, occur only in the humerus. Such findings support the supposition that microscopic bone mass will be conserved in skeletal elements under higher mechanical loads, such as the femur, and less conserved in relatively less mechanically loaded elements, such as the humerus.

Under Seven Years. Mann-Whitney *U*-test results in the younger subadult sample support ANCOVA results in the entire Alytus sample. Based on these results, there is no evidence of different relative distribution of microscopic properties within long bone elements between the stress groups. Unfortunately, due to small sample sizes in this subset, it was not possible to conduct a chi-square test to determine if the patterns that support Hypothesis 2c in the

total Alytus sample are also present when older subadults are removed from the analysis. Thus, age effects could be driving the patterns revealed in the chi-square results above. However, as discussed briefly in Chapter 5, ANCOVA results on individuals of all ages showed no significant differences in humeral I_{max}:I_{min} between the stress groups. There are no demonstrable patterns in the magnitudes of I_{max} relative to I_{min} that would explain the histological differences. Therefore, it is arguable, based on current evidence, that differences in the relative cross-sectional properties of these axes caused by differences in mechanical loading associated with age are not responsible for the differences between the stress groups in histological distribution along I_{max} versus I_{min}. Future research will be necessary to address this issue.

Interaction of Mechanics and Metabolism: Comparisons Across Stress Groups

When considering the patterns in cortical bone properties within the Alytus subadults as a whole, regardless of inferred metabolic status, the trends generally support mechanical and metabolic expectations set out in previous research (see Chapters 2 and 3). The examination of general macromorphic and micromorphic patterns across elements, especially in light of the findings reported above regarding stress categories, is important for understanding how bone structure varies across elements in subadult skeletons. These interpretations also shed light on which relationships are most disrupted with chronic metabolic stress and assist with evaluating the interaction between mechanical and metabolic factors.

Variation in cross-sectional properties across the skeletons of Alytus subadults support mechanical expectations given loading differences among these elements. Bones under high loading demands tend to have more cortical bone relative to diaphyseal size (%CA); this is especially true of long bones in relation to ribs but is also mainly true of the femur in relation to

the humerus. The femur also tends to have higher strength in bending and torsion than the humerus. These patterns are evident when all individuals are considered in analyses, as well as when the younger subset is evaluated. That these patterns match mechanical expectations based on previous research in adults lends credence to the argument that mechanical loading has a discernible effect on diaphyseal cortical bone mass and structure and, more importantly, that this effect is present early in ontogeny (Cowgill et al., 2010).

Based on the previous research cited in Chapter 2, increasing mechanical loads are associated with increased resistance to compression (reflected by %CA), bending (reflected by I_{max} and I_{min}), and torsion (reflected by J and Z_p). Even in Alytus individuals who have stress lesions, these patterns are still present in the majority of variables. Thus, one can conclude that, although chronic metabolic stress results in reduced macroscopic bone mass and increased compensatory strength in all three skeletal elements, it does not cause such considerable shifts in diaphyseal cortical morphology that the strength relationships across these elements with loading are disturbed. All three skeletal elements appear to respond to metabolic bone loss by maintaining relative resistances to mechanical loading, although the response varies depending on the element and not in clear association with the level of mechanical loading. Nevertheless, loading appears to continue to have a significant influence on cortical bone morphology regardless of the effects of metabolic stress, as defined in this study. Furthermore, while metabolic stress does affect cortical bone morphology systemically, mechanical loading-induced compensation seems to mitigate its effects across the skeleton.

Histological variation across the skeleton in all Alytus subadults also supports previous research concerning mechanical and metabolic effects on intracortical remodeling. Regardless of whether the entire sample or the younger subset is analyzed, skeletal elements under more

mechanical demand (e.g., femora, humeri) tend to have larger osteons and greater amounts of intact osteonal, fragmented osteonal, and total osteonal bone. These findings verify previous analyses of increased BMU resorption and increased remodeling rates with high levels of mechanical loading (see Chapter 2). Interestingly, elements under higher mechanical loading also generally tend to have smaller resorption spaces and pore size compared to elements that experience lower mechanical loading (e.g., ribs). Increased resorption space size in less mechanically loaded elements supports hypothesized targeting of less mechanically influenced skeletal elements for mineral homeostasis. Additionally, this may indicate either more resorption on average by BMUs or convergence of porosities during multiple remodeling events in elements like the ribs. Moreover, results of this study suggest that intracortical resorption associated with mineral metabolism is limited to localized regions within these elements (resulting in fewer, larger pores) rather than removing bone profusely and stochastically (resulting in many, smaller pores). This phenomenon has been identified in age-related bone loss in adults (Bell et al., 1999; Stein et al., 1999; Bousson et al., 2001); however, whether this strategy is advantageous or disadvantageous from a structural perspective or is simply a by-product of the remodeling process requires additional research.

While elements that experience low mechanical demands demonstrate larger resorption spaces and pores, total resorption space area and total porosity do not show a clear relationship with mechanical loading. However, this lack of relationship is mainly caused by the divergent patterns in individuals possessing stress lesions. In all other cross-sectional and histological variables discussed thus far, patterns among skeletal elements are generally similar in both stress groups; even if one group shows more similarity between the two long bones or opposite patterns between the long bones compared to the other group, the rib is always differentiated from the

two long bones. However, for total resorption area and total area of porous structures, chronic stress does considerably disrupt the patterns among the elements by increasing porosity in the humerus relative to other elements. In individuals without lesions, these variables decrease as loading decreases; more cortical bone is removed during remodeling in highly loaded bones, which likely reflects higher targeted remodeling rates in these elements. Chronic stress, on the other hand, creates deviations from this normal baseline pattern.

Thus, one can conclude that chronic metabolic stress causes changes that disrupt the normal relationship between resorption in relation to mechanical loading, which in turn affects porosity differences in cortical bone under different loads. In this sense, it can be argued that persistent metabolic stress in the Alytus sample has a stronger effect on these microscopic bone mass variables than do mechanical loading demands. Unlike macroscopic cortical bone morphology, there is no known loading-induced mechanism at the histological level that would compensate for this metabolic bone loss. However, as discussed above, higher resorption and porosity are present in the element with the highest conservation of %CA (i.e., the humeri of individuals in the lesion group). Moreover, the patterns across the elements for %CA and total porosity are the same within individuals in the lesion group (i.e., Humerus > Femur > Rib) and within individuals in the no lesion group (i.e., Femur > Humerus > Rib), even though there is a reversal in the humerus and femur between the two groups. Therefore, there appears to be an association between the amount of intracortical microscopic bone mass and the relative amount of cortical area in these bones, and this association occurs regardless of metabolic status.

One of the most interesting outcomes of this study is the relationship between macroscopic and microscopic bone loss across the elements. In contrast to hypothesized expectations, reduced bone mass was not found at the microscopic level in the femora and ribs of

individuals in the lesion group, elements that demonstrated relatively larger reductions in %CA. Humeri, on the other hand, exhibit the least amount of macroscopic bone loss and are the only elements with evidence of microscopic bone loss in the lesion group. What could explain this opposing pattern? One explanation could be that intracortical bone loss will occur preferentially in elements that can withstand the associated tissue-level reductions in strength, because they contain more cortical bone relative to their size and are stronger in bending and torsion.

Another explanation, and one which is more complicated, is that all three elements are undergoing microscopic bone loss but that this loss is only visible in elements that retain high values of %CA. Because macroscopic alterations in bone mass are ultimately the combined results of individual cellular processes, histological alterations in bone mass will eventually lead to changes in cortical structure at the organ level. Thus, increased levels of porosity in the endosteal portion of the diaphysis are likely to have caused the endosteal bone loss detected at the macroscopic level in all three elements from the lesion group. It would appear that in chronic stress, this bone loss leads to more significant removal of cortical bone surrounding the medullary cavity in the femur compared to the other elements. In the humerus, intracortical bone loss is only visible because it has not been erased by large-scale endosteal bone loss. Therefore, microscopic bone loss may only be detectable in elements that have not undergone significant endosteal resorption.

It remains unclear why the humerus would experience less macroscopic cortical bone loss than other elements, but it is possible that activity in the upper limb within the Alytus population (e.g., forestry-related tasks, swordplay) places strong mechanical demands on humeri, leading to retention of humeral cortical bone mass. However, this would involve individuals below the age of seven engaging in behaviors not typically attributed to this developmentally immature stage;

thus, additional research is necessary to determine why metabolic bone loss is greater in femora relative to humeri.

Caveats, Limitations, and Implications for Broader Biological Anthropology Studies

Caveats and Limitations

In the analyses summarized above, many of the specific research hypotheses regarding the nature of the interaction among mechanical and metabolic factors were either not supported or only partially supported, and there were often unexpected patterns and/or no statistically significant differences in cortical bone properties between the stress groups, especially in the histological analyses. Although non-significant differences between the stress groups supported some of the research hypotheses, relatively few statistically significant differences were found in bone properties when stress categories were compared directly. Hypothesized systemic metabolic bone loss was not always associated with the presence of pathological lesions in the Alytus sample; surprisingly, both stress groups demonstrated similar trends among the bone elements for many variables. And, furthermore, analyses within individuals demonstrated more variation in patterns across the skeletal elements than that captured by mean values alone.

General lack of statistical significance may suggest a lack of statistical power to detect such differences and/or a lack of significant metabolic effects in subadults with stress lesions (i.e., inappropriate assumptions regarding the definition of chronic stress). On the statistical argument, power analyses will undoubtedly show that the sample sizes were insufficient to reach statistical significance, especially in the ANCOVAs. Given the low degrees of freedom in these analyses, increasing the sample size may not necessarily increase the ability to distinguish many of the subtle differences observed in the results. Statistical power is also dependent on effect

sizes; to reach relatively large effect sizes (e.g., 0.75) would require sample sizes much greater than the total sample available for this study (i.e., greater than 54), and even then an increase in sample size is not a guarantee for increased effect sizes (B.M. Auerbach, personal communication). In fact, as outlined in Chapter 5, there are instances where no difference in weighted means occurs, even though they would be expected. This calls for further consideration of the nature of the sample and assumptions made in categorizing stress groups.

Arguably, some of these discrepancies between expectations and observations could have been caused by the small sample sizes within stress categories, especially for histological comparisons. Diagenetic change in Alytus skeletal remains precluded analysis of many skeletal elements and lead to different numbers of elements being included in statistical analyses. With an increased sample size, these non-significant trends could arguably reach significance; yet whether this is the case awaits further research. As discussed in Chapter 4, statistical significance is not always indicative of biological significance (and vice versa). Determining whether the trends and differences among properties reported have biological consequences is difficult to discern, especially as, arguably, all of the observed effects (both macroscopic and microscopic) may have been ultimately consequential. Additionally, it is not possible, given our current understanding of bone mechanics, to determine the exact consequences of structural alterations in both macroscopic and microscopic properties to whole bone strength and rigidity. Though generalizations can be made considering previous research on cortical reductions at these scales independently, the direct biological impact of the reported reductions in bone mass cannot be determined and is beyond the scope of this research.

Despite the potential explanations above, and focusing on analyses that attempted to account for age effects (on individuals 1.0-6.99 years of age), lesion presence was indeed

associated with evidence for reduced bone mass at both macroscopic and microscopic levels, even though it did not occur exactly as hypothesized in relation to variance in mechanical loading across elements. Such results do call into question the assumption that metabolic bone loss will occur systemically without being influenced by differences in mechanical demands within the skeleton. Thus, even taking into account the limitations to this study, the results do address and impact interpretations of interaction effects between mechanics and metabolism and provide a basis for further assessment.

Implications for Bioarchaeological Studies of Subadults

Overall, the results outlined in the "Addressing Research Hypotheses" section appear to call into question the way metabolic stress is defined in human skeletal samples and directly impact the interpretation of metabolic bone loss from skeletal remains. It may be that, in light of the lack of differences in some bone properties, chronic metabolic stress in the Alytus sample did not reach a high enough level of severity or duration to induce metabolic bone loss. That is, the individuals possessing stress lesions may not have been unhealthy *enough* to lead to systemic effects. Yet, pathological lesions that are commonly used as bioarchaeological indicators of chronic stress developed in these individuals. As discussed in Chapter 3, the threshold for induction of metabolic bone loss is unknown. It is possible that pathological lesions appear more quickly with chronic stress than metabolic bone loss. Unlike metabolic bone loss, traditional stress indicators themselves do not cause serious structural detriments to the skeleton; and, thus, it is logical that these lesions could develop more easily in cases of chronic stress than significant, detectable metabolic bone loss. These results may suggest that cortical bone is a relatively conserved tissue in the body, and that only in cases of severe and/or prolonged

metabolic disturbance will the body begin to resorb significant amounts of cortical bone tissue systemically to maintain mineral homeostasis (e.g., in groups like the Kulubnarti; see Chapter 3).

Special attention should be given here to the use of DEH as a criterion for assigning individuals to the lesion group, and the cryptic nature of using a pathological indicator that does not appear, at least in the Alytus sample, in individuals with unerupted permanent dentition. In cases of excellent skeletal preservation, conditions necessary to perform the methodology for collecting data on cross-sectional and histomorphometric properties, stress categories utilizing DEH as a pathological criterion will not be directly comparable if older subadults are included. For this study, younger subadults who could not be assessed for the presence of DEH were compared because, it was argued, they represent different magnitudes of metabolic stress relative to each other regardless of whether some individuals in the no lesion group had unobservable DEH. In future research, to include the entire range of ontogenetic variation in cortical bone properties, it may be necessary to refine the way stress groups are defined in archaeological samples. This issue is discussed further with constructive suggestions for future studies in the "Future Directions" section.

Additionally, taking into consideration that Alytus individuals with pathological indicators of chronic stress also did not demonstrate reduced body mass and stature estimates or retarded long bone growth relative to individuals without such indicators, perhaps pathological lesions are not necessarily associated with other indicators of metabolic stress at the *individual* level. Previous research has linked reduced bone mass, body mass, and bone growth with increased frequencies of stress lesions across populations, but few studies have compared the correlation between stress lesion presence and metabolic bone loss within individuals (e.g., Paine and Brenton, 2006). It may not be appropriate to assume that metabolic bone loss will occur

systemically in all individuals with pathological lesions; there may be some individuals who present pathological lesions who have not endured enough chronic stress to induce bone loss at all much less throughout the skeleton. While this fact was recognized at the implementation of the study, the small sample sizes do not allow for subdividing the Alytus individuals into fewer, graded groups (e.g., individuals with few lesions versus individuals with many lesions) to test this idea.

Furthermore, all inferences drawn from the analyses in this study are based on the assumption that individuals who lack pathological indicators of chronic stress represent the normal baseline from which chronically stressed individuals deviate. One of the assumptions in this study is that acute stress does not result in metabolic bone loss, because it is not of a high enough severity or duration. Likewise, individuals who have died from non-metabolic causes are not expected to show bone loss. However, it is possible that, because individuals in both groups are non-survivors, both groups deviate from healthy individuals who survived into adulthood, but whose subadult remains obviously are not in cemetery samples. Were this true, the implication is that both of the stress groups in the Alytus sample are gradations of metabolic stress. Of course, whether this is the case cannot be tested.

It is important to note, however, that if this scenario were true of the Alytus subadult sample, individuals possessing stress lesions continue to demonstrate logical patterns in cortical bone loss relative to those individuals assigned to the no lesion group. That these patterns are consistently present in many variables supports the argument that individuals in the lesion group are experiencing bone loss in generally anticipated ways. Whether or not subadults in the no lesion group are considered to have “normal” bone mass or if they have reduced bone mass relative to survivors may ultimately be moot for this particular study. Yet, this observation, in

addition to the discussion of DEH in the paragraph above, calls for caution in the assignment of subadults to stress categories based on skeletal lesions.

It is possible that activity differences between individuals and/or between the stress groups are causing some of the differences in bone properties found in the statistical analyses. In the Alytus cemetery, there are no clear indicators of status in burial goods or burial practice. If chronically stressed subadults at the Alytus site are more frequently those from the lower class, the reduction in %CA and increased second moments of area and polar section modulus found in the younger subadult sample could be due to higher activity levels (in both the upper and lower limb) rather than an indication of metabolic disturbance. This supposition, of course, assumes two things: first, Alytus individuals in the lower classes were more highly active because they engaged more frequently in manual or skilled labor than higher class individuals and, second, these activity differences are present early in ontogeny (1.0-6.99 years of age). As explored in Chapter 4, even though nobility lived in Alytus in addition to the vast peasantry, it is unlikely that the entirety of either stress group would be comprised of one social class or another. In addition, few ethnographic studies (see Chapter 2) show individuals younger than six engaging in the increased activity levels associated with labor.

Even placing these two arguments aside, the explanation for confounding of activity and stress group does not account for the significantly expanded rib dimensions (more likely a metabolic effect) and the unexpectedly reduced remodeling rates (not a result of increased loading activity) in Alytus individuals with stress lesions. Thus, while it is important that the possible covariance of stress frequency and duration with activity levels should be taken into account, the evidence in this study diminishes the possibility that such covariance is present.

Two final, important methodological implications emerge from this study, in addition to those discussed above. The first concerns the procedures used for measuring the histomorphometric data, particularly with the size and location of regions of interest (ROIs) within a cross-section. Secondly, there are implications for the application of subadult body mass estimate methods to individuals who were likely less healthy, or at least empirically had a different correlation between body size and age, than the reference sample on which the estimate was developed.

The histological ROIs assessed herein represent a relatively small portion of the entire diaphyseal cross-section of these bone elements; standard histological practice does not require measuring entire cross-sections mainly due to the exceptional amount of time involved to complete such a task. If intracortical bone loss in chronically stressed individuals tends to occur outside of the ROIs used in this study (i.e., not along I_{max} or I_{min}), it could explain lack of significant differences between the stress groups for histomorphometric properties. Previous research has demonstrated that ROIs containing 3% of cortical area in the anterior cortex of adult femora contained 95% of variation in histomorphometry in that section of the cortex (Iwaniec et al., 1998). Whether this finding holds true in subadults has not been tested. Future research will examine microscopic bone loss in areas of the cross-section that do not fall along these axes of maximum and minimum bending rigidity to evaluate whether differences between the stress groups are present.

Similarly, due to cortical drift during growth and variance in mean tissue age among the Alytus individuals, the ROIs may have been placed on cortical bone sections that formed at various times across individuals' lifetimes. In individuals with expanded periosteal and endosteal dimensions, older cortical tissue containing potential evidence of previous stress events may,

therefore, have been removed. Further research is necessary to determine the rate of bone replacement in subadult individuals and how modeling would affect interpretations of loading behavior and health status from histological properties. Future study, as discussed below, will also look at ROIs away from the maximum and minimum second moments of area to determine whether these are atypical representatives of the rest of the cortical area.

Equally as important are the complications involved with standardizing cross-sectional properties by body mass estimates in chronically stressed individuals. Metabolic stress of prolonged duration will lead to reduced body mass, and this reduction may not be detectable in portions of the skeletal system (i.e., metaphyses and epiphyses) that are genetically canalized (Ruff et al., 1991; Lieberman et al., 2001; Auerbach and Ruff, 2006). Thus, because body mass in this study was predicted from distal metaphyseal femoral breadth using equations calculated from modern, relatively healthy subadults, Alytus individuals in the lesion group may have overestimated body mass estimates compared to their actual body mass during life. Long bone strength properties that are standardized by these overestimated body masses would, thus, appear lower than they actually are. However, long bone strength properties in the younger subset of the lesion group were higher than those in the no lesion group, not lower. Thus, if body mass is overestimated in subadults with chronic stress, their long bones are actually stronger relative to subadults lacking lesions than reported herein.

Conversely, it is possible that the entire sample, based on discrepancies between the ages estimated from dental formation versus femoral length, will have *underestimated* body mass estimates. Metaphyseal size is likely to scale positively with bone length (Ruff, 2007), and thus, body mass estimates for individuals who have relatively shortened bones for their age may be underestimated. If this is a systematic bias in estimation, without different effects between the

two groups, then the results are unaffected as far as analytical comparisons within the site are concerned. However, if the skeletal cross-sectional geometric properties calculated from this sample were compared with subadults from another site, the researcher would need to assess whether the sample from the other site expressed the same kind of discrepancy in age estimations. Even if these were similar, it is not known how comparable the scaled cross-sectional properties would be, especially in light of the potential effects that arise due to metabolic stress. Therefore, this calls for caution in the direct comparison of subadult mechanical properties derived from archaeological samples and the need for researchers to pay attention to skeletal and dental stress markers—even in light of the many caveats above—when collecting data.

Future Directions

This study was an initial investigation of the interaction between mechanics and metabolism in human cortical bone development. As is the case with most dissertations, the results summarized in this chapter raise just as many questions as they answer. More studies are needed to disentangle interaction effects among these factors, and the current study highlights the areas where continued research is needed.

Given the bias associated with archaeological samples and complications with defining metabolic stress, future analyses may benefit from exploring relationships between macroscopic and microscopic cortical bone mass in subadults without utilizing stress categories. Not all individuals with stress lesions will necessarily have reduced bone mass; identifying individuals with reduced bone mass for their age may be an alternative to relying on traditional metabolic stress indicators. This approach would require a much larger sample size to establish normal

bone mass for a given age and population and would still not address hidden heterogeneity and mortality bias in subadult cemetery samples. This solution would, however, create criteria for identifying metabolic bone loss that are currently missing in health studies on skeletal remains. Nevertheless, this approach assumes that reduced bone mass for a given age is caused by metabolic stress rather than normal variation among individuals, and this assumption may artificially improve the likelihood of detecting differences, whether of biological significance or not.

It follows from the arguments presented above that a larger sample is needed to continue to explore the interaction effects between mechanics and metabolism. Given the issues in comparing stress groups utilizing traditional stress markers (especially DEH) and the logical trends in cortical bone properties reported here for the younger subsample (< 7 years old), it seems that future analyses would benefit from focusing on younger subadults and excluding older individuals. In populations like Alytus, where metabolic disruptions appear to be significant stressors with obvious skeletal effects evident in the majority of the Alytus cemetery sample, the likelihood of individuals surviving to late childhood and early adolescence without developing a skeletal lesion is low. In populations where metabolic stress is less influential, based on reduced frequencies of pathological lesions and concordance between dental and skeletal age estimates, the capacity for identifying differences in cortical morphology caused by metabolic stress is diminished. Thus, limiting evaluations of interaction effects to younger subadults is advisable, despite the potential restrictions to observing DEH when skeletal preservation is good.

Alternatively, future analyses can explore relationships and patterns in cortical morphology in subadult individuals of all ages only if it can be demonstrated that DEH presence

in older subadult individuals does not correlate with reduced metabolic bone loss. This scenario would categorize older subadults with DEH but no other indicators of chronic stress into the no lesion group and make comparisons between the two age categories (i.e., < seven years old and ≥ seven years old) comparable. As discussed in Chapter 3, DEH in subadults and adults is used as a criterion for identifying health status in cemetery samples due to its correlation with other pathological lesions and indicators of metabolic disturbance, such as reduced bone mass. These correlations have been demonstrated more consistently among cemetery samples than within cemetery samples; thus, if DEH presence in the older subadults of a particular sample is not indicative of reduced bone mass, an argument can be made for eliminating DEH from the categorization of individuals into stress groups. However, future research is necessary to address this issue.

Chapter 4 outlines the argument for performing this study on human skeletal remains rather than experimentally in non-human analogues. In light of unexpected results and discussion of the impact that the osteological paradox has on metabolic interpretations from skeletal samples, it is important to review this issue again. Given limitations to both experimental non-human studies and those employing a cemetery sample, which is the best approach to addressing the interaction between mechanics and metabolism? Arguably, if the research question simply asked what the nature of the interaction is, an experimental approach would be more appropriate. In experimental studies, variables such as the threshold of metabolic disturbance and length of stress duration, as well as level and type of mechanical loading can be controlled. As discussed in Chapters 2 and 3, previous experimental studies have assisted with understanding how mechanical loading and metabolic stress interact on cortical bone and have helped formulate the hypotheses tested in this study.

However, this research is specifically concerned with the influence that this interaction has on bioanthropological interpretations of physical activity and health status from human skeletal samples. Experimental studies in non-human animals cannot address how this interaction influences human cortical bone structure and strength across the skeleton with specific human locomotor patterns. Moreover, results concerning the distribution of macroscopic and microscopic bone loss with metabolic stress that arise from experimental studies must always be tested and confirmed in human samples. This being said, studies such as this one can benefit substantially from continued experimental research on interactions among mechanical and metabolic factors. With a more complete understanding of how variation in loading and metabolic stress expression influence cortical bone structure, more thorough analyses may be conducted on human skeletal remains in the future.

Conclusions

In sum, this study made an initial investigation into the main effects and interactions of general mechanical and metabolic factors on cortical bone throughout the skeleton. Ultimately, the conclusions may be summarized by answering three research questions set out in the Introduction:

1) **How does the interaction between mechanical loading and metabolic stress influence macroscopic and microscopic cortical bone structure?**

At the macroscopic level, chronic metabolic stress causes endosteal bone loss (increased MA) leading to cortical bone loss (reduced %CA) in all three skeletal elements analyzed in this study. This bone loss is not equivalent in magnitude across these bone elements; the femur

experiences the greatest cortical bone loss, the humerus demonstrates the least loss, and the rib is intermediate. Cortical bone loss is somewhat compensated by mechanical alterations to cross-sectional geometry that vary in their level of compensation depending on the skeletal element. Periosteal bone deposition (increased TA) is evident in all three bones; however, the least amount of periosteal deposition occurs in the most heavily loaded element (i.e., femur). Mechanical compensation for metabolic bone loss results in increased long bone strength properties in both the humerus and femur of individuals with stress lesions; however relatively more compensation appears to occur in the humerus. Thus, in contrast to expectations, mechanical compensation for endosteal bone loss is greatest in the humerus, not the femur, and compensation also occurs in the relatively least loaded rib elements. Whether these compensations are adequate to withstand the loads placed on these elements during physical activity is unknown and cannot be determined from an archaeological skeletal sample.

At the microscopic level, bone loss (enhanced resorption) occurs in individuals with stress lesions only in the humerus, whereas microscopic bone mass is actually higher in the femur and rib of these individuals relative to those without lesions. Chronic metabolic stress is also not associated with extended bone removal during remodeling or higher rates of remodeling. Histological variables indicative of microscopic bone mass removal during remodeling are *reduced* in all three chronically stressed elements and total osteonal areas are also reduced in the humeri and ribs of individuals possessing stress lesions. The distribution of microscopic bone loss appears to occur regardless of the inferred level of mechanical loading based on the mechanical demands placed on the elements; more intracortical bone loss does not occur preferentially in the least loaded elements.

However, the amount of intracortical bone loss appears to correlate negatively with the relative amount of cortical bone present in the cross-section (%CA) and strength properties (J, Z_p). The humeri of subadults with stress lesions undergo the least amount of macroscopic bone loss and the highest level of microscopic bone loss relative to the femora and ribs of these individuals. This may suggest either that microscopic bone loss occurs preferentially in elements that are structurally reinforced at the macroscopic level or enhanced macroscopic bone loss will erase evidence of microscopic bone loss. Additionally, the current analyses do not support preferential microscopic bone loss along axes of minimum bending rigidity in long bone elements. In long bone diaphyseal cross-sections, microscopic bone loss occurs in equal amounts within the cortex.

2) Does this interaction affect bone strength within and across individuals?

As discussed above**,** at both macroscopic and microscopic levels, chronic metabolic stress has an influence on cortical bone structure that, when viewed in isolation, seems to alter bone strength both within and across individuals. This effect, however, only disrupts the relationship between loading patterns and cortical bone structure at the microscopic level. Mechanical loading leads to macroscopic compensations for bone mass reductions (i.e., from the endosteal surface of the bone) and generally maintains loading relationships across the skeleton. Although microscopic bone mass is altered with metabolic stress, its distribution within the skeleton (preferentially in elements with higher %CA) may mitigate potential reductions in strength at the tissue-level.

Metabolic bone loss at the endosteal surface will induce a mechanical compensatory response to reduced bone mass that serves to redistribute cortical bone further from the cross-

sectional centroid, thus increasing strength properties. Therefore, the femora and humeri of subadults with stress lesions are stronger under bending and torsion than the long bones of subadults without lesions. A similar response occurs in rib elements (inferred from expanded endosteal and periosteal dimensions). The fact that this compensation is not equivalent in all three skeletal elements causes changes in the relative strength relationships among skeletal elements in individuals with stress lesions but not enough to disrupt the general patterns across elements. In other words, femora are still stronger than humeri, which remain stronger than ribs. Thus, while metabolic stress does affect cross-sectional geometry, mechanical loading mitigates this effect.

At the microscopic level, however, chronic metabolic stress disrupts the relative pattern in microscopic porosity among the elements associated with different levels of mechanical loading; patterns in intracortical porosity among the bones of subadults with stress lesions do not follow expectations based on loading demands (i.e., increased porosity with decreased loading). Based on microscopic bone mass alone, the humeri of individuals with lesions are more likely to incur microdamage during loading due to the increase in tissue-level porosity. However, the tendency for microscopic bone loss to be negatively associated with %CA suggests that whole bone strength may not actually be reduced with metabolic reductions in microscopic mass.

3) Does the interaction potentially restrict interpretations of physical activity and health status from skeletal samples?

Given the alterations in cortical bone structure associated with chronic metabolic stress in the Alytus sample, it follows that the interpretation of either physical activity or health status in isolation from skeletal samples could result in erroneous conclusions in some bioarchaeological

studies. Analyses of both subadult and adult skeletal samples are likely to be affected by the interaction between these factors. Although cortical bone continues to be influenced somewhat by environmental factors after skeletal maturity, the majority of adult cortical morphology is the result of developmental processes, which are considerably responsive to mechanical and metabolic inputs, as well as other factors.

Mechanical compensation for metabolic bone loss in chronically stressed individuals makes long bone cross-sectional geometric properties appear more robust, but this is not necessarily the result of activity differences between these individuals. Moreover, if patterns present in the above analyses are confirmed in continued research, individuals under chronic metabolic stress will appear to load their upper limbs more heavily or frequently than other individuals. Therefore, comparisons of cross-sectional strength properties both within and among populations with different health statuses could potentially be biased.

Similarly, evaluations of cross-sectional geometric properties across populations to infer health status could be spurious if they do not account for mechanical compensation. For example, similar %CA is not indicative of similar health statuses. If periosteal deposition balances endosteal loss, relative reductions in cortical bone mass will not occur, even though metabolic stress effects are present. What the current study does demonstrate is that macroscopic bone loss is evident in all three elements, suggesting that accounting for metabolic effects cannot be avoided simply by limiting mechanical interpretations to more heavily loaded elements. If, for example, metabolic bone loss occurred only in rib elements but not long bone elements, researchers could continue to evaluate long bone cross-sectional properties to infer physical activity without the need to account for metabolic effects. However, this research suggests that interaction effects complicate behavioral interpretation from long bone cross-sections.

Nevertheless, researchers may examine health status more accurately by analyzing cortical bone mass in elements under low mechanical demands, such as rib elements, to avoid potential activity effects.

At the microscopic level, assuming patterns in these analyses hold true with continued research, metabolic bone loss will not necessarily be present in any single element analyzed. The ability to detect microscopic bone loss seems to be dependent on the amount of cortical bone present in the cross-section. Therefore, it may be necessary to evaluate multiple skeletal elements to determine the bone most appropriate for histological analysis.

REFERENCES

Abbott S, Trinkaus E, Burr D. Dynamic bone remodeling in Later Pleistocene fossil hominids. Am J Phys Anthropol 99:585-601.

Agarwal SC. 2008. Light and broken bones: examining and interpreting bone loss and osteoporosis in past populations. In: Katzenberg MA, Saunders SR, editors. Biological anthropology of the human skeleton, 2nd edition. Hoboken, New Jersey: John Wiley & Sons, Inc. p 387-410.

Agnew AM, Stout SD. 2012. Brief communication: reevaluating osteoporosis in human ribs: the role of intracortical porosity. Am J Phys Anthropol 148:462-466.

Ahlqvist J, Damsten O. 1969. A modification of Kerley's method for the microscopic determination of age in human bone. J Forensic Sci 14:205-213.

Alfredson H, Nordstrom P, Lorentzon R. 1996. Total and regional bone mass in female soccer players. Calcif Tissue Int 59:438-442.

Alfredson H, Nordstrom P, Lorentzon R. 1997. Bone mass in female volleyball players: a comparison of total and regional bone mass in female volleyball players and nonactive females. Calcif Tissue Int 60:338-342.

Alfredson H, Nordstrom P, Pietila T, Lorentzon R. 1998. Long-term loading and regional bone mass of the arm in female volleyball players. Calcif Tissue Int 62:303-308.

Ammann P, Bourrin S, Bonjour JP, Meyer JM, Rizzoli R. 2000. Protein undernutrition-induced bone loss is associated with decreased IGF-I levels and estrogen deficiency. J Bone Miner Res 15:683–690.

Ammann P, Laib A, Bonjour J-P, Meyer JM, Ruegsegger P, Rizzoli R. 2002. Dietary essential amino acid supplements increase bone strength by influencing bone mass and bone microstructure in ovariectomized adult rats fed an isocaloric low-protein diet. J Bone Miner Res 17:1264-1272.

Anderson JJB. 1999. Nutritional mechanisms of age-related bone loss. In: Rosen C, Glowacki J, Bilezikian JP, editors. The aging skeleton. San Diego: Academic Press. p 229-234.

Andriušis A. 2006. Lietuvos medicinos istorijos apybraiža: mokomoji knyga. Vilnius, Lithuania: Vilniaus universiteto leidykla.

Ariès P. 1962. Centuries of childhood: a social history of family life. Translated by R. Baldick. New York: Vintage Books.

Armelagos GJ, Mielke JH, Owen KH, Van Gerven DP. 1972. Bone growth and development in prehistoric populations from Sudanese Nubia. J Hum Evol 1:89-119.

Ashizawa N, Nonaka K, Michikami S, Mizuki T, Amagai H, Tokuyama K, Suzuki M. 1999. Tomographical description of tennis-loaded radius: reciprocal relation between bone size and volumetric BMD. J Appl Physiol 86:1347-1351.

Auerbach BM, Ruff CB. 2006. Limb bone bilateral asymmetry: variability and commonality among modern humans. J Hum Evol 50:203-218.

Auerbach BM, Sylvester AD. 2011. Allometry and apparent paradoxes in human limb proportions: implications for scaling factors. Am J Phys Anthropol 144:382–391.

Bailey DA, Faulkner RA, McKay HA. 1996. Growth, physical activity, and bone mineral acquisition. Exerc Sport Sci Rev 24:233-266.

Bailey DA, McKay HA, Mirwald RL, Crocker PR, Faulkner RA. 1999. A six-year longitudinal study of the relationship of physical activity to bone mineral accrual in growing children: the university of Saskatchewan bone mineral accrual study. J Bone Miner Res 14:1672–1679.

Baker D, Roberts R, Towell T. 2000. Factors predictive of bone mineral density in eating-disordered women: a longitudinal study. Int J Eat Disorder 27:29–35.

Baldwin KM, White TP, Arnaud SB, Edgerton VR, Kraemer WJ, Kram R, Raab-Cullen D, Snow CM. 1996. Musculoskeletal adaptations to weightlessness and development of effective countermeasures. Med Sci Sport Exer 28:1247–1253.

Balena R, Shih M-S, Parfitt AM. 1992. Bone resorption and formation on the periosteal envelope of the ilium: a histomorphometric study in healthy women. J Bone Miner Res 7:1475-1482.

Baliulis A. 2009. Lietuvos metrika, 593. Vilnius, Lithuania: Lietuvos istorijos instituto leidykla.

Baliulis A, Meilus E. 2001. Lietuvos Didžiosios Kunigaikštystės kasdienis gyvenimas. Vilnius, Lithuania: Vilniaus Dailės Akademijos leidykla.

Baronas D, Dubonis A, Petrauskas R. 2011. Lietuvos istorija, t. 3. XIII a. 1385m. Vilnius, Lithuania: Valstybes iškilimas tarp Rytu ir Vakaru.

Barth RW, Williams JL, Kaplan FS. 1992. Osteon morphometry in females with femoral neck fractures. Clin Orthop 283:178–186.

Bass SL, Pearce G, Bradney M, Hendrich E, Delmas PD, Harding A, Seeman E. 1998. Exercise before puberty may confer residual benefits in bone density in adulthood: studies in active prepubertal and retired female gymnasts. J Bone Miner Res 13:500-507.

Bass SL, Delmas PD, Pearce G, Hendrich E, Tabensky A, Seeman E. 1999. The differing tempo of growth in bone size, mass, and density in girls is region-specific. J Clin Invest 104:795–804.

Bass SL, Saxon L, Daly RM, Turner CH, Robling AG, Seeman E, Stuckey S. 2002. The effect of mechanical loading on the size and shape of bone in pre-, peri-, and postpubertal girls: a study in tennis players. J Bone Miner Res 17:2274-2280.

Bass SL, Eser P, Daly R. 2005. The effect of exercise and nutrition on the mechanostat. J Musculoskel Neuronal Interact 5:239-254.

Bassett JHG, Nordström K, Boyde A, Howell PGT, Kelly S, Vennström B, Williams GR. 2007. Thyroid status during skeletal development determines adult bone structure and mineralization. Mol Endocrinol 21:1893-1904.

Bell KL, Loveridge N, Power J, Garrahan N, Stanton M, Lunt M, Meggitt BF, Reeve J. 1999a. Structure of the femoral neck in hip fracture: cortical bone loss in the inferoanterior to superoposterior axis. J Bone Miner Res 14:111–119.

Bell KL, Loveridge N, Power J, Rushton N, Reeve J. 1999b. Intracapsular hip fracture: increased cortical remodeling in the thinned and porous anterior region of the femoral neck. Osteoporosis Int 10:248–257.

Bennike P, Lewis ME, Schutkowski H, Valentin F. 2005. Comparison of child morbidity in two contrasting medieval cemeteries from Denmark. Am J Phys Anthropol 128:734-746.

Beresnevičius G. 2008. Lietuvių religija ir mitologija. Vilnius, Lithuania: Tyto Alba.

Bertelsen PK, Clement JG, Thomas CD. 1995. A morphometric study of the cortex of the human femur from early childhood to advanced old age. Forensic Sci Int 74:63-77.

Bertram JE, Biewener AA. 1988. Bone curvature: sacrificing strength for load predictability? J Theor Biol 131:75-92.

Bertram JE, Swartz SM. 1991. The “law of bone transformation”: a case of crying Wolff? Biol Rev Cambridge Philosophic Soc 66:245-273.

Bianchi ML. 2007. Osteoporosis in children and adolescents. Bone 41:486-495.

Biewener AA. 1983. Locomotor stresses in the limb bones of two small mammals: the ground squirrel and chipmunk. J Exp Biol 103:135-154.

Biewener AA, Bertram JEA. 1994. Structural response of growing bone to exercise and disuse. J Appl Physiol 76:946-955.

Biewener AA, Swartz SM, Bertram JE. 1986. Bone modeling during growth: dynamic strain equilibrium in the chick tibiotarsus. Calcif Tissue Int 39:390-395.

Binns CW. 1998. Infant-feeding and growth. In: Ulijaszek S, Johnston FE, Preece MA, editors. The Cambridge encyclopedia of human growth and development. Cambridge, UK: Cambridge University Press. p 320-325.

Bird DW, Bliege Bird R. 2000. The ethnoarchaeology of juvenile foragers: shellfishing strategies among Meriam children. J Anthropol Archaeol 19:461-476.

Bird DW, Bliege Bird R. 2002. Children on the reef: slow learning or strategic foraging? Human Nature 13:269-297.

Bird DW, Bliege Bird R. 2005. Martu children's hunting strategies in the western desert, Australia. In: Hewlett BS, Lamb ME, editors. Hunter-gatherer childhoods: evolutionary, developmental and cultural perspectives. New Brunswick: Transaction Publishers. p 129-146.

Bird-David N. 2005. Studying children in hunter-gatherer societies: reflections from a Nayaka perspective. In: Hewlett BS, Lamb ME, editors. Hunter-gatherer childhoods: evolutionary, developmental and cultural perspectives. New Brunswick: Transaction Publishers. p 92-102.

Blakey ML, Armelagos GJ. 1985. Deciduous enamel defects in prehistoric Americans from Dickson Mounds: prenatal and postnatal stress. Am J Phys Anthropol 66:371-380.

Block JE, Friedlander AL, Brooks GA, Steiger P, Stubbs HA, Genant HK. 1989. Determinants of bone density among athletes engaged in weight-bearing and non-weight bearing activity. J Appl Physiol 67:1100-1105.

Blom DE, Buikstra JE, Keng L, Tomczak PD, Shoreman E, Stevens-Tuttle D. 2005. Anemia and childhood mortality: latitudinal patterning along the coast of pre-Columbian Peru. Am J Phys Anthropol 127:152-169.

Blurton Jones N, Marlowe FR. 2002. Selection for delayed maturity: does it take 20 years to learn to hunt and gather? Human Nature 13:199-238.

Bock J. 2005. What makes a competent adult forager? In: Hewlett BS, Lamb ME, editors. Hunter-gatherer childhoods: evolutionary, developmental and cultural perspectives. New Brunswick: Transaction Publishers. p 109-128.

Bogin B. Evolutionary hypotheses for human childhood. Yearb Phys Anthropol 40:63-89.

Boivin GY, Chavassieux PM, Santora AC, Yates J, Meunier PJ. 2000. Alendronate increases bone strength by increasing the mean degree of mineralization of bone tissue in osteoporotic women. Bone 27:687-694.

Bolotin HH. 2011. Bone loss without the loss of bone mineral material? A new perspective on anorexia nervosa. Bone 44:1034-1042.

Bonjour JP, Rizzoli R. 1996. Bone acquisition in adolescence. In: Marcus R, Feldman D, editors. Osteoporosis. San Diego: Academic Press. p 465-476.

Bonjour JP, Theintz G, Law F, Slosman D, Rizzoli R. 1994. Peak bone mass. Osteoporosis Int 4:7-13.

Bourne GH. 1942. The effect of graded doses of vitamin C upon the generation of bone in guinea-pigs on a scorbutic diet. J Physiol 101:327-336.

Bourrin S, Ammann P, Bonjour JP, Rizzoli R. 2000. Dietary protein restriction lowers plasma insulin-like growth factor I (IGF-I), impairs cortical bone formation, and induces osteoblastic resistance to IGF-I in adult female rats. Endocrinology 141:3149-3155.

Bousson V, Bergot C, Meunier A, Barbot F, Parlier-Cuau C, Laval-Jeantet AM. 2000. CT of the middiaphyseal femur: cortical bone mineral density and relation to porosity. Radiology 217:179-187.

Bousson V, Meunier A, Bergot C, Vicaut E, Rocha MA, Morais MH, Laval-Jeantet AM, Laredo JD. 2001. Distribution of intracortical porosity in human midfemoral cortex by age and gender. J Bone Miner Res 16:1308-1317.

Bouvier M, Hylander WL. 1981. Effect of bone strain on cortical bone structure in macaques (*Macaca mullatta*). J Morphol 167:1-12.

Bouxsein ML. 2001. Biomechanics of age-related fractures. In: Marcus R, Feldman D, Kelsey J, editors. Osteoporosis. New York: Academic Press. p 509-531.

Bradley C. 1984. Sexual division of labor and the value of children. Behav Sci Res 19:159-185.

Bradley C. 1993. Women's power, children's labor. Cross-cult Res 27:70-96.

Brand MD. 1997. Regulation analysis of energy metabolism. J Exper Biol 200:193-202.

Bredella MA, Misra M, Miller KK, Madisch I, Sarwar A, Cheung A, Klibanski A, Gupta R. 2008. Distal radius in adolescent girls with anorexia nervosa: trabecular structure analysis with high resolution flat-panel volume CT. Radiology 249:938–946.

Bredella MA, Fazeli PK, Miller KK, Misra M, Torriani M, Thomas BJ, Ghomi RH, Rosen CJ, Klibanski A. 2009. Increased bone marrow fat in anorexia nervosa. J Clin Endocrinol Metab 94:2129-2136.

Brenton BP, Paine RR. 2007. Reevaluating the health and nutritional status of maize-dependent populations: evidence for the impact of pellagra on human skeletons from South Africa. Ecol Food Nutr 46:345-360.

Brickley M, Agarwal SC. 2003. Techniques for the investigation of age-related bone loss and osteoporosis in archaeological bone. In: Agarwal SC, Stout SD, editors. Bone loss and osteoporosis: an anthropological perspective. New York: Kluwer Academic Press. p 157–172.

Brickley M, Ives R. 2006. Skeletal manifestations of infantile scurvy. Am J Phys Anthropol 129:163-172.

Brickley M, Ives R. 2008. The bioarchaeology of metabolic bone disease. San Diego: Elsevier.

Bridges PS. 1989. Bone cortical area in the evaluation of nutrition and activity levels. Am J Hum Biol 1:785-792.

Bridges PS. 1991. Skeletal evidence of changes in subsistence activities between the Archaic and Mississippian time periods in northwestern Alabama. In: Powell ML, Bridges PS, Mires AMW, editors. What mean these bones? Studies in Southeastern bioarchaeology. Tuscaloosa: Alabama University Press. p 89–101.

Bridges PS, Blitz J, Solano MC. 2000. Changes in long bone diaphyseal strength with horticultural intensification in west-central Illinois. Am J Phys Anthropol 112:217-238.

Burger EH, Klein Nulend J. Mechanotransduction in bone: role of the lacunocanalicular network. FASEB J 13:S101-S112.

Burghardt AJ, Kazakia GJ, Ramachandran S, Link TM, Majumdar S. 2010. Age- and gender-related differences in the geometric properties and biomechanical significance of intracortical porosity in the distal radius and tibia. J Bone Miner Res 25:983-993.

Burr DB. 1992. Orthopedic principles of skeletal growth, modeling and remodeling. In: Carlson DS, Goldstein SA, editors. Bone biodynamics in orthodontic and orthopedic treatment. Ann Arbor: University of Michigan Press. p 15–50.

Burr DB. 2002. Targeted and nontargeted remodeling. Bone 30:2-4.

Burr D, Martin RB. 1989. Errors in bone remodeling: toward a unified theory of metabolic bone disease. Am J Anat 186:186-216.

Burr DB, Martin RB, Schaffler MB, Radin EL. 1985. Bone remodeling in response to in vivo fatigue microdamage. J Biomech 18:189–200.

Burr DB, Ruff CB, Thompson DD. 1990. Patterns of skeletal histological change through time: comparison of an archaic Native American population with modern population. Anat Rec 226:307–313.

Burr DB, Forwood MR, Fyhrie DP, Martin RB, Schaffler MB, Turner CH. 1997. Bone microdamage and skeletal fragility in osteoporotic and stress fractures. J Bone Miner Res 12:6-15.

Burr DB, Robling AG, Turner CH. 2002. Effects of biomechanical stress on bones in animals. Bone 30:781-786.

Buzon MR. 2006. Health of the non-elites at Tombos: nutritional and disease stress in New Kingdom Nubia. Am J Phys Anthropol 130:26-37.

Cabin RJ, Mitchell RJ. 2000. To Bonferroni or not to Bonferroni: when and how are the questions. Bulletin of the Ecological Society of America 81:246-248.

Cain M. 1977. The economic activities of children in a village in Bangladesh. Popul Dev Rev 3: 201-227.

Cameron N, Demerath EW. 2002. Critical periods in human growth and their relationship to diseases of aging. Yearb Phys Anthropol 45:159-184.

Carter DR. 1984. Mechanical loading histories and cortical bone remodeling. Calcif Tissue Int 36:19-24.

Carter DR. 1987. Mechanical loading history and skeletal biology. J Biomech 20:1095–1109.

Carter DR, Beaupre G. 2001. Skeletal function and form: mechanobiology of skeletal development, aging, and regeneration. New York: Cambridge University Press.

Carter DR, Hayes WC. 1977a. The compressive behavior of bone as a two phase porous structure. J Bone Joint Surg 59A: 954-967.

Carter DR, Hayes WC. 1977b. Compact bone fatigue damage. I: residual strength and stiffness. J Biomech 10:325-337.

Carter DR, Hayes WC, Schurman DJ. 1976. Fatigue life of compact bone. II: effects of microstructure and density. J Biomech 9:211-218.

Carter DR, Smith DJ, Spengler DM, Daly CH, Frankel VH. 1980. Measurement and analysis of in vivo bone strains on the canine radius and ulna. J Biomech 13:27–38.

Carter DR, van der Meulen MC, Beaupre GS. 1996. Skeletal development: mechanical consequences of growth, aging, and disease. In: Marcus R, Feldmen D, Kelsey J, editors. Osteoporosis. San Diego: Academic Press. p 333-350.

Casazza K, Hanks LJ, Hidalgo B, Hu HH, Affuso O. 2012. Short-term physical activity intervention decreases femoral bone marrow adipose tissue in young children: a pilot study. Bone 50:23-27.

Chan A, Crowder C, Rogers T. 2007. Variation in cortical bone histology within the human femur and its impact on estimating age at death. Am J Phys Anthropol 132:80-88.

Cho H, Stout SD. 2001. Age-associated bone loss in an Imperial Roman population. Am J Phys Anthropol 32:49-50.

Christiansen P. 2001. The skeleton in primary hyperparathyroidism: a review focusing on bone remodeling, structure, mass, and fracture. APMIS Suppl 102:1-52.

Chiu J-F, Lan S-J, Yang C-Y, Wang P-W, Yao W-J, Su I-H, Hsieh C-C. 1997. Long-term vegetarian diet and bone mineral density in postmenopausal Taiwanese women. Calcif Tissue Int 60:245–249.

Churchill SE. 1994. Human upper body evolution in the Eurasian Late Pleistocene. Ph.D. dissertation. University of New Mexico, Albuquerque.

Clark EM, Ness AR, Tobias JH. 2008. Bone fragility contributes to the risk of fracture in children, even after moderate and severe trauma. J Bone Miner Res 23:173-179.

Clark NG, Sheard NF, Kelleher JF. 1992. Treatment of iron-deficiency anemia complicated by scurvy and folic acid deficiency. Nutr Rev 50:134-137.

Cohen MN. 1989. Health and the rise of civilization. New Haven: Yale University Press

Cook DC. 1979. Subsistence base and health in prehistoric Illinois Valley: evidence from the human skeleton. Med Anthropol 4:109-124.

Cook DC. 1984. Subsistence and health in the lower Illinois valley: osteological evidence. In: Cohen M, Armelagos G, editors. Paleopathology at the origins of agriculture. New York: Academic Press. p 237-269.

Cooper C, Westlake S, Harvey N, Javaid K, Dennison E, Hanson M. 2006. Review: developmental origins of osteoporotic fracture. Osteoporosis Int 17:337–347.

Cooper DM, Thomas CD, Clement JG, Hallgrimsson B. Three-dimensional microcomputed tomography imaging of basic multicellular unit-related resorption spaces in human cortical bone. Anat Rec A 288:806-816.

Cormier JM, Stitzel JD, Duma SM, Matsuoka F. 2005. Regional variation in the structural response and geometrical properties of human ribs. Proceedings of Association for the Advancement of Automotive Medicine 9:153–170.

Cowgill LW. 2006. Postcranial growth and development of immature skeletons from Point Hope, Alaska. Am J Phys Anthropol 129 (S42):78.

Cowgill LW. 2008. The ontogeny of recent and Late Pleistocene human postcranial robusticity. Ph.D. dissertation. Washington University, St. Louis.

Cowgill LW. 2010 The ontology of Holocene and Late Pleistocene human postcranial strength. Am J Phys Anthropol 141:16-37.

Cowgill LW, Hager LD. 2007. Variation in the development of postcranial robusticity: an example from Çatalhöyük, Turkey. Int J Osteoarchaeol 17:235-252.

Cowgill LW, Warrener A, Pontzer H, Ocobock C. 2010. Waddling and toddling: the biomechanical effects of an immature gait. Am J Phys Anthropol 143:52-61.

Cowin SC. 2001a. The false premise in Wolff's law. In: Cowin SC, editor. Bone biomechanics handbook. Boca Raton: CRC Press. p 30-32.

Cowin SC. 2001b. Handbook of bone mechanics. Raton, FL: CRC Press.

Cowin SC, Moss-Salentijn L, Moss ML. 1991. Candidate for the mechanosensory system in bone. J Biomech Eng 113:191-197.

Crowder C. 2013. Estimation of age at death using cortical bone histomorphometry. U.S. Department of Justice, National Institute of Justice.

Crowder C, Heinrich J, Stout SD. 2012. Rib histomorphometry for adult age estimation. In: Bell LS, editor. Forensic microscopy for skeletal tissues: methods and protocols. New York: Springer. p 109-127.

Currey JD. 1964. Some effects of aging in human Haversian systems. J Anat 98:69-75.

Currey JD. 1984. The mechanical adaptations of bones. Princeton: Princeton University Press.

Currey JD. 1988. The effect of porosity and mineral content on the Young's modulus of elasticity of compact bone. J Biomech 2:131–139.

Currey JD. 2002. Bones: structure and mechanics. Princeton: Princeton University Press.

Currey JD. 2003. How well are bones designed to resist fracture? J Bone Miner Res 18:591-598.

Dabernat H, Crubézy E. 2010. Multiple bone tuberculosis in a child from predynastic Upper Egypt (3200 BC). Int J Osteoarchaeol 20:719-730.

Daly RM. 2007. The effect of exercise on bone mass and structural geometry during growth. In: Daly RM, Petit M, editors. Optimizing bone mass and strength: the role of physical activity and nutrition during growth. Med Sports Sci 51:33-49.

Daly RM, Bass SL. 2006. Lifetime sport and leisure activity participation is associated with greater bone size, quality and strength in older men. Osteoporosis Int 17:1258-1267.

Danforth ME. 1999. Nutrition and politics in prehistory. Annu Rev Anthropol 28:1-15.

Davison KS, Siminoski K, Adachi JD, Hanley DA, Goltzman D, Hodsman AB, Josse R, Kaiser S, Olszyanski WP, Papaioannou A, Ste-Marie L-G, Kendler DL, Tenenhouse A, Brown JP. 2006. Bone strength: the whole is greater than the sum of its parts. Semin Arthritis Rheum 36:22–31.

de Boer WF, Blijdenstein AF, Longamane F. 2000. Between the tides: the impact of human exploitation on an intertidal ecosystem, Mozambique. Ph.D. Dissertation. Rijksuniversiteit te Groningen.

Demirjian A. 1978. Dentition. In: Falkner F, Tanner JM, editors. Human growth, Vol. II, Postnatal growth. New York: Plenum Press. p 413–444.

DeVista AD, Beck TJ, Petit MA, Feldman HA, LeBoff MS, Gordon CM. 2007. Bone cross-sectional geometry in adolescents and young women with anorexia nervosa: a hip structural analysis study. Osteoporosis Int 18:797-804.

Devlin MJ, Cloutier AM, Thomas NA, Panus DA, Lotinun S, Pinz I, Baron R, Rosen CJ, Bouxsein ML. 2010. Caloric restriction leads to high marrow adiposity and low bone mass in growing mice. J Bone Miner Res 25:2078-2088.

Dickerson JWT, McCance RA. 1961. Severe undernutrition in growing and adult animals: the dimensions and chemistry of the long bones. Brit J Nutr 15:567-576.

Dong XN, Guo XE. 2004. The dependence of transversely isotropic elasticity of human femoral cortical bone on porosity. J Biomech 37:1281:1287.

Doppler S, Neuberger FM, Grupe G. 2006. Histomorphology of archaeological human compact bone: a neglected methodological approach. In: Grupe G, Peters J, editors. Documenta archaeobiologiae 4. Microscopic examinations of bioarchaeological remains: keeping a close eye on ancient tissues. Rahden/Westfahlen:Verlag. p 29-48.

Drapeau MSM, Streeter MA. 2006. Modeling and remodeling responses to normal loading in the human lower limb. Am J Phys Anthropol 129:403-409.

Dubonis A. 1996. Lietuvos didžiojo kunigaikščio leičiai XIII–XVI a.: lietuvių ankstyvojo feodalizmo visuomenės tyrimas. Daktaro disertacijos tezės (Humanitarinių mokslų sritis, istorijos kryptis). PhD dissertation. Vilnius University.

Dudar JC. 1993. Identification of rib number and assessment of intercostal variation at the sternal rib end. J Forensic Sci 38:788-797.

Dunnigan MG, Henderson JB. 1997. An epidemiological model of privational rickets and osteomalacia. Proc Nutr Soc 56:939-956.

Dupras TL, Pfeiffer. 1996. Determination of sex from adult human ribs. Can Soc Forensic Sci J 29:221-231.

Dyson K, Blimkie CJ, Davison KS, Webber CE, Adachi JD. 1997. Gymnastic training and bone density in pre-adolescent females. Med Sci Sports Exerc 29:443-450.

Enlow DH. 1963. Principles of bone remodeling. Springfield, IL: Charles C. Thomas.

Epker BN, Frost HM. 1966. Periosteal appositional bone growth from age two to age seventy in man, a tetracycline evaluation. Anat Rec 154:573-577.

Erben RG. 1996. Trabecular and endocortical bone surfaces in the rat: modeling or remodeling. Anat Rec 246:39-46.

Ericksen M. 1980. Patterns of microscopic bone remodeling in three aboriginal American populations. In: Browman D, editor. Early Native Americans: prehistoric demography, economy, and technology. The Hague: Mouton Publishers. p 239-270.

Erickson GM, Catanese J, Keaveny TM. 2002. Evolution of the biomechanical material properties of the femur. Anat Rec 268:115–124.

Evans FG, Bang S. 1967. Differences and relationships between the physical properties and microscopic structure of human femoral, tibial, and fibular cortical bone. Am J Anat 120:79-88.

Eveleth PB, Tanner JM. 1990. Worldwide variation in human growth. Cambridge: Cambridge University Press.

Faerman M, Jankauskas R, Gorski A, Bercovier H, Greenblatt CL. 1999. Detecting Mycobacterium tuberculosis DNA in medieval skeletal remains from Lithuania. In: Palfi GY, Dutour O, Deak J, Kutas I, editors. Tuberculosis: past and present. Budapest, Szeged: Golden Book and Tuberculosis Foundation. p 371-376.

Fain O. 2005. Musculoskeletal manifestations of scurvy. Joint Bone Spine 72:124-128.

Fazekas IG, Kósa F. 1978. Forensic fetal osteology. Budapest: Akadémiai Kiadó.

Feik SA, Thomas CD, Clement JG. 1997. Age-related changes in cortical porosity of the midshaft of the human femur. J Anat 191:407-416.

Feja K, Saiman L. 2005. Tuberculosis in children. Clin Chest Med 26:295-312.

Fernándaz-Garcia D, Rodríguez M, García Alemán J, García-Almeida JM, Picón MJ, Fernández-Aranda F, Tinahones FJ. 2009. Thin healthy women have a similar bone mass to women with anorexia nervosa. Brit J Nutr 102:709-714.

Foote K, Marriott L. 2003. Weaning of infants. Arch Dis Childhood 88:488-492.

Forwood MR. 2008. Physical activity and bone development during childhood: insights from animal models. J Appl Physiol 105:334-341.

Forwood MR, Burr DB. 1993. Physical activity and bone mass: exercise in futility? Bone Miner 21:89-112.

Forwood MR, Turner CH. 1995. Skeletal adaptations to mechanical usage: results from tibial loading studies in rats. Bone 17:197S–205S.

Forwood MR, Baxter-Jones AD, Beck N, Mirwald RL, Howard A, Bailey DA. 2006. Physical activity and strength of the femoral neck during the adolescent growth spurt: a longitudinal analysis. Bone 38:576-583.

Fratzl-Zelman N, Roschger P, Misof BM, Nawrot-Wawrzyniak K, Potter-Lang S, Muschitz C, Resch H, Klaushofer K, Zwettler E. 2011. Fragility fractures in men with idiopathic osteoporosis are associated with undermineralization of the bone matrix without evidence of increased bone turnover. Calcif Tissue Int 88:378-387.

Frost HM. 1960. Presence of microscopic cracks in vivo in bone. Henry Ford Hospital Bulletin 8:25-35.

Frost HM. 1963. Bone remodeling dynamics. The Henry Ford Hospital surgical monographs. Springfield, IL: Charles C. Thomas.

Frost HM. 1964a. The laws of bone structure. The Henry Ford Hospital surgical monographs. Springfield, IL: Charles C. Thomas

Frost HM. 1964b. Mathematical elements of lamellar bone remodeling. The Henry Ford Hospital surgical monographs. Springfield, IL: Charles C. Thomas.

Frost HM. 1966. The bone dynamics in osteoporosis and osteomalacia. The Henry Ford Hospital surgical monographs. Springfield, IL: Charles C. Thomas.

Frost HM. 1969. Tetracycline-based histological analysis of bone remodeling. Calcif Tissue Res 3:211-237.

Frost HM. 1973. Bone: remodeling and its relationship to metabolic bone disease. Orthopaedic lectures Vol. 3. Springfield, IL: Charles C. Thomas.

Frost HM. 1987. Bone "mass" and the "mechanostat": a proposal. Anat Rec 219:1-9.

Frost, HM. 1988. Structural adaptations to mechanical usage: a proposed three-way rule for lamellar bone modeling. Vet Comp Orthop Traumatol 1:7-17.

Frost HM. 1990a. Skeletal structural adaptations to mechanical usage (SATMU): 1. Redefining Wolff's law: the bone modeling problem. Anat Rec 4:403-413.

Frost HM. 1990b. Skeletal structural adaptations to mechanical usage (SATMU): 2. Redefining Wolff's law: the remodeling problem. Anat Rec 4:414-422.

Frost HM. 1997. Perspectives on increased fractures during the human adolescent growth spurt: summary of a new vital-biomechanical explanation. J Bone Miner Metab 15:115–121.

Frost HM. 2003. Bone's mechanostat: a 2003 update. Anat Rec 275A:1081–1101.

Frost HM, Schönau E. 2000. The "muscle-bone unit" in children and adolescents: a 2000 overview. J Pediatr Endocrinol Metab 13:571-590.

Fuchs RK, Allen MR, Ruppel ME, Diab T, Phipps RJ, Miller LM, Burr DB. 2008. In situ examination of the time-course for secondary mineralization of Haversian bone using synchrotron Fourier transform infrared microspectroscopy. Matrix Biol 27:34-41.

Galusca B, Zouch M, Germain N, Bossu C, Frere D, Lang F, Lafage-Proust M-H, Thomas T, Vico L, Estour B. 2008. Constitutional thinness: unusual human phenotype of low bone quality. J Clin Endocrinol Metab 93:110-117.

Garn S. 1970. The earlier gain and later loss of cortical bone. Springfield, IL: Charles C. Thomas.

Garn S, Rohmann C, Behar M, Viteri F, Guzman M. 1964. Compact bone deficiency in protein calorie malnutrition. Science 145:1444-1445.

Garn S, Guzman M, Wagner B. 1969. Subperiosteal gain and endosteal loss in protein-calorie malnutrition. Am J Phys Anthropol 30:153-156.

Garofalo E. 2012. Environmental and genetic effects on growth of the human skeleton: a bioarchaeological investigation. PhD dissertation. Johns Hopkins University.

Glencross B, Stuart-Macadam P. 2000. Childhood trauma in the archaeological record. Int J Osteoarch 10:198-209.

Goldman HM, McFarlin SC, Cooper DLM, Thomas CDL, Clement JG. 2009. Ontogenetic patterning of cortical bone microstructure and geometry at the human mid-shaft femur. Anat Rec 292:48-64.

Goodman AH. 1991. Health, adaptation, and maladaptation in past societies. In: Bush H, Zvelebil M, editors. Health in past societies. London: BAR International Series. p 31-38.

Goodman AH, Armelagos GJ. 1988. Childhood stress and decreased longevity in a prehistoric population. Am Anthropol 90:936-944.

Goodman AH, Armelagos GJ. 1989. Infant and childhood morbidity and mortality risks in archaeological populations. World Arch 21:225-243.

Goodman AH, Martin DL. 2002. Reconstructing health profiles from skeletal remains. In: Steckel RH, Rose JC, editors. The backbone of history: health and nutrition in the western hemisphere. London: Cambridge University Press. p 11-59.

Goodman AH, Rose JC. 1990. Assessment of systemic physiological perturbations from dental enamel hypoplasias and associated histological structures. Yearb Phys Anthropol 33:59-110.

Goodman AH, Rose JC. 1991. Dental enamel hypoplasias as indicators of nutritional status. In: Kelley MA, Larsen CS, editors. Advances in dental anthropology. New York: Wiley-Liss. p 279-293.

Goodman AH, Martin D, Armelagos GJ, Clark G. 1984. Indications of stress from bone and teeth. In: Cohen MN, Armelagos GJ, editors. Paleopathology at the origins of agriculture. New York: Academic Press. p 13-49.

Goodman AH, Thomas R, Swedlund A, Armelagos G. 1988. Biocultural perspectives on stress in prehistoric, historical, and contemporary population research. Yearb Phys Anthropol 31:169-202.

Goodship AE, Cunningham JL. 2001. Pathophysiology of functional adaptation of bone in remodeling and repair *in vivo*. In: Cowin SC, editor. Bone biomechanics handbook. Boca Raton: CRC Press. p 26-31.

Gottlieb A. 2000. Where have all the babies gone?: toward an anthropology of infants (and their caretakers). Anthropol Quarterly 73:121-132.

Goulding A, Jones IE, Taylor RW, Manning PJ, Williams SM. 2000. More broken bones: a 4-year double cohort study of young girls with and without distal forearm fractures. J Bone Miner Res 15:2011–2018.

Goulding A, Jones IE, Taylor RW, Williams SM, Manning PJ. 2001. Bone mineral density and body composition in boys with distal forearm fractures: a dual-energy x-ray absorptiometry study. J Pediatr 139:509–515.

Granik G, Stein I. 1973. Human ribs: static testing as a promising medical application. J Biomech 6:237–240.

Grech P, Martin TJ, Barrington NA, Ell PJ. 1985. Diagnosis of metabolic bone disease. London: Chapman & Hall Medical.

Grewar D. 1965. Infantile scurvy. Clin Pediatr 4:82-89.

Grupe G, Peters J, editors. Documenta archaeobiologiae 4. Microscopic examinations of bioarchaeological remains: keeping a close eye on ancient tissues. Rahden/Westfahlen:Verlag.

Grynpas MD. 2003. The role of bone quality on bone loss and bone fragility. In: Agarwal SC, Stout SD, editors. Bone loss and osteoporosis: an anthropological perspective. New York: Kluwer Academic Press. p. 33-44.

Grynpas MD, Holmyard D. 1988. Changes in quality of bone mineral on aging and in disease. Scanning Microscopy 2:1045-1054.

Guadalupe-Grau A, Fuentes T, Guerra B, Calbet JA. 2009. Exercise and bone mass in adults. Sports Med 39:439-468.

Gudavičius E. 1989. Alytaus žemė. In: Leščinskienė D, editor. Alytaus miesto ir apylinkių istorijos bruožai: straipsnių rinkinys. Vilnius, Lithuania: Mokslas.

Gurven M, Kaplan H, Gutierrez M. 2006. How long does it take to become a proficient hunter? Implications for the evolution of extended development and long life span. J Hum Evol 51:454-470.

Haapasalo H, Sievanen H, Kannus P, Heinonen A, Oja P, Vuori I. 1996. Dimensions and estimated mechanical characteristics of the humerus after long-term tennis loading. J Bone Miner Res 11:864-872.

Haapasalo H, Kannus P, Sievänen H, Pasanen M, Uusi-Rasi K, Heinonen A, Oja P, Vuori I. 1998. Effect of long-term unilateral activity on bone mineral density of female junior tennis players. J Bone Miner Res 13:310–319.

Haapasalo H, Kontulainen S, Sievänen H, Kannus P, Järvinen M, Vouri I. 2000. Exercise induced bone gain is due to enlargement in bone size with a change in volumetric bone density: a peripheral quantitative computed tomography study of the upper arms of male tennis players. Bone 27:351-357.

Halcrow SE, Tayles N. 2008. The bioarchaeological investigation of childhood and social age: problems and prospects. J Archaeol Method Theory 15:190-215.

Halioua L, Anderson JJB. 1989. Lifetime calcium intake and physical activity habits: independent and combined effects on the radial bone of healthy premenopausal Caucasian women. Am J Clin Nutr 49:534-541.

Hall MC. 1965. The locomotor system: functional histology. The Henry Ford Hospital surgical monographs. Springfield, IL: Charles C. Thomas.

Hanson DB, Buikstra JE. 1987. Histomorphological alteration in buried human bone from the Lower Illinois Valley: implications for paleodietary research. J Archaeol Sci 14:594-563.

Harel Z, Gold M, Cromer B, Bruner A, Stager M, Bachrach L, Wolter K, Reid C, Hertweck P, Nelson A, Nelson D, Coupey S, Johnson C, Burkman R, Bone H. 2007. Bone mineral density in postmenarchal adolescent girls in the United States: associated biopsychosocial variables and bone turnover markers. J Adolesc Health 40:44–53.

Hatch JW, Eiley PS, Hunt EE. 1983. Indicators of status-related stress in Dallas society: transverse lines and cortical thickness in long bones. Midcontinental Journal of Archaeology 8:49-71.

Hattner R, Epker BN, Frost HM. 1965. Suggested sequential mode of control of changes in cell behavior in adult bone remodelling. Nature 206:489-490.

Hawkes K, O'Connell JF, Blurton Jones NG. 1995. Hadza children's foraging: juvenile dependency, social arrangements, and mobility among hunter-gatherers. Curr Anthropol 36:688-700.

Heaney RP. 1997. Vitamin D: role in the calcium economy. In: Feldman D, Glorieux F, Pike J, editors. Vitamin D. San Diego: Academic Press. p 485-497.

Heaney RP. 2000. Calcium, dairy products and osteoporosis. J Am Coll Nutr. 19:83S-99S.

Heinonen A, Oja P, Kannus P, Sievänen H, Mänttäri A, Vuori I. 1993. Bone mineral density of female athletes in different sports. Bone Miner 23:1-14.

Heinonen A, Kannus P, Sievänen H, Oja P, Pasanen P, Rinne M, Uusi-Rasi K, Vuori I. 1996. Randomized controlled trial of effect of high-impact exercise on selected risk factors of osteoporotic fractures. Lancet 348:1343-1347.

Heinonen A, Sievanen H, Kannus P, Oja P, Vuori I. 2002. Site-specific skeletal response to long-term weight training seems to be attributable to principal loading modality: a pQCT study of female weightlifters. Calcif Tissue Int 70:469–474.

Heinrich CH, Going SB, Pamenter RW, Perry CD, Boyden TW, Lohman TG. 1990. Bone mineral content of cyclically menstruating female resistance and endurance trained athletes Med Sci Sports Exerc 22*:* 558–563.

Henderson JH, Carter DR. 2002. Mechanical induction in limb morphogenesis: The role of growth-generated strains and pressures. Bone 31:645-653.

Hernandez CJ, Beaupre GS, Carter DR. 2003. A theoretical analysis of the relative influences of peak BMD, age-related bone loss and menopause on the development of osteoporosis. Osteoporosis Int 14:843–847.

Herring DA, Saunders SR, Katzenberg MA. 1998. Investigating the weaning process in past populations. Am J Phys Anthropol 105:425–439.

Hert J, Kucera P, Vavra M, Volenik V. 1965. Comparison of the mechanical properties of both the primary and Haversian bone tissue. Acta Anat 61:412-423.

Hewlett BS, Lamb ME, editors. 2005. Hunter-gatherer childhoods: evolutionary, developmental, and cultural perspectives. New Brunswick: Transaction Publishers.

Higgins RW, Ruff CB. 2011. The effects of distal limb segment shortening on locomotor efficiency in sloped terrain: implications for Neandertal locomotor behavior. Am J Phys Anthropol 146:336–345.

Hill K, Hurtado AM. 1996. Ache life history: the ecology and demography of a foraging people. New York: Aldine de Gruyter.

Hillson SW. 1992. Dental enamel growth, perikymata and hypoplasia in ancient tooth crowns. J Roy Soc Med 85:460-466.

Hillson SW. 2000. Dental pathology. In: Katzenberg MA, Saunders SR, editors. Biological anthropology of the human skeleton. New York: Wiley-Liss. p 249-286.

Hoc T, Henry L, Verdier M, Aubry D, Sedel L, Meunier A. 2006. Effect of microstructure on the mechanical properties of Haversian cortical bone. Bone 38:466-474.

Holland TD, O'Brien MJ. 1997. Porotic hyperostosis and the implications of changing perspectives. Am Antiquity 62:183-193.

Hoppa RD, Vaupel JW. 2002. Paleodemography: age distributions from skeletal samples. Cambridge: Cambridge University Press.

Hotta M, Shibasaki T, Sato K, Demura H. 1998. The importance of body weight history in the occurrence and recovery of osteoporosis in patients with anorexia nervosa: evaluation by dual X-ray absorptiometry and bone metabolic markers. Eur J Endocrinol 139:276–283.

Huiskes R. 1982. On the modeling of long bones in structural analysis. J Biomech 15:65-69.

Hummert JR. 1983 Cortical bone growth and dietary stress among subadults from Nubia's Batn El Hajar. Am J Phys Anthropol 62:167-176.

Hummert JR, Van Gerven DP. 1983. Skeletal growth in a medieval population from Sudanese Nubia. Am J Phys Anthropol 62:471-478.

Humphrey L. 2000. Interpretations of the growth of past populations. In: Derevenski JS, editor. Children and material culture. London: Routledge. p 193-205.

Huss-Ashmore R, Goodman A, Armelagos G. 1982. Nutritional inference from paleopathology. In: Schiffer M, editor. Advances in archaeological method and theory. New York: Academic Press. p 395-474.

Iorgi N, Rosol M, Mittelman SD, Gilsanz V. 2008. Reciprocal relation between marrow adiposity and the amount of bone in the axial and appendicular skeleton of young adults. J Clin Endocrinol Metab 93:2281-2286.

Iwaniec UT, Crenshaw TD, Schoeninger MJ, Stout SD, Ericksen MF. 1998. Methods for improving the efficiency of estimating total osteon density in the human anterior mid-diaphyseal femur. Am J Phys Anthropol 107:13-24.

Jankauskas R. 1994. Variability of vertebral column measurements in Lithuanian paleopopulation. Int J Anthropol 9:137-151.

Jankauskas R. 1998. History of human tuberculosis in Lithuania: possibilities and limitations of paleoosteological evidences. Bulletins et Mémoires de la Société d'anthropologie de Paris, Nouvelle Série 10:357-374.

Jankauskas R. 1999. Tuberculosis in Lithuania: paleopathological and historical correlations. In: Palfi GY, Dutour O, Deak J, Kutas I, editors. Tuberculosis: past and present. Budapest, Szeged: Golden Book and Tuberculosis Foundation. p 551-558.

Jankauskas R, Schultz M. 1999. Infant diseases in Eastern Europe during the Late Middle Ages and early modern times. Am J Phys Anthropol S28:160-161.

Jankauskas R, Urbanavičius A. 1998. Diseases in European historical populations and their effects on individuals and society. Collegium Antropologicum 22:465-476.

Jantz RL, Owsley DW. 1984. Long bone growth variation among Arikara skeletal populations. Am J Phys Anthropol 63:13-20.

Jee WSS, Li XJ. 1990. Adaptation of cancellous bone to overloading in the adult rat: a single photon absorptiometry and histomorphometry study. Anat Rec 227:418-426.

Jee WSS, Yao W. 2001. Overview: animal models of osteopenia and osteoporosis. J Musculoskel Neuron Interact 1:193-207.

Jelliffe DB. 1955. Infant feeding in the subtropics and tropics. Geneva: World Health Organization.

Johnson YJ, Kaneene JB, Gardiner JC, Lloyd JW, Sprecher DJ, Coe PH. 2001. The effect of subclinical Mycobacterium paratuberculosis infection on milk production in Michigan dairy cows. J Dairy Sci 84:2188-2194.

Jones D, Leivseth G, Tenbosch J. 1995. Mechano-reception in osteoblast-like cells. Biochem Cell Biol 73:525-534.

Jones HH, Priest JD, Hayes WC, Tichenor CC, Nagel DA. 1977. Humeral hypertrophy in response to exercise. J Bone Joint Surg 59:204-208.

Jowsey J. 1960. Age changes in human bone. Clin Orthop 17:210–217.

Jowsey J. 1966. Studies of Haversian systems in man and some animals. J Anat 100:857-864.

Jowsey J. 1968. Age and species differences in bone. Cornell Vet 56 (Suppl): 74-94.

Kalediene R, Petrauskiene J. 2000. Regional life expectancy patterns in Lithuania. Eur J Public Health 10:101-104.

Kamp KA. 2001. Where have all the children gone?: the archaeology of childhood. J Archaeol Method Theory 8:1-34.

Kannus P, Haapasalo H, Sankelo M, Sievänen H, Pasanen M, Heinonen A, Pekka O, Vuori I. 1995. Effect of starting age of physical activity on bone mass in the dominant arm of tennis and squash players. Ann Intern Med 123:27-31.

Kaplan H, Hill K, Lancaster J, Hurtado AM. 2000. A theory of human life history evolution: diet, intelligence, and longevity. Evol Anthropol 9:149-186.

Karlsson MK, Johnell O, Obrant KJ. 1993. Bone mineral density weight lifters. Calcif Tissue Int 52:212-215.

Katz JL. 1980. The structure and biomechanics of bone. In: Currey JD, Vincent JFV, editors. Mechanical properties of biological materials. Cambridge: Cambridge University Press. p 137–168.

Katzenberg MA, Herring DA, Saunders SR. 1996. Weaning and infant mortality: evaluating the skeletal evidence. Am J Phys Anthropol 101:177-199.

Keller TS, Mao Z, Spengler DM. 1990. Young's modulus, bending strength, and tissue physical properties of human compact bone. J Orthop Res 8:592-603.

Kemper AR, McNally C, Kennedy EA, Manoogian SJ, Rath AL, Ng TP, Stitzel JD, Smith EP, Duma SM. 2005. Material properties of human rib cortical bone from dynamic tension coupon testing. Stapp Car Crash Journal 49:199–230.

Kemper AR, McNally C, Pullins CA, Freeman LJ, Duma S. 2007. The biomechanics of human ribs: material and structural properties from dynamic tension and bending tests. Stapp Car Crash Journal 5:235–273.

Kerley ER. 1965. The microscopic determination of age in human bone. Am J Phys Anthropol 23:149-164.

Kerr D, Morton A, Dick I, Prince R. 1996. Exercise effects on bone mass in postmenopausal women are site-specific and load-dependent. J Bone Miner Res 11:218-225.

Kiaupa Z. 1989. XVI a. Alytus: miestelis ir miestas. In: Leščinskienė D, editor. Alytaus miesto ir apylinkių istorijos bruožai: straipsnių rinkinys. Vilnius, Lithuania: Mokslas. p 44.

King SE, Ulijaszek SJ. 2000. Invisible insults during growth and development: contemporary theories and past populations. In: Hoppa RD, FitzGerald CM, editors. Human growth in the past: studies from bones and teeth. Cambridge: Cambridge University Press. p 161-182.

Kipp DE, McElvain M, Kimmel DB, Akhter MP, Robinson RG, Lukert BP. 1996. Scurvy results in decreased collagen synthesis and bone density in the guinea pig animal model. Bone 18:281-288.

Klaus HD, Tam ME. 2009. Contact in the Andes: bioarchaeology of systemic stress in colonial Morrope, Peru. Am J Phys Anthropol 138:356-368.

Klein-Nulend J, Bakker AD, Bacabac RG, Vatsa A, Weinbaum S. 2013. Mechanosensation and transduction in osteocytes. Bone 54:182-190.

Klibanski A, Biller BMK, Schoenfeld DA, Herzog DB, Saxe VC. 1995. The effects of estrogen administration on trabecular bone loss in young women with anorexia nervosa. J Endocrinol Metab 80:898-904.

Konigsberg LW, Frankenberg SR. 1994. Paleodemography: "not quite dead." Evol Anthropol 3:92-105.

Kontulainen S, Kannus P, Haapasalo H, Heinonen A, Sievänen, H, Oja P, Vuori I. 1999. Changes in bone mineral content with decreased training in competitive young adult tennis players and controls: a prospective 4-year follow-up. Med Sci Sports Exerc 31:646–652.

Kontulainen S, Kannus P, Haapasalo H, Sievänen H, Pasanen M, Heinonen A, Oja P, Vuori I. 2001. Good maintenance of exercise-induced bone gain with decreased training of female tennis and squash players: a prospective 5-year follow-up study of young and old starters and controls. J Bone Miner Res 16:195-201.

Kontulainen S, Sievanen H, Kannus P, Pasanen M, Vuori I. 2002. Effect of long-term impact-loading on mass, size, and estimated strength of humerus and radius of female racquet sports players: a peripheral quantitative computed tomography study between young and old starters and controls. J Bone Miner Res 17:2281-2289.

Kooh SW, Noriega E, Leslie K, Müller C, Harrison JE. Bone mass and soft tissue composition in adolescents with anorexia nervosa. Bone 19:181-188.

Kotev-Emeth S, Savion N, Pri-chen S, Pitaru S. 2000. Effect of maturation on the osteogenic response of cultured stromal bone marrow cells to basic fibroblast growth factor. Bone 27:777-783.

Kozakaitė J. 2011. The analysis of long bone fractures and dislocations in 14^{th} – 17^{th} century Alytus, Lithuania. PhD dissertation. Durham University.

Kumar A, Mittal S, Orito S, Ishitani K, Ohta H. 2010. Impact of dietary intake, education, and physical activity on bone mineral density among North Indian women. J Bone Miner Metab 28:192-201.

Lambert J, Lamothe JM, Zernicke RF, Auer RN, Reimer RA. 2005. Dietary restriction does not adversely affect bone geometry and mechanics in rapidly growing male wistar rats. Pediatr Res 57:227-231.

Landeros O, Frost HM. 1964. The cross-sectional size of the osteon. Henry Ford Hosp Med Bull 12:517-525.

Lanyon LE. 1984. Functional strain as a determinant for bone remodeling. Calcif Tissue Int 36:S56-S61.

Lanyon LE, Baggott DG. 1976. Mechanical function as an influence on the structure and form of bone. J Bone Joint Surg 58B:436–443.

Lanyon LE, Rubin CT. 1984. Static versus dynamic loads as an influence on bone remodeling. J Biomech 17:897–905.

Larsen CS. 1995. Biological changes in human populations with agriculture. Annu Rev Anthropol 24:185-213.

Larsen CS. 1997. Bioarchaeology: interpreting behavior from the human skeleton. Cambridge: Cambridge University Press.

Larsen CS. 2003. Animal source foods and human health during evolution. J Nutr 133:3893S 3897S.

Larsen CS, Ruff CB. 1991. Biomechanical adaptation and behavior on the prehistoric Georgia Coast. In: Powell ML, Bridges PS, Mires AM, editors. What mean these bones? Studies in southeastern bioarchaeology. Tuscaloosa: University of Alabama Press. p 102-113.

Larsen CS, Schoeninger MJ, Hutchinson DL, Russell KF, Ruff CB. 1990. Beyond demographic collapse: biological adaptation and change in native populations of La Florida. In: Thomas DH, editor. Columbian consequences, vol. 2: archaeological and historical perspectives on the Spanish borderlands east. Washington: Smithsonian Institution Press. p 409-428.

Larsen CS, Ruff CB, Kelly RL. 1995. Structural analysis of the Stillwater postcranial human remains: behavioral implications of articular joint pathology and long bone diaphyseal morphology. In: Larsen CS, Kelly RL, editors. Bioarchaeology of the Stillwater marsh: prehistoric human adaptation in the western Great Basin. New York: American Museum of Natural History. p 107-133.

Lawson EA, Miller KK, Bredella MA, Phan C, Misra M, Meenaghan E, Rosenblum L, Donoho D, Gupta R, Klibanski A. 2010. Hormone predictors of abnormal bone microstructure in women with anorexia nervosa. Bone 46:458-463.

Lazenby R. 1986a. The interaction of bone porosity and cross-sectional geometry for the conservation of bone strength. M.A. Thesis. Simon Fraser University.

Lazenby R. 1986b. Porosity-geometry interaction in the conservation of bone strength. J Biomech 19:257-258.

Lazenby R. 1990a. Continuing periosteal apposition I: the significance of peak bone mass, strain equilibrium, and age-related activity differentials for mechanical compensation in human tubular bones. Am J Phys Anthropol 82:451-72.

Lazenby R. 1990b. Continuing periosteal apposition II: the significance of peak bone mass, strain equilibrium, and age-related activity differentials for mechanical compensation in human tubular bones. Am J Phys Anthropol 82:473-484.

Leblanc AD, Schneider VS, Evans HJ, Engelbretson DA, Krebs JM. 1990. Bone mineral loss and recovery after 17 weeks of bed rest. J Bone Miner Res 5:843-850.

LeBlanc AD, Schneider VS, Shackelford L, West S, Oganov V, Bakulin A, Voronin L. 2000. Bone mineral and lean tissue loss after long duration space flight. J Musculoskelet Neuronal Interact 1:157–160.

Legroux-Gerot I, Vignau J, D'Herbomez M, Collier F, Marchandise X, Duquesnoy B, Cortet B. 2007. Evaluation of bone loss and its mechanisms in anorexia nervosa. Calcif Tissue Int 81:174–182

Lewis M. 2007. The bioarchaeology of children: perspectives from biological and forensic anthropology. London: Cambridge University Press.

Lewis M, Roberts C. 1997. Growing pains: the interpretation of stress indicators. Int J Osteoarch 7:581–586.

Li XJ, Jee WSS. 1991. Adaptation of diaphyseal structure to aging and decreased mechanical loading in the adult rat: a densitometric and histomorphometric study. Anat Rec 229:291-297.

Li XJ, Jee WSS, Chow S-Y, Woodbury DM. 1990. Adaptation of cancellous bone to aging and immobilization in the rat: a single photon absorptiometry and histomorphometry study. Anat Rec 227:12-24.

Lieberman DE. 1997. Making behavioral and phylogenetic inferences from hominid fossils: considering the developmental influence of mechanical forces. Annu Rev Anthropol 26:185-210.

Lieberman DE, Crompton AW. 1998. Responses of bone to stress: constraints on symmorphosis. In: Webel ER, Taylor CR, Bolis L, editors. Principles of animal design: the optimization and symmorphosis debate. Cambridge: Cambridge University Press. p 78-86.

Lieberman DE, Pearson OM. 2001. Trade-off between modeling and remodeling responses to loading in the mammalian limb. Bull Mus Comp Zool 156:269-282.

Lieberman DE, Devlin M, Pearson O. 2001. Articular area responses to mechanical loading: effects of exercise, age, and skeletal location. Am J Phys Anthropol 116:266-277.

Lieberman DE, Pearson O, Polk J, Demes B, Crompton A. 2003. Optimization of bone growth and remodeling in response to loading in tapered mammalian limbs. J Exper Biol 206:3125-3138.

Lincoln EM, Sewell EM. 1963. Tuberculosis in children. New York: McGraw-Hill.

Maggiano CM. 2012. Histomorphometry of humeral primary bone: evaluating modeling drift in ancient and modern skeletal samples. Ph.D. dissertation. Ohio State University.

Maggiano IS, Schultz M, Kierdorf H, Sierra Sosa T, Maggiano CM, and Tiesler Blos V. 2008. Cross-sectional analysis of long bones, occupational activities and long-distance trade of the Classic Maya from Xcambo': archaeological and osteological evidence. Am J Phys Anthropol 136:470–477.

Mailhot G, Petit J-L, Dion N, Deschênes C, Ste-Marie L-G, Gascon-Barré M. 2007. Endocrine and bone consequences of cyclic nutritional changes in the calcium, phosphate and vitamin D status in the rat: an in vivo depletion-repletion-redepletion study. Bone 41:422-436.

Mankin H. 1974. Rickets, osteomalacia and renal osteodystrophy. Part I. J Bone Joint Surg Am 56A:101-128.

Marie P, Pettifor JM, Ross P, Glorieux FH. 1982. Histological osteomalacia due to dietary calcium deficiency in children. New Engl J Med 307:584-588.

Martin DL, Armelagos G. 1979. Morphometrics of compact bone: an example from Sudanese Nubia. Am J Phys Anthropol 51:571-577.

Martin DL, Armelagos G. 1985. Skeletal remodeling and mineralization as indicators of health: An example from prehistoric Sudanese Nubia. J Hum Evol 14:527-537.

Martin DL, Armelagos GJ, Goodman AH, Van Gerven D. 1984. The effects of socio-economic change in prehistoric Africa: Sudanese Nubia as a case study. In: Cohen MN, Armelagos GJ, editors. Paleopathology at the origins of agriculture. New York: Academic Press. p 93-213.

Martin DL, Goodman AH, Armelagos GJ. 1985. Skeletal pathologies as indicators of quality and quantity of diet. In: Gilbert RI, Mielke JH, editors. The analysis of prehistoric diets. Orlando: Academic Press. p 227-279.

Martin DL, Magennis AL, Rose JC. 1987. Cortical bone maintenance in an historic Afro-American cemetery sample from Cedar Grove, Arkansas. Am J Phys Anthropol 74:255-264.

Martin RB. 1993. Aging and strength of bone as a structural material. Calcif Tissue Int 53:S34-40.

Martin RB. 2000. Toward a unifying theory of bone remodeling. Bone 26:1-6.

Martin RB. 2004. Functional adaptation and fragility of the skeleton. In: Agarwal SC, Stout SD, editors. Bone loss and osteoporosis: an anthropological perspective. New York: Kluwer Academic Press. p 121–138.

Martin RB. 2007. Targeted bone remodeling involves BMU steering as well as activation. Bone 40:1574-1580.

Martin RB, Boardman DL. 1993. The effects of collagen fiber orientation, porosity, density, and mineralization on bovine cortical bone bending properties. J Biomech 26:1047-1054.

Martin RB, Burr DB. 1982. A hypothetical mechanism for the stimulation of osteonal remodeling by fatigue damage. J Biomech 15:137-139.

Martin RB, Burr DB. 1984. Mechanical implications of porosity distribution in bone of the appendicular skeleton. Orthopaedic Transactions 8:342–343.

Martin RB, Burr DB. 1989. Structure, function, and adaptation of compact bone. New York: Raven Press.

Martin RB, Ishida J. 1989. The relative effects of collagen fiber orientation, porosity, density, and mineralization on bone strength. J Biomech 22:419-426.

Martin RB, Pickett JC, Zinaich S. 1980. Studies of skeletal remodeling in aging men. Clin Orthop Relat Res 149:268 –282.

Martin RB, Burr D, Sharkey M. 1998. Skeletal tissue mechanics. New York: Springer-Verlag.

Martin TJ, Seeman E. 2008. Bone remodelling: its local regulation and the emergence of bone fragility. Best Pract Res Clin Endocrinol Metab 22:701-722.

Matkovic V, Fontana D, Tominac C, Goel P, Chesnut CH. 1990. Factors that influence peak bone mass formation: a study of calcium balance and the inheritance of bone mass in adolescent females. Am J Clin Nutr 52:878-888.

Mays S, Brickley M, Ives R. 2006. Skeletal manifestations of rickets in infants and young children in a historic population from England. Am J Phys Anthropol 129:362-374.

Mays S, Ives R, Brickley M. 2009. The effects of socioeconomic status on endochondral and appositional bone growth, and acquisition of cortical bone in children from 19th century Birmingham, England. Am J Phys Anthropol 140:410–416.

Mays S, Rogers J, Watt I. 2001. A possible case of hyperparathyroidism in a burial of 15th-17th century A.D .date from Wharram Percy, England. Am J Phys Anthropol 129:362-374.

McCalden RW, McGeough JA, Barker MB, Court-Brown CM. 1993. Age-related changes in the tensile properties of cortical bone: the relative importance of changes in porosity, mineralization, and microstructure. J Bone Joint Surg Am 75:1193-1205.

McCance RA, Dickerson JWT, Bell GH, Dunbar O, Gibb A. 1962. Severe undernutrition in growing and adult animals: the effect of undernutrition and its relief on the mechanical properties of bone. Brit J Nutr 16:1-12.

McCann P. 1962. The incidence and value of radiological signs of scurvy. Br J Radiol 35:683-686.

McCulloch RG, Bailey DA, Whalen RL, Houson CS, Faulkner RA, Craven BR. 1992. Bone density and bone mineral content of adolescent soccer athletes and competitive swimmers. Pediatr Exerc Sci 4:319-330.

Menkes A, Mazel S, Redmond RA, Koffler K, Libanati CR, Gundberg CM, Zizik TM, Hagsberg JM, Pratley RE, Hurley BF. 1993. Strength training increases regional bone mineral density and bone remodeling in middle-aged and older men. J Appl Physiol 74:2478-2484.

Mensforth RP. 1985. Relative tibia long bone growth in the Libben and Bt-5 prehistoric skeletal populations. Am J Phys Anthropol 68:247-262.

Mensforth RP, Lovejoy CO, Lallo JW, Armelagos GJ. 1978. The role of constitutional factors, diet and infectious disease in the etiology of porotic hyperostosis and periosteal reactions in prehistoric infants and children. Med Anthropol 2:1-59.

Metz LN, Martin RB, Turner AS. 2003. Histomorphometric analysis of the effects of osteocyte density on osteonal morphology and remodeling. Bone 33:753-759.

Meyer U, Romann M, Zahner L, Schindler C, Puder JJ, Kraenzlin M, Rizzoli R, Kreimler S. 2011. Effect of a general school-based physical activity intervention on bone mineral content and density: a cluster-randomized controlled trial. Bone 48:792–797.

Meyer U, Ernst D, Zahner L, Schindler C, Puder JJ, Kraenzlin M, Rizzoli R, Kreimler S. 2013. 3-year follow-up results of bone mineral content and density after a school-based physical activity randomized controlled trial. Bone 55:16-22.

Milos G, Spindler A, Rüegsegger P, Seifert B, Mühlebach S, Uebelhart D, Häuseelmann HJ. 2005. Cortical and trabecular bone density and structure in anorexia nervosa. Osteoporosis Int 16:783-790.

Miškinis A. 1989. Alytaus urbanistinės raidos bruožai. In: Leščinskienė D, editor. Alytaus miesto ir apylinkių istorijos bruožai: straipsnių rinkinys. Vilnius, Lithuania: Mokslas.

Moberg M. 1985. Household production and the value of children: a microeconomic approach to third world population trends. Anthropol UCLA 14:41-52.

Moran MD. 2003. Arguments for rejecting the sequential Bonferroni in ecological studies. Oikos 100:403-305.

Mori S, Burr DB. 1993. Increased intracortical remodeling following fatigue damage. Bone 14:103–109.

Mosekilde L. 2008. Primary hyperparathyroidism and the skeleton. Clin Endocrinol 69:1-19.

Mulhern DM, Ubelaker DH. 2003. Histologic examination of bone development in juvenile chimpanzees. Am J Phys Anthropol 122:127-133.

Munoz MT, Argente J. 2002. Anorexia nervosa in female adolescents: endocrine and bone mineral density disturbances. Eur J Endocrinol 147:275–286.

Nag M, White B, Peet RC. 1978. An anthropological approach to the study of the economic value of children in Java and Nepal. Curr Anthropol 19:293-306.

Nakagawa S. 2004. A farewell to Bonferroni: the problems of low statistical power and publication bias. Behav Ecol 15:1044-1045.

Navickas T. 1988. Alytus ir jo apylinkės. Chicago: Lithuanian Historical Society.

New S. 2003. Intake of fruit and vegetables: implications for bone health. Proc Nutr Soc 62:889-899.

Nickols-Richardson SM, Miller LE, Wootten DF, Ramp WK, Herbert WG. 2007. Concentric and eccentric isokinetic resistance training similarly increases muscular strength, fat-free soft tissue mass, and specific bone mineral measurements in young women. Osteoporosis Int 18: 789-796.

Nishida S, Endo N, Yamagiwa H, Tanizawa T, Takahashi H. 1999. Number of osteoprogenitor cells in human bone marrow markedly decrease after skeletal maturation. J Bone Miner Metab 17:171-177.

O'Neill MC, Ruff CB. 2004. Estimating human long bone cross-sectional geometric properties: a comparison of noninvasive methods. J Hum Evol 47:221-235.

Ortner D. 1991. Theoretical and methodological issues in paleopathology. In: Ortner D, Aufderheide AC, editors. Human paleopathology: current syntheses and future options. Washington, D.C.: Smithsonian Institution Press. p 5-11.

Ortner D. 2003. Identification of pathological conditions in human skeletal remains. San Diego: Elsevier.

Ortner D, Putschar WGJ. 1985. Identification of pathological conditions in human skeletal remains. Washington, D.C.: Smithsonian Institution Press.

Ortner D, Butler W, Cafarella J, Milligan L. 2001. Evidence of probably scurvy in subadults from archaeological sites in North America. Am J Phys Anthropol 114:343-351.

Ott SM, Lipkin EW, Newell-Morris L. 1999. Bone physiology during pregnancy and lactation in young macaques. J Bone Miner Res 14:1779–1788.

Paine RR, Brenton BP. 2006. Dietary health does affect histological age assessment: an evaluation of the Stout and Paine (1992) age estimation equation using secondary osteons from the rib. J Forensic Sci 51:1-4.

Paknys M. 2001. Mirtis. In: Ališauskas V, Jovaiša L, Paknys M, Petrauskas R, Raila E, editors. Lietuvos didžiosios kunigaikštijos kultūra: tyrinėjimai ir vaizdai. Vilnius, Lithuania: Aidai. p 365-377.

Pankovich AM, Simmons DJS, Kulkarni VV. 1974. Zonal osteons in cortical bone. Clin Orthop Relat Res 100:356-363.

Parfitt AM. 1983. The physiological and clinical significance of bone histomorphometric data. In: Recker RR, editor. Bone histomorphometry techniques and interpretation. Boca Raton: CRC Press. p 143-223.

Parfitt AM. 1984. Age-related structural changes in trabecular and cortical bone: cellular mechanisms and biomechanical consequences. Calcif Tissue Int 36:S123-S128.

Parfitt AM. 1986. Bone fragility in osteomalacia: mechanisms and consequences. In: Uhthoff H, Jaworski ZFG, editors. Current concepts of bone fragility. Berlin: Springer-Verlag. p 265–270.

Parfitt AM. 1998. Osteomalacia and related disorders. In: Aviolo LV, Krane SM, editors. Metabolic bone disease and clinically related disorders. San Diego: Academic Press. p 327-386.

Parfitt AM. 2002. High bone turnover is intrinsically harmful: two paths to a similar conclusion. J Bone Miner Res 17:1558-1559.

Parfitt AM. 2003. Renal bone disease: a new conceptual framework for the interpretation of bone histomorphometry. Curr Opin Nephrol Hypertens 12:387-403.

Pearson OM. 2000. Activity, climate, and postcranial robusticity: implications for modern human origins and scenarios of adaptive change. Curr Anthropol 41:569-607.

Pearson OM, Lieberman DE. 2004. The aging of Wolff's "law": ontogeny and responses to mechanical loading in cortical bone. Yearb Phys Anthropol 47:63-99.

Peck J, Stout SD. 2007. Intraskeletal variability in bone mass. Am J Phys Anthropol 132:89-97.

Pettersson U, Nordstrom P, Lorentzon R. 1999. A comparison of bone mineral density and muscle strength in young male adults with different exercise level. Calcif Tissue Int 64: 490-498.

Pettifor JM. 2003. Nutritional rickets. In: Gloriuex FH, Pettifor JM, Jüppner H, editors. Pediatric bone: biology and diseases. San Diego: Academic Press. p 541-565.

Pettifor JM. 2004. Nutritional rickets: deficiency of vitamin D, calcium, or both? Am J Clin Nutr 80: 1725S-1729S.

Pettifor JM, Daniels ED. 1997. Vitamin D deficiency and nutritional rickets in children. In: Feldman D, Glorieux F, Pike J, editors. Vitamin D. San Diego: Academic Press. p 663-679.

Pettifor JM, Marie PJ, Sly MR, du Bruyn DB, Ross F, Isdale JM, de Klerk WA, van der Walt WH. 1984. The effect of differing dietary calcium and phosphorus contents on mineral metabolism and bone histomorphometry in young vitamin D-replete baboons. Calcif Tissue Int 36:668-676.

Pfeiffer S. 1998. Variability in osteon size in recent human populations. Am J Phys Anthropol 106:219-227.

Pfeiffer S. 2006. Cortical bone histology in juveniles. In: Grupe G, Peters J, editors. Documenta archaeobiologiae 4. Microscopic examinations of bioarchaeological remains: keeping a close eye on ancient tissues. Rahden/Westfahlen: Verlag. p 15-28.

Pfeiffer S, King P. 1983. Cortical bone formation and diet among protohistoric Iroquoians. Am J Phys Anthropol 60:23-28.

Pfeiffer S, Lazenby RA. 1994. Low bone mass in past and present aboriginal populations. In: Draper HH, editor. Advances in nutritional research. Vol 9. New York: Plenum. p 35-51.

Pfeiffer S, Lazenby R, Chiang J. 1995. Brief communication: cortical remodeling data are affected by sampling location. Am J Phys Anthropol 96:89-92.

Pfeiffer S, Crowder C, Harrington L, Brown M. 2006. Secondary osteon and Haversian canal dimensions as behavioral indicators. Am J Phys Anthropol 131:460-468.

Pitt M. 1988. Rickets and osteomalacia. In: Resnick D, Niwayama G, editors. Diagnosis of bone and joint disorders. Vol 8, 2nd edition. Philadelphia: W.B. Daunders. p 2086-2119.

Pomeroy RS. 1987. The role of women and children in small scale fishing households: a case study in Matalom, Leyte, Philippines. Philipp Q Cult Soc 15:353-360.

Pontzer H, Raichlen DA, Sockol MD. 2009. The metabolic cost of walking in humans, chimpanzees, and early hominins. J Hum Evol 56:43-54.

Porter KA. 1996. The agency of children, work, and social change in the South Pare Mountains, Tanzania. Anthropol Work Rev 17:8-19.

Prais D, Diamond G, Kattan A, Salzberg J, Inbar D. 2008. The effect of calcium intake and physical activity on bone quantitative ultrasound measurements in children: a pilot study. J Bone Miner Metab 26:248–253.

Pratt CWM, McCance RA. 1961. Severe undernutrition in growing and adult animals: changes in the long bones during rehabilitation of cockerels. Brit J Nutr 15:121-129.

Prentice A, Parsons TA, Cole TJ. 1994. Uncritical use of bone mineral density in absorptiometry may lead to size-related artifacts in the identification of bone mineral determinants. Am J Clin Nutr 60:837-842.

Puntila E, Kroger H, Lakka T, Honkanen R, Tuppurainen M. 1997. Physical activity in adolescence and bone density in peri- and postmenopausal women. Bone 21:363-367.

Raab DM, Crenshaw TD, Kimmel DB, Smith EL. 1991. A histomorphometric study of cortical bone activity during increased weight-bearing exercise. J Bone Miner Res 6:741–749.

Ragauskienė R. 2004. Karališkojo Birštono praeitis: istorinė raida iki XIX a. Vilnius, Lithuania: UAB Petro ofsetas.

Raisz LG. 1999. Physiology and pathophysiology of bone remodeling. Clin Chem 45:1353-1358.

Raisz LG. 2005. Pathogenesis of osteoporosis: concepts, conflicts, and prospects. J Clin Invest 115:3318-3325.

Ratha SN, Mahakud NK. 1988. The Kisan children at work: data from a west Orissa village. Man India, Vol. I.

Rauch F, Schönau E. 2001. The developing bone: slave or master of its cells and molecules? Pediatr Res 50:309-314.

Reilly DT, Burstein AH. 1974. The mechanical properties of cortical bone. J Bone Joint Surg 56A:1001-1021.

Reilly DT, Burstein AH. 1975. The elastic and ultimate properties of compact bone tissue. J Biomech 8:393-405.

Reilly GC, Currey JD, Goodship AE. 1997. Exercise of young thoroughbred horses increases impact strength of the third metacarpal bone. J Orthop Res 15:862–868.

Richman E, Ortner D, Schulter-Ellis F. 1979. Differences in intracortical bone remodeling in three aboriginal American populations: possible dietary factors. Calcif Tissue Int 28:209-214.

Riggs BL, O'Fallon WM, Muhs J, O'Connor MK, Kumar R, Melton LJ. 1998. Long-term effects of calcium supplementation on serum parathyroid hormone level, bone turnover, and bone loss in elderly women. J Bone Miner Res 13:168-174.

Riggs CM, Vaughan LC, Evans GP, Lanyon LE, Boyde A. 1993. Mechanical implications of collagen fiber orientation in cortical bone of the equine radius. Anat Embryol (Berl) 187:239–248.

Ritzman TB, Baker BJ, Schwartz GT. 2008. A fine line: a comparison of methods for estimating ages of linear enamel hypoplasia formation. Am J Phys Anthropol 135:348-361.

Rizzoli R, Bonjour JP. 1999. Determinants of peak bone mass and mechanisms of bone loss. Osteoporosis Int 2:S17-S23

Rizzoli R, Bianchi ML, Garabédian M, McKay HA, Moreno LA. 2010. Maximizing bone mineral mass gain during growth for the prevention of fractures in the adolescents and the elderly. Bone 46:294-305.

Robling AG, Stout SD. 1999. Morphology of the drifting osteon. Cells Tissues Organs 164:192–204.

Robling AG, Stout SD. 2000. Methods of determining age at death using bone microstructure. In: Katzenberg MA, Saunders SR, editors. Biological anthropology of the human skeleton. New York: Wiley-Liss. p 187-205.

Robling AG, Stout SD. 2008. Histomorphometry of human cortical bone: applications to age estimation. In: Katzenberg MA, Saunders SR, editors. Biological anthropology of the human skeleton. New York: Wiley-Liss. p 149-171.

Robling AG, Burr DB, Turner CH. 2000. Partitioning a daily mechanical stimulus into discrete loading bouts improves the osteogenic response to loading. J Bone Miner Res 15:1596-1602.

Robling AG, Burr DB, Turner CH. 2001. Recovery periods restore mechanosensitivity to dynamically loaded bone. J Exp Biol 204:3389–3399.

Robling AG, Hinant F, Burr DB, Turner CH. 2002. Improved bone structure and strength after long-term mechanical loading is greatest if loading is separated into short bouts. J Bone Miner Res 17:1545–1554.

Robling AG, Castillo AB, Turner CH. 2006. Biomechanical and molecular regulation of bone remodeling. Annu Rev Biomed Eng 8:455-498.

Rosenbaum Chou TG, Child JR, Naughtin RJ, Rigdon RR, Schumann C, Bloebaum RD. 2008. The relationship between femoral periprosthetic cortical bone geometry and porosity after total hip arthoplasty. J Biomedic Mater Res A 87:107-115.

Ross DS. 1998. Bone disease in hyperparathyroidism. In: Aviolo LV, Krane SM, editors. Metabolic bone disease and clinically related disorders. 3rd edition. San Diego: Academic Press. p 531-544.

Rowell SC. 2001. Iš viduramžių ūkų kylanti Lietuva: pagonių imperija Rytų ir Vidurio Europoje, 1295-1345. Vilnius, Lithuania: Baltos lankos.

Rubin CT, Lanyon LE. 1982. Limb mechanics as a function of speed and gait: a study of functional strains in the radius and tibia of horse and dog. J Exp Biol 101:187-211.

Rubin CT, Lanyon LE. 1984a. Dynamic strain similarity in vertebrates: an alternative to allometric limb bone scaling. J Theor Biol 107:321-327.

Rubin CT, Lanyon LE. 1984b. Regulation of bone formation by applied dynamic loads. J Bone Joint Surg 66:367-402.

Rubin CT, Lanyon LE. 1985. Regulation of bone mass by mechanical strain magnitude. Calcif Tissue Int 37:411–417.

Rubin CT, Judex S, Hadjiargyrou M. 2002. Skeletal adaptation to mechanical stimuli in the absence of formation or resorption of bone. J Musculoskelet Neuronal Interact 2:264–267.

Ruff CB. 1987. Sexual dimorphism in human lower limb bone structure: relationship to subsistence strategy and sexual division of labor. J Hum Evol 5:391-416.

Ruff CB. 1988. Hindlimb articular surface allometry in *Hominoidea* and *Macaca*, with comparisons to diaphyseal scaling. J Hum Evol 17:687-714.

Ruff CB. 1991. Aging and osteoporosis in Native Americans from Pecos Pueblo, New Mexico: behavioral and biomechanical effects. New York: Garland Publishing.

Ruff CB. 1992. Biomechanical analyses of archaeological human skeletal samples. In: Saunders SR, Katzenberg MA, editors. The skeletal biology of past peoples: advances in research methods. New York: Wiley-Liss. p 37-58.

Ruff CB. 1994. Biomechanical analysis of northern and southern plains femora: behavioral implications. In: Owsley DW, Jantz RL, editors. Skeletal biology in the Great Plains: migration, warfare, health, and subsistence. Washington, D.C.: Smithsonian Institution Press. p 235-245.

Ruff CB. 1995. Biomechanics of the hip and birth in early *Homo.* Am J Phys Anthropol 98:527-574.

Ruff CB. 1999. Skeletal structure and behavioral patterns of prehistoric Great Basin populations. In: Hemphill BE, Larsen CS, editors. Prehistoric lifeways in the Great Basin wetlands: bioarchaeological reconstruction and interpretation. Salt Lake City: University of Utah Press. p 290-320.

Ruff CB. 2000. Body size, body shape, and long bone strength in modern humans. J Hum Evol 38:269-290.

Ruff CB. 2002. Long bone articular and diaphyseal structure in Old World monkeys and apes, I: locomotor effects. Am J Phys Anthropol 119:305-342.

Ruff CB. 2003a. Growth in bone strength, body size, and muscle size in a juvenile longitudinal sample. Bone 33:317-329.

Ruff CB. 2003b. Ontogenetic adaptation to bipedalism: age changes in femoral to humeral length and strength proportions in humans, with a comparison to baboons. J Hum Evol 45:317-349.

Ruff CB. 2006. Environmental influences on skeletal morphology. In: Ubelaker DH, editor. Handbook of North American Indians, Vol. 3: environment, origins and population. Washington, D.C.: Smithsonian Institution Press. p 685-694.

Ruff CB. 2007. Body size prediction from juvenile skeletal remains. Am J Phys Anthropol 133:698-716.

Ruff CB. 2008a. Biomechanical analyses of archaeological human skeletons. In: Katzenberg MA, Saunders SR, editors. Biological anthropology of the human skeleton. New York: Wiley-Liss. p 71-102.

Ruff CB. 2008b. Femoral/humeral strength in early African *Homo erectus*. J Hum Evol 54:383-390.

Ruff CB. 2009. Relative limb strength and locomotion in *Homo habilis*. Am J Phys Anthropol 138:90–100.

Ruff CB, Hayes WC. 1982. Subperiosteal expansion and cortical remodeling of the human femur and tibia with aging. Science 217:945–948.

Ruff CB, Hayes W. 1983a. Cross-sectional geometry of Pecos Pueblo femora and tibiae: a biomechanical investigation: I. method and general patterns of variation. Am J Phys Anthropol 60:359-381.

Ruff CB, Hayes W. 1983b. Cross-sectional geometry of Pecos Pueblo femora and tibiae: a biomechanical investigation: II. sex, age, and side differences. Am J Phys Anthropol 60:383-400.

Ruff CB, Hayes WC. 1988. Sex differences in age-related remodeling of the femur and tibia. J Orthop Res 6:886-896.

Ruff CB, Larsen CS. 1990. Postcranial biomechanical adaptations to subsistence strategy changes on the Georgia Coast. In: Larsen CS, editor. The archaeology of Mission Santa Catalina de Guale: 2: biocultural interpretations of a population in transition. Anthropol Pap Am Mus Nat Hist 68: 94-120.

Ruff CB, Larsen C. 2001. Reconstructing behavior in Spanish Florida: the biomechanical evidence. In: Larsen CS, editor. Bioarchaeology of Spanish Florida: the impact of colonialism. University Press of Florida, Gainesville. p 113-145.

Ruff CB, Larsen C, Hayes W. 1984. Structural changes in the femur with the transition to agriculture on the Georgia Coast. Am J Phys Anthropol 64:125-136.

Ruff CB, Scott W, Liu A. 1991. Articular and diaphyseal remodeling of the proximal femur with changes in body mass in adults. Am J Phys Anthropol 86:397–413.

Ruff CB, Walker A, Trinkaus E. 1994. Postcranial robusticity in Homo. III: Ontogeny. Am J Phys Anthropol 9:35-54.

Ruff CB, McHenry HM, Thackeray F. 1999. Cross-sectional morphology of the SK 82 and 97 proximal femora. Am J Phys Anthropol 109:509-521.

Ruff CB, Holt B, Trinkaus E. 2006. Who's afraid of the big bad Wolff?: "Wolff's law" and bone functional adaptation. Am J Phys Anthropol 129:484-498.

Russo CR, Lauretani F, Bandinelli S, Bartali B, DiIorio S, Volpoto S, Guralnik JM, Harris T, Ferrucci L. 2003. Aging bone in men and women: beyond changes in bone mineral density. Osteoporosis Int 14:531-538.

Saunders SR. 1992. Subadult skeletons and growth related studies. In: Saunders SR, Katzenberg MA, editors. Skeletal biology of past peoples: advances in research methods. New York: Wiley-Liss. p 1-20.

Saunders SR, Hoppa RD. 1993. Growth deficit in survivors and non-survivors: biological mortality bias in subadult skeletal samples. Yearb Phys Anthropol 36:127-151.

Sazawal S, Black RE, Bhan MK. 1995. Zinc supplementation in young children with acute diarrhea in India. N Engl J Med 333:839-844.

Schaffler MB, Burr DB. 1988. Stiffness of compact bone: effects of porosity and density. J Biomech 21:13–16.

Schaffler MB, Choi K, Milgrom C. 1995. Aging and matrix microdamage accumulation in human compact bone. Bone 17:521-525.

Schaffler MB, Radin EL, Burr DB. 1989. Mechanical and morphological effects of strain rate on fatigue of compact bone. Bone 10:207–214.

Schaffler MB, Radin EL, Burr DB. 1990. Long-term fatigue behavior of compact bone at low strain magnitude and rate. Bone 11:321–326.

Schneider V, Oganov V, LeBlanc A. 1995. Bone and body mass changes during space flight. Acta Astronaut 36:463-466.

Schoenau E, Neu CM, Rauch F, Manz F. 2001. The development of bone strength at the proximal radius during childhood and adolescence. J Clin Endocrinol Metab 86:613-618.

Schultz DR, Benson AB, Hirsch C. 1974. Force-deformation properties of human ribs. J Biomech 7:303–309.

Schultz M. 2001. Paleohistopathology of bone: a new approach to the study of ancient diseases. Yearb Phys Anthropol 44:106-147.

Schwartz-Dabney CL, Dechow PC. 2003. Variations in cortical material properties throughout the human dentate mandible. Am J Phys Anthropol 120:252–277.

Sedlin ED. 1964. The ratio of cortical area to total cross-section area in rib diaphysis: a quantitative index of osteoporosis. Clin Orthop 36:161-168.

Sedlin ED, Frost H, Villanueva A. 1963. Age changes in resorption in the human rib cortex. J Gerontol 18:345-349

Seeman E. 2001. Sexual dimorphism in skeletal size, density, and strength. J Clin Endocrinol Metab 86:4576-4584.

Seeman E. 2003a. Reduced bone formation and increased bone resorption: rational targets for the treatment of osteoporosis. Osteoporosis Int 14:S2–S8.

Seeman E. 2003b. Periosteal bone formation—a neglected determinant for bone strength. N Engl J Med 349:320-323.

Seeman E, Delmas PD. 2006. Bone quality: the material and structural basis of bone strength and fragility. N Engl J Med 354:2250-2261.

Seeman E, Szmukler GI, Formica C, Tsalamandris C, Mestrovic R. 1992. Osteoporosis in anorexia nervosa: the influence of peak bone density, bone loss, oral contraceptive use, and exercise. J Bone Miner Res 7:1467-1474.

Seeman E, Karlsson MK, Duan Y. 2000. On exposure to anorexia nervosa, the temporal variation in axial and appendicular skeletal development predisposes to site-specific deficits in bone size and density: a cross-sectional study. J Bone Miner Res 15:2259–2265.

Seow WK, Masel JP, Weir C. 1989. Mineral deficiency in the pathogenesis of enamel hypoplasia in prematurely born, very low birth weight children. Pediatr Dent 11:297-302.

Šereikienė I, Jankauskas R. 2002. Late medieval Lithuanian children growth (according to paleo-osteological material of 14^{th}-17^{th} cc. Alytus burial ground. Anthropologie 40:157-163.

Šereikienė I, Jankauskas R. 2004. Lithuanian children's growth in the past –an updated medieval sample. Papers on Anthropology 13:226-238.

Severs D, Williams T, Davies JW. 1961. Infantile scurvy: a public health problem. Can J Public Health 52:214-220.

Shackelford LL. 2007. Regional variation in the postcranial robusticity of late Upper Paleolithic humans. Am J Phys Anthropol 133:655–668.

Shapiro R, Heaney RP. 2003. Co-dependence of calcium and phosphorus for growth and development under conditions of varying deficiency. Bone 32:532-540.

Shaw CN, Stock JT. 2009a. Intensity, repetitiveness, and directionality of habitual adolescent mobility patterns influence the tibial diaphysis morphology of athletes. Am J Phys Anthropol 140:149–159.

Shaw CN, Stock JT. 2009b. Habitual throwing and swimming correspond with upper limb diaphyseal strength and shape in modern human athletes. Am J Phys Anthropol 140:160-172.

Sims NA, Gooi JH. 2008. Bone remodeling: multiple cellular interactions required for coupling of bone formation and resorption. Semin Cell Dev Biol 19:444-451.

Siraisi NG. 1990. Medieval and early Renaissance medicine: an introduction to knowledge and practice. Chicago: University of Chicago Press.

Skedros JG. 2000. Do BMUs adapt osteon cross-sectional shape for habitual tension vs. compression loading? J Bone Miner Res 15:S347.

Skedros JG, Bloebaum RD, Mason MW, Bramble DM. 1994a. Analysis of a tension/compression skeletal system: possible strain-specific differences in the hierarchical organization of bone. Anat Rec 239:396–404.

Skedros JG, Mason MW, Bloebaum RD. 1994b. Differences in osteonal micromorphologies between tensile and compressive cortices of a bending skeletal system: indications of potential strain-specific differences in bone microstructure. Anat Rec 239:405–413.

Skedros JG, Mason MW, Nelson MC, Bloebaum RD. 1996. Evidence of structural and material adaptation to specific strain features in cortical bone. Anat Rec 246:47–63.

Skedros JG, Su SC, Bloebaum RD. 1997. Biomechanical implications of mineral content and microstructural variations in cortical bone of horse, elk and sheep calcanei. Anat Rec 249:297–316.

Skedros JG, Mason MW, Bloebaum RD. 2001a. Modeling and remodeling in a developing artiodactyl calcaneus: a model for evaluating Frost's mechanostat hypothesis and its corollaries. Anat Rec 263:167–185.

Skedros JG, Hunt KJ, Bloebaum RD. 2001b. Expanding Wolff's law: variant and invariant strain stimuli in bone adaptation and maintenance. Trans Orthop Res Soc 26:548.

Skedros JG, Knight AN, Clark GC, Crowder CM, Dominguez VM, Qiu S, Mulhern DM, Donahue SW, Busse B, Hulsey BI, Zedda M, Sorenson SM. 2013. Scaling of Haversian canal surface area to secondary osteon bone volume in ribs and limb bones. Am J Phys Anthropol 151:230-244.

Skerry TM. 2008. The response of bone to mechanical loading and disuse: fundamental principles and influences on osteoblast/osteocyte homeostasis. Arch Biochem Biophys 473:117-123.

Sladek V, Berner M, Sailer R. 2006. Mobility in central European late eneolithic and early Bronze Age: femoral cross-sectional geometry. Am J Phys Anthropol 130:320–332.

Slemenda CW, Miller JZ, Hui SL, Reister TK, Johnston CC. 1991. Role of physical activity in the development of skeletal mass in children. J Bone Miner Res 6:1227-1233.

Slemenda CW, Reister TK, Hui SL, Miller JZ, Christian JC, Johnston CC. 1994. Influences of skeletal mineralization in children and adolescents: evidence for varying effects of sexual maturation and physical activity. J Pediatr 125:201-207.

Smith BH. 1991. Standards of human tooth formation and dental age assessment. In: Kelley MA, Larsen CS, editors. Advances in dental anthropology. New York: Wiley-Liss. p 143-168.

Smith EL, Gilligan C. 1987. Effects of inactivity and exercise on bone. Physician Sportsmed 15:91-100.

Sockol MD, Raichlen DA, Pontzer H. 2007. Chimpanzee locomotor energetics and the origin of human bipedalism. Proc Natl Acad Sci USA 30:12265-12269.

Sofaer Derevenski JR. 1997. Engendering children, engendering archaeology. In: Moore J, Scott EC, editors. Invisible people and processes. London: Leicester University Press. p 192–202.

Soafer Deverenski JR. 2000. Children and material culture. London, Routledge.

Specker B, Binkley T. 2003. Randomized trial of physical activity and calcium supplementation on bone mineral content in 3- to 5-year-old children. J Bone Miner Res 18:885-892.

Specker B, Vukovich M. 2007. Evidence for an interaction between exercise and nutrition for improved bone health during growth. In: Daly R, Petit M, editors. Optimizing bone mass and strength: the role of physical activity and nutrition during growth. Med Sport Sci 51:50-63.

Squillante RG, Williams JL. 1993. Videodensitometry of osteons in females with femoral neck fractures. Calcif Tissue Int 52:273–277.

Srinivasan S, Keilin SA, Judex S, Bray RC, Zernicke RF, Gross TS. 2000. Aging-induced Osteopenia in avian cortical bone. Bone 26:361-365.

Srinivasan S, Weimer DA, Agans SC, Bain SD, Gross TS. 2002. Low-magnitude mechanical loading becomes osteogenic when rest is inserted between each load cycle. J Bone Miner Res 17:1613–1620.

Stein ID, Granik G. 1976. Rib structure and bending strength: an autopsy study. Calcif Tissue Res 20:61–73.

Stein MS, Feik SA, Thomas CD, Clement JG, Ward JD. 1999. An automated analysis of intracortical porosity in human femoral bone across age. J Bone Miner Res 14:624-632.

Stitzel JD, Cormier JM, Barretta JT, Kennedy EA, Smith EP, Rath AL, Duma SM, Matsuoka F. 2003. Defining regional variation in the material properties of human rib cortical bone and its effect on fracture prediction. Stapp Car Crash Journal 47:243–265.

Stratakis CA, Gold PW, Chrousos GP. 1995. Neuroendochronology of stress: implications for growth and development. Horm Res 43:162-167.

Stock JT. 2006. Hunter-gatherer postcranial robusticity relative to patterns of mobility, climatic adaptation, and selection for tissue economy. Am J Phys Anthropol 131:194-204.

Stock JT, Pfeiffer SK. 2001. Linking structural variability in long bone diaphyses to habitual behaviors: foragers from the southern African Later Stone Age and the Andaman Islands. Am J Phys Anthropol 115:337-348.

Stock JT, Pfeiffer SK. 2004. Long bone robusticity and subsistence behaviour among Later Stone Age foragers of the forest and fynbos biomes of South Africa. J Archaeol Sci 31:999–1013.

Stone KL, Seeley DG, Lui L-Y, Cauley JA, Ensrud K, Browner WS, Nevitt MC, Cummings SR. 2003. BMD at multiple sites and risk of fracture of multiple types: long-term results from the study of osteoporotic fractures. J Bone Miner Res 18:1947-1954.

Stout SD. 1978. Histological structure and its preservation in ancient bone. Curr Anthropol 19:601-604.

Stout SD. 1989. Histomorphometric analysis of human skeletal remains. In: Iscan MY, Kennedy KAR, editors. Reconstruction of life from the skeleton. New York: Alan R. Liss, Inc. p 41-52.

Stout S, Lueck R. 1995. Bone remodeling rates and skeletal maturation in three archaeological skeletal populations. Am J Phys Anthropol 98:161-171.

Stout SD, Paine RR. 1992. Brief communication: histological age estimation using rib and clavicle. Am J Phys Anthropol 87:111-115.

Stout SD, Simmons DJ. 1979. Use of histology in ancient bone research. Yearb Phys Anthropol 22:228-249.

Stout SD, Teitelbaum SL. 1976. Histomorphometric determination of formation rates of archaeological bone. Calcif Tissue Res 21:163-169.

Streeter M. 2005. Histomorphometric characteristics of the subadult rib cortex: normal patterns of dynamic bone modeling and remodeling during growth and development. Ph.D. dissertation. University of Missouri, Columbia.

Streeter M, Stout S, Trinkaus E, Burr D. 2010. Brief communication: bone remodeling rates in Pleistocene humans are not slower than rates observed in modern populations: a reexamination of Abbott et al. (1996). Am J Phys Anthropol 141:315-318.

Stuart-Macadam P. 1989. Porotic hyperostosis: relationship between orbital and vault lesions. Am J Phys Anthropol 80:187-193.

Stuart-Macadam P. 1992. Porotic hyperostosis: a new perspective. Am J Phys Anthropol 87:39-47.

Sumner DR, Andriacchi TP. 1996. Adaptation to differential loading: comparison of growth-related changes in cross-sectional properties of the human femur and humerus. Bone 19:121-126.

Svetikas E. 2003. Alytaus kapinynas: christianizacijos šaltiniai. Vilnius, Lithuania: Diemedžio leidykla.

Szulc P, Seeman E, Dabouef F, Sornay-Rendu E, Delmas P. 2006. Bone fragility: failure of periosteal apposition to compensate for increased endocortical resorption in postmenopausal women. J Bone Miner Res 21:1856-1863.

Taaffe DR, Robinson TL, Snow CM, Robert M. 1997. High-impact exercise promotes bone gain in well-trained female athletes. J Bone Miner Res 12:255-260.

Takahashi H, Frost HM. 1966. Age and sex related changes in the amount of cortex in normal human ribs. Acta Orthop Scand 37:122–130.

Teitelbaum SL, Tondravi MM, Ross FP. 1996. Osteoclast biology. In: Marcus R, Feldman D, Kelsey J, editors. Osteoporosis. San Diego: Academic Press. p 61-94.

Temple DH. 2007. Dietary variation and stress among prehistoric Jomon foragers from Japan. Am J Phys Anthropol 133:1035-1046.

Tersigni MA. 2005. Serial long bone histology: inter- and intra-bone age estimation. PhD dissertation. University of Tennessee, Knoxville.

Thomas CD, Feik SA, Clement JG. 2005. Regional variation of intracortical porosity in the midshaft of the human femur: age and sex differences. J Anat 206:115-125.

Thompson B. 1984. Infant mortality in nineteenth-century Bradford. In Woods R, Woodward J, editors. Urban disease and mortality in nineteenth-century England. London: Batsford. P 120-147.

Thompson DD. 1979. The core technique in the determination of age at death in skeletons. J Forensic Sci 44:902-915.

Tilton FE, Degioanni JC, Schneider VS. 1980. Long term follow-up of skylab bone demineralization. Aviat Space Environ Med 51:1209-1213.

Tommerup LJ, Raab DM, Crenshaw TD, Smith EL. 1993. Does weight bearing exercise affect non-weight bearing bone? J Bone Miner Res 8:1053-1058.

Trinkaus E, Ruff CB. 1999. Diaphyseal cross-sectional geometry of Near Eastern Middle Paleolithic humans: the femur. J Archaeol Sci 26:409-424.

Trinkaus E, Stringer CB, Ruff CB, Hennessy R, Roberts M, Parfitt S. 1999. Diaphyseal cross-sectional geometry of the Boxgrove 1 Middle Pleistocene human tibia. J Hum Evol 37:1–25.

Trinkaus E, Ruff CB, Esteves F, Coelho JMS, Silva M, Mendova M. 2002. The lower limb remains. In: Zilhão J, Trinkaus E, editors. Portrait of the artist as a child. Lisbon: Intituto Português de Arquelogis. p 466-488.

Tucker B, Young AG. 2005. Growing up Mikea: children's time allocation and tuber foraging in southwestern Madagascar. In: Hewlett BS, Lamb ME, editors. Hunter-gatherer childhoods: evolutionary, developmental and cultural perspectives. New Brunswick: Transaction Publishers. p 147-172.

Turner CH. 1992. Functional determinants of bone structure: beyond Wolff's law of bone transformation. Bone 13:403-409.

\Turner CH. 1998. Three rules for bone adaptation to mechanical stimuli. Bone 23:399-407.

Turner CH. 2001. Animal models of osteoporosis: necessity and limitations. Eur Cell Mater 1:66-81.

Turner CH. 2002. Biomechanics of bone: determinants of skeletal fragility and bone quality. Osteoporosis Int 13:97-104.

Turner CH, Forwood MR, Otter MW. 1994. Mechanotransduction in bone: do bone cells act as sensors of fluid flow? FASEB J 8:875–878.

Turner CH, Owan I, Takano Y. 1995. Mechanotransduction in bone: role of strain rate. Am J Physiol Endocrinol Metab 269:E438–42.

Turner CH, Rho J, Takano Y, Tsui T, Pharr G. 1999. The elastic properties of trabecular and cortical bone tissues are similar: results from two microscopic measurement techniques. J Biomech 32:437–441.

Turner C, Robling A, Duncan R, Burr D. 2002. Do bone cells behave like a neuronal network? Calcif Tissue Int 70:435-442.

Turner CH, Sun Q, Schriefer J, Pitner N, Price R, Bouxsein ML, Rosen CJ, Donahue LR, Schultz KL, Beamer WG. 2003. Congenic mice reveal sex-specific genetic regulation of femoral structure and strength. Calcif Tissue Int 73:297-303.

Tyla A. 1989. XVI-XVIII a. Alytaus ekonomijos valdymas. In: Leščinskienė D, editor. Alytaus miesto ir apylinkių istorijos bruožai: straipsnių rinkinys. Vilnius, Lithuania: Mokslas.

Ulijaszek SJ. 1991. Human dietary change. Philos Trans R Soc Lond B Biol Sci 334:271-279.

Urbanavičius A. 2001. Imigracija į Vilnių iš Alytaus XVII a. 2-oje pusėje – XVIII a. In: Jakunskienė A, editor. Alytaus miesto istorijos fragmentai. Alytus: Alytaus Kraštotyros muziejus. p 28-39.

Vajda EG, Kneissel M, Muggenburg B, Miller SC. 1999. Increased intracortical bone remodeling during lactation in beagle dogs. Biol Reprod 61:1439–1444.

van der Meulen MC, Beaupré GS, Carter DR. 1993. Mechanobiologic influences in long bone cross-sectional growth. Bone 14:635-642.

van der Meulen MC, De Ausen JM, Kiratli BJ, Bachrach LK, Carter DR. 1995. Race and gender effects on bone mass and strength acquisition during adolescence. Trans Orthop Res Soc 20:542.

van der Meulen MC, Ashford MWJ, Kiratli BJ, Backrach LK, Carter DR. 1996. Determinates of femoral geometry and structure during adolescent growth. J Orthop Res 14:22-29.

van der Meulen MC, Marcus R, Backrach LK, Carter DR. 1997. Correspondence between theoretical models and dual energy x-ray absorptiometry measurements of femoral cross-sectional growth during adolescence. J Orthop Res 15:473-475.

van Gerven D, Hummert J, Burr D. 1985. Cortical bone maintenance and geometry of the tibia in prehistoric children from Nubia's Batn el Hajar. Am J Phys Anthropol 66:275-280.

Vatanparast H, Whiting SJ, Bailey DA, Baxter-Jones A. 2007. The beneficial effect of dietary protein on bone mineral mass is influenced by habitual dietary calcium intake in young adult females. J Nutr 137:2674-2679.

Vėlius G. 2003. Kernavė in the context of towns of the Grand Duchy of Lithuania. In: Archaeologia Lituana 4:161–174.

Vėlius G. 2005. Kernavės miesto bendruomenė XIII–XIV amžiuje. Vilnius: Vilniaus universiteto leidykla. p 112.

Wachter NJ, Augat P, Krischak GD, Sarkar MR, Mentzel M, Kinzl L, Claes L. 2001. Prediction of strength of cortical bone in vitro by microcomputed tomography. Clin Biomech 16:252–256.

Wachter NJ, Krischak GD, Mentzel M, Sarkar MR, Ebinger T, Kinzl L. 2002. Correlation of bone mineral density with strength and microstructural parameters of cortical bone in vitro. Bone 31:90-95.

Walker PL, Bathurst RR, Richman R, Gjerdrum T, Andrushko VA. 2009. The causes of porotic hyperostosis and cribra orbitalia: a reappraisal of the iron-deficiency-anemia hypothesis. Am J Phys Anthropol 139:109–125.

Wapler U, Crube´zy E, Schultz M. 2004. Is cribra orbitalia synonymous with anemia?: analysis and interpretation of cranial pathology in Sudan. Am J Phys Anthropol 123:333–339.

Wang QJ, Seeman E. 2008. Skeletal growth and peak bone strength. Best Pract Res Clin Endocrinol Metab 22:687-700.

Wang QJ, Suominen H, Nicholson PH, Zou LC, Alen M, Koistinen A, Cheng S. 2004. Influence of physical activity and maturation status on bone mass and geometry in early pubertal girls. Scand J Med Sci Sports 15:100-106.

Wang QJ, Ashley DW, Dechow PC. 2010. Regional, ontogenetic, and sex-related variations in elastic properties of cortical bone in baboon mandibles. Am J Phys Anthropol 141:526–549.

Ward KA, Roberts SA, Adams JE, Mughal MZ. 2005. Bone geometry and density in the skeleton of prepubertal gymnasts and school children. Bone 36:1012-1018.

Weiss E. 2003. Humeral cross-sections and the physical environment. Am J Phys Anthropol 121:293–302.

Wescott DJ. 2001. Structural variation in the humerus and femur in the American Great Plains and adjacent regions: differences in subsistence strategy and physical terrain. Ph.D. dissertation. The University of Tennessee, Knoxville.

Wescott DJ. 2006. Effect of mobility on femur midshaft external shape and robusticity. Am J Phys Anthropol 130:201-213.

White B. 1975. The economic importance of children in a Javanese village. In: Nag M, editor. Population and social organization. The Hague: Mouton. p 127-146.

White TD. 2000. Human osteology. San Diego: Academic Press.

Wildt AR, Ahtola O. 1978. Analysis of covariance: quantitative applications in the social sciences. Series 12. Thousand Oaks, CA: SAGE Publications, Inc.

Wolff J. 1986. The law of bone remodeling (translated from the 1892 original, Das Gesetz de Transformation der Knochen, by P. Maquet and R. Ferlong). Berlin: Springer Verlag.

Wong MW, Carter DR. 1990. A theoretical model of endochondral ossification and bone architectural construction in long bone ontogeny. Anat Embryol 181:523-532.

Wong S, Au B, Lau E, Lee Y, Sham A, Lee S. 2004. Osteoporosis in Chinese patients with anorexia nervosa. Int J Eat Disord 36:104–108.

Wood JW, Milner GR, Harpending HC, Weiss KM. 1992. The osteological paradox: problems of inferring prehistoric health from skeletal samples. Curr Anthropol 33:343-370.

Wu K, Schubeck KE, Frost HM, Villanueva AR. 1970. Haversian bone formation rates determined by a new method in a mastodon, and in human diabetes mellitus and osteoporosis. Calcif Tissue Int 22:204-219.

Yaeger J, Sharawy M. 1986. Enamel. In: Behaskar SN, editor. Orban’s oral histology and embryology. St. Louis: CV Mosby. p 45-100.

Yao W, Jee WSS, Zhou H, Lu J, Cui L, Setterberg R, Liang T, Ma YF. 1999. Anabolic effect of prostaglandin E2 on cortical bone of aged male rats comes mainly from modeling dependent bone gain. Bone 25:697-702.

Yeni YN, Norman TL. 2000. Fracture toughness of human femoral neck: effect of microstructure, composition, and age. Bone 26:499-504.

Yeni YN, Brown CU, Wang Z, Norman TL. 1997. The influence of bone morphology on fracture toughness of the human femur and tibia. Bone 21:453–459.

Yeni YN, Brown CU, Norman TL. 1998. Influence of bone composition and apparent density on fracture toughness of the human femur and tibia. Bone 22:79–84.

Yoganandan N, Pintar FA. 1998. Biomechanics of human thoracic ribs. J Biomech Eng 120:100–104.

Young N, Formica C, Szmukler G, Seeman E. 1994. Bone density at weight-bearing and nonweight-bearing sites in ballet dancers: the effects of exercise, hypogonadism, and body weight. J Clin Endocrinol Metab 78:449-454.

Zebaze R, Ghasem-Zadeh A, Mbala A, Seeman E. 2013. A new method of segmentation of compact-appearing, transitional and trabecular compartments and quantification of cortical porosity from high resolution peripheral quantitative computed topographic images. Bone 54:8-20.

Žepkaitė R. 2001. Prisiminkime Alytaus praeitį. In: Jakunskienė A, editor. Alytaus miesto istorijos fragmentai. Alytus: Alytaus Kraštotyros muziejus. p 5-9.

Zink AR, Panzer S, Fesq-Martin M, Burger-Heinrich E, Wahl J, Nerlich AG. 2005. Evidence for a 7000-year-old case of primary hyperparathyroidism. JAMA 293:40-42.

APPENDICES

APPENDIX I: Age methodology and age estimates for each individual.

			Age Estimation Method		
PC.Inv.No[1]	**Cr.Inv.No[1]**	**Age Estimate[2]**	**Dental (radiographic)**	**Dental (visual)**	**Skeletal**
314A	3913	7.4	X		
348A	3909	3.5	X		
348B	3923A	4.0		X	
350C	3904	8.8	X		
350D	3614	9.3			X
464G	4159	3.0		X	
465A	4182	10.1	X		
465B	4334E	1.5			X
470B	3955A	7.2	X		
474B	4382	5.6	X		
478C	4369	1.8	X		
478D	4398	5.1	X		
478F	4397	5.3	X		
483H	3956A	2.7	X		
486B	4167	6.5	X		
490B	3956B	3.9	X		
492C	4387	4.5	X		
553B	4412	7.5	X		
553C	3991	7.9	X		
634C	3975D	2.1	X		
634R	3975A	1.3	X		
637B	4235	5.5	X		
674B	4158	10.9	X		
730B	4781	13.0	X		
736B	4446	9.0			X
742B	4439	11.3	X		
745A	4454	12.0			X
746B	4458	7.3			X
753B	4448	11.3	X		
790A	4456	12.7	X		
824A	4645	12.0		X	
956A	4817	13.5		X	
969A	4522	13.5		X	
976A	4655	13.5		X	

APPENDIX I (cont.): Age methodology and age estimates for each individual.

			Age Estimation Method		
PC.Inv.No[1]	**Cr.Inv.No[1]**	**Age Estimate[2]**	**Dental (radiographic)**	**Dental (visual)**	**Skeletal**
979A	4799	11.0		X	
980B	4819	9.7	X		
983B	4516	12.0		X	
991C	4756	6.1	X		
991D	4478	5.7	X		
994H	4758	2.5	X		
999B	4558I	1.5			X
1000F	4558D	2.5	X		
1000G	4544H	5.1	X		
1000H	4510	8.8	X		
1002C	4572D	1.5			X
1003D	4752	1.7	X		
1004D	4762	2.0		X	
1005A	4534	8.9	X		
1005C	4443	4.4	X		
1005D	4778	10.0		X	
1006K	4489	11.5		X	
1007B	4783	2.9	X		
1007D	4731	2.8	X		
1007I	4442	4.7	X		
1008E	4578	3.6	X		
1008H	4482	8.0	X		
1011A	4440	5.0	X		

[1] PC.Inv.No = Post Cranial Inventory Number; Cr.Inv.No = Cranial Inventory Number.
[2] Final age estimate for each individual in years.

APPENDIX II: Pathological lesion presence and absence for each individual.

			Cranial					Postcranial	
PC.Inv. No[1]	**Cr.Inv. No[1]**	**Age Est.[2]**	PH[1] (Vault)	PH (Orbital)	Total PH	Other Lesions	DEH[1]	Osteo-periostitis	Other Lesions
314A	3913	7.4					X		
348A	3909	3.5							
348B	3923A	4.0	X		X				
350C	3904	8.8					X		
350D	3614	9.3							
464G	4159	3.0		X	X	X		X	
465A	4182	10.1					X	X	
465B	4334E	1.5	X		X			X	
470B	3955A	7.2	X		X		X	X	
474B	4382	5.6						X	
478C	4369	1.8	X		X				
478D	4398	5.1				X			
478F	4397	5.3							
483H	3956A	2.7				X			
486B	4167	6.5		X	X				
490B	3956B	3.9							
492C	4387	4.5							
553B	4412	7.5							
553C	3991	7.9						X	
634C	3975D	2.1						X	
634R	3975A	1.3							
637B	4235	5.5							
674B	4158	10.9		X	X				
730B	4781	13.0	X		X	X	X		
736B	4446	9.0				X		X	
742B	4439	11.3		X	X		X	X	X
745A	4454	12.0						X	
746B	4458	7.3	X		X				
753B	4448	11.3					X		
790A	4456	12.7		X	X			X	X
824A	4645	12.0		X	X		X		
956A	4817	13.5					X		
969A	4522	13.5					X	X	
976A	4655	13.5					X	X	X

APPENDIX II (cont.): Pathological lesion presence and absence for each individual.

			Cranial					Postcranial	
PC.Inv. No[1]	**Cr.Inv. No[1]**	**Age Est.[2]**	PH[1] (Vault)	PH (Orbital)	Total PH	Other Lesions	DEH[1]	Osteo-periostitis	Other Lesions
979A	4799	11.0					X		
980B	4819	9.7					X		
983B	4516	12.0					X		
991C	4756	6.1							
991D	4478	5.7							
994H	4758	2.5				X		X	
999B	4558I	1.5						X	
1000F	4558D	2.5							
1000G	4544H	5.1							
1000H	4510	8.8		X	X				
1002C	4572D	1.5							
1003D	4752	1.7							
1004D	4762	2.0		X	X				
1005A	4534	8.9						X	
1005C	4443	4.4						X	
1005D	4778	10.0					X	X	X
1006K	4489	11.5					X		
1007B	4783	2.9						X	
1007D	4731	2.8	X	X	X				
1007I	4442	4.7						X	
1008E	4578	3.6							
1008H	4482	8.0					X	X	
1011A	4440	5.0						X	

[1] PC.Inv.No = Postcranial Inventory Number; Cr.Inv.No = Cranial Inventory Number, PH = Porotic Hyperostosis, DEH = Dental Enamel Hypoplasia.

[2] Final age estimate for each individual in years.

APPENDIX III: Representative photographs of the pathological lesions analyzed.

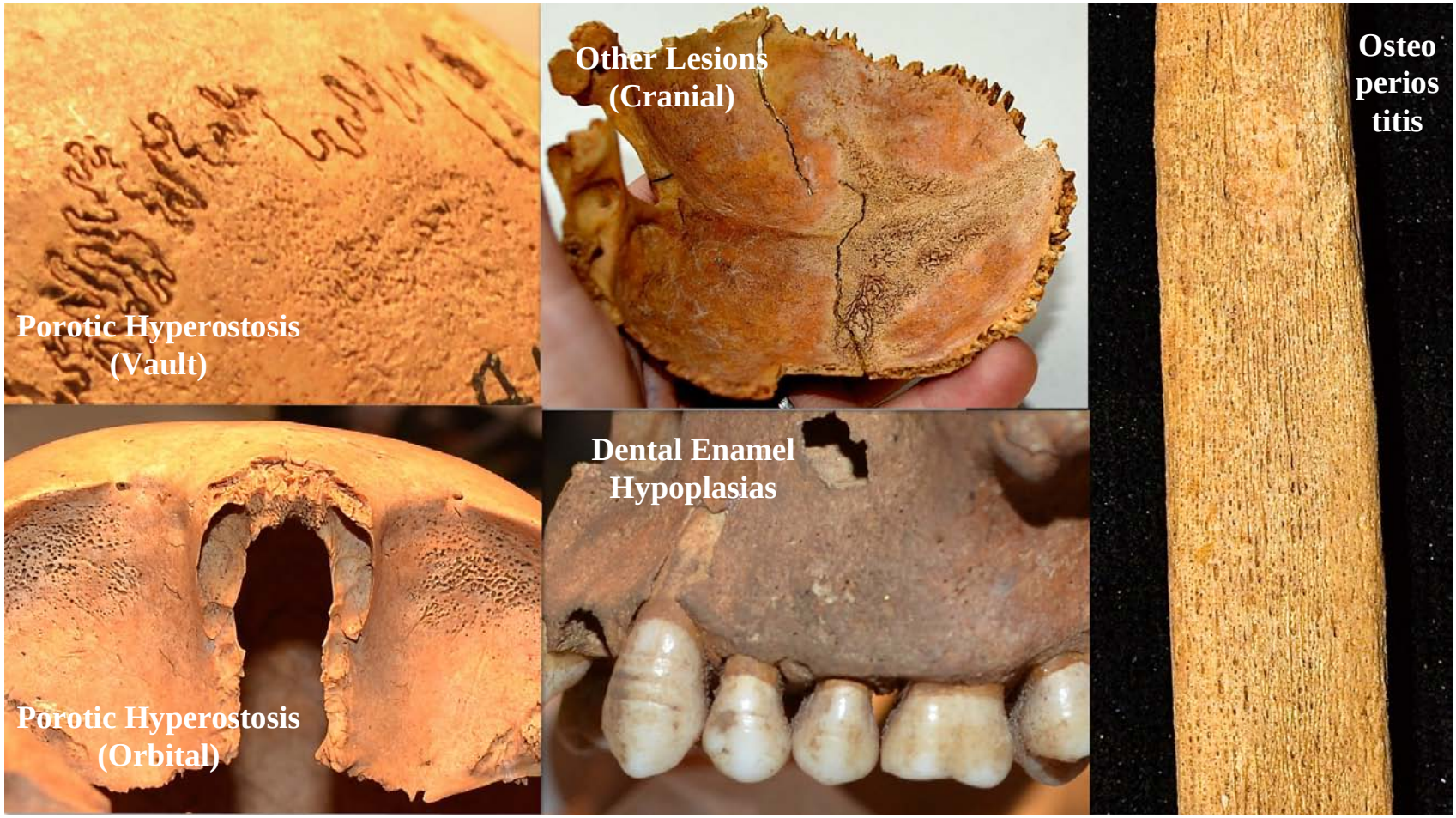

APPENDIX IV: MATLAB code for calculation of cross-sectional geometric properties

```
function [XSex] = FileLoader
%Select BMP file list from MATLAB directory
datafiles = dir('*.bmp');
XSex = zeros(numel(datafiles),9);
for k = 1:numel(datafiles);
   currentImage = datafiles(k).name %Uses BMP file name for current file name
   A = imread(currentImage);
   XSex(k,:) = CSProperties(A, currentImage);
end


function [properties] = CSProperties(A, currentImage)
%This code does not include total area, see FileLoader2.
%All images must be converted to 1 bit bitmap files with all cancellous
%bone removed from the image.
%The code assumes that 80 pixels = 1 mm.

BoneSearchArea = size(find(A),1); %counts all non-zero elements in the matrix
CA = BoneSearchArea*(0.011719^2); %scales these by number of pixels/nm for cortical area

[ml,ap] = find(A); %produces a matrix of m*n elements equal to dimensions of bone

row = ml*0.011719; %scales ML
col = ap*0.011719; %scales AP

ctrml = mean(row); %finds the centroid of ML axis
ctrap = mean(col); %finds the centroid of AP axis

radml = row-ctrml; %radius vector of ML axis
radap = col-ctrap; %radius vector of AP axis

%calculation of I around the AP axis
Iap = radap.^2*(0.011719^2); %takes the square of radap element by element * y^2 (pixel area)
Iap = sum(Iap); %summation of squared elements by pixel area

%calculation of I around the ML axis
Iml = radml.^2*(0.011719^2); %takes the square of radml element by element * y^2 (pixel area)
Iml = sum(Iml); %summation of squared elements by pixel area

%calculate J
J = Iap + Iml;
```

APPENDIX IV (cont.): MATLAB code for calculation of cross-sectional geometric properties

```
%calculate the principal axes of the cross-section
[PC,SCORE] = princomp([radml,radap]); %extracts the scores of PCA of ML & AP axes

plotk = figure;
biplot(PC(:,1:2),'Scores',SCORE(:,1:2)); %produces a rotated plot of the cross-section showing
major & minor axes
saveas(plotk,strcat(currentImage,'plot'), 'pdf');

%calculate Imax
MaxRad1 = (SCORE(:,1).^2)*(0.011719^2); %takes the square of 1st column of PCA scores *
y^2 (pixel area)
Imax = sum(MaxRad1); %summation of squared major axis elements by pixel area

%calculate Imin
MaxRad2 = (SCORE(:,2).^2)*(0.011719^2); %takes the square of 2nd column of PCA scores *
y^2 (pixel area)
Imin = sum(MaxRad2); %summation of squared minor axis elements by pixel area

%calculate theta
B = radap/norm(radap); %makes the AP vector into unit length
C = (SCORE(:,1))/norm(SCORE(:,1)); %makes the maximum PC vector into unit length
theta = acos(C'*B)*180/pi; %calculates the cosine of the arc length between the vectors to obtain
theta

%calculate Zml
Zml = Iml/max(abs(radml));

%calculate Zap
Zap = Iap/max(abs(radap));

properties = [CA, Iml, Iap, J, Imax, Imin, theta, Zml, Zap]

end
```

APPENDIX IV (cont.): MATLAB code for calculation of cross-sectional geometric properties

```
function [result] = momentcalculator(data)

BoneArea = size(find(data),1)
BoneArea = BoneArea*(0.625^2);

[r,c] = find(data);

r = r-.5;
c = c-.5;

r = r*0.625;
c = c*0.625;

MeanR = mean(r);
MeanC = mean(c);

r = r-MeanR;
c = c-MeanC;

%I about the row axes (vertical axes)
Ic = c.^2;
Ic = Ic*(0.625^2);
Ic = sum(Ic);

%I about the column axes (horizontal axes)
Ir = r.^2;
Ir = Ir*(0.625^2);
Ir = sum(Ir);

%Run PCA on these coordinates
[~,score] = princomp([r,c]);

%Im1
Im1 = (score(:,1).^2)*(0.625^2);
Im1 = sum(Im1);

Im2 = (score(:,2).^2)*(0.625^2);
Im2 = sum(Im2);

%Max rows and column values
MaxR = max(abs(r));
```

APPENDIX IV (cont.): MATLAB code for calculation of cross-sectional geometric properties

```
MaxC = max(abs(c));

%Imax max rad
MaxRad1 = max(score(:,1));
MaxRad2 = max(score(:,2));

result = [BoneArea, Ir, Ic, MaxC, MaxR, (Ir/MaxR), (Ic/MaxC), Im1, Im2];

end



function [TA] = FileLoader2
%Select BMP file list from MATLAB directory
datafiles = dir('*.bmp');
TA = zeros(numel(datafiles),1);
for k = 1:numel(datafiles);
   currentImage = datafiles(k).name %Uses BMP file name for current file name
   A = imread(currentImage);
   TA(k,:) = TotalArea(A, currentImage);
end



function [TotArea] = TotalArea(A, currentImage)
%This code does not include total area, as it is unnecessary for analyses.
%All images must be converted to 1 bit bitmap files with medullary cavity filled in with black.
%The code assumes that 85.333 pixels = 1 mm.

BoneSearchArea = size(find(A),1); %counts all non-zero elements in the matrix

TA = BoneSearchArea*(0.011719^2); %scales these by number of pixels/nm for cortical area

TotArea = [TA]

end
```

APPENDIX V: Means and standard deviations for estimated body mass, stature, femoral length, and humeral length by age cohort.

Dimension	Total n	1.0-1.99 yrs			2.0-2.99 yrs			3.0-6.99 yrs			7.0-11.99 yrs			12.0-13.99 yrs	
		n	Mean	StDev	n	Mean	StDev	n	Mean	StDev	n	Mean	StDev	n	Mean	StDev
Estimated Body Mass (kg)	57	6	8.08	1.42	7	9.83	1.31	17	13.65	1.70	19	24.70	5.02	8	42.13	32.24
Estimated Stature (cm)	57	6	69.39	8.35	7	80.54	3.95	17	94.79	7.61	19	121.73	8.78	8	130.05	6.38
Femur Length (mm)	57	6	121.42	27.56	7	152.51	13.43	17	194.19	24.75	19	278.89	28.75	8	322.31	22.01
Humerus Length (mm)	57	6	97.76	18.91	7	119.10	12.15	17	146.97	15.56	19	205.55	18.83	8	233.75	13.10

APPENDIX VI: Means and standard deviations for size-standardized cross-sectional geometric properties by age cohort.

Dimension[1]		1.0-1.99 yrs			2.0-2.99 yrs			3.0-6.99 yrs			7.0-11.99 yrs			12.0-13.99 yrs	
Element		n	Mean	St Dev	n	Mean	St Dev	n	Mean	St Dev	n	Mean	St Dev	n	Mean	St Dev
Femur	48	6			6			14			16			6		
TA			16.54	3.23		20.57	3.01		19.25	3.59		18.02	2.50		18.05	3.80
CA			8.39	2.45		10.15	2.34		10.98	2.26		11.09	1.04		12.27	2.25
MA			8.15	2.21		10.41	1.39		8.27	2.09		6.93	1.83		5.78	1.87
%CA			50.77	9.56		49.05	6.00		57.18	7.06		62.08	5.55		68.51	5.08
I_{max}			4.99×10^{-3}	1.15×10^{-3}		6.08×10^{-3}	1.81×10^{-3}		4.89×10^{-3}	0.56×10^{-3}		3.80×10^{-3}	0.91×10^{-3}		3.47×10^{-3}	0.92×10^{-3}
I_{min}			3.94×10^{-3}	0.72×10^{-3}		4.71×10^{-3}	1.61×10^{-3}		4.25×10^{-3}	1.37×10^{-3}		3.19×10^{-3}	0.77×10^{-3}		3.01×10^{-3}	0.86×10^{-3}
I_{max}:I_{min}			1.26	0.09		1.31	0.10		1.15	0.08		1.20	0.12		1.16	0.13
J			8.93×10^{-3}	1.85×10^{-3}		10.78×10^{-3}	3.41×10^{-3}		9.14×10^{-3}	2.97×10^{-3}		6.99×10^{-3}	1.7×10^{-3}		6.48×10^{-3}	1.73×10^{-3}
Z_p			32.3×10^{-3}	3.5×10^{-3}		31.75×10^{-3}	5.49×10^{-3}		26.24×10^{-3}	4.59×10^{-3}		17.65×10^{-3}	2.44×10^{-3}		16.58×10^{-3}	3.54×10^{-3}
Humerus	51	6			6			16			16			7		
TA			11.28	1.29		14.12	1.76		11.52	1.42		10.83	2.07		10.41	2.56
CA			5.95	0.54		6.61	1.59		6.51	1.19		6.80	0.81		7.24	1.66
MA			5.33	1.52		7.50	1.52		5.01	1.56		4.03	1.37		3.17	1.03
%CA			53.42	8.81		46.71	8.82		56.97	10.85		63.77	6.47		69.87	4.04
I_{max}			3.73×10^{-3}	0.63×10^{-3}		4.47×10^{-3}	1.33×10^{-3}		2.97×10^{-3}	0.56×10^{-3}		2.64×10^{-3}	0.91×10^{-3}		2.44×10^{-3}	0.92×10^{-3}
I_{min}			3.01×10^{-3}	0.50×10^{-3}		3.43×10^{-3}	0.96×10^{-3}		2.44×10^{-3}	0.53×10^{-3}		2.24×10^{-3}	0.87×10^{-3}		1.91×10^{-3}	0.64×10^{-3}
I_{max}:I_{min}			1.24	0.13		1.30	0.12		1.23	0.13		1.20	0.15		1.27	0.13
J			6.73×10^{-3}	1.06×10^{-3}		7.90×10^{-3}	2.26×10^{-3}		5.40×10^{-3}	1.06×10^{-3}		4.87×10^{-3}	1.75×10^{-3}		4.34×10^{-3}	1.55×10^{-3}
Z_p			28.9×10^{-3}	4.78×10^{-3}		26.96×10^{-3}	6.77×10^{-3}		20.15×10^{-3}	2.16×10^{-3}		14.96×10^{-3}	2.93×10^{-3}		13.25×10^{-3}	3.63×10^{-3}
Rib	57	6			7			17			19			8		
TA			5.36×10^{-3}	1.37×10^{-3}		4.77×10^{-3}	0.75×10^{-3}		3.48×10^{-3}	0.81×10^{-3}		2.17×10^{-3}	0.63×10^{-3}		1.74×10^{-3}	0.000.55
CA			2.34×10^{-3}	0.44×10^{-3}		2.34×10^{-3}	0.50×10^{-3}		1.68×10^{-3}	0.35×10^{-3}		1.04×10^{-3}	0.32×10^{-3}		0.87×10^{-3}	0.000.33
MA			3.02×10^{-3}	0.98×10^{-3}		2.43×10^{-3}	0.39×10^{-3}		1.81×10^{-3}	0.64×10^{-3}		1.13×10^{-3}	0.41×10^{-3}		0.88×10^{-3}	0.000.26
%CA			44.78	6.72		48.82	5.60		49.16	8.90		48.29	9.89		49.37	5.73

[1] Cross-sectional long bone areas (TA, CA, MA) standardized by body mass estimated from distal femoral metaphyseal breadth. Second moments of area (*I*, *J*) standardized by body mass × bone length^2 (Ruff, 2007). Section modulus (Z_p) standardized by body mass × bone length (Ruff, 2008a). Rib areas standardized by estimated stature as a body size approximation.

APPENDIX VII: Means and standard deviations for unstandardized and size-standardized histomorphometric properties by age cohort.

Element	Dimension[1]		1.0-1.99 yrs			2.0-2.99 yrs			3.0-6.99 yrs			7.0-11.99 yrs			12.0-13.99 yrs	
			n	Mean	St Dev	n	Mean	St Dev	n	Mean	St Dev	n	Mean	St Dev	n	Mean	St Dev
Femur		25	5			3			9			8			0		
	Avg. On.Ar			22843.87	4263.13		37979.46	11919.28		40649.47	8082.94		56103.42	39110.63		--	--
	Avg. On.Fg.Ar			1520.00	3398.82		29691.43	8893.65		30317.17	12750.81		45513.07	35099.28		--	--
	Avg. On.C.Ar			20913.20	4541.08		34646.63	10797.82		36684.94	6811.75		53068.71	36890.07		--	--
	Avg. HC.Ar			2527.86	807.26		3919.27	925.35		3407.46	978.38		4195.95	4061.61		--	--
	Avg. RS.Ar			7964.13	4125.76		13014.74	3289.94		12568.19	8939.64		16547.02	17982.81		--	--
	Avg. Por.Ar			2894.69	361.95		4320.68	693.74		3929.68	1452.10		6254.36	6838.90		--	--
	Total On.Ar			0.7162	0.5943		2.2897	0.7425		3.3819	1.4618		7.6977	5.2494		--	--
	Total On.Fg.Ar			0.0041	0.0045		0.0344	0.0107		0.0207	0.0114		0.0293	0.0323		--	--
	Total On.C.Ar			0.1329	0.0878		0.2689	0.0534		0.2341	0.0567		0.3560	0.2389		--	--
	Total HC.Ar			0.0164	0.0112		0.0323	0.0086		0.0235	0.0071		0.0299	0.0264		--	--
	Total RS.Ar			0.0941	0.0842		0.0460	0.0109		0.0240	0.0150		0.0286	0.0346		--	--
	Total Por.Ar			0.1269	0.0829		0.0817	0.0059		0.0518	0.0162		0.0636	0.0629		--	--
	Total On.B.Ar			0.1481	0.0909		0.3360	0.0746		0.2900	0.0713		0.4304	0.3366		--	--
Humerus		29	6			3			13			7			0		
	Avg. On.Ar			24061.44	10084.30		35916.74	9204.02		37412.40	11004.56		42768.68	6428.08		--	--
	Avg. On.Fg.Ar			11984.89	11517.91		19470.16	16870.90		24783.50	17748.76		30852.15	5619.92		--	--
	Avg. On.C.Ar			22120.21	10150.41		32846.00	7556.96		35019.74	10059.81		39724.18	5891.34		--	--
	Avg. HC.Ar			2151.97	835.72		3488.12	799.81		2979.81	1171.15		3059.14	1140.76		--	--
	Avg. RS.Ar			32495.14	25543.70		6044.78	2524.43		14922.25	14304.41		9238.01	7322.55		--	--
	Avg. Por.Ar			6941.97	4256.64		2903.82	658.93		5278.46	5224.89		3912.73	2034.06		--	--
	Total On.Ar			0.6747	0.4364		0.8889	0.2055		1.6066	0.9498		3.7266	1.8580		--	--
	Total On.Fg.Ar			0.0182	0.0106		0.0618	0.0497		0.0235	0.0176		0.0370	0.0124		--	--
	Total On.C.Ar			0.1526	0.0706		0.2193	0.0832		0.2147	0.0849		0.2926	0.0850		--	--
	Total HC.Ar			0.0166	0.0069		0.0278	0.0090		0.0179	0.0068		0.0237	0.0103		--	--

APPENDIX VII (cont.): Means and standard deviations for unstandardized and size-standardized histomorphometric properties by age cohort.

		1.0-1.99 yrs			2.0-2.99 yrs			3.0-6.99 yrs			7.0-11.99 yrs			12.0-13.99 yrs	
Element	**Dimension[1]**	n	Mean	St Dev	n	Mean	St Dev	n	Mean	St Dev	n	Mean	St Dev	n	Mean	St Dev
Humerus	Total RS.Ar		0.1635	0.1711		0.0562	0.0500		0.0306	0.0240		0.0201	0.0184		--	--
	Total Por.Ar		0.1908	0.1684		0.0949	0.0469		0.0524	0.0235		0.0469	0.0225		--	--
	Total On.B.Ar		0.1897	0.0763		0.3028	0.0734		0.2577	0.1027		0.3601	0.1011		--	--
Rib	35	5			3			14			11			2		
	Avg. On.Ar		13259.71	7595.51		25638.20	7834.07		25238.81	10586.23		31749.25	12364.54		45281.90	12309.99
	Avg. On.Fg.Ar		6909.58	11164.45		9795.78	8608.46		16123.29	16071.66		23607.89	10271.96		23980.43	6043.90
	Avg. On.C.Ar		11995.11	6796.56		22956.46	6476.15		23278.96	9779.77		28966.54	11482.68		40098.02	8778.83
	Avg. HC.Ar		1210.21	825.26		2340.43	1323.87		2028.71	1132.32		2650.31	746.87		5081.49	3675.95
	Avg. RS.Ar		12103.16	8297.00		19570.13	4652.28		21788.49	14970.82		24124.71	14927.99		28215.74	30155.84
	Avg. Por.Ar		4897.78	4002.88		10544.95	3789.75		9501.67	7913.33		9391.27	4978.28		11005.90	10801.46
	Total On.Ar		0.3577	0.2822		0.7405	0.6259		1.2276	0.5539		2.6709	1.9732		2.7717	0.8476
	Total On.Fg.Ar		0.0012	0.0019		0.0042	0.0062		0.0063	0.0090		0.0108	0.0092		0.0068	0.0062
	Total On.C.Ar		0.0428	0.0355		0.0595	0.0523		0.0932	0.0440		0.1371	0.0792		0.1742	0.0701
	Total HC.Ar		0.0044	0.0039		0.0067	0.0058		0.0082	0.0045		0.0118	0.0040		0.0185	0.0030
	Total RS.Ar		0.0186	0.0165		0.0617	0.0136		0.0512	0.0414		0.0317	0.0212		0.0298	0.0247
	Total Por.Ar		0.0346	0.0199		0.0693	0.0174		0.0597	0.0400		0.0572	0.0264		0.0484	0.0276
	Total On.B.Ar		0.0486	0.0407		0.0745	0.0684		0.1082	0.0542		0.1636	0.0880		0.2019	0.0767

[1] Average size variables are not standardized and mean values are presented in nanometers-squared. Total area variables are size-standardized by the area encompassed by the histological region of interest measured (ROI.Ar).

APPENDIX VIII: Weighted means and standard deviations for size-standardized cross-sectional geometric properties by stress group.

Element	Dimension[1]	No lesion group		Lesion group		ANCOVA
		Mean $_{weighted}$	St Dev $_{weighted}$	Mean $_{weighted}$	St Dev$_{weighted}$	***p*-value**
Femur	TA	18.64	2.32	18.46	2.80	0.865
	CA	10.68	0.98	10.78	2.08	0.271
	MA	7.97	1.77	7.68	1.88	0.150
	%CA	57.51	5.34	58.78	8.02	0.021*
	I_{max}	4.85 x10^{-3}	1.35 x10^{-3}	4.37 x10^{-3}	1.27 x10^{-3}	0.516
	I_{min}	4.13 x10^{-3}	1.13 x10^{-3}	3.61 x10^{-3}	1.02 x10^{-3}	0.967
	I_{max}:I_{min}	1.17	0.08	1.21	0.07	0.024*
	J	8.99 x10^{-3}	2.45 x10^{-3}	7.98 x10^{-3}	2.28 x10^{-3}	0.738
	Z_p	27.52 x10^{-3}	5.88 x10^{-3}	22.00 x10^{-3}	6.87 x10^{-3}	0.956
Humerus	TA	11.51	1.57	11.40	1.92	0.399
	CA	6.33	0.59	6.80	0.96	0.423
	MA	5.18	1.85	4.60	1.53	0.623
	%CA	56.10	9.99	60.69	8.44	0.570
	I_{max}	3.03 x10^{-3}	0.60 x10^{-3}	3.07 x10^{-3}	0.92 x10^{-3}	0.031*
	I_{min}	2.44 x10^{-3}	0.51 x10^{-3}	2.51 x10^{-3}	0.69 x10^{-3}	0.023*
	I_{max}:I_{min}	1.25	0.08	1.23	0.10	0.701
	J	5.47 x10^{-3}	1.10 x10^{-3}	5.57 x10^{-3}	1.59 x10^{-3}	0.023*
	Z_p	20.97 x10^{-3}	4.19 x10^{-3}	18.70 x10^{-3}	6.53 x10^{-3}	0.053
Rib	TA	3.51 x10^{-3}	1.06 x10^{-3}	3.02 x10^{-3}	1.44 x10^{-3}	0.007*
	CA	1.69 x10^{-3}	0.41 x10^{-3}	1.43 x10^{-3}	0.67 x10^{-3}	0.071
	MA	1.82 x10^{-3}	0.67 x10^{-3}	1.59 x10^{-3}	0.83 x10^{-3}	0.008*
	%CA	49.90	5.50 x10^{-3}	47.81	6.23 x10^{-3}	0.119

- Asterisks denote significant differences between the stress groups for the given dimension.

[1] Cross-sectional long bone areas (TA, CA, MA) standardized by body mass estimated from distal femoral metaphyseal breadth. Second moments of area (*I*, *J*) standardized by body mass × bone length^2 (Ruff, 2007). Section modulus (Z_p) standardized by body mass × bone length (Ruff, 2008a). Rib areas standardized by estimated stature as a body size approximation.

APPENDIX IX: Weighted means and standard deviations for unstandardized and size-standardized histomorphometric properties by stress group.

Element	Dimension[1]	No lesion group		Lesion group		ANCOVA
		$Mean_{weighted}$	$St\ Dev_{weighted}$	$Mean_{weighted}$	$St\ Dev_{weighted}$	***p*-value**
Femur	Avg. On.Ar (nm^2)	36207.13	12636.81	43854.47	21037.75	0.760
	Avg. On.Fg.Ar (nm^2)	20760.21	12570.54	32683.99	21738.22	0.558
	Avg. On.C.Ar (nm^2)	32666.77	11023.90	40808.48	20073.88	0.709
	Avg. HC.Ar (nm^2)	3527.92	860.21	3552.03	2042.08	0.935
	Avg. RS.Ar (nm^2)	14063.78	302.01	12550.46	357.85	0.638
	Avg. Por.Ar (nm^2)	4145.78	1294.13	4656.50	3356.15	0.954
	Total On.Ar / ROI.Ar	2.75	1.80	4.62	3.84	0.680
	Total On.Fg.Ar / ROI.Ar	0.0199	0.0117	0.0225	0.0203	0.695
	Total On.C.Ar / ROI.Ar	0.2128	0.0737	0.2743	0.1410	0.984
	Total HC.Ar / ROI.Ar	0.0231	0.0027	0.0260	0.0159	0.772
	Total RS.Ar / ROI.Ar	0.0583	0.5633	0.0358	0.5579	0.535
	Total Por.Ar / ROI.Ar	0.0884	0.0550	0.0686	0.0355	0.699
	Total On.B.Ar / ROI.Ar	0.2565	0.0923	0.3337	0.1898	0.663
Humerus	Avg. On.Ar (nm^2)	37137.85	9555.51	34691.79	9961.77	0.196
	Avg. On.Fg.Ar (nm^2)	20628.81	4546.64	25018.48	11010.74	0.655
	Avg. On.C.Ar (nm^2)	35017.75	9040.80	31834.65	9355.97	0.108
	Avg. HC.Ar (nm^2)	2755.78	836.22	2981.41	1037.86	0.500
	Avg. RS.Ar (nm^2)	19066.55	353.92	13993.45	325.52	0.617
	Avg. Por.Ar (nm^2)	5807.79	2660.66	4429.45	2198.90	0.192
	Total On.Ar / ROI.Ar	1.62	1.06	2.04	1.71	0.113
	Total On.Fg.Ar / ROI.Ar	0.0204	0.0064	0.0372	0.0168	0.787
	Total On.C.Ar / ROI.Ar	0.2193	0.0821	0.2227	0.0814	0.450
	Total HC.Ar / ROI.Ar	0.0181	0.0045	0.0216	0.0062	0.340

APPENDIX IX (cont.): Weighted means and standard deviations for unstandardized and size-standardized histomorphometric properties by stress group.

		No lesion group		Lesion group		ANCOVA
Element	**Dimension[1]**	$Mean_{weighted}$	St $Dev_{weighted}$	$Mean_{weighted}$	St $Dev_{weighted}$	***p*-value**
Humerus	Total RS.Ar / ROI.Ar	0.0504	0.5521	0.0646	0.6868	0.400
	Total Por.Ar / ROI.Ar	0.0722	0.0437	0.0938	0.0787	0.277
	Total On.B.Ar / ROI.Ar	0.2588	0.0924	0.2845	0.0979	0.836
Rib	Avg. On.Ar (nm^2)	26548.81	5506.29	26859.84	11650.76	0.326
	Avg. On.Fg.Ar (nm^2)	17240.23	9810.91	16975.06	9627.07	0.456
	Avg. On.C.Ar (nm^2)	24397.91	5217.70	24382.76	10334.82	0.282
	Avg. HC.Ar (nm^2)	2306.62	493.51	2309.18	1448.41	0.342
	Avg. RS.Ar (nm^2)	21831.65	364.98	21047.32	523.88	0.672
	Avg. Por.Ar (nm^2)	10183.02	3213.05	8359.42	4306.89	0.415
	Total On.Ar / ROI.Ar	1.35	0.73	1.74	1.68	0.711
	Total On.Fg.Ar / ROI.Ar	0.0068	0.0041	0.0068	0.0060	0.549
	Total On.C.Ar / ROI.Ar	0.0968	0.0243	0.1040	0.0700	0.461
	Total HC.Ar / ROI.Ar	0.0091	0.0027	0.0094	0.0050	0.461
	Total RS.Ar / ROI.Ar	0.0441	0.5289	0.0380	0.6939	0.760
	Total Por.Ar / ROI.Ar	0.0595	0.0119	0.0534	0.0237	0.877
	Total On.B.Ar / ROI.Ar	0.1125	0.0291	0.1232	0.0796	0.626

* Asterisks denote significant differences between the stress groups for the given dimension.

[1] Average size variables are not standardized and mean values are presented in nanometers-squared. Total area variables are size-standardized by the area encompassed by the histological region of interest measured (ROI.Ar).

APPENDIX X: Weighted means for unstandardized and size-standardized histomorphometric properties for maximum (I_{max}) minus minimum (I_{min}) long bone second moments of area between stress groups.

Element	Dimension[1]	No lesion group $Mean_{weighted}$	Lesion group $Mean_{weighted}$	ANCOVA *p*-value
Femur	Avg. On.Ar (nm^2)	-1710.70	1859.42	0.502
	Avg. On.Fg.Ar (nm^2)	-3546.66	-431.59	0.761
	Avg. On.C.Ar (nm^2)	-3497.88	3153.84	0.428
	Avg. HC.Ar (nm^2)	1238.23	1425.06	0.861
	Avg. RS.Ar (nm^2)	6769.89	-1103.93	0.242
	Avg. Por.Ar (nm^2)	566.02	-263.22	0.990
	Total On.Ar / ROI.Ar	-0.0559	0.0321	0.398
	Total On.Fg.Ar / ROI.Ar	-0.0098	-0.0025	0.767
	Total On.C.Ar / ROI.Ar	-0.0490	0.0472	0.363
	Total HC.Ar / ROI.Ar	-0.0005	-0.0023	0.674
	Total RS.Ar / ROI.Ar	-0.0071	0.0001	0.474
	Total Por.Ar / ROI.Ar	-0.0044	-0.0003	0.524
	Total On.B.Ar / ROI.Ar	-0.0661	0.0289	0.449
Humerus	Avg. On.Ar (nm^2)	9048.27	-1968.43	0.150
	Avg. On.Fg.Ar (nm^2)	1449.86	-3752.81	0.514
	Avg. On.C.Ar (nm^2)	7309.76	-1947.03	0.178
	Avg. HC.Ar (nm^2)	1425.06	-480.83	0.038*
	Avg. RS.Ar (nm^2)	-137.75	12270.90	0.990
	Avg. Por.Ar (nm^2)	-69.21	2589.92	0.343
	Total On.Ar / ROI.Ar	-0.0007	-0.0338	0.701
	Total On.Fg.Ar / ROI.Ar	0.0014	-0.0122	0.392
	Total On.C.Ar / ROI.Ar	-0.0057	-0.0297	0.786
	Total HC.Ar / ROI.Ar	0.0031	-0.0007	0.445
	Total RS.Ar / ROI.Ar	0.0034	0.0247	0.331
	Total Por.Ar / ROI.Ar	0.0071	0.0235	0.417
	Total On.B.Ar / ROI.Ar	-0.0008	-0.0469	0.600

* Asterisks denote significant differences between the stress groups for I_{max}-I_{min}.

[1] Average size variables are not standardized and mean values are presented in nanometers-squared. Total area variables are size-standardized by the area encompassed by the histological region of interest measured (ROI.Ar).

APPENDIX XI: Medians for size-standardized cross-sectional geometric properties by stress group (1.0-6.99 years).

Element	Dimension[1]	No lesion group Median	Lesion Group Median	Mann-Whitney *p*-value
Femur	TA	18.17	18.97	0.990
	CA	10.64	8.45	0.169
	MA	7.98	8.95	0.153
	%CA	55.12	52.01	0.064
	I_{max}	4.48 $x10^{-3}$	4.89 $x10^{-3}$	0.479
	I_{min}	3.68 $x10^{-3}$	3.91 $x10^{-3}$	0.960
	I_{max}:I_{min}	1.18	1.25	0.064
	J	8.36 $x10^{-3}$	8.83 $x10^{-3}$	0.153
	Z_p	26.99 $x10^{-3}$	29.42 $x10^{-3}$	0.418
Humerus	TA	11.53	12.19	0.329
	CA	6.09	6.87	0.734
	MA	5.59	6.07	0.376
	%CA	53.32	52.57	0.701
	I_{max}	3.05 $x10^{-3}$	3.25 $x10^{-3}$	0.210
	I_{min}	2.32 $x10^{-3}$	2.95 $x10^{-3}$	0.056
	I_{max}:I_{min}	1.25	1.23	0.571
	J	5.34 $x10^{-3}$	6.12 $x10^{-3}$	0.104
	Z_p	20.98 $x10^{-3}$	23.35 $x10^{-3}$	0.125
Rib	TA	3.68 $x10^{-3}$	4.32 $x10^{-3}$	0.017*
	CA	1.76 $x10^{-3}$	2.22 $x10^{-3}$	0.028*
	MA	1.88 $x10^{-3}$	2.37 $x10^{-3}$	0.047*
	%CA	48.36	47.65	0.423

- Asterisks denote significant differences between the stress groups for the given dimension.

[1] Cross-sectional long bone areas (TA, CA, MA) standardized by body mass estimated from distal femoral metaphyseal breadth. Second moments of area (*I*, *J*) standardized by body mass × bone length^2 (Ruff, 2007). Section modulus (Z_p) standardized by body mass × bone length (Ruff, 2008a). Rib areas standardized by estimated stature as a body size approximation.

APPENDIX XII: Medians for unstandardized and size-standardized histomorphometric properties by stress group (1.0-6.99 years).

Element	Dimension[1]	No lesion group Median	Lesion group Median	Mann-Whitney *p*-value
Femur	Avg. On.Ar (nm^2)	38170.54	31653.46	0.760
	Avg. On.Fg.Ar (nm^2)	24483.74	24560.64	0.558
	Avg. On.C.Ar (nm^2)	36799.40	28806.70	0.709
	Avg. HC.Ar (nm^2)	3315.00	3082.71	0.935
	Avg. RS.Ar (nm^2)	13248.57	7654.18	0.638
	Avg. Por.Ar (nm^2)	3542.79	3037.59	0.954
	Total On.Ar / ROI.Ar	2.10	1.97	0.680
	Total On.Fg.Ar / ROI.Ar	0.0172	0.0146	0.695
	Total On.C.Ar / ROI.Ar	0.2137	0.2276	0.984
	Total HC.Ar / ROI.Ar	0.0224	0.0205	0.772
	Total RS.Ar / ROI.Ar	0.0403	0.0360	0.535
	Total Por.Ar / ROI.Ar	0.0650	0.0680	0.699
	Total On.B.Ar / ROI.Ar	0.2402	0.2650	0.663
Humerus	Avg. On.Ar (nm^2)	39801.48	28876.10	0.196
	Avg. On.Fg.Ar (nm^2)	23650.84	20728.33	0.655
	Avg. On.C.Ar (nm^2)	38007.17	27500.71	0.108
	Avg. HC.Ar (nm^2)	2652.78	2877.23	0.500
	Avg. RS.Ar (nm^2)	18132.49	7745.24	0.617
	Avg. Por.Ar (nm^2)	4422.40	3098.67	0.192
	Total On.Ar / ROI.Ar	1.52	0.97	0.113
	Total On.Fg.Ar / ROI.Ar	0.0189	0.0310	0.787
	Total On.C.Ar / ROI.Ar	0.2173	0.1805	0.450
	Total HC.Ar / ROI.Ar	0.0202	0.0196	0.340
	Total RS.Ar / ROI.Ar	0.0365	0.0424	0.400
	Total Por.Ar / ROI.Ar	0.0605	0.0718	0.277
	Total On.B.Ar / ROI.Ar	0.2571	0.2318	0.836

APPENDIX XII (cont.): Medians for unstandardized and size-standardized histomorphometric properties by stress group (1.0-6.99 years).

Element	Dimension[1]	No lesion group Median	Lesion group Median	Mann-Whitney *p*-value
Rib	Avg. On.Ar (nm^2)	26457.54	17828.37	0.326
	Avg. On.Fg.Ar (nm^2)	14604.39	0.00	0.456
	Avg. On.C.Ar (nm^2)	24183.57	16434.19	0.282
	Avg. HC.Ar (nm^2)	2070.67	1735.20	0.342
	Avg. RS.Ar (nm^2)	21046.13	14699.29	0.672
	Avg. Por.Ar (nm^2)	9036.03	7480.47	0.415
	Total On.Ar / ROI.Ar	1.30	0.78	0.711
	Total On.Fg.Ar / ROI.Ar	0.0034	0.0000	0.549
	Total On.C.Ar / ROI.Ar	0.0881	0.0739	0.461
	Total HC.Ar / ROI.Ar	0.0072	0.0058	0.461
	Total RS.Ar / ROI.Ar	0.0443	0.0212	0.760
	Total Por.Ar / ROI.Ar	0.0550	0.0503	0.877
	Total On.B.Ar / ROI.Ar	0.0978	0.0843	0.626

* Asterisks denote significant differences between the stress groups for the given dimension.

[1] Average size variables are not standardized and median values are presented in nanometers-squared. Total area variables are size-standardized by the area encompassed by the histological region of interest measured (ROI.Ar).

APPENDIX XIII: Medians for unstandardized and size-standardized histomorphometric properties for maximum (I_{max}) minus minimum (I_{min}) long bone second moments of area between stress groups (1.0-6.99 years).

Element	Dimension[1]	No lesion group Median	Lesion group Median	ANCOVA *p*-value
Femur	Avg. On.Ar (nm^2)	734.89	5059.02	0.601
	Avg. On.Fg.Ar (nm^2)	0.00	0.00	0.887
	Avg. On.C.Ar (nm^2)	-167.30	6544.76	0.364
	Avg. HC.Ar (nm^2)	207.60	666.72	0.536
	Avg. RS.Ar (nm^2)	8263.79	-968.89	0.364
	Avg. Por.Ar (nm^2)	1277.91	-123.77	0.364
	Total On.Ar / ROI.Ar	-0.0450	0.0105	0.133
	Total On.Fg.Ar / ROI.Ar	-0.0065	-0.0008	0.475
	Total On.C.Ar / ROI.Ar	-0.0098	0.0205	0.109
	Total HC.Ar / ROI.Ar	0.0048	-0.0001	0.813
	Total RS.Ar / ROI.Ar	-0.0075	-0.0054	0.999
	Total Por.Ar / ROI.Ar	-0.0018	0.0007	0.999
	Total On.B.Ar / ROI.Ar	-0.0507	0.0035	0.315
Humerus	Avg. On.Ar (nm^2)	10970.97	-3969.38	0.080
	Avg. On.Fg.Ar (nm^2)	0.00	0.00	0.771
	Avg. On.C.Ar (nm^2)	10310.12	-4348.83	0.123
	Avg. HC.Ar (nm^2)	1563.68	-95.47	0.025*
	Avg. RS.Ar (nm^2)	1433.26	5979.14	0.159
	Avg. Por.Ar (nm^2)	985.03	1773.18	0.418
	Total On.Ar / ROI.Ar	0.0525	-0.0406	0.254
	Total On.Fg.Ar / ROI.Ar	0.0112	-0.0038	0.418
	Total On.C.Ar / ROI.Ar	0.0406	-0.0291	0.228
	Total HC.Ar / ROI.Ar	0.0072	-0.0032	0.093
	Total RS.Ar / ROI.Ar	-0.0029	0.0132	0.123
	Total Por.Ar / ROI.Ar	0.0036	0.0192	0.381
	Total On.B.Ar / ROI.Ar	0.0569	-0.0725	0.346

* Asterisks denote significant differences between the stress groups for I_{max}-I_{min}.

[1] Average size variables are not standardized and mean values are presented in nanometers-squared. Total area variables are size-standardized by the area encompassed by the histological region of interest measured (ROI.Ar).

APPENDIX XIV: Presence and absence of DEH in the adult dentition and estimated age of disruption for each individual.

			DEH[3] Age Estimate (years)															
PC.Inv. No[1]	**Cr.Inv. No[1]**	**Indiv Age Est.[2]**	**0.25**	**0.75**	**1.25**	**1.75**	**2.25**	**2.75**	**3.25**	**3.75**	**4.25**	**4.75**	**5.25**	**5.75**	**6.25**	**6.75**	**7.25**	**Total**
314A	3913	7.4							X									**1**
348A	3909	3.5																
348B	3923A	4.0																
350C	3904	8.8						X		X								**2**
350D	3614	9.3																
464G	4159	3.0																
465A	4182	10.1		X	X		X	X										**4**
465B	4334E	1.5																
470B	3955A	7.2						X										**1**
474B	4382	5.6																**0**
478C	4369	1.8																
478D	4398	5.1																
478F	4397	5.3																**0**
483H	3956A	2.7																
486B	4167	6.5																**0**
490B	3956B	3.9																
492C	4387	4.5																
553B	4412	7.5																**0**
553C	3991	7.9																**0**
634C	3975D	2.1																
634R	3975A	1.3																
637B	4235	5.5																**0**
674B	4158	10.9																**0**

APPENDIX XIV (cont.): Presence and absence of DEH in the adult dentition and estimated age of disruption for each individual.

			DEH[3] Age Estimate (years)															
PC.Inv. No[1]	**Cr.Inv. No[1]**	**Indiv Age Est.[2]**	**0.25**	**0.75**	**1.25**	**1.75**	**2.25**	**2.75**	**3.25**	**3.75**	**4.25**	**4.75**	**5.25**	**5.75**	**6.25**	**6.75**	**7.25**	**Total**
730B	4781	13.0				X	X	X	X	X	X	X	X					8
736B	4446	9.0																
742B	4439	11.3						X	X	X	X							4
745A	4454	12.0																
746B	4458	7.3																
753B	4448	11.3				X	X	X	X	X	X	X						7
790A	4456	12.7																0
824A	4645	12.0				X	X	X		X	X	X	X	X				8
944A	4817	13.5																
956A	4522	13.5					X		X	X		X						4
969A	4655	13.5									X		X					2
976A	4799	11.0						X		X								2
979A	4819	9.7											X					1
980B	4516	12.0			X					X		X						3
983B	4756	6.1					X	X	X	X	X							5
991C	4478	5.7																
991D	4758	2.5																0
997F	4558I	1.5																
1000F	4558D	2.5																
1000G	4544H	5.1																
1000H	4510	8.8																0
1002C	4572D	1.5																
1003D	4752	1.7																
1004D	4762	2.0																

APPENDIX XIV (cont.): Presence and absence of DEH in the adult dentition and estimated age of disruption for each individual.

			DEH[3] Age Estimate (years)															
PC.Inv. No[1]	**Cr.Inv. No[1]**	**Indiv Age Est.[2]**	**0.25**	**0.75**	**1.25**	**1.75**	**2.25**	**2.75**	**3.25**	**3.75**	**4.25**	**4.75**	**5.25**	**5.75**	**6.25**	**6.75**	**7.25**	**Total**
1005A	4534	8.9																**0**
1005C	4443	4.4																
1005D	4778	10.0					**X**											**1**
1006K	4489	11.5				**X**	**X**	**X**	**X**			**X**	**X**	**X**				**7**
1007B	4783	2.9																
1007D	4731	2.8																
1007I	4442	4.7																
1008E	4578	3.6																
1008H	4482	8.0						**X**	**X**									**2**
1011A	4440	5.0																
Total				1	2	4	8	11	8	9	6	6	5	2				

[1] PC.Inv.No = Postcranial Inventory Number; Cr.Inv.No = Cranial Inventory Number.
[2] Final age estimate for each individual in years.
[3] DEH = Dental Enamel Hypoplasia; X indicates the presence of a DEH as defined under the pathological criteria outlined in Chapter 4; grey boxes indicate individuals who could not be assessed for DEH presence, whether due to inadequate numbers of present teeth (e.g., undeveloped adult dentition, poor dental preservation) or intact, but unerupted, adult dentition.

VITA

Courtney Eleazer was born in Tallahassee, FL to parents Ed and Nancy Eleazer. She attended West Florence High School in Florence, SC and received her B.S. in Anthropology from Florida State University in 2004. She attended the University of Tennessee, Knoxville to pursue her interests in biological anthropology, graduating with an M.A. degree in 2007. She continued her doctoral education at the University of Tennessee and obtained her Ph.D. in August 2013. During her tenure in graduate school, Courtney was a graduate teaching assistant in introductory biology and human anatomy. She is currently employed in the Department of Biological Sciences at Florida International University in Miami, FL.